Forest Service
U.S. DEPARTMENT OF AGRICULTURE

Southern Research Station | General Technical Report SRS-273 | October 2023

Forest Health Monitoring: National Status, Trends, and Analysis 2022

EDITORS: Kevin M. Potter and Barbara L. Conkling

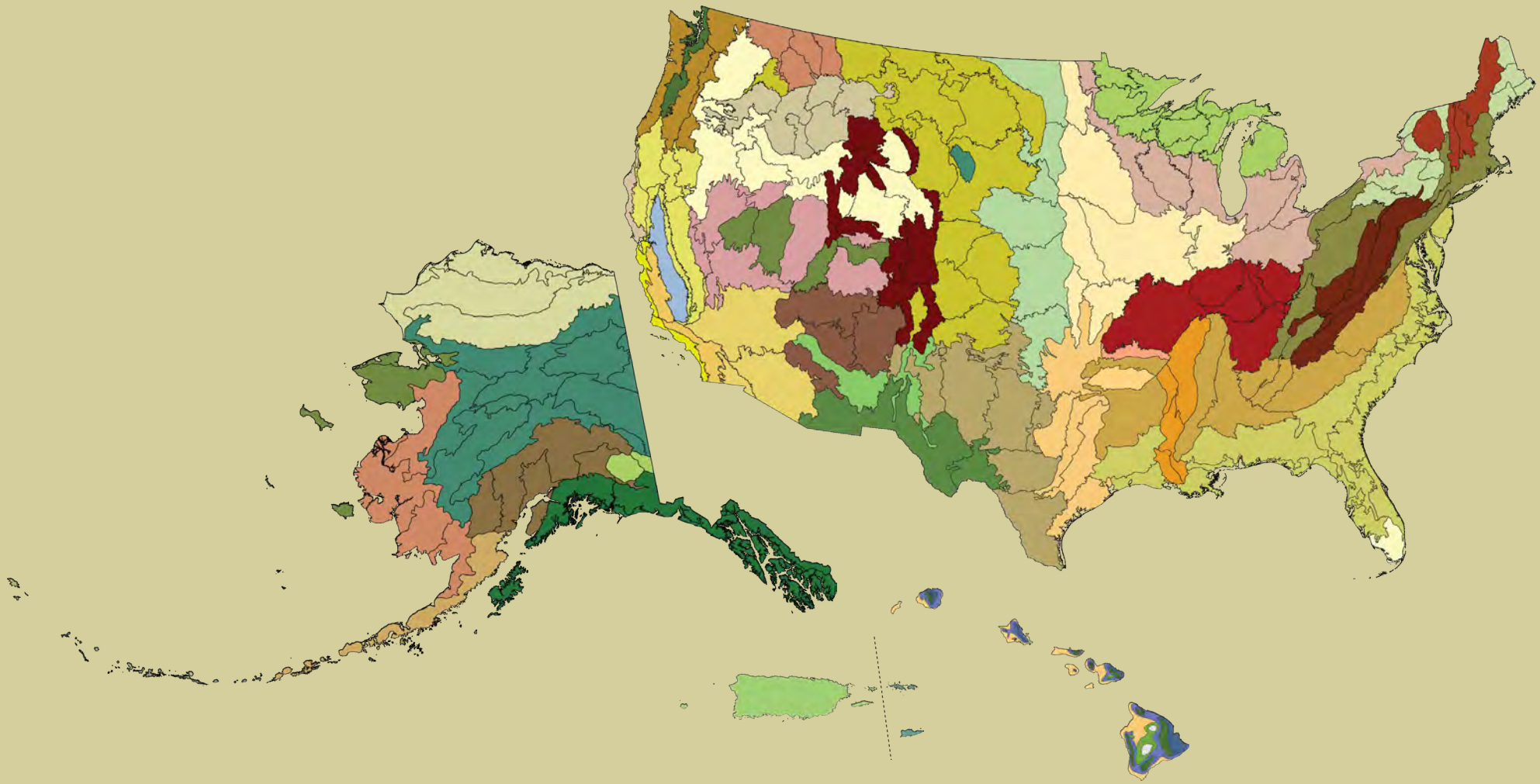

FRONT COVER MAP: Ecoregion provinces and ecoregion sections for the conterminous United States (Cleland and others 2007) and for Alaska (Spencer and others 2002), and ecoregions within the islands of Hawaii (Potter 2023), along with Puerto Rico and the U.S. Virgin Islands, for which no corresponding ecoregion treatments exist.

BACK COVER MAPS: Tree canopy cover (green) for the conterminous United States, Hawaii, Puerto Rico, and the U.S. Virgin Islands based on data from a cooperative project between the Multi-Resolution Land Characteristics Consortium and the U.S. Department of Agriculture, Forest Service, Geospatial Technology and Applications Center using the 2011 National Land Cover Database (NLCD). Forest and shrubland cover for Alaska derived from the 2011 NLCD.

PESTICIDE PRECAUTIONARY STATEMENT: This publication reports research involving pesticides. It does not contain recommendations for their use, nor does it imply that the uses discussed here have been registered. All uses of pesticides must be registered by appropriate State and/or Federal agencies before they can be recommended.

DISCLAIMER: The use of trade or firm names in this publication is for reader information and does not imply endorsement by the U.S. Department of Agriculture of any product or service.

October 2023

https://doi.org/10.2737/SRS-GTR-273

Forest Service
Research & Development
Southern Research Station
General Technical Report SRS-273

Southern Research Station
200 W.T. Weaver Blvd.
Asheville, NC 28804
www.srs.fs.usda.gov

Forest Health Monitoring: National Status, Trends, and Analysis 2022

EDITORS:

Kevin M. Potter, Research Professor, North Carolina State University, Department of Forestry and Environmental Resources, Raleigh, NC 27695 (now Research Ecologist, U.S. Department of Agriculture, Forest Service, Eastern Forest Environmental Threat Assessment Center, Research Triangle Park, NC 27709)

Barbara L. Conkling, Research Assistant Professor, North Carolina State University, Department of Forestry and Environmental Resources, Raleigh, NC 27695

ABSTRACT

The annual national report of the Forest Health Monitoring (FHM) program of the U.S. Department of Agriculture, Forest Service, presents forest health status and trends from a national or multistate regional perspective using a variety of sources, introduces new techniques for analyzing forest health data, and summarizes results of recently completed Evaluation Monitoring projects funded through the FHM national program. In this 22nd edition in a series of annual reports, national survey data are used to identify recent geographic patterns of insect and disease activity. Satellite data are employed to detect geographic patterns of forest fire occurrence. Fine-scale changes in Normalized Difference Vegetation Index (NDVI) are used to detect broad patterns of forest disturbance across the conterminous United States. Data collected by the Forest Inventory and Analysis (FIA) program are employed to detect regional differences in tree mortality. Twenty years of crown dieback trends are presented for the most common tree species and genera in the Eastern United States. The new National FIA Lichen Database and the National Lichen Atlas are described to illustrate the breadth of 23 years of lichen indictor data. Four recently completed Evaluation Monitoring projects are summarized, addressing forest health concerns at smaller scales.

Keywords—Change detection, disturbance, fire, forest health, forest insects and disease, lichens, tree canopy, tree crown dieback, tree mortality.

CONTENTS

CONTENTS

CONTENTS

LIST OF FIGURES

LIST OF FIGURES

LIST OF FIGURES

LIST OF FIGURES

LIST OF FIGURES

LIST OF FIGURES

LIST OF FIGURES

LIST OF FIGURES

LIST OF FIGURES

LIST OF TABLES

EXECUTIVE SUMMARY

Healthy ecosystems are those that are stable and sustainable, able to maintain their organization and autonomy over time while remaining resilient to stress (Costanza 1992). Healthy forests are vital to our future (Edmonds and others 2011), and consistent, large-scale, and long-term monitoring of key indicators of forest health status, change, and trends is necessary to identify forest resources deteriorating across large regions (Riitters and Tkacz 2004). The Forest Health Monitoring (FHM) program of the Forest Service, U.S. Department of Agriculture, with cooperating researchers within and outside the Forest Service and with State partners, quantifies status and trends in the health of U.S. forests in the Forest Health Monitoring: National Status, Trends, and Analysis report (ch. 1). The 2022 FHM national report is the 22nd edition in the annual series of reports. The analyses and results outlined in sections 1 and 2 of this report offer a snapshot of the current condition of U.S. forests from a national or multistate regional perspective, incorporating baseline investigations of forest ecosystem health, examinations of change over time in forest health metrics, and assessments of developing threats to forest stability and sustainability. For datasets collected on an annual basis, analyses are presented from 2021 data. For datasets collected over several years, analyses are presented at a longer temporal scale. Section 3 of this report presents four summaries of results from recently completed Evaluation Monitoring (EM) projects that have been funded through the FHM national program to determine the extent, severity, and/or causes of specific forest health problems (FHM 2022).

Monitoring the occurrence of forest pest and pathogen outbreaks is important at regional scales because of the potential forest health impacts of insects and disease across landscapes (ch. 2). In 2021, national Insect and Disease Survey data identified 60 mortality-causing agents and complexes across the conterminous United States (CONUS) on approximately 2.21 million ha. Emerald ash borer (*Agrilus planipennis*) was the most widely detected mortality agent, identified on about 878 000 ha across the Eastern FHM megaregion, causing a hot spot of extremely high mortality density in the Midwest. Fir engraver (*Scolytus ventralis*) caused extensive mortality in parts of the West, but the area of its impact had declined from recent years. As in recent years, Alaska experienced extensive mortality from spruce beetle (*Dendroctonus rufipennis*), while much mortality in Hawaii may be associated with rapid ōhiʻa death. Meanwhile, forest health surveyors reported damage from 56 defoliation agents and complexes affecting approximately 1.67 million ha across the CONUS. Most of this defoliation was the result of a spongy moth (*Lymantria dispar*) outbreak, primarily in the Eastern FHM megaregion but in the Southern FHM megaregion as well. Alaska had extensive defoliation, caused mostly by western blackheaded budworm (*Acleris gloverana*).

Forest fire occurrence outside the historic range of frequency and intensity can result in extensive economic and ecological impacts. The detection of regional patterns of fire occurrence density can allow for the identification of areas at greatest risk of significant impact (ch. 3). In 2021, the number of satellite-detected forest fire occurrences in the

CONUS was the fourth highest in 21 full years of data collection but represented a 9-percent decrease in fire activity from the 2020 fire season. Parts of California and the Pacific Northwest in 2021 had extremely high fire occurrence densities, while other areas of the West had high or very high densities. The extensive fire activity in these regions resulted in geographic hot spots of extremely active or very high fire occurrence density. These areas experienced fire occurrence densities that were much higher than normal in 2021 compared to the previous 20-year mean and accounting for variability over time. Alaska experienced a large increase in fire occurrences from 2020, but this was a decrease from the extremely active fire year of 2019 and less than the mean for the preceding 2 decades. Hawaiian forests in 2021 had fire occurrence densities that were low and within expectations. Parts of both Puerto Rico and the U.S. Virgin Islands had higher than expected fire occurrence densities.

Recent advances in high-spatial-resolution imagery and high-speed computation have revolutionized forest canopy monitoring. With more efficient use of higher resolution imagery, the capacity to understand the mechanisms of forest change and precise disturbance impacts at a fine scale has grown (ch. 4). Moderate Resolution Imaging Spectroradiometer (MODIS) satellite imagery was accessed using Google Earth Engine to produce 250-m-resolution national maps of the Normalized Difference Vegetation Index (NDVI) for the 2021 growing season. One-year absolute change (departure) in NDVI was determined by comparing 2021 to 2020, with forest-only change below a threshold of -0.05 NDVI summarized nationally using hexagons of 834 km^2. The map of NDVI departure shows drought as the major detected disturbance for the West during 2021; the major detected disturbances in the East were spongy moth-caused tree defoliation in Michigan and the Northeast, and the effects of commercial logging operations in the Southeastern Coastal Plain. The patterns shown in the map of NDVI departure represent the more prominent disturbances while contextualizing them within the forested landscape in which they occur. Such regional or national analyses provide a coarse-filter perspective on forest disturbance, with a full understanding requiring landscape or site analysis that involves multiple years of context and regional expertise.

Mortality is a natural process in all forested ecosystems, but high levels of mortality at large scales may be an indicator of forest health problems. Phase 2 data collected by the Forest Inventory and Analysis (FIA) program of the Forest Service offer tree mortality information on a relatively spatially intense basis of approximately one plot per 6,000 acres, and mortality analysis is possible for areas where data are available from repeated plot measurements using consistent sampling protocols (ch. 5). Due to the COVID-19 pandemic, FIA data collection was slowed during 2020 and 2021, so no new data were available from any Western States. Analyses focused on States in the Eastern and Central United States. Preliminary analyses of FIA data from these States indicated especially high mortality as a percentage of live volume in the Black Hills (due to insects and fire), the south-central Great Plains in Kansas and Oklahoma (due to fire, disease, and weather-related issues), and the western Great

Plains in South Dakota and Nebraska (due to fire and weather-related issues). These mortality-causing agents are related in that weather events can stress trees, making them more susceptible to insect attack. Both insect-killed trees and damage from weather events, such as tornadoes, can create conditions favorable for wildfires. Mortality as a percentage of live volume was lower in Eastern U.S. areas, with insects and weather-related issues dominating the major causes of mortality.

Assessments of tree crown conditions, which are visually assessed by the FIA program as an indicator of forest health, are useful because tree photosynthetic capacity depends on the size and condition of the crown (ch. 6). A fourth national summary of crown condition in the United States indicated that recent crown conditions were as expected for most species and overall exemplified the presence of known stressors in the Eastern United States, such as beech bark disease, emerald ash borer, hemlock woolly adelgid (*Adelges tsugae)*, spongy moth, and eastern spruce budworm *(Choristoneura fumiferana)*. With only a few exceptions, average crown dieback has remained stable or declined over the last 20 years. Among the softwood species groups included in the analyses, crown dieback was greatest among northern white-cedar (*Thuja occidentalis*) trees in the Northern region and pinyon-juniper (*Pinus-Juniperus*) trees in the Southern region. Among the hardwood species groups, crown dieback was greatest among ash (*Fraxinus* spp.) and elm (*Ulmus* spp.) trees in the Northern region and honey mesquite (*Prosopis glandulosa*) trees in the Southern region. Favorably, a downward trend in crown dieback was observed for northern white-cedar over the last 20 years and for elm within the last 10 years; however, crown dieback continued to trend upward for ash. The first remeasurement of trees in central and western Texas is incomplete, so it is unclear if the high levels of crown dieback for pinyon-juniper and honey mesquite are characteristic for these species groups.

Since its inception in 1989, the National Lichen Indicator has been the single most extensive lichen community monitoring program in the world with nearly 10,000 standardized surveys of epiphytic (tree-dwelling) lichen communities conducted (ch. 7). Used widely by Federal land managers and researchers, these surveys provide valuable information on air quality, climate, biodiversity, and lichen floristics in U.S. forests. Lichen indicator data were packaged from across three Forest Service programs using a consistent, user-friendly format. This comprehensive National FIA Lichen Database (NFLD) was used to create a National Lichen Atlas to illustrate the breadth of the combined Indicator datasets. These products mark a significant milestone, making thousands of lichen surveys conducted between 1989 and 2012 available to the public for the first time. Despite reduced data collection since 2012, FIA and the National Forest System's Air Resource Management (ARM) program have maintained their long-term partnership to continue serving clients of the Indicator, making data more readily available and, when possible, supporting additional data collection to answer specific research or management questions. Future versions of the NFLD will incorporate these newer datasets, including assay data where available.

Finally, four recently completed EM projects address a wide variety of forest health concerns at a scale smaller than the national or multistate regional analyses included in the first two sections of the report. These EM projects (funded by the FHM program):

- Studied the impacts of emerald ash borer on white ash (*F. americana*), green ash (*F. pennsylvanica*), pumpkin ash (*F. profunda*), black ash (*F. nigra*), and blue ash (*F. quadrangulata*) in different landscape contexts in Ohio and Pennsylvania, tracking individual trees on a yearly basis during a rapid mortality event that allowed for an accurate quantification of the effects of emerald ash borer (ch. 8)
- Described a flexible moving-window approach for Landsat-based harmonic condition monitoring (HCM) that considers both spatial and temporal variability in forest disturbance dynamics, comparing HCM results with comparable fixed-baseline results for a set of field sites in central Massachusetts and testing the utility of HCM scores for assessing relationships between defoliation and growth and mortality rates of oaks (*Quercus spp.)* in Pennsylvania (ch. 9)
- Summarized results of a study to examine the spread and impact of laurel wilt caused by the fungus *Harringtonia lauricola*, an ambrosial symbiont of the redbay ambrosia beetle (*Xyleborus glabratus*), in sassafras (*Sassafras albidum*) across 46 sites in the Gulf-Atlantic Coastal Plain, Piedmont, and Central and Eastern Mountains of the Southeastern United States (ch. 10)
- Determined the effects of spruce beetle outbreaks on Rocky Mountain spruce-fir stand characteristics in northern Colorado and southern Wyoming, including quantifying fuels structure and regeneration across a chronosequence of outbreaks, aging seedlings to understand tree regeneration and recruitment in relation to the disturbances and long-term climate, and quantifying fuels in sites after spruce beetle disturbance (ch. 11)

The FHM program, in cooperation with forest health specialists and researchers inside and outside the Forest Service, continues to investigate a broad range of issues relating to forest health using a wide variety of data and techniques. This report presents some of the latest results from ongoing national-scale detection monitoring and smaller scale environmental monitoring efforts by FHM and its cooperators. For more information about efforts to determine the status, changes, and trends in indicators of the condition of U.S. forests, please visit the FHM website at https://www.fs.usda.gov/foresthealth/protecting-forest/forest-health-monitoring.

LITERATURE CITED

Costanza, R. 1992. Toward an operational definition of ecosystem health. In: Costanza, R.; Norton, B.G.; Haskell, B.D., eds. Ecosystem health: new goals for environmental management. Washington, DC: Island Press: 239–256.

Edmonds, R.L.; Agee, J.K.; Gara, R.I. 2011. Forest health and protection. Long Grove, IL: Waveland Press, Inc. 667 p.

Forest Health Monitoring (FHM). 2022. Program description. Forest Health Monitoring fact sheet series. https://www.fs.usda.gov/foresthealth/protecting-forest/forest-health-monitoring/. [Date accessed: August 10, 2022].

Riitters, K.H.; Tkacz, B. 2004. The U.S. Forest Health Monitoring program. In: Wiersma, G.B., ed. Environmental monitoring. Boca Raton, FL: CRC Press: 669–683. https://doi.org/10.1201/9780203495476.ch30.

CHAPTER 1

Introduction

Kevin M. Potter

Forests and woodlands cover an extensive area of the United States, 333 million ha or approximately 36 percent of the Nation's land area (Oswalt and others 2019). These forests provide a broad range of goods and services for current and future generations, safeguard biological diversity, and contribute to the resilience of ecosystems, societies, and economies (USDA Forest Service 2011). Their socioeconomic benefits include wood products, nontimber goods, recreational opportunities, and natural beauty. Their ecological roles include supplying large and consistent quantities of clean water, preventing soil erosion, and providing habitat for a broad diversity of plant and animal species. At the same time, both the ecological integrity and the continued capacity of these forests to provide ecological and economic goods and services face a long list of threats, including insect and disease infestation, drought, fragmentation and forest conversion to other land uses, catastrophic fire, invasive species, and the effects of climate change.

Natural and anthropogenic stresses vary among biophysical regions and local environments; they also change over time and interact with each other. These and other factors make it challenging to establish baselines of forest health and to detect important departures from normal forest ecosystem functioning (Riitters and Tkacz 2004). Monitoring the health of forests is a critically important task, reflected within the Criteria and Indicators for the Conservation and Sustainable Management of Temperate and Boreal Forests (Montréal Process Working Group 1995), which the U.S. Department of Agriculture, Forest Service uses as a forest sustainability assessment framework (USDA Forest Service 2004, 2011). The primary objective of such monitoring is to identify ecological resources whose condition is deteriorating in subtle ways over large regions in response to cumulative stresses, a goal that requires consistent, large-scale, and long-term monitoring of key indicators of forest health status, change, and trends (Riitters and Tkacz 2004). Given the magnitude of this task, it is best accomplished through the participation of multiple Federal, State, academic, and private partners.

The concept of a healthy forest has universal appeal, but forest ecologists and managers have struggled with how exactly to define forest health (Teale and Castello 2011). There is no universally accepted definition. Most definitions of forest health can be categorized as representing either an ecological or a utilitarian perspective (Kolb and others 1994). From an ecological perspective, the current understanding of ecosystem dynamics suggests that healthy ecosystems are those that maintain their organization and autonomy over time while remaining resilient to stress (Costanza 1992), and that evaluations of forest health should emphasize factors that affect the inherent processes and resilience of forests (Edmonds and others 2011, Kolb and others 1994, Raffa and others 2009). On the other hand, the utilitarian perspective holds that a forest is healthy if management objectives are met, and that a forest is unhealthy if these objectives are not met (Kolb and others 1994). Although this definition may be appropriate when a single, unambiguous management objective exists, such as the production of wood fiber or the maintenance of

How to cite this chapter:

Potter, Kevin M. 2023. Introduction. In: Potter, Kevin M.; Conkling, Barbara L., eds. Forest Health Monitoring: national status, trends, and analysis 2022. Gen. Tech. Rep. SRS-273. Asheville, NC: U.S. Department of Agriculture, Forest Service, Southern Research Station: 5–22. https://doi.org/10.2737/SRS-GTR-273-Chap1.

wilderness attributes, it can be too narrow when multiple management objectives are required (Edmonds and others 2011, Teale and Castello 2011). Teale and Castello (2011) incorporate both ecological and utilitarian perspectives into their two-component definition of forest health: first, a healthy forest must be sustainable with respect to its size structure, including a correspondence between baseline and observed mortality; second, a healthy forest must meet the landowner's objectives, provided that these objectives do not conflict with sustainability.

This Forest Health Monitoring: National Status, Trends, and Analysis report, the 22nd in an annual series sponsored by the Forest Health Monitoring (FHM) program of the Forest Service, attempts to quantify the status of, changes to, and trends in a wide variety of broadly defined indicators of forest health. The indicators described in this report encompass forest insect and disease activity, wildland fire occurrence, tree mortality, crown condition, lichen diversity, and general forest disturbance, among others. The previous reports in this series are Ambrose and Conkling (2007, 2009), Conkling (2011), Conkling and others (2005), Coulston and others (2005a, 2005b, 2005c), and Potter and Conkling (2012a, 2012b, 2013a, 2013b, 2014, 2015a, 2015b, 2016, 2017, 2018, 2019, 2020, 2021, 2022). Visit https://www.fs.usda.gov/foresthealth/publications/fhm/fhm-annual-national-reports.shtml for links to each of these reports in their entirety and for searchable lists of links to chapters included in the reports.

This report has three specific objectives. The first is to present information about forest health from a national perspective, or from a multistate regional perspective when appropriate, using data collected by the Forest Health Protection (FHP) and Forest Inventory and Analysis (FIA) programs of the Forest Service, as well as from other sources available at a wide extent. The chapters that present analyses at a national scale, or multistate regional scale, are divided between sections 1 and 2 of the report. Section 1 presents analyses of forest health data that are available on an annual basis. Such repeated analyses of regularly collected indicator measurements allow for the detection of trends over time and help establish a baseline for future comparisons (Riitters and Tkacz 2004). Section 2 presents longer term forest health trends and describes new techniques for analyzing forest health data at national or regional scales (the second objective of the report, see below). While in-depth interpretation and analysis of specific geographic or ecological regions are beyond the scope of these parts of the report, the chapters in sections 1 and 2 present information that can be used to identify areas that may require investigation at a finer scale.

The second objective of the report is to present new techniques for analyzing forest health data as well as new applications of established techniques, often applied to longer timescales; these are presented in section 2. The examples in this report are in chapter 6, which presents current crown dieback, current crown-damaging agents, and 20-year crown dieback trends for the most common genera and species in the Eastern United States, and chapter 7, which provides an overview of the 23 years of epiphytic lichen data summarized recently in the National Lichen Atlas (Jovan and others 2021).

The third objective of the report is to present results of recently completed Evaluation Monitoring (EM) projects funded through the FHM national program. These project summaries, presented in section 3, determine the extent, severity, and/or cause of forest health problems (FHM 2022), generally at a finer scale than that addressed by the analyses in sections 1 and 2. Each of the four chapters in section 3 contains an overview of an EM project, key results, and contacts for more information.

When appropriate throughout this report, authors use the Forest Service revised ecoregions for the conterminous United States (CONUS) and Alaska (Cleland and others 2007, Spencer and others 2002) as a common ecologically based spatial framework for their forest health assessments (fig. 1.1). Specifically, when the spatial scale of the data and the expectation of an identifiable pattern in the data are appropriate, authors use ecoregion sections, larger scale provinces, or smaller scale subsections as assessment units for their analyses. Bailey's hierarchical system bases the two broadest ecoregion scales, domains and divisions, on large ecological climate zones, while each division is broken into provinces based on vegetation macrofeatures (Bailey 1995). Provinces are further divided into sections, which may be thousands of km^2 in area and are expected to encompass regions similar in their geology, climate, soils, potential natural vegetation, and potential natural communities (Cleland and others 1997). Subsections are nested within sections as the smallest level in the hierarchy. This hierarchical system does not address either Hawaii or Puerto Rico beyond including each in a unique, single ecoregion province (Bailey 1995). A set of Hawaii ecoregions based on moisture and elevational characteristics was developed for use in FHM national reports (Potter 2020, 2023) because a finer scale and ecologically oriented spatial assessment framework was needed to estimate the impacts of a destructive forest disease (ch. 2) and of forest fire occurrences (ch. 3) (fig. 1.2, table 1.1).

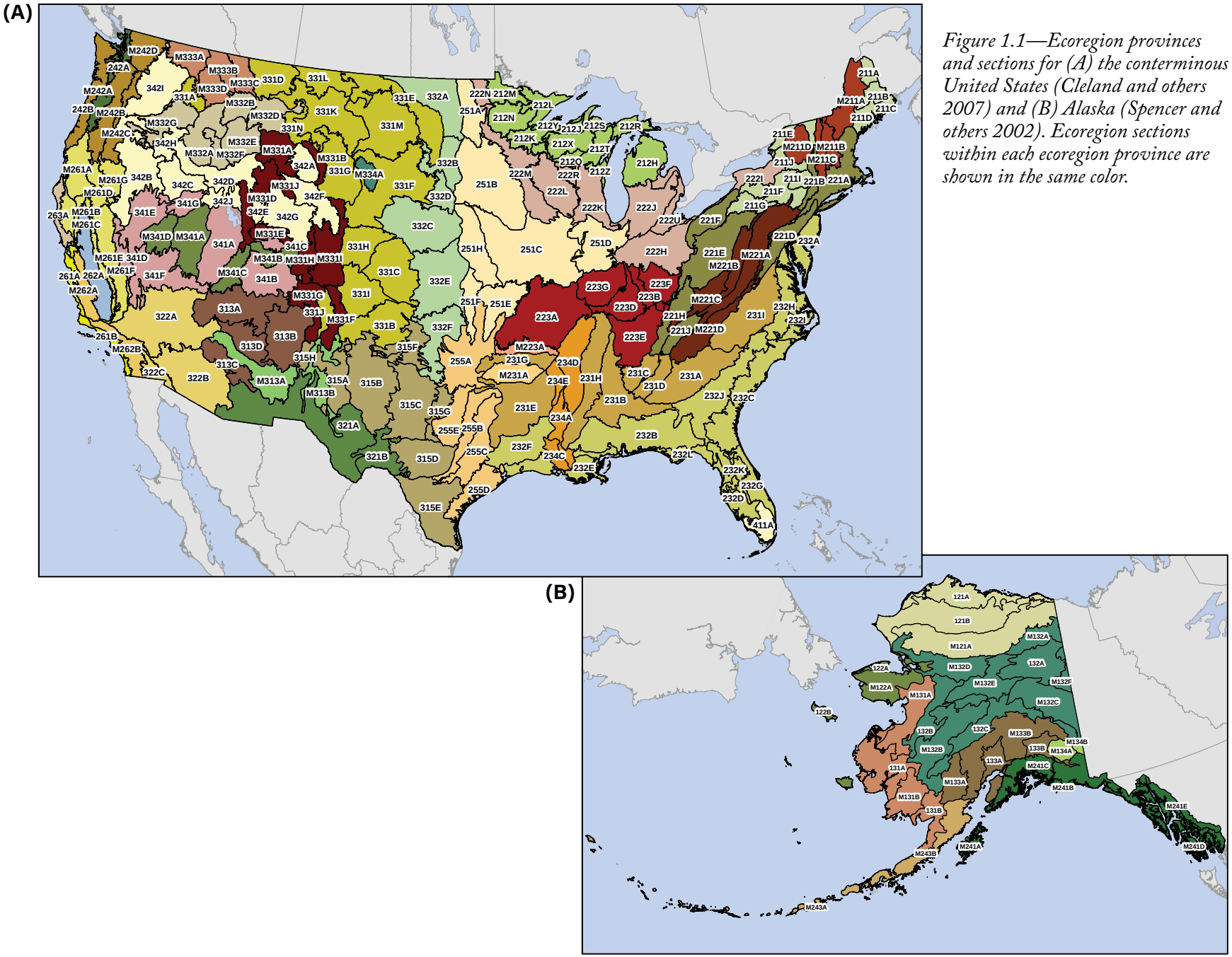

Figure 1.1—Ecoregion provinces and sections for (A) the conterminous United States (Cleland and others 2007) and (B) Alaska (Spencer and others 2002). Ecoregion sections within each ecoregion province are shown in the same color.

Conterminous States ecoregion provinces

- 211: Northeastern Mixed Forest
- M211: Adirondack-New England Mixed Forest—Coniferous Forest—Alpine Meadow
- 212: Laurentian Mixed Forest
- 221: Eastern Broadleaf Forest
- M221: Central Appalachian Broadleaf Forest—Coniferous Forest—Meadow
- 222: Midwest Broadleaf Forest
- 223: Central Interior Broadleaf Forest
- M223: Ozark Broadleaf Forest
- 231: Southeastern Mixed Forest
- M231: Ouachita Mixed Forest—Meadow
- 232: Outer Coastal Plain Mixed Forest
- 234: Lower Mississippi Riverine Forest
- 242: Pacific Lowland Mixed Forest
- 251: Prairie Parkland (Temperate)
- 255: Prairie Parkland (Subtropical)
- M242: Cascade Mixed Forest—Coniferous Forest—Alpine Meadow
- 261: California Coastal Chaparral Forest and Shrub
- M261: Sierran Steppe—Mixed Forest—Coniferous Forest—Alpine Meadow
- 262: California Dry Steppe
- M262: California Coastal Range Open Woodland—Shrub—Coniferous Forest—Meadow
- 263: California Coastal Steppe—Mixed Forest—Redwood Forest
- 313: Colorado Plateau Semi-Desert
- M313: Arizona-New Mexico Mountains Semi-Desert—Open Woodland—Coniferous Forest—Alpine Meadow
- 315: Southwest Plateau and Plains Dry Steppe and Shrub
- 321: Chihuahuan Semi-Desert
- 322: American Semi-Desert and Desert
- 331: Great Plains—Palouse Dry Steppe
- M331: Southern Rocky Mountain Steppe—Open Woodland—Coniferous Forest—Alpine Meadow
- 332: Great Plains Steppe
- M332: Middle Rocky Mountain Steppe—Coniferous Forest—Alpine Meadow
- M333: Northern Rocky Mountain Forest-Steppe—Coniferous Forest—Alpine Meadow
- M334: Black Hills Coniferous Forest
- 341: Intermountain Semi-Desert and Desert
- M341: Nevada-Utah Mountains Semi-Desert—Coniferous Forest—Alpine Meadow
- 342: Intermountain Semi-Desert
- 411: Everglades

Alaska ecoregion provinces

- 121: Arctic Tundra
- M122: Bering Tundra
- M131: Bering Taiga
- M132: Intermontane Boreal
- 133: Alaska Range Transition
- M134: Coastal Mountains Transition
- M241: Coastal Rainforest
- M243: Aleutian Meadows

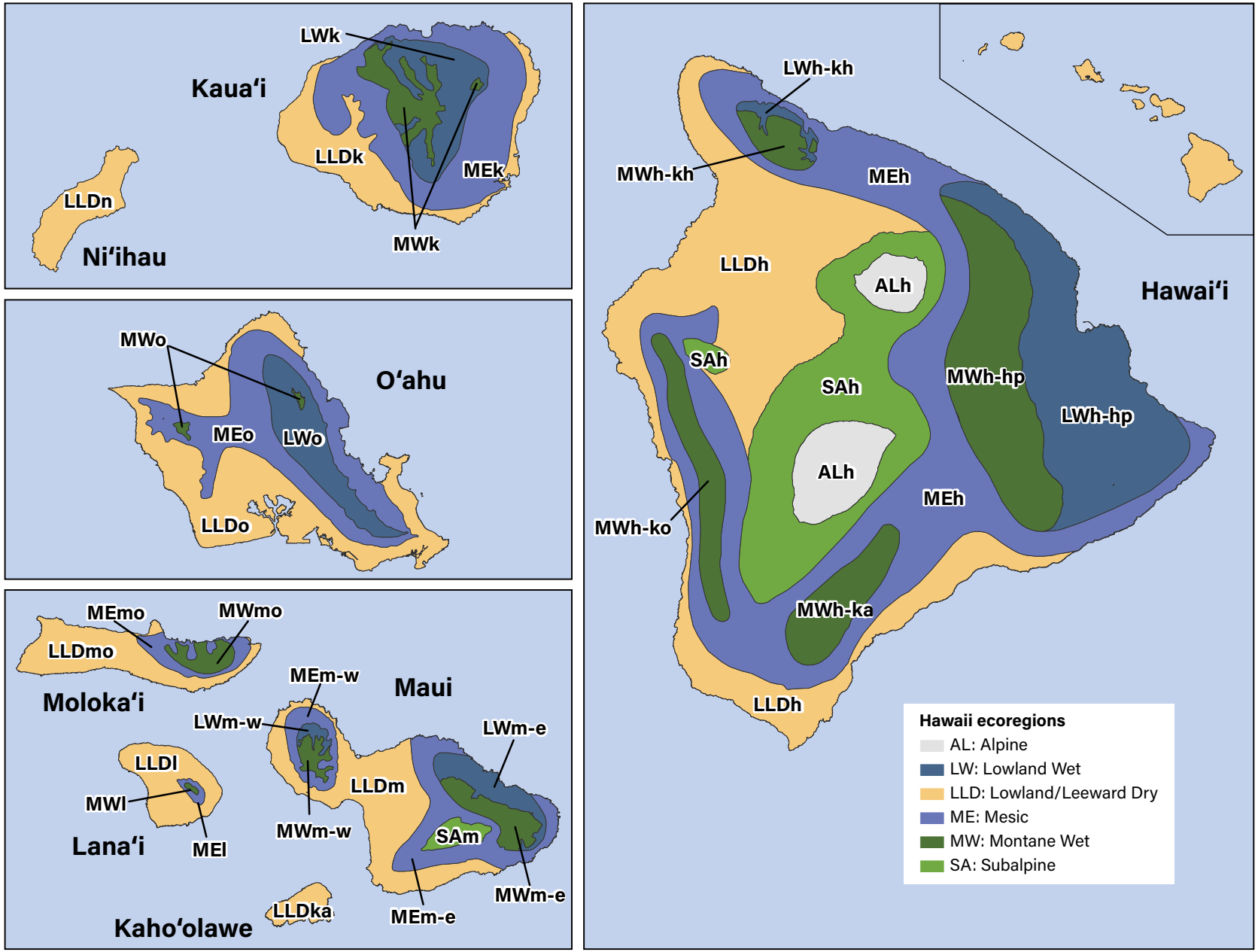

Figure 1.2—Ecoregions, and ecoregion subunits, for Hawaii (Potter 2023), developed based on moisture zones and elevation (see box 1.1). Ecoregion subunits are shown in the same color by ecoregion. See table 1.1 for the names of the ecoregion subunits listed on the map.

Table 1.1—The six ecoregions and 34 ecoregion subunits for the State of Hawaii (Potter 2023)

Ecoregion	Subunit
AL: Alpine	Alh: Alpine-Hawai‘i
LW: Lowland Wet	LWh-hp: Lowland Wet-Hawai‘i-Hilo-Puna
	LWh-kh: Lowland Wet-Hawai‘i-Kohala-Hāmākua
	LWk: Lowland Wet-Kaua‘i
	LWm-e: Lowland Wet-Maui-East
	LWm-w: Lowland Wet-Maui-West
	LWo: Lowland Wet-O‘ahu
LLD: Lowland/ Leeward Dry	LLDh: Lowland/Leeward Dry-Hawai‘i
	LLDka: Lowland/Leeward Dry-Kaho‘olawe
	LLDk: Lowland/Leeward Dry-Kaua‘i
	LLDl: Lowland/Leeward Dry-Lāna‘i
	LLDm: Lowland/Leeward Dry-Maui
	LLDmo: Lowland/Leeward Dry-Moloka‘i
	LLDn: Lowland/Leeward Dry-Ni‘ihau
	LLDo: Lowland/Leeward Dry-O‘ahu
ME: Mesic	MEh: Mesic-Hawai‘i
	MEk: Mesic-Kaua‘i
	MEl: Mesic-Lāna‘i
	MEm-e: Mesic-Maui-East
	MEm-w: Mesic-Maui-West
	MEmo: Mesic-Moloka‘i
	MEo: Mesic-O‘ahu
MW: Montane Wet	MWh-hp: Montane Wet-Hawai‘i-Hilo-Puna
	MWh-ka: Montane Wet-Hawai‘i-Ka‘ū
	MWh-kh: Montane Wet-Hawai‘i-Kohala-Hāmākua
	MWh-ko: Montane Wet-Hawai‘i-Kona
	MWk: Montane Wet-Kaua‘i
	MWl: Montane Wet-Lāna‘i
	MWm-e: Montane Wet-Maui-East
	MWm-w: Montane Wet-Maui-West
	MWmo: Montane Wet-Moloka‘i
	MWo: Montane Wet-O‘ahu
SA: Subalpine	SAh: Subalpine-Hawai‘i
	SAm: Subalpine-Maui

Source: Potter (2023)

THE FOREST HEALTH MONITORING PROGRAM

The national FHM program is designed to determine the status, changes, and trends in indicators of forest condition on an annual basis and covers all forested lands through a partnership encompassing the Forest Service, State foresters, and other State and Federal agencies and academic groups (FHM 2022). The FHM program utilizes data from a wide variety of data sources, both inside and outside the Forest Service, and develops analytical approaches for addressing forest health issues that affect the sustainability of forest ecosystems. The FHM program has four major components (fig. 1.3):

- **Detection Monitoring**—nationally standardized aerial and ground surveys to evaluate status and change in condition of forest ecosystems (sections 1 and 2 of this report)
- **Evaluation Monitoring**—projects to determine the extent, severity, and causes of undesirable changes in forest health identified through Detection Monitoring (section 3 of this report)
- **Research on Monitoring Techniques**—work to develop or improve indicators, monitoring systems, and analytical techniques, such as urban and riparian forest health monitoring, early detection of invasive species, multivariate analyses of forest health indicators, and spatial scan statistics (section 2 of this report)

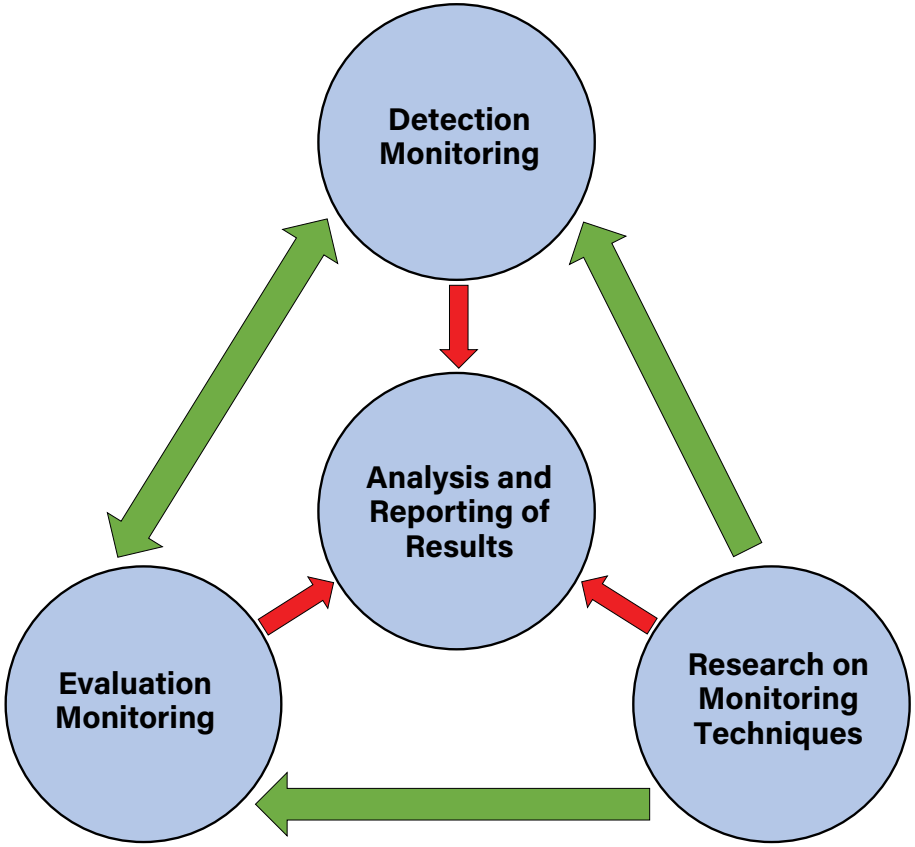

Figure 1.3—The design of the Forest Health Monitoring program (FHM 2003).

- **Analysis and Reporting of Results**—synthesis of information from various data sources within and external to the Forest Service to produce issue-driven reports on status and change in forest health at national, regional, and State levels (sections 1, 2, and 3 of this report)

The FHM program, in addition to national reporting, generates regional and State reports, often in cooperation with FHM partners, both

within the Forest Service and in State forestry and agricultural departments. For example, the FHM megaregions cooperate with their respective State partners to produce the annual Forest Health Highlights report series, available on the FHM website at https://www.fs.usda.gov/foresthealth/protecting-forest/forest-health-monitoring/monitoring-forest-highlights.shtml. Other examples include Steinman (2004) and Harris and others (2011).

The FHM program is divided into four "megaregions." These correspond with the two Forest Service regions in the Eastern United States (Eastern and Southern) while joining four Forest Service regions into the Interior West megaregion (Northern, Rocky Mountain, Southwestern, and Intermountain), and three Forest Service regions into the West Coast megaregion (Pacific Southwest, Pacific Northwest, and Alaska) (fig. 1.4). Some analyses in this FHM national report provide results by FHM megaregion, though they separate Alaska and Hawaii from the rest of the West Coast megaregion.

The FHM program and its partners also produce peer-reviewed reports and journal articles on monitoring techniques and analytical methods (see https://www.fs.usda.gov/foresthealth/publications/fhm/fhm-publications.shtml). The emphases of these publications include forest health data (Potter and others 2016, Siry and others 2018, Smith and Conkling 2004); soils as an indicator of forest health (O'Neill and others 2005); urban forest health monitoring (Bigsby and others 2014; Cumming and others 2006, 2007; Lake and others 2006); remote sensing of forest disturbances (Chastain and others 2015, Rebbeck and others 2015); health conditions in national forests (Morin and others 2006); crown conditions (Morin and others 2015; Randolph 2010a, 2010b, 2013; Randolph and Moser 2009; Schomaker and others 2007); indicators of regeneration (McWilliams and others 2015); vegetation diversity and structure (Schulz and Gray 2013, Schulz and others 2009, Simkin and others 2016); forest lichen communities (Jovan and others 2012, Root and others 2014); down woody materials in forests (Woodall and others 2012, 2013); drought (Vose and others 2016); ozone monitoring (Rose and Coulston 2009); patterns of nonnative invasive plant occurrence (Guo and others 2015, 2017; Iannone and others 2015, 2016a, 2016b, 2018; Jo and others 2018; Oswalt and others 2015; Potter and others 2022, 2023; Riitters and others 2018a, 2018b); assessments of forest risk or tree species vulnerability to exotic invasive forest insects and diseases (Koch and others 2011, 2014; Krist and others 2014; Potter and others 2019a, 2019b; Vogt and Koch 2016; Yemshanov and others 2014); spatial patterns of land cover and forest fragmentation (Guo and others 2018; Riitters 2011; Riitters and Costanza 2019; Riitters and Wickham 2012; Riitters and others 2012, 2016, 2017); impacts of deer browse on forest structure (Russell and others 2017); broad-scale assessments of forest biodiversity (Guo and others 2019; Potter 2018; Potter and Koch 2014; Potter and Woodall 2012, 2014); predictions and indicators of climate change effects on forests and forest tree species (Anderson and others 2021, Fei and others 2017, Heath and others 2015, Potter and Hargrove 2013); legal, institutional, and economic indicators of forest conservation and sustainable management (McGinley and Cubbage 2020); and the overall forest health indicator program (Woodall and others 2010).

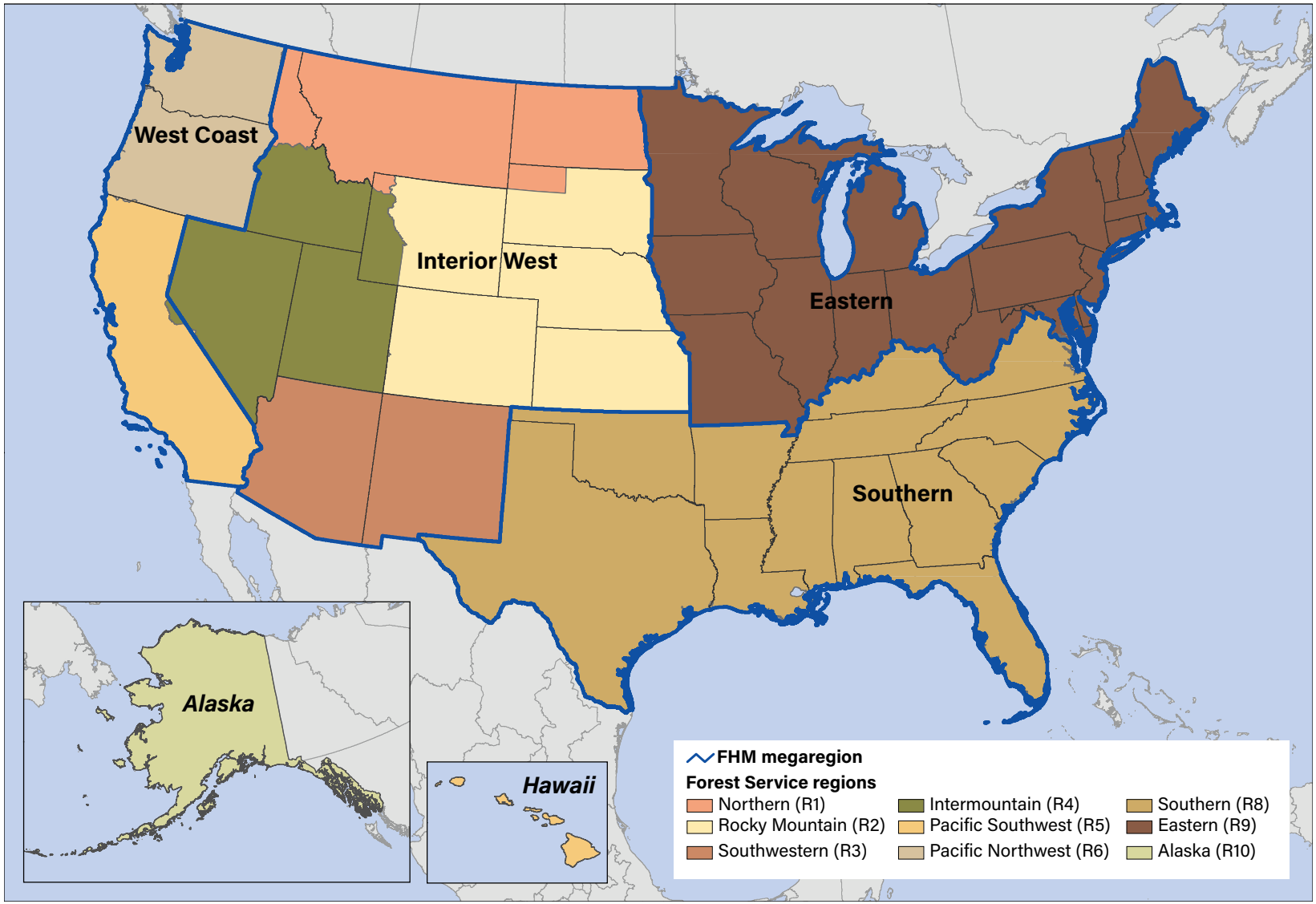

Figure 1.4—The four megaregions of the Forest Health Monitoring program and their relationship to Forest Service regions. Note that Alaska and Hawaii are parts of the West Coast megaregion, but data from these States are analyzed separately in most cases in this report.

DATA SOURCES

Forest Service data sources in this edition of the FHM national report include FIA annualized Phase 2 survey data (Bechtold and Patterson 2005, Burrill and others 2018, Woodall and others 2010); FHP national Insect and Disease Survey forest mortality and defoliation data for 2021 (FHP 2022); Moderate Resolution Imaging Spectroradiometer (MODIS) Active Fire Detections for the United States data for 2021 (NASA Fire Information for Resource Management System 2022); tree canopy cover data generated from the 2011 National Land Cover Database (NLCD) (Homer and others 2015) through a cooperative project between the Multi-Resolution Land Characteristics Consortium and Forest Service Geospatial Technology and Applications Center (GTAC) (Coulston and others 2012); and FIA's publicly available Environmental Monitoring and Assessment Program (EMAP) hexagons (Brand and others 2000). Other sources of data include MODIS 8-day composite Normalized Difference Vegetation Index (NDVI) data for the CONUS at 250 m during parts of the 2020 and 2021 growing seasons, information from the National FIA Lichen Database (Jovan and others 2020), and Alaskan forest and shrub cover derived from the 2011 NLCD. For more information about the FIA program, which is a major source of data for several FHM analyses, see box 1.1.

FOREST HEALTH MONITORING REPORT PRODUCTION

The FHM national report is produced annually by forest health monitoring researchers at the Eastern Forest Environmental Threat Assessment Center (EFETAC) in collaboration with North Carolina State University cooperators in the Forest Health Monitoring Research Group (https://go.ncsu.edu/foresthealth). A unit of the Southern Research Station of the Forest Service, EFETAC was established under the Healthy Forests Restoration Act of 2003 to generate the knowledge and tools needed to anticipate and respond to environmental threats. For more information about the research team and about threats to U.S. forests, please visit https://forestthreats.org/about.

BOX 1.1

The Forest Inventory and Analysis (FIA) program collects forest inventory information across all forest land ownerships in the United States and maintains a network of more than 130,000 permanent forested ground plots across the conterminous United States, southeastern Alaska, Hawaii, Caribbean territories, and U.S.-Affiliated Pacific Islands with a sampling intensity of approximately one plot/2428 ha (one plot per 6,000 acres). Forest Inventory and Analysis Phase 2 encompasses the annualized inventory measured on plots at regular intervals, with each plot surveyed every 5 to 7 years in most Eastern States but with plots in the Rocky Mountain and Pacific Northwest regions surveyed once every 10 years (Reams and others 2005). The standard 0.067-ha plot (see figure) consists of four 7.315-m (24-foot) radius subplots (approximately 168.6 m^2 or 1/24th acre), on which field crews measure trees at least 12.7 cm (5 inches) in diameter. Within each of these subplots is nested a 2.073-m (6.8-foot) radius microplot (approximately 13.48 m^2 or 1/300th acre), on which crews measure trees smaller than 12.7 cm (5 inches) in diameter. A core-optional variant of the standard design includes four "macroplots," each with a radius of 17.953 m or 58.9 feet (approximately 0.1012 ha or 1/4 acre) that originates at the center of each subplot (Burrill and others 2018).

Forest Inventory and Analysis Phase 3 plots previously represented a subset of these Phase 2 plots, with one Phase 3 plot for every 16 standard FIA Phase 2 plots. In addition to traditional forest inventory measurements, data for a variety of important ecological indicators were from Phase 3 plots, including tree crown condition, lichen communities, down woody material, soil condition, and vegetation structure and diversity, whereas data on ozone bioindicator plants were collected on a separate grid of plots (Woodall and others 2010, 2011). Most of these additional forest health indicators were measured as part of the Forest Health Monitoring Detection Monitoring ground plot system prior to 2000[1] (Palmer and others 1991). The FIA program recently updated its sampling techniques with flexible spatial and temporal intensities for some of these ecosystem health indicators (including down woody material, vegetation diversity and structure, and crown conditions) to improve field operation efficiency, address emerging user demands, and adjust to evolving forest health science (Castillo and Alvarez 2020). This "Phase 2 Plus Program/ Ecosystem Indicator Program" (P2+) sampling scheme facilitates the collection of a national core set of indicator information on more plots for less cost than the original indicator protocols, with sampling based on a systematic subsample that can change in response to budgetary fluctuations without compromising long-term analytical capabilities. The enhanced indicator protocols collect less-detailed information on each sampled plot than on the previous Phase 3 plots, but substantially more plots are sampled, increasing the statistical power of forest health analyses and improving the reliability of estimates in important national assessments (Castillo and Alvarez 2020).

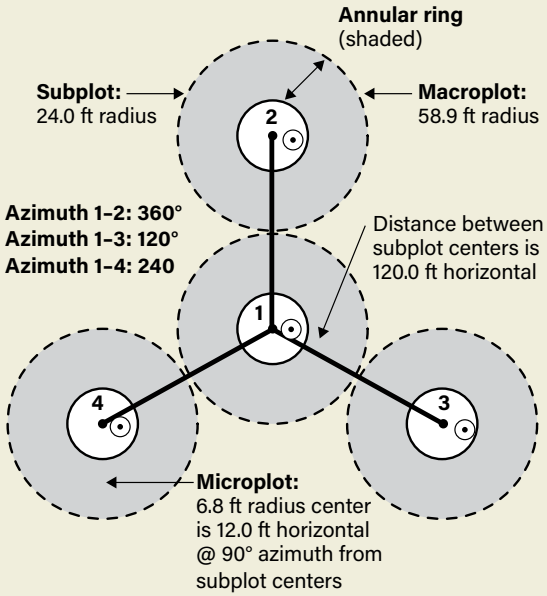

Box 1.1 figure—The Forest Inventory and Analysis mapped plot design. Subplot 1 is the center of the cluster with subplots 2, 3, and 4 located 120 feet away at azimuths of 360°, 120°, and 240°, respectively (Burrill and others 2018).

[1] *U.S. Department of Agriculture, Forest Service. 1998. Forest Health Monitoring 1998 field methods guide. Research Triangle Park, NC: U.S. Department of Agriculture, Forest Service, Forest Health Monitoring program. 473 p. On file with: Forest Health Monitoring program, 3041 Cornwallis Rd., Research Triangle Park, NC 27709.*

LITERATURE CITED

Ambrose, M.J.; Conkling, B.L., eds. 2007. Forest Health Monitoring 2005 national technical report. Gen. Tech. Rep. SRS-104. Asheville, NC: U.S. Department of Agriculture, Forest Service, Southern Research Station. 76 p. https://doi.org/10.2737/SRS-GTR-104.

Ambrose, M.J.; Conkling, B.L., eds. 2009. Forest Health Monitoring 2006 national technical report. Gen. Tech. Rep. SRS-117. Asheville, NC: U.S. Department of Agriculture, Forest Service, Southern Research Station. 118 p. https://doi.org/10.2737/SRS-GTR-117.

Anderson, S.M.; Heath, L.S.; Emery, M.R. [and others]. 2021. Developing a set of indicators to identify, monitor, and track impacts and change in the forests of the United States. Climatic Change.165: 13. https://doi.org/10.1007/s10584-021-02993-6.

Bailey, R.G. 1995. Descriptions of the ecoregions of the United States. 2d ed. Misc. Publ. No. 1391. Washington, DC: U.S. Department of Agriculture, Forest Service. Map; presentation scale 1:7,500,000. 108 p.

Bechtold, W.A.; Patterson, P.L., eds. 2005. The enhanced Forest Inventory and Analysis program—national sampling design and estimation procedures. Gen. Tech. Rep. SRS-80. Asheville, NC: U.S. Department of Agriculture, Forest Service, Southern Research Station. 85 p. https://doi.org/10.2737/SRS-GTR-80.

Bigsby, K.M.; Ambrose, M.J.; Tobin, P.C.; Sills, E.O. 2014. The cost of gypsy moth sex in the city. Urban Forestry & Urban Greening. 13(3): 459–468. https://doi.org/10.1016/j.ufug.2014.05.003.

Brand, G.J.; Nelson, M.D.; Wendt, D.G.; Nimerfro, K.K. 2000. The hexagon/panel system for selecting FIA plots under an annual inventory. In: McRoberts, R.E.; Reams, G.A.; Van Deusen, P.C., eds. Proceedings of the first annual Forest Inventory and Analysis symposium. Gen. Tech. Rep. NC-213. St. Paul, MN: U.S. Department of Agriculture, Forest Service, North Central Research Station: 8–13.

Burrill, E.A.; Wilson, A.M.; Turner, J.A. [and others]. 2018. The Forest Inventory and Analysis Database: database description and user guide for Phase 2 (version 8.0). Washington, DC: U.S. Department of Agriculture, Forest Service. 946 p. http://www.fia.fs.usda.gov/library/database-documentation/. [Date accessed: August 8, 2022].

Castillo, P.S.B.; Alvarez, M. 2020. Forest Inventory and Analysis: fiscal year 2018 business report. FS-1153. Washington, DC: U.S. Department of Agriculture, Forest Service. 71 p. https://www.fia.fs.usda.gov/library/bus-org-documents/docs/17973%20FS%20FIA%20Fiscal%20Year%202018%20Business%20Reportv3%20508.pdf. [Date accessed: August 10, 2022].

Chastain, R.A.; Fisk, H.; Ellenwood, J.R. [and others]. 2015. Near-real time delivery of MODIS-based information on forest disturbances. In: Lippitt, C.D.; Stow, D.A.; Coulter, L.L., eds. Time-sensitive remote sensing. New York: Springer: 147–164. https://doi.org/10.1007/978-1-4939-2602-2_10.

Cleland, D.T.; Avers, P.E.; McNab, W.H. [and others]. 1997. National hierarchical framework of ecological units. In: Boyce, M.S.; Haney, A., eds. Ecosystem management applications for sustainable forest and wildlife resources. New Haven, CT: Yale University Press: 181–200.

Cleland, D.T.; Freeouf, J.A.; Keys, J.E. [and others]. 2007. Ecological subregions: sections and subsections for the conterminous United States. Gen. Tech. Rep. WO-76D. Washington, DC: U.S. Department of Agriculture, Forest Service. Map; Sloan, A.M., cartographer; presentation scale 1:3,500,000; colored. https://doi.org/10.2737/WO-GTR-76D.

Conkling, B.L., ed. 2011. Forest Health Monitoring 2007 national technical report. Gen. Tech. Rep. SRS-147. Asheville, NC: U.S. Department of Agriculture, Forest Service, Southern Research Station. 159 p. https://doi.org/10.2737/SRS-GTR-147.

Conkling, B.L.; Coulston, J.W.; Ambrose, M.J., eds. 2005. Forest Health Monitoring 2001 national technical report. Gen. Tech. Rep. SRS-81. Asheville, NC: U.S. Department of Agriculture, Forest Service, Southern Research Station. 204 p. https://doi.org/10.2737/SRS-GTR-81.

Costanza, R. 1992. Toward an operational definition of ecosystem health. In: Costanza, R.; Norton, B.G.; Haskell, B.D., eds. Ecosystem health: new goals for environmental management. Washington, DC: Island Press: 239–256.

Coulston, J.W.; Riitters, K.H.; Conkling, B.L., eds. 2005a. Forest Health Monitoring 2002 national technical report. Gen. Tech. Rep. SRS-84. Asheville, NC: U.S. Department of Agriculture, Forest Service, Southern Research Station. 97 p. https://doi.org/10.2737/SRS-GTR-84.

Coulston, J.W.; Ambrose, M.J.; Riitters, K.H. [and others], eds. 2005b. Forest Health Monitoring 2003 national technical report. Gen. Tech. Rep. SRS-85. Asheville, NC: U.S. Department of Agriculture, Forest Service, Southern Research Station. 97 p. https://doi.org/10.2737/SRS-GTR-85.

Coulston, J.W.; Ambrose, M.J.; Riitters, K.H.; Conkling, B.L., eds. 2005c. Forest Health Monitoring 2004 national technical report. Gen. Tech. Rep. SRS-90. Asheville, NC: U.S. Department of Agriculture, Forest Service, Southern Research Station. 81 p. https://doi.org/10.2737/SRS-GTR-90.

Coulston, J.W.; Moisen, G.G.; Wilson, B.T. [and others]. 2012. Modeling percent tree canopy cover: a pilot study. Photogrammetric Engineering and Remote Sensing. 78(7): 715–727. https://doi.org/10.14358/PERS.78.7.715.

Cumming, A.B.; Nowak, D.J.; Twardus, D.B. [and others]. 2007. Urban forests of Wisconsin: pilot monitoring project 2002. NA-FR-05-07. Newtown Square, PA: U.S. Department of Agriculture, Forest Service, Northeastern Area State and Private Forestry. 33 p.

Cumming, A.B.; Twardus, D.B.; Smith, W.D. 2006. National Forest Health Monitoring program, Maryland and Massachusetts street tree monitoring pilot projects. NA-FR-01-06. Newtown Square, PA: U.S. Department of Agriculture, Forest Service, Northeastern Area State and Private Forestry. 23 p.

Edmonds, R.L.; Agee, J.K.; Gara, R.I. 2011. Forest health and protection. Long Grove, IL: Waveland Press, Inc. 667 p.

Fei, S.; Desprez, J.M.; Potter, K.M. [and others]. 2017. Divergence of species responses to climate change. Science Advances. 3(5): e1603055. https://doi.org/10.1126/sciadv.1603055.

Forest Health Monitoring (FHM). 2003. Forest Health Monitoring: a national strategic plan. 7 p.

Forest Health Monitoring (FHM). 2022. Program description. Forest Health Monitoring fact sheet series. https://www.fs.usda.gov/foresthealth/protecting-forest/forest-health-monitoring/. [Date accessed: August 10, 2022].

Forest Health Protection (FHP). 2022. Insect and Disease Detection Survey (IDS) data downloads. Fort Collins, CO: U.S. Department of Agriculture, Forest Service, Forest Health Technology Enterprise Team. https://www.fs.usda.gov/foresthealth/applied-sciences/mapping-reporting/detection-surveys.shtml. [Date accessed: June 13, 2022].

Guo, Q.; Fei, S.; Dukes, J.S. [and others]. 2015. A unified approach to quantify invasibility and degree of invasion. Ecology. 95(10): 2613–2621. https://doi.org/10.1890/14-2172.1.

Guo, Q.; Fei, S.; Potter, K.M. [and others]. 2019. Tree diversity regulates forest pest invasion. Proceedings of the National Academy of Sciences. 116(15): 7382–7386. https://doi.org/10.1073/pnas.1821039116.

Guo, Q.; Iannone, B.V.; Nunez-Mir, G.C. [and others]. 2017. Species pool, human population, and global vs. regional invasion patterns. Landscape Ecology. 32(2): 229–238. https://doi.org/10.1007/s10980-016-0475-6.

Guo, Q.; Riitters, K.H.; Potter, K.M. [and others]. 2018. A subcontinental analysis of forest fragmentation and pest invasion. Forests. 9(12): 744. https://doi.org/10.3390/f9120744.

Harris, J.L., comp.; Region 2 Forest Health Protection staff. 2011. Forest health conditions, 2009–2010: Rocky Mountain Region (R2). R2-11-RO-31. Golden, CO: U.S. Department of Agriculture, Forest Service, Renewable Resources, Forest Health Protection, Rocky Mountain Region. 108 p.

Heath, L.S.; Anderson, S.; Emery, M.R. [and others]. 2015. Indicators for climate change impacts for forests: National Climate Assessment indicators. Gen. Tech. Rep. NRS-155. Newtown Square, PA: U.S. Department of Agriculture, Forest Service, Northern Research Station. 143 p.

Homer, C.G.; Dewitz, J.A.; Yang, L. [and others]. 2015. Completion of the 2011 National Land Cover Database for the conterminous United States: representing a decade of land cover change information. Photogrammetric Engineering and Remote Sensing. 81(5): 345–354.

Iannone, B.V.; Oswalt, C.M.; Liebhold, A.M. [and others]. 2015. Region-specific patterns and drivers of macroscale forest plant invasions. Diversity and Distributions. 21: 1181–1192. https://doi.org/10.1111/ddi.12354.

Iannone, B.V.; Potter, K.M.; Guo, Q. [and others]. 2016a. Biological invasion hotspots: a trait-based perspective reveals new sub-continental patterns. Ecography. 39: 961–969. https://doi.org/10.1111/ecog.01973.

Iannone, B.V.; Potter, K.M.; Guo, Q. [and others]. 2018. Environmental harshness drives spatial heterogeneity in biotic resistance. NeoBiota. 40: 87–105. https://doi.org/10.3897/neobiota.40.28558.

Iannone, B.V.; Potter, K.M.; Hamil, K.-A.D. [and others]. 2016b. Evidence of biotic resistance to invasions in forests of the Eastern USA. Landscape Ecology. 31: 85–99. https://doi.org/10.1007/s10980-015-0280-7.

Jo, I.; Potter, K.M.; Domke, G.; Fei, S. 2018. Dominant forest tree mycorrhizal type mediates understory plant invasions. Ecology Letters. 21: 217–224. https://doi.org/10.1111/ele.12884.

Jovan, S.; Haldeman, M.; Will-Wolf, S. [and others]. 2021. National atlas of epiphytic lichens in forested habitats of the United States. Gen. Tech. Rep. PNW-986. Portland, OR: U.S. Department of Agriculture, Forest Service, Pacific Northwest Research Station. 96 p.

Jovan, S.; Riddell, J.; Padgett, P.E.; Nash, T.H., III. 2012. Eutrophic lichens respond to multiple forms of N: implications for critical levels and critical loads research. Ecological Applications. 22(7): 1910–1922. https://doi.org/10.1890/11-2075.1.

Jovan, S.; Will-Wolf, S.; Geiser, L. [and others]. 2020. User guide for the national Forest Inventory and Analysis lichen database (version 1.0). Gen. Tech. Rep. PNW-988. Portland, OR: U.S. Department of Agriculture, Forest Service, Pacific Northwest Research Station. 83 p.

Koch, F.H.; Yemshanov, D.; Colunga-Garcia, M. [and others]. 2011. Potential establishment of alien-invasive forest insect species in the United States: where and how many? Biological Invasions. 13: 969–985. https://doi.org/10.1007/s10530-010-9883-8.

Koch, F.H.; Yemshanov, D.; Haack, R.A.; Magarey, R.D. 2014. Using a network model to assess risk of forest pest spread via recreational travel. PLOS ONE. 9(7): e102105. https://doi.org/10.1371/journal.pone.0102105.

Kolb, T.E.; Wagner, M.R.; Covington, W.W. 1994. Concepts of forest health: utilitarian and ecosystem perspectives. Journal of Forestry. 92: 10–15.

Krist, F.J., Jr.; Ellenwood, J.R.; Woods, M.E. [and others]. 2014. 2012–2027 national insect and disease forest risk assessment. FHTET-14-01. U.S. Department of Agriculture, Forest Service, Forest Health Technology Enterprise Team. 199 p. http://www.fs.usda.gov/foresthealth/technology/pdfs/2012_RiskMap_Report_web.pdf. [Date accessed: August 9, 2022].

Lake, M.; Marshall, P.; Mielke, M. [and others]. 2006. National Forest Health Monitoring program monitoring urban forests in Indiana: pilot study 2002, part 1. Analysis of field methods and data collection. NA-FR-06-06. Newtown Square, PA: U.S. Department of Agriculture, Forest Service, Northeastern Area State and Private Forestry. 22 p.

McGinley, K.A.; Cubbage, F.W., tech. eds. 2020. Legal, institutional, and economic indicators of forest conservation and sustainable management in the United States: analyzing criterion 7 of the Montréal Process criteria and indicators framework. Gen. Tech. Rep. IITF-52. Río Piedras, PR: U.S. Department of Agriculture, Forest Service, International Institute of Tropical Forestry. 174 p.

McWilliams, W.H.; Westfall, J.A.; Brose, P.H. [and others]. 2015. A regeneration indicator for Forest Inventory and Analysis: history, sampling, estimation, analytics, and potential use in the Midwest and Northeast United States. Gen. Tech. Rep. NRS-148. Newtown Square, PA: U.S. Department of Agriculture, Forest Service, Northern Research Station. 74 p. https://doi.org/10.2737/NRS-GTR-148.

Montréal Process Working Group. 1995. Criteria and indicators for the conservation and sustainable management of temperate and boreal forests. https://montreal-process.org. [Date accessed: July 26, 2023].

Morin, R.S.; Liebhold, A.M.; Gottschalk, K.W. [and others]. 2006. Analysis of Forest Health Monitoring surveys on the Allegheny National Forest (1998–2001). Gen. Tech. Rep. NE-339. Newtown Square, PA: U.S. Department of Agriculture, Forest Service, Northeastern Research Station. 102 p. https://doi.org/10.2737/NE-GTR-339.

Morin, R.S.; Randolph, K.C.; Steinman, J. 2015. Mortality rates associated with crown health for eastern forest tree species. Environmental Monitoring and Assessment. 187(3): 87. https://doi.org/10.1007/s10661-015-4332-x.

NASA Fire Information for Resource Management System. 2022. MODIS fire archive download tool. https://firms.modaps.eosdis.nasa.gov/download/. [Date accessed: April 26, 2022].

O'Neill, K.P.; Amacher, M.C.; Perry, C.H. 2005. Soils as an indicator of forest health: a guide to the collection, analysis, and interpretation of soil indicator data in the Forest Inventory and Analysis program. Gen. Tech. Rep. NC-258. St. Paul, MN: U.S. Department of Agriculture, Forest Service, North Central Research Station. 53 p. https://doi.org/10.2737/NC-GTR-258.

Oswalt, C.M.; Fei, S.; Guo, Q. [and others]. 2015. A subcontinental view of forest plant invasions. NeoBiota. 24: 49–54. https://doi.org/10.3897/neobiota.24.4526.

Oswalt, S.N.; Smith, W.B.; Miles, P.D.; Pugh, S.A., coords. 2019. Forest resources of the United States, 2017: a technical document supporting the Forest Service 2020 RPA Assessment. Gen. Tech. Rep. WO-97. Washington, DC: U.S. Department of Agriculture, Forest Service, Washington Office. 223 p. https://doi.org/10.2737/WO-GTR-97.

Palmer, C.J.; Riitters, K.H.; Strickland, T. [and others]. 1991. Monitoring and research strategy for forests—Environmental Monitoring and Assessment Program (EMAP). EPA/600/4-91/012. Washington, DC: U.S. Environmental Protection Agency. 189 p.

Potter, K.M. 2018. Do United States protected areas effectively conserve forest tree rarity and evolutionary distinctiveness? Biological Conservation. 224: 34–46. https://doi.org/10.1016/j.biocon.2018.05.007.

Potter, K.M. 2020. Introduction. In: Potter, K.M.; Conkling, B.L., eds. Forest Health Monitoring: national status, trends, and analysis 2019. Gen. Tech. Rep. SRS-250. Asheville, NC: U.S. Department of Agriculture, Forest Service, Southern Research Station: 5–24.

Potter, K.M. 2023. Ecological regions of Hawai'i. Fort Collins, CO: Forest Service Research Data Archive. https://doi.org/10.2737/RDS-2023-0018. [Date accessed: July 31, 2023].

Potter, K.M.; Conkling, B.L., eds. 2012a. Forest Health Monitoring 2008 national technical report. Gen. Tech. Rep. SRS-158. Asheville, NC: U.S. Department of Agriculture, Forest Service, Southern Research Station. 179 p. https://doi.org/10.2737/SRS-GTR-158.

Potter, K.M.; Conkling, B.L., eds. 2012b. Forest Health Monitoring 2009 national technical report. Gen. Tech. Rep. SRS-167. Asheville, NC: U.S. Department of Agriculture, Forest Service, Southern Research Station. 252 p. https://doi.org/10.2737/SRS-GTR-167.

Potter, K.M.; Conkling, B.L., eds. 2013a. Forest Health Monitoring: national status, trends, and analysis 2010. Gen. Tech. Rep. SRS-176. Asheville, NC: U.S. Department of Agriculture, Forest Service, Southern Research Station. 162 p. https://doi.org/10.2737/SRS-GTR-176.

Potter, K.M.; Conkling, B.L., eds. 2013b. Forest Health Monitoring: national status, trends, and analysis 2011. Gen. Tech. Rep. SRS-185. Asheville, NC: U.S. Department of Agriculture, Forest Service, Southern Research Station. 149 p. https://doi.org/10.2737/SRS-GTR-185.

Potter, K.M.; Conkling, B.L., eds. 2014. Forest Health Monitoring: national status, trends, and analysis 2012. Gen. Tech. Rep. SRS-198. Asheville, NC: U.S. Department of Agriculture, Forest Service, Southern Research Station. 192 p. https://doi.org/10.2737/SRS-GTR-198.

Potter, K.M.; Conkling, B.L., eds. 2015a. Forest Health Monitoring: national status, trends, and analysis 2013. Gen. Tech. Rep. SRS-207. Asheville, NC: U.S. Department of Agriculture, Forest Service, Southern Research Station. 199 p. https://doi.org/10.2737/SRS-GTR-207.

Potter, K.M.; Conkling, B.L., eds. 2015b. Forest Health Monitoring: national status, trends, and analysis 2014. Gen. Tech. Rep. SRS-209. Asheville, NC: U.S. Department of Agriculture, Forest Service, Southern Research Station. 190 p. https://doi.org/10.2737/SRS-GTR-209.

Potter, K.M.; Conkling, B.L., eds. 2016. Forest Health Monitoring: national status, trends, and analysis 2015. Gen. Tech. Rep. SRS-213. Asheville, NC: U.S. Department of Agriculture, Forest Service, Southern Research Station. 199 p. https://doi.org/10.2737/SRS-GTR-213.

Potter, K.M.; Conkling, B.L., eds. 2017. Forest Health Monitoring: national status, trends, and analysis 2016. Gen. Tech. Rep. SRS-222. Asheville, NC: U.S. Department of Agriculture, Forest Service, Southern Research Station. 195 p. https://doi.org/10.2737/SRS-GTR-222.

Potter, K.M.; Conkling, B.L., eds. 2018. Forest Health Monitoring: national status, trends, and analysis 2017. Gen. Tech. Rep. SRS-233. Asheville, NC: U.S. Department of Agriculture, Forest Service, Southern Research Station. 190 p. https://doi.org/10.2737/SRS-GTR-233.

Potter, K.M.; Conkling, B.L., eds. 2019. Forest Health Monitoring: national status, trends, and analysis 2018. Gen. Tech. Rep. SRS-239. Asheville, NC: U.S. Department of Agriculture, Forest Service, Southern Research Station. 168 p. https://doi.org/10.2737/SRS-GTR-239.

Potter, K.M.; Conkling, B.L., eds. 2020. Forest Health Monitoring: national status, trends, and analysis 2019. Gen. Tech. Rep. SRS-250. Asheville, NC: U.S. Department of Agriculture, Forest Service, Southern Research Station. 189 p. https://doi.org/10.2737/SRS-GTR-250.

Potter, K.M.; Conkling, B.L., eds. 2021. Forest Health Monitoring: national status, trends, and analysis, 2020. Gen. Tech. Rep. SRS-261. Asheville, NC: U.S. Department of Agriculture, Forest Service, Southern Research Station. 211 p. https://doi.org/10.2737/SRS-GTR-261.

Potter, K.M.; Conkling, B.L., eds. 2022. Forest Health Monitoring: national status, trends, and analysis, 2021. Gen. Tech. Rep. SRS-266. Asheville, NC: U.S. Department of Agriculture, Forest Service, Southern Research Station. 193 p. https://doi.org/10.2737/SRS-GTR-266.

Potter, K.M.; Escanferla, M.E.; Jetton, R.M.; Man, G. 2019a. Important insect and disease threats to United States tree species and geographic patterns of their potential impacts. Forests. 10(4): 304. https://doi.org/10.3390/f10040304.

Potter, K.M.; Escanferla, M.E.; Jetton, R.M. [and others]. 2019b. Prioritizing the conservation needs of United States tree species: evaluating vulnerability to forest insect and disease threats. Global Ecology and Conservation. 18: e00622. https://doi.org/10.1016/j.gecco.2019.e00622.

Potter, K.M.; Giardina, P.; Hughes, F. [and others]. 2023. How invaded are Hawaiian forests? Non-native understory tree dominance signals potential canopy replacement. Landscape Ecology. https://doi.org/10.1007/s10980-023-01662-6.

Potter, K.M.; Hargrove, W.W. 2013. Quantitative metrics for assessing predicted climate change pressure on North American tree species. Mathematical and Computational Forestry and Natural Resources Sciences. 5(2): 151–169.

Potter, K.M.; Koch, F.H. 2014. Phylogenetic community structure of forests across the conterminous United States: regional ecological patterns and forest health implications. Forest Science. 60(5): 851–861. https://doi.org/10.5849/forsci.13-115.

Potter, K.M.; Koch, F.H.; Oswalt, C.M.; Iannone, B.V. 2016. Data, data everywhere: detecting spatial patterns in fine-scale ecological information collected across a continent. Landscape Ecology. 31: 67–84. https://doi.org/10.1007/s10980-015-0295-0.

Potter, K.M.; Riitters, K.H.; Guo, G. 2022. Non-native tree regeneration indicates regional and national risks from current invasions. Frontiers in Forests and Global Change. 5:966407. https://doi.org/10.3390/f13010019.

Potter, K.M.; Woodall, C.W. 2012. Trends over time in tree and seedling phylogenetic diversity indicate regional differences in forest biodiversity change. Ecological Applications. 22(2): 517–531. https://doi.org/10.1890/10-2137.1.

Potter, K.M.; Woodall, C.W. 2014. Does biodiversity make a difference? Relationships between species richness, evolutionary diversity, and aboveground live tree biomass across U.S. forests. Forest Ecology and Management. 321: 117–129. https://doi.org/10.1016/j.foreco.2013.06.026.

Raffa, K.F.; Aukema, B.; Bentz, B.J. [and others]. 2009. A literal use of "forest health" safeguards against misuse and misapplication. Journal of Forestry. 107: 276–277.

Randolph, K.C. 2010a. Equations relating compacted and uncompacted live crown ratio for common tree species in the South. Southern Journal of Applied Forestry. 34(3): 118–123. https://doi.org/10.1093/sjaf/34.3.118.

Randolph, K.C. 2010b. Comparison of the arithmetic and geometric means in estimating crown diameter and crown cross-sectional area. Southern Journal of Applied Forestry. 34(4): 186–189. https://doi.org/10.1093/sjaf/34.4.186.

Randolph, K.C. 2013. Development history and bibliography of the U.S. Forest Service crown-condition indicator for forest health monitoring. Environmental Monitoring and Assessment. 185(6): 4977–4993. https://doi.org/10.1007/s10661-012-2919-z.

Randolph, K.C.; Moser, W.K. 2009. Tree crown condition in Missouri, 2000–2003. Gen. Tech. Rep. SRS-113. Asheville, NC: U.S. Department of Agriculture, Forest Service, Southern Research Station. 11 p. https://doi.org/10.2737/SRS-GTR-113.

Reams, G.A.; Smith, W.D.; Hansen, M.H. [and others]. 2005. The Forest Inventory and Analysis sampling frame. In: Bechtold, W.A.; Patterson, P.L., eds. The enhanced Forest Inventory and Analysis program—national sampling design and estimation procedures. Gen. Tech. Rep. SRS-80. Asheville, NC: U.S. Department of Agriculture, Forest Service, Southern Research Station: 11–26.

Rebbeck, J.; Kloss, A.; Bowden, M. [and others]. 2015. Aerial detection of seed-bearing female *Ailanthus altissima*: a cost-effective method to map an invasive tree in forested landscapes. Forest Science. 61: 1068–1078. https://doi.org/10.5849/forsci.14-223.

Riitters, K.H. 2011. Spatial patterns of land cover in the United States: a technical document supporting the Forest Service 2010 RPA assessment. Gen. Tech. Rep. SRS-136. Asheville, NC: U.S. Department of Agriculture, Forest Service, Southern Research Station. 64 p. https://doi.org/10.2737/SRS-GTR-136.

Riitters, K.; Costanza, J. 2019. The landscape context of family forests in the United States: anthropogenic interfaces and forest fragmentation from 2001 to 2011. Landscape and Urban Planning. 188: 64–71. https://doi.org/10.1016/j.landurbplan.2018.04.001.

Riitters, K.H.; Costanza, J.K.; Buma, B. 2017. Interpreting multiscale domains of tree cover disturbance patterns in North America. Ecological Indicators. 80: 147–152. https://doi.org/10.1016/j.ecolind.2017.05.022.

Riitters, K.H.; Coulston, J.W.; Wickham, J.D. 2012. Fragmentation of forest communities in the Eastern United States. Forest Ecology and Management. 263: 85–93. https://doi.org/10.1016/j.foreco.2011.09.022.

Riitters, K.; Potter, K.M.; Iannone, B.V. [and others]. 2018a. Exposure of protected forest to plant invasions in the Eastern United States. Forests. 9(11): 723. https://doi.org/10.3390/f9110723.

Riitters, K.; Potter, K.M.; Iannone, B.V. [and others]. 2018b. Landscape correlates of forest plant invasions: a high-resolution analysis across the Eastern United States. Diversity and Distributions. 24: 274–284. https://doi.org/10.1111/ddi.12680.

Riitters, K.H.; Tkacz, B. 2004. The U.S. Forest Health Monitoring program. In: Wiersma, G.B., ed. Environmental monitoring. Boca Raton, FL: CRC Press: 669–683. https://doi.org/10.1201/9780203495476.ch30.

Riitters, K.H.; Wickham, J.D. 2012. Decline of forest interior conditions in the conterminous United States. Scientific Reports. 2: 653. https://doi.org/10.1038/srep00653.

Riitters, K.H.; Wickham, J.D.; Costanza, J.K.; Vogt, P. 2016. A global evaluation of forest interior area dynamics using tree cover data from 2000 to 2012. Landscape Ecology. 31: 137–148. https://doi.org/10.1007/s10980-015-0270-9.

Root, H.T.; McCune, B.; Jovan, S. 2014. Lichen communities and species indicate climate thresholds in southeast and south-central Alaska, USA. The Bryologist. 117(3): 241–252. https://doi.org/10.1639/0007-2745-117.3.241.

Rose, A.K.; Coulston, J.W. 2009. Ozone injury across the Southern United States, 2002–06. Gen. Tech. Rep. SRS-118. Asheville, NC: U.S. Department of Agriculture, Forest Service, Southern Research Station. 25 p. https://doi.org/10.2737/SRS-GTR-118.

Russell, M.B.; Woodall, C.W.; Potter, K.M. [and others]. 2017. Interactions between white-tailed deer density and the composition of forest understories in the Northern United States. Forest Ecology and Management. 384: 26–33. https://doi.org/10.1016/j.foreco.2016.10.038.

Schomaker, M.E.; Zarnoch, S.J.; Bechtold, W.A. [and others]. 2007. Crown-condition classification: a guide to data collection and analysis. Gen. Tech. Rep. SRS-102. Asheville, NC: U.S. Department of Agriculture, Forest Service, Southern Research Station. 78 p. https://doi.org/10.2737/SRS-GTR-102.

Schulz, B.K.; Bechtold, W.A.; Zarnoch, S.J. 2009. Sampling and estimation procedures for the vegetation diversity and structure indicator. Gen. Tech. Rep. PNW-781. Portland, OR: U.S. Department of Agriculture, Forest Service, Pacific Northwest Research Station. 53 p. https://doi.org/10.2737/PNW-GTR-781.

Schulz, B.K.; Gray, A.N. 2013. The new flora of Northeastern USA: quantifying introduced plant species occupancy in forest ecosystems. Environmental Monitoring and Assessment. 185: 3931–3957. https://doi.org/10.1007/s10661-012-2841-4.

Simkin, S.M.; Allen, E.B.; Bowman, W.D. [and others]. 2016. Conditional vulnerability of plant diversity to atmospheric nitrogen deposition across the United States. Proceedings of the National Academy of Sciences. 113: 4086–4091. https://doi.org/10.1073/pnas.1515241113.

Siry, J.; Cubbage, F.W.; Potter, K.M.; McGinley, K. 2018. Current perspectives on sustainable forest management: North America. Current Forestry Reports. 4(3): 138–149. https://doi.org/10.1007/s40725-018-0079-2.

Smith, W.D.; Conkling, B.L. 2004. Analyzing forest health data. Gen. Tech. Rep. SRS-77. Asheville, NC: U.S. Department of Agriculture, Forest Service, Southern Research Station. 33 p. https://doi.org/10.2737/SRS-GTR-77.

Spencer, P.; Nowacki, G.; Fleming, M. [and others]. 2002. Home is where the habitat is: an ecosystem foundation for wildlife distribution and behavior. Arctic Research of the United States. 16: 6–17.

Steinman, J. 2004. Forest Health Monitoring in the Northeastern United States: disturbances and conditions during 1993–2002. NA-TP-01-04. Newtown Square, PA: U.S. Department of Agriculture, Forest Service, Northeastern Area State and Private Forestry. 46 p.

Teale, S.A.; Castello, J.D. 2011. The past as key to the future: a new perspective on forest health. In: Castello, J.D.; Teale, S.A., eds. Forest health: an integrated perspective. New York: Cambridge University Press: 3–16. https://doi.org/10.1017/CBO9780511974977.002.

U.S. Department of Agriculture (USDA) Forest Service. 2004. National report on sustainable forests—2003. FS-766. Washington, DC. 139 p.

U.S. Department of Agriculture (USDA) Forest Service. 2011. National report on sustainable forests—2010. FS-979. Washington, DC. 134 p.

Vogt, J.T.; Koch, F.H. 2016. The evolving role of Forest Inventory and Analysis data in invasive insect research. American Entomologist. 62(1): 46–58. https://doi.org/10.1093/ae/tmv072.

Vose, J.M.; Clark, J.S.; Luce, C.H.; Patel-Weynand, T., eds. 2016. Effects of drought on forests and rangelands in the United States: a comprehensive science synthesis. Gen. Tech. Rep. WO-93b. Washington, DC: U.S. Department of Agriculture, Forest Service, Washington Office. 289 p. https://doi.org/10.2737/WO-GTR-93b.

Woodall, C.W.; Amacher, M.C.; Bechtold, W.A. [and others]. 2011. Status and future of the forest health indicators program of the USA. Environmental Monitoring and Assessment. 177: 419–436. https://doi.org/10.1007/s10661-010-1644-8.

Woodall, C.W.; Conkling, B.L.; Amacher, M.C. [and others]. 2010. The Forest Inventory and Analysis Database version 4.0: database description and users manual for Phase 3. Gen. Tech. Rep. NRS-61. Newtown Square, PA: U.S. Department of Agriculture, Forest Service, Northern Research Station. 180 p. https://doi.org/10.2737/NRS-GTR-61.

Woodall, C.W.; Walters, B.F.; Oswalt, S.N. [and others]. 2013. Biomass and carbon attributes of downed woody materials in forests of the United States. Forest Ecology and Management. 305: 48–59. https://doi.org/10.1016/j.foreco.2013.05.030.

Woodall, C.W.; Walters, B.F.; Westfall, J.A. 2012. Tracking downed dead wood in forests over time: development of a piece matching algorithm for line intercept sampling. Forest Ecology and Management. 277: 196–204. https://doi.org/10.1016/j.foreco.2012.04.031.

Yemshanov, D.; Koch, F.H.; Lu, B. [and others]. 2014. There is no silver bullet: the value of diversification in planning invasive species surveillance. Ecological Economics. 104: 61–72. https://doi.org/10.1016/j.ecolecon.2014.04.024.

SECTION 1

Analyses of Short-Term Forest Health Data

CHAPTER 2

Broad-Scale Patterns of Insect and Disease Activity Across the United States From the National Insect and Disease Survey, 2021

Kevin M. Potter and
Jeanine L. Paschke

INTRODUCTION

Forest insects and diseases have widespread ecological and economic impacts on forests in the United States and may represent the most serious threats to the Nation's forests (Logan and others 2003, Lovett and others 2016, Tobin 2015). U.S. law, therefore, authorizes the U.S. Department of Agriculture, Forest Service to "conduct surveys to detect and appraise insect infestations and disease conditions and man-made stresses affecting trees and establish a monitoring system throughout the forests of the United States to determine detrimental changes or improvements that occur over time, and report annually concerning such surveys and monitoring" (FHP 2022). Insects and diseases cause changes in forest structure and function, species succession, and biodiversity, which may be considered negative or positive depending on management objectives (Edmonds and others 2011). Nearly all native tree species of the United States are affected by at least one injury-causing insect or disease agent, with exotic agents, on average, being considerably more severe than native ones (Potter and others 2019a). Additionally, the genetic integrity of several native tree species is highly vulnerable to exotic diseases and insects (Potter and others 2019b).

An important task for forest managers, pathologists, and entomologists is to recognize and distinguish between natural and excessive mortality, a task relating to ecologically based or commodity-based management objectives (Teale and Castello 2011). Impacts of insects and diseases on forests vary from natural thinning to disruption of valued ecosystem processes due to tree mortality, but insects and diseases that kill trees are not necessarily the enemies of forests (Teale and Castello 2011). If disturbances, including insects and diseases, are viewed in their full ecological context, then some amount can be considered "healthy." Disturbances can sustain forest structures (Manion 2003, Zhang and others 2011) by facilitating a sanitation role, culling weak competitors, and releasing resources needed to support the growth of surviving trees (Teale and Castello 2011).

Analyzing patterns of forest insect infestations, disease occurrences, forest declines, and related biotic stress factors is necessary to monitor the health of forested ecosystems and their potential impacts on forest structure, composition, biodiversity, and species distributions (Castello and others 1995). Introduced insects and diseases are of particular concern because they can extensively damage the biodiversity, ecology, and economy of affected areas (Brockerhoff and others 2006, Mack and others 2000). Few forests remain unaffected by invasive species, and their impacts to forest ecosystems are undeniable. These impacts can include wholesale changes in structures and function of ecosystems (Parry and Teale 2011).

Examining insect pest occurrences and related stress factors from a landscape-scale perspective is useful, given the regional extent of many infestations and the large-scale complexity of interactions between host distribution, stress factors, and the development of outbreaks (Holdenrieder and others 2004, Liebhold and others 2013). One such landscape-scale approach is detecting geographic patterns of disturbance, allowing for the identification of areas at greater

How to cite this chapter:

Potter, Kevin M.; Paschke, Jeanine L. 2023. Broad-scale patterns of insect and disease activity across the United States from the National Insect and Disease Survey, 2021. In: Potter, Kevin M.; Conkling, Barbara L., eds. Forest Health Monitoring: national status, trends, and analysis 2022. Gen. Tech. Rep. SRS-273. Asheville, NC: U.S. Department of Agriculture, Forest Service, Southern Research Station: 25–53. https://doi.org/10.2737/SRS-GTR-273-Chap2.

risk of significant ecological and economic impacts, and for selecting locations for more intensive monitoring and analysis. National Insect and Disease Survey (IDS) data (FHP 2022), coordinated by the Forest Service's Forest Health Protection (FHP) program, provide an important source of information on forest disturbances and their causal agents across broad regions. Recent long-term analyses of these data highlight insects as more widely detected agents of mortality compared to diseases, with bark beetles consistently the most important mortality agents across regions and time (Potter and others 2020a). (These results may be somewhat skewed toward insects because the visible signatures of insect damage are easier for IDS surveyors to detect.)

Here, we report the area affected in 2021 by insect and disease mortality and defoliation agents across all 50 States using IDS data collected by the Forest Service and its State partners. We further estimate the percentage of surveyed tree canopy cover area with insect- and disease-related mortality or defoliation within ecoregions across the United States and identify statistically significant geographic hot spots of mortality or defoliation in the conterminous United States (CONUS).

METHODS

Data

The IDS data (FHP 2022) consist of information from low-altitude aerial survey and ground survey efforts by FHP and its partners in State agencies. These data can be used to summarize insect and disease activity by regions in the CONUS, Alaska, and Hawaii (Potter 2012, 2013; Potter and Koch 2012; Potter and Paschke 2013, 2014, 2015a, 2015b, 2016, 2017, 2022; Potter and others 2018, 2019c, 2020b, 2021). The 2021 data collection season was more typical than 2020, when the global COVID-19 pandemic precluded the ability of many State partners and regional Forest Service personnel to conduct aerial survey flights because of risks posed by spending extended periods of time in the confined space of an aircraft. In 2020, a group of forest health specialists worked together to generate new workflows, training materials, and help sessions to address this challenge, including "scan and sketch" methods to outline damage polygons and points directly on base imagery (Hanavan and others 2021). In 2021, however, most data in the IDS data stream were collected using aerial and ground survey methods.

The IDS data identify areas with mortality and defoliation caused by insect and disease activity, although some important forest insects (such as emerald ash borer [*Agrilus planipennis*] and hemlock woolly adelgid [*Adelges tsugae*]), diseases (such as laurel wilt [*Harringtonia lauricola*], Dutch elm disease [*Ophiostoma novo-ulmi*], white pine blister rust [*Cronartium ribicola*], and thousand cankers disease [*Geosmithia morbida*]), and mortality complexes (such as oak decline) have not been not easily detected or thoroughly quantified through aerial detection and other remote sensing methods. (Recent efforts, however, have successfully used remotely sensed data to map damage caused by hemlock woolly adelgid, laurel wilt, and emerald ash borer in urban settings [Abdulridha and others 2018, Hanavan and others 2015, Pontius and others

2017].) Such pests may attack hosts that are widely dispersed throughout forests with high tree species diversity or may cause mortality or defoliation that is otherwise difficult to detect. A visual interpreter might consider a pathogen or insect to be a mortality-causing agent in one location and a defoliation-causing agent in another, depending on the level of damage to the forest in an area and the convergence of other stress factors (such as drought). In some cases, identified agents of mortality or defoliation are actually complexes of multiple agents summarized under an impact label related to a specific host tree species (e.g., "beech bark disease complex" or "yellow-cedar decline"). In other cases, one or more agents (such as ash yellows [caused by the *Candidatus Phytoplasma fraxini* bacterium], ash rust [*Puccinia sparganioides*], and verticillium wilt [*Verticillium albo-atrum*] in ash [*Fraxinus* spp.]) may cause stress to a tree that may ultimately increase its susceptibility to another agent to which the damage is attributed (such as emerald ash borer). Additionally, differences in data collection, attribute recognition, and coding procedures among States and regions can complicate data analysis and interpretation of results. A comparison of aerial survey data by four aerial observers with ground presence/absence observations found the accuracy of aerial survey data exceeded 70 percent, and damage type observations for tree mortality and defoliation had high levels of accuracy, but further showed the accuracy declined for severity estimates and as specificity for observations went from the genus to the species level for tree species and damage agents (Coleman and others 2018).

In 2021, IDS surveys of the CONUS covered about 191.05 million ha of both forested and unforested area (fig. 2.1), of which approximately 131.35 million ha were forested, representing about 41.6 percent of the 315.99-million-ha tree canopy area of the CONUS. This was approximately twice the percentage of tree-canopied area surveyed in 2020 but similar to the amount surveyed in 2018 (46.6 percent) and 2019 (49.2 percent) (Potter and Paschke 2022; Potter and others 2020b, 2021). Meanwhile, about 7.2 percent (5.60 million ha) of Alaska's 77.78 million ha of forest and shrubland was surveyed in 2021, out of a total of 7.35 million ha surveyed across land cover types. This compares to 12.7 percent in 2018, 10.8 percent in 2019, and 2.8 percent in 2020. Finally, surveyors covered about 860 000 ha of Hawaii during 2021. Approximately 564 000 ha of that area had tree canopy cover, or about 65.5 percent of the 861 000 ha total, compared to 69.4 percent in 2018, 63.9 percent in 2019, and 60.3 percent in 2020.

The Digital Mobile Sketch Mapping (DMSM) platform includes tablet hardware, software, and data support processes allowing trained aerial surveyors in light aircraft, as well as ground observers and those using other remote sensing data, to record forest disturbances and their causal agents. Digital Mobile Sketch Mapping enhances the quality and quantity of forest health data while having the potential to improve safety by integrating with remote sensing platforms (FHP 2019). Geospatial data collected with DMSM are stored in the national IDS database. In an important change from the legacy Digital Aerial Sketch Mapping (DASM) approach,

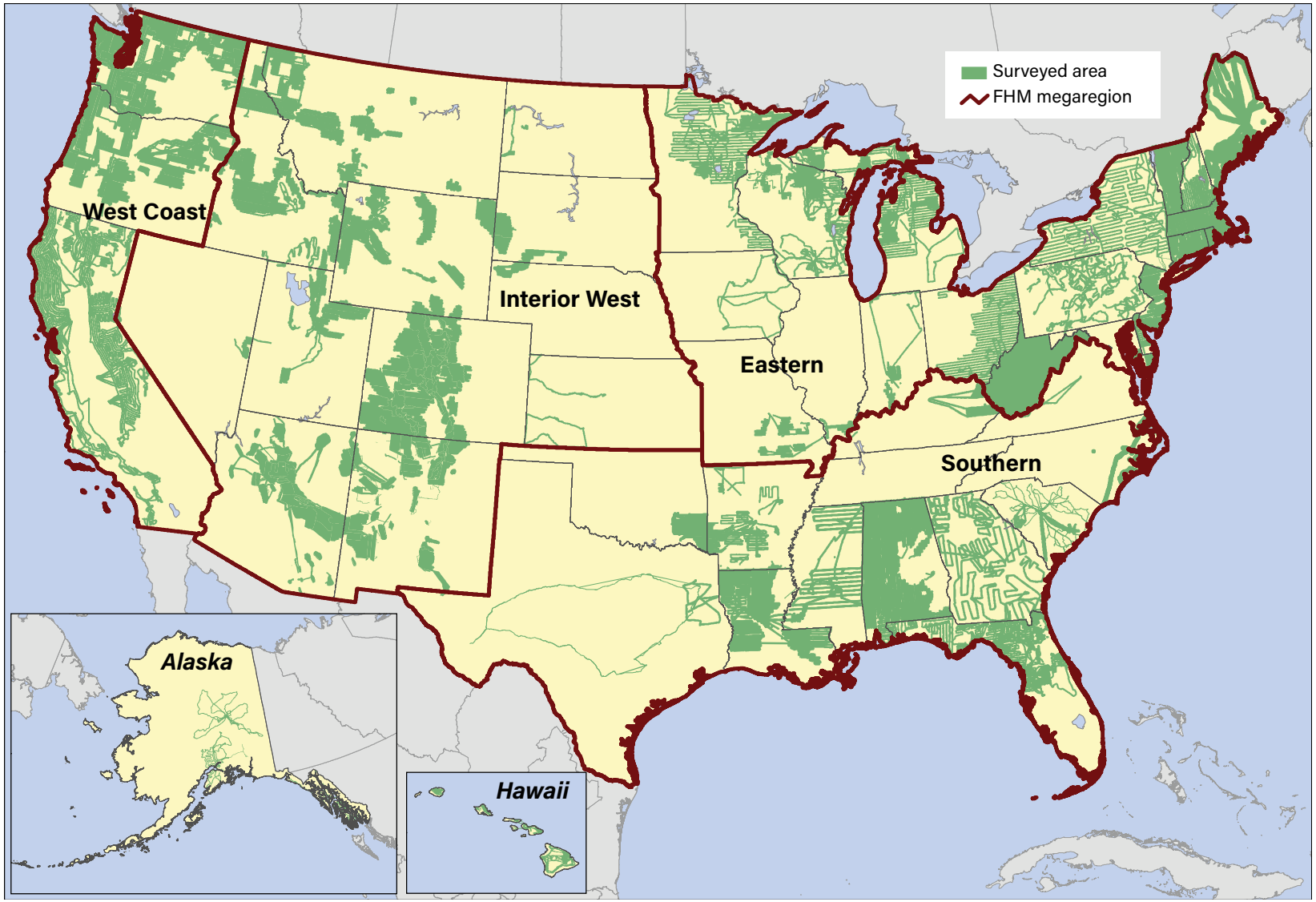

Figure 2.1—The extent of surveys for insect and disease activity conducted in the conterminous United States (CONUS), Alaska, and Hawaii in 2021. The red lines delineate Forest Health Monitoring (FHM) megaregions in the CONUS. Note: Alaska and Hawaii are not shown to scale with map of the CONUS. (Data source: U.S. Department of Agriculture, Forest Service, Forest Health Protection)

the DMSM platform allows surveyors to both define the extent of an area experiencing damage and estimate the percent range of the area within polygons that is affected (Berryman and McMahan 2019). While additional validation is required for this new metric, it should increase the accuracy of derived damage metrics because it potentially corrects for previous overestimation caused by "lassoing" areas of undamaged trees into large areas of damage (Coleman and others 2018, Slaton and others 2021). For this reason, IDS analysis chapters in FHM reports before 2019 did not incorporate derived damage estimates beyond the areal footprint damage with mortality or defoliation polygon boundaries. However, these are now possible because of the inclusion of damage percentage estimates within polygons (see "Analyses" below).

Digital Mobile Sketch Mapping includes both polygon geometry, used for damage areas where boundaries are discrete and obvious, and point geometry, used for small clusters of damage where size and shape of the damage are less important than recording the location. Examples of insects and diseases for which point data are utilized include sudden oak death (caused by the pathogen *Phytophthora ramorum*), southern pine beetle (*Dendroctonus frontalis*), and some types of bark beetle damage in the West. For analyses in this report, these points were assigned an area of 0.8 ha (about 2 acres). Additionally, DMSM allows for the use of grid cells (240-, 480-, 960-, or 1920-m resolution) to estimate the percentage of trees affected by damages that may be widespread and diffuse, such as those associated with spongy moth (*Lymantria dispar*) and emerald ash borer. When calculating the total areas affected by each damage agent, we used the entire areas of these grid cells (e.g., 240-m cell = 5.76 ha).

Analyses

To estimate the extent of damaging insect and disease agents in 2021, we conducted three types of analyses: (1) compiling a series of tables reporting the most widely detected mortality and defoliation agents, (2) describing the percentage of surveyed tree canopy cover area with insect- and disease-related mortality or defoliation within ecoregions across the United States, and (3) using a geographic hot spot analytical approach to identify statistically significant geographic hot spots of mortality or defoliation in the CONUS.

For the first of these, we used the 2021 mortality and defoliation polygons to identify the select mortality and defoliation agents and complexes causing damage on >5000 ha of forest in the CONUS that year. Similarly, we listed the five most widely reported mortality and defoliation agents and complexes within each of the four FHM megaregions in the CONUS (West Coast, Interior West, Eastern, and Southern), as well as for Alaska and Hawaii where data were available. Because of the insect and disease aerial sketch-mapping process (i.e., digitization of polygons by a human interpreter aboard aircraft or by a forest health specialist applying the "scan and sketch" approach with remotely sensed data), all quantities are approximate "footprint" areas for each agent or complex, delineating areas of visible damage within which the agent or complex is present.

Unaffected trees may exist within the footprint, and the amount of damage within the footprint is not reflected in the estimates of forest area affected. The sum of areas affected by all agents and complexes is not equal to the total affected area because of overlapping polygons and the reporting of multiple agents per polygon in some situations.

In our second set of analyses, we used the IDS data for 2021 to more directly estimate impacts of insect- and disease-related mortality and defoliation on U.S. forests. These results are reported in a set of figures describing the percentage of surveyed tree canopy cover area with insect- and disease-related mortality or defoliation within ecoregions across the United States. For these indicators of the extent of damaging insect and disease agents, we summarized the percentage of surveyed tree canopy cover area experiencing mortality or defoliation for ecoregions within the CONUS and Hawaii, and for surveyed forest and shrubland in Alaska ecoregions. This is a change from FHM reports before 2019, in which we reported on the percentage of regions exposed to mortality and defoliating agents based only on the footprint with mortality or defoliation polygon boundaries (masked by forest cover) because information on the percentage of damage within polygons was not yet completely available. As noted above, DMSM now allows surveyors to both define the extent of an area experiencing damage and estimate percent range of the area within the polygon affected (specifically, 1–3 percent, 4–10 percent, 11–29 percent, 30–50 percent, and >50 percent). By multiplying the area of damage within each polygon (after masking by tree canopy cover) by the midpoint of the estimated percent-affected range, it is possible to generate an adjusted estimate of the area affected by each mortality or defoliation agent detection (Berryman and McMahan 2019). These individual estimates can be summed for all polygons within an ecoregion (intersected and dissolved) and divided by the total surveyed tree canopy cover area within the ecoregion to generate an estimate of the percentage of its canopy cover area affected by defoliating or mortality-causing agents. (Digital Mobile Sketch Mapping point data are also included in this estimate. Surveyors have the option to estimate the number of trees affected at a point and are required to assign an area value associated with each point, which is assumed to be 100 percent affected by its mortality or defoliation agent. For simplicity, we transformed each point into a 2-acre [0.809-ha] polygon. These areas for all the points in an ecoregion were then added to the polygon-adjusted affected area estimates for the ecoregion.)

We calculated the percentage of surveyed tree canopy area with mortality or defoliation within each of the 190 ecoregion sections in the CONUS (Cleland and others 2007). Similarly, we summarized mortality and defoliation data for each of the 32 ecoregion sections in Alaska (Spencer and others 2002). For Hawaii, we calculated the percentage of surveyed tree canopy area affected by mortality and defoliation agents in 34 ecoregion subunits on each of the major islands of the archipelago (Potter 2023). We did not calculate statistics for analysis regions in the

CONUS and Hawaii with ≤5 percent of the tree canopy cover area surveyed, nor in Alaska with ≤2.5 percent of the forest and shrubland area surveyed.

We resampled tree canopy data for the CONUS and Hawaii to 240 m from a 30-m raster dataset that estimates percentage of tree canopy cover (0–100 percent) for each grid cell; this dataset was generated from the 2011 National Land Cover Database (NLCD) (Homer and others 2015) through a cooperative project between the Multi-Resolution Land Characteristics Consortium and the Forest Service Geospatial Technology and Applications Center (GTAC) (Coulston and others 2012). For our purposes, we treated any cell with >0-percent tree canopy cover as forest. Comparable tree canopy cover data were not available for Alaska, so we instead created a 240-m-resolution layer of forest and shrub cover from the 2011 NLCD.

Finally, we used the Spatial Association of Scalable Hexagons (SASH) analytical approach to identify statistically significant geographic hot spots of mortality or defoliation in the CONUS. This method identifies locations where ecological phenomena occur at greater or lower frequency than expected by random chance and is based on a sampling frame optimized for spatial neighborhood analysis, adjustable to the appropriate spatial resolution, and applicable to multiple data types (Potter and others 2016). Specifically, it consists of dividing an analysis area into scalable equal-area hexagonal cells within which data are aggregated, followed by identifying statistically significant geographic clusters of hexagonal cells within which mean values are greater or less than those expected by chance. To identify these clusters, we employed a Getis-Ord (G_i^*) hot spot analysis (Getis and Ord 1992) in ArcMap® 10.3 (ESRI 2017) separately for both mortality- and defoliation-causing agents across the CONUS. The low density of survey data in 2021 from Alaska, as well as the small spatial extent of Hawaii (fig. 2.1), precluded the use of Getis-Ord G_i^* hot spot analyses in these areas.

The units of analysis were 9,810 hexagonal cells, each approximately 834 km^2 in area, generated in a lattice across the CONUS using intensification of the Environmental Monitoring and Assessment Program (EMAP) North American hexagon coordinates (White and others 1992). These coordinates are the foundation of a sampling frame in which a hexagonal lattice was projected onto the CONUS by centering a large base hexagon over the region (Reams and others 2005, White and others 1992). This base hexagon can be subdivided into many smaller hexagons, depending on sampling needs, and serves as the basis of the plot sampling frame for the Forest Service's Forest Inventory and Analysis (FIA) program (Reams and others 2005). Importantly, hexagons maintain equal areas across the study region regardless of the degree of intensification of the EMAP hexagon coordinates. In addition, hexagons are compact and uniform in their distance to the centroids of neighboring hexagons, meaning a hexagonal lattice has a higher degree of isotropy (uniformity in all directions) than a square grid (Shima and others 2010). These are convenient and highly useful attributes for spatial neighborhood analyses. These scalable hexagons are independent of geopolitical and

ecological boundaries, avoiding the possibility of different sample units (such as counties, States, or watersheds) encompassing vastly different areas (Potter and others 2016). We selected hexagons 834 km^2 in area because this is a manageable size for making monitoring and management decisions in analyses that are national in extent (Potter and others 2016).

We then used the Getis-Ord G_i^* statistic to identify clusters of hexagonal cells within which the percentage of surveyed tree canopy area with mortality or defoliation was higher than expected by chance. This statistic allows for the decomposition of a global measure of spatial association into its contributing factors, by location, and is therefore particularly suitable for detecting instances of nonstationarity in a dataset, such as when spatial clustering is concentrated in one subregion of the data (Anselin 1992). We excluded hexagons if they contained <5-percent tree canopy cover or if <1 percent of the tree canopy cover was surveyed in 2021.

The Getis-Ord G_i^* statistic for each hexagon summed differences between mean values in a local sample, determined by a moving window consisting of the hexagon and its 18 first- and second-order neighbors (the 6 adjacent hexagons and the 12 additional hexagons contiguous to those 6) and a global mean. The G_i^* statistic was standardized as a z-score with a mean of 0 and a standard deviation of 1, with values >1.96 representing significant (p <0.025) local clustering of high values and values <-1.96 representing significant clustering of low values (p <0.025), since 95 percent of observations under a normal distribution should be within approximately two (exactly 1.96) standard deviations of the mean (Laffan 2006). In other words, a G_i^* value of 1.96 indicates the local mean of the percentage of forest exposed to mortality- or defoliation-causing agents for a hexagon and its 18 neighbors is approximately two standard deviations greater than the mean expected in the absence of spatial clustering, while a G_i^* value of -1.96 indicates the local mortality or defoliation mean for a hexagon and its 18 neighbors is approximately two standard deviations less than the mean expected in the absence of spatial clustering. Values between -1.96 and 1.96 have no statistically significant concentration of high or low values. In other words, when a hexagon has a G_i^* value between -1.96 and 1.96, mortality or defoliation damage within it and its 18 neighbors is not statistically different from a normal expectation. As described in Laffan (2006), it is calculated as:

$$G_i^*(\boldsymbol{d}) = \frac{\sum_j w_{ij}(\boldsymbol{d}) x_j - W_i^* \bar{x}^*}{s^* \sqrt{\frac{(n s_{1i}^*) - W_i^{*2}}{n-1}}}$$

where

G_i^* = the local clustering statistic (in this case, for the target hexagon)

i = the center of local neighborhood (the target hexagon)

d = the width of local sample window (the target hexagon and its first- and second-order neighbors)

x_j = the value of neighbor j

w_{ij} = the weight of neighbor j from location i (all the neighboring hexagons in the moving window were given an equal weight of 1)

n = number of samples in the dataset (the 4,303 hexagons containing >5-percent tree cover and with at least 1 percent of the canopy cover surveyed)

W_i^* = the sum of the weights

s^*_{1i} = the number of samples within d of the central location (19: the focal hexagon and its 18 first- and second-order neighbors)

$\overline{x}^*$= mean of whole dataset (in this case, the 4,303 hexagons)

s^* = the standard deviation of whole dataset (for the 4,303 hexagons)

It is worth noting that the -1.96 and 1.96 threshold values are not exact because the correlation of spatial data violates the assumption of independence required for statistical significance (Laffan 2006). The Getis-Ord approach does not require the input data to be normally distributed because the local G_i^* values are computed under a randomization assumption, with G_i^* equating to a standardized z-score that asymptotically tends to a normal distribution (Anselin 1992). The z-scores are reliable, even with skewed data, if the distance band used to define the local sample around the target observation is large enough to include several neighbors for each feature (ESRI 2017).

RESULTS AND DISCUSSION

Conterminous United States Mortality

The national IDS data in 2021 identified 60 mortality-causing agents and complexes across the CONUS on approximately 2.21 million ha, slightly less than the land area of New Hampshire. Of the 60 mortality agents, 13 were detected on >5000 ha within the area surveyed. These numbers were higher than in 2020, when 45 agents and complexes were detected on 1.17 million ha (Potter and Paschke 2022), largely because of the challenges associated with collecting insect and disease damage data during the COVID-19 pandemic. They are more consistent with the numbers during a typical year of data collection, such as 2.69 million ha from 58 agents and complexes in 2019 (Potter and others 2021).

Emerald ash borer was the most widely detected mortality agent in 2021, identified on about 878 000 ha (table 2.1), which represents about 40 percent of the total CONUS mortality area. It is important to note, however, that emerald ash borer damage is challenging to map during aerial surveys, that it is difficult to differentiate the occurrence of damage between years, and that agents other than emerald ash borer affect ash species. Fir engraver (*Scolytus ventralis*), identified on 412 000 ha, was the next most widely detected mortality agent, as in 2020 (Potter and Paschke 2022). Three other agents were detected on >100 000 ha. The first of these is characterized as an "unknown bark beetle" on approximately 230 000 ha, with damage primarily in ponderosa pine (*Pinus ponderosa*) forests by a group of known and varied bark beetles impossible to distinguish using IDS data. This also has been characterized as "Southwest bark beetle complex" consisting mainly of damage caused by roundheaded pine beetle (*D. adjunctus*), western pine beetle (*D. brevicomis*), and ips beetles. As a separate individual agent, western pine beetle was detected on almost 158 000 ha, while eastern larch beetle

Table 2.1—Mortality agents and complexes affecting >5000 ha in the conterminous United States during 2021

Agents/complexes causing mortality, 2021	Area (ha)[a]
Emerald ash borer	877 631
Fir engraver	411 511
Unknown bark beetle[b]	230 426
Western pine beetle	157 550
Eastern larch beetle	101 516
Mountain pine beetle	72 636
Pinyon ips	66 706
Douglas-fir beetle	61 653
Spruce beetle	57 443
Unknown	51 406
Western balsam bark beetle	35 521
Flatheaded fir borer	22 739
Balsam woolly adelgid	18 952
Oak decline	16 832
Jeffrey pine beetle	10 630
Subalpine fir decline	10 104
Ips engraver beetles	7822
Sudden oak death	6578
Other (42)	21 611
Total, all mortality agents	2 213 302

[a] All values are "footprint" areas for each agent or complex. The sum of the individual agents is not equal to the total for all agents due to the reporting of multiple agents per polygon.

[b] In the Interior West, this is primarily damage on ponderosa pines. The group of bark beetles is known and varied but not distinguishable from the air. Regions have characterized it as "Southwest bark beetle complex" consisting mainly of damage caused by roundheaded pine beetle, western pine beetle, and ips beetles.

(*D. simplex)* was identified on 102 000 ha. Meanwhile, mortality from the 14 IDS agents constituting the western bark beetle group (table 2.2) encompassed about 49 percent of all the 2021 mortality area across the CONUS (1.09 million ha in the West).

The Eastern FHM megaregion in 2021 had the largest area on which mortality agents and complexes were detected, about 1.02 million ha (table 2.3), within the surveyed area. The large majority of this (86.2 percent) was associated with emerald ash borer, which was detected on 878 000 ha. Eastern larch beetle was next, at 102 000 ha (10 percent of the total). Oak decline represented 1.7 percent and southern pine beetle was 0.5 percent of the total. Overall, 35 agents and complexes were identified in the megaregion. The ecoregion sections with the greatest mortality of surveyed tree canopy cover were 222M–Minnesota and Northeast Iowa Morainal-Oak Savannah (6.66 percent) and 222L–North Central U.S. Driftless and Escarpment of southwestern Wisconsin, northeastern Iowa, and southeastern Minnesota (5.87 percent), places where emerald ash borer killed white, green, and black ash (*F. americana, F. pennsylvanica*, and *F. nigra*) (fig. 2.2). Parts of these ecoregion sections, along with 251C–Central Dissected Till Plains and 251B–North Central Glaciated Plains, encompassed hot spots of extremely high and very high mortality density (fig. 2.3).

Other ecoregion sections in the Eastern FHM megaregion with relatively high mortality were 212M–Northern Minnesota and Ontario (1.92 percent of surveyed tree canopy cover), following an infestation of eastern larch beetle, and

Table 2.2—Beetle taxa included in the "western bark beetle" group in 2021

Western bark beetle mortality agents	
Douglas-fir beetle	*Dendroctonus pseudotsugae*
Douglas-fir engraver	*Scolytus unispinosus*
Fir engraver	*Scolytus ventralis*
Ips engraver beetles	*Ips* spp.
Jeffrey pine beetle	*Dendroctonus jeffreyi*
Mountain pine beetle	*Dendroctonus ponderosae*
Pine engraver	*Ips pini*
Pinyon ips	*Ips confusus*
Roundheaded pine beetle	*Dendroctonus adjunctus*
Silver fir beetle	*Pseudohylesinus sericeus*
Spruce beetle	*Dendroctonus rufipennis*
Unknown bark beetle	—
Western balsam bark beetle	*Dryocoetes confusus*
Western pine beetle	*Dendroctonus brevicomis*

222I–Erie and Ontario Lake Plain (1.51 percent) because of emerald ash borer-caused mortality in white ash. Both ecoregion sections were locations of hot spots of moderate mortality density (fig. 2.3). Oak decline was an issue in 223B–Interior Low Plateau-Transition Hills (0.49 percent) in south-central Indiana, while eastern larch beetle, emerald ash borer, and eastern spruce budworm (*Choristoneura fumiferana*) all caused mortality in 212T–Northern Green Bay Lobe (0.31 percent).

The West Coast FHM megaregion had the second largest area of detected mortality within the area surveyed, about 748 000 ha linked to 24 agents and complexes (table 2.3). Slightly more than half of this area (53.1 percent) was attributed to fir engraver (397 000 ha). Three other bark beetles were detected on large areas: western pine beetle on 157 000 ha (21.0 percent of the total), mountain pine beetle (*D. ponderosae*) on 66 000 ha (8.8 percent), and Douglas-fir beetle (*D. pseudotsugae*) on 30 000 ha (4.0 percent). Much of eastern and northern California, as well as southwestern Oregon, had at least moderate mortality detected in their surveyed areas (>0.25 percent) (fig. 2.2). First among these ecoregion sections was M261E–Sierra Nevada (1.13 percent), where fir engraver caused mortality in California red fir (*Abies magnifica* var. *shastensis*), mountain pine beetle killed lodgepole pine (*P. contorta*), Jeffrey pine beetle (*D. jeffrey*i) resulted in mortality in Jeffrey pine (*P. jeffreyi*), and western pine beetle affected ponderosa pine stands. Neighboring ecoregion sections also had high mortality: M261D–Southern Cascades (0.94-percent mortality of surveyed areas), M261A–Klamath Mountains (0.93 percent),

Table 2.3—The top five mortality agents or complexes for each Forest Health Monitoring megaregion and for Alaska and Hawaii in 2021

Mortality agents and complexes, 2021	Area (ha)[a]
Eastern	
Emerald ash borer	877 631
Eastern larch beetle	101 516
Oak decline	16 832
Unknown	11 147
Southern pine beetle	4789
Other mortality agents (30)	6171
Total, all mortality agents and complexes	1 018 029
Interior West	
Unknown bark beetle[b]	224 720
Pinyon ips	66 463
Spruce beetle	56 884
Douglas-fir beetle	30 642
Western balsam bark beetle	15 218
Other mortality agents (12)	51 930
Total, all mortality agents and complexes	441 007
Southern	
Ips engraver beetles	2831
Unknown bark beetle[c]	1930
Douglas-fir beetle[c]	1115
Unknown	762
Needlecast	257
Other mortality agents (7)	482
Total, all mortality agents and complexes	6499

Mortality agents and complexes, 2021	Area (ha)[a]
West Coast	
Fir engraver	397 297
Western pine beetle	156 989
Mountain pine beetle	65 673
Unknown	36 755
Douglas-fir beetle	29 896
Other mortality agents (19)	81 338
Total, all mortality agents and complexes	747 768
Alaska	
Spruce beetle	78 325
Hemlock sawfly	8510
Yellow-cedar decline	3299
Western balsam bark beetle	36
Aspen running canker	23
Other mortality agents (4)	5
TOTAL	90 196
Hawaii	
Unknown[d]	36 415
Total, all mortality agents and complexes	36 415

[a] The total area affected by other agents is listed at the end of each section. All values are "footprint" areas for each agent or complex. The sum of the individual agents is not equal to the total for all agents due to the reporting of multiple agents per polygon.

[b] In the Interior West, this is primarily damage on ponderosa pines. The group of bark beetles is known and varied but not distinguishable from the air. Regions have characterized it as "Southwest bark beetle complex" consisting mainly of damage caused by roundheaded pine beetle, western pine beetle, and ips beetles.

[c] Personnel from Forest Service Region 3 (Southwestern Region) conducted surveys into southwestern Texas (Region 8 [Southern Region]) because of extended damage in the Guadalupe Mountains which included Douglas-fir beetle and "unknown bark beetle" damage on ponderosa pines (see note b in table 2.1).

[d] Most of the mortality recorded in Hawaii is coded as "unknown" mortality on ʻōhiʻa lehua. Damage is likely attributed to rapid ʻōhiʻa death but has not been confirmed in all cases.

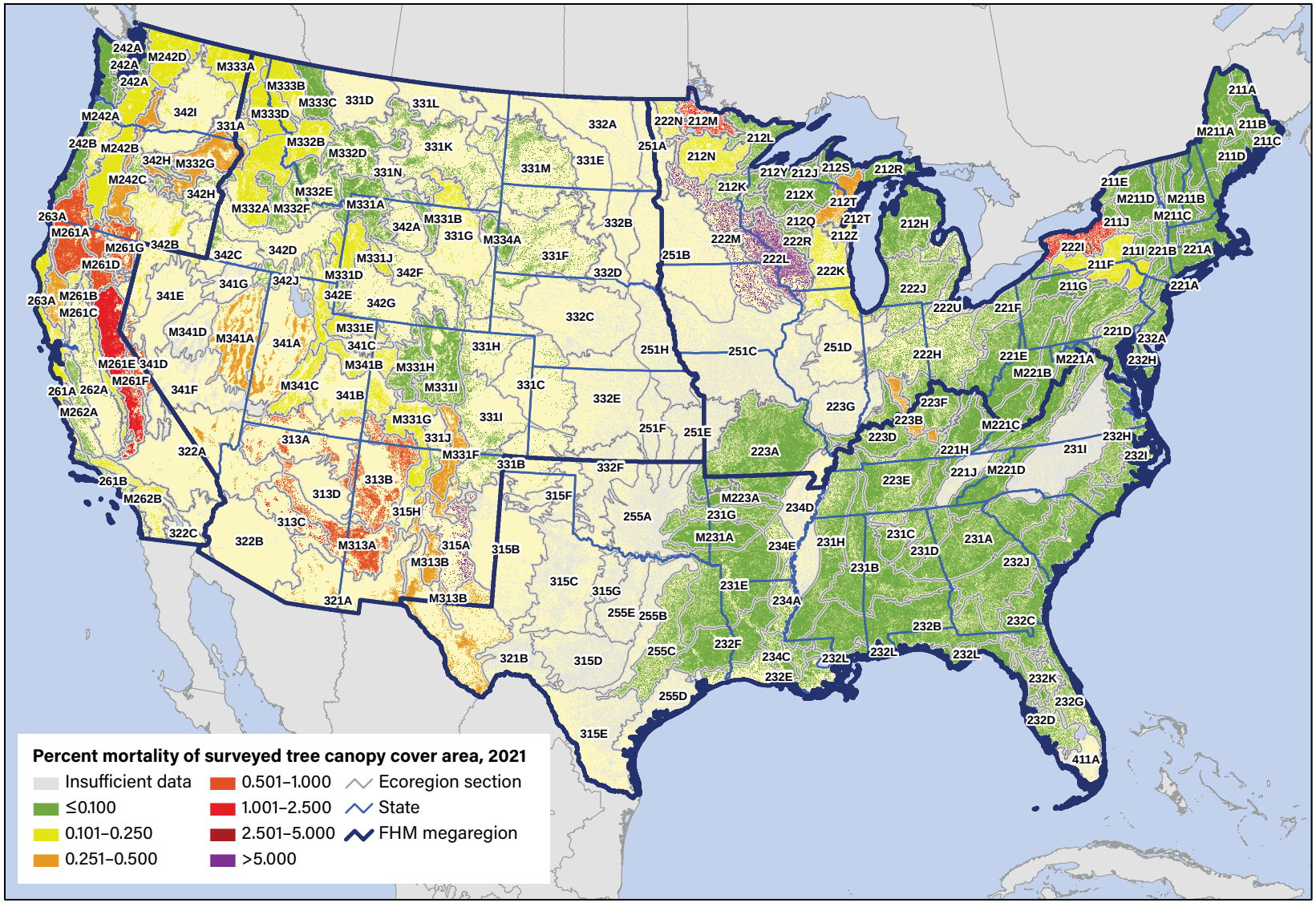

Figure 2.2—The percentage of surveyed tree canopy cover area with insect and disease mortality, by ecoregion section within the conterminous United States, for 2021. The gray lines delineate ecoregion sections (Cleland and others 2007), and blue lines delineate Forest Health Monitoring megaregions. The 240-m tree canopy cover is based on data from a cooperative project between the Multi-Resolution Land Characteristics Consortium (Coulston and others 2012) and the Forest Service Geospatial Technology and Applications Center using the 2011 National Land Cover Database. (Data source: U.S. Department of Agriculture, Forest Service, Forest Health Protection)

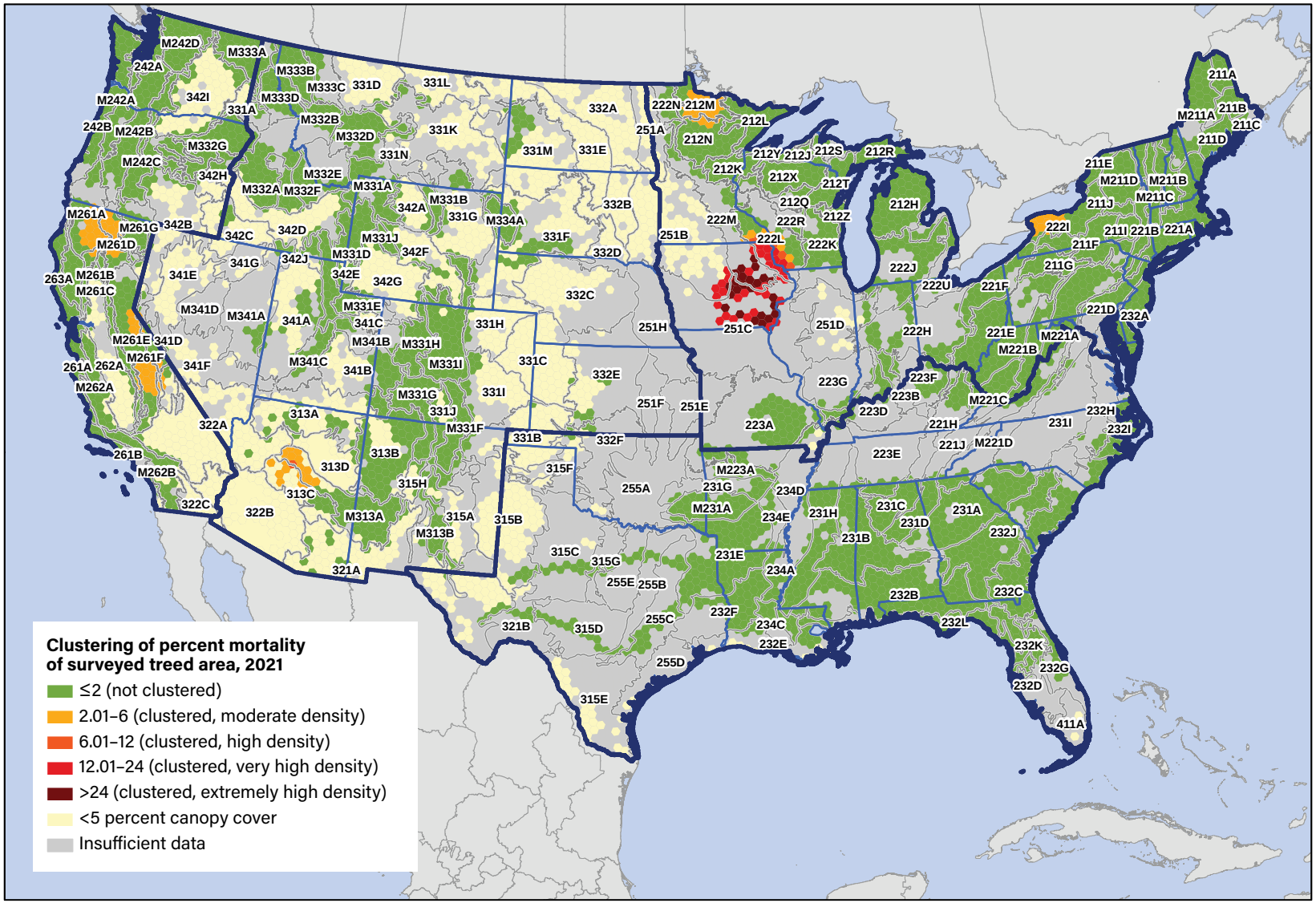

Figure 2.3—Hot spots of percentage of surveyed tree canopy cover area with insect and disease mortality in 2021 for the conterminous United States by hexagons containing >5-percent tree canopy cover. Values are Getis-Ord Gi scores, with values >2 representing significant clustering of high mortality occurrence densities and values <-2 representing significant clustering of low mortality occurrence densities. The gray lines delineate ecoregion sections (Cleland and others 2007), and blue lines delineate Forest Health Monitoring megaregions. Tree canopy cover is based on data from a cooperative project between the Multi-Resolution Land Characteristics Consortium (Coulston and others 2012) and the Forest Service Geospatial Technology and Applications Center using the 2011 National Land Cover Database. (Data source: U.S. Department of Agriculture, Forest Service, Forest Health Protection)*

M261G–Modoc Plateau (0.68 percent), and 341D–Mono (0.56 percent). California encompassed three hot spots of moderate mortality density, one in the northern part of the State and two in the Sierra Nevada (fig. 2.3).

Damage from 17 mortality agents and complexes was identified across 441 000 ha in the Interior West FHM megaregion in 2021 (table 2.3). The primary agent was the set of unknown bark beetles characterized as "Southwest bark beetle complex" in ponderosa pine forests, described above. This was associated with mortality on approximately 225 000 ha, or 51 percent of the total in the region. Other widespread agents were pinyon ips (*Ips confusus*) (66 000 ha, 15.1 percent), spruce beetle (*D. rufipennis*) (57 000 ha, 12.9 percent), Douglas-fir beetle (31 000 ha, 6.9 percent), and western balsam bark beetle (*Dryocoetes confusus*) (15 000 ha, 3.5 percent).

The Interior West ecoregion section with the highest mortality was 315A–Pecos Valley in east-central New Mexico (fig. 2.2), with mortality on 5.17 percent of surveyed tree canopy cover within the surveyed area. This mortality was associated with Southwest bark beetle complex, Douglas-fir beetle, and pinyon ips. These agents, along with fir engraver in white fir (*A. concolor*), were responsible for the relatively high levels of mortality in other ecoregion sections of the Southwest: 313C–Tonto Transition (1.56 percent), M313A–White Mountains-San Francisco Peaks-Mogollon Rim (0.93 percent), 313D–Painted Desert (0.75 percent), 313B–Navajo Canyonlands[1] (0.57 percent), and 313A–Grand Canyon (0.56 percent). A hot spot of moderate and high mortality densities occurred in M313A–White Mountains-San Francisco Peaks-Mogollon Rim and 313C–Tonto Transition (fig. 2.3).

Approximately 6500 ha in the Southern FHM megaregion had recorded damage from 12 mortality agents and complexes in 2021 (table 2.3). Ips engraver beetles represented the most widely detected agent, on 2800 ha or 44 percent of the total. The next two most widespread agents, the "unknown bark beetle" agent noted above and Douglas-fir beetle, caused damage in ponderosa pine forests of the Guadalupe Mountains of western Texas. As a result of these two agents, the 321A–Basin and Range ecoregion section of far-west Texas had 0.28-percent mortality of the surveyed tree canopy area (fig. 2.2).

Conterminous United States Defoliation

The national IDS in 2021 identified 56 defoliation agents and complexes affecting approximately 1.67 million ha within the area surveyed across the CONUS (table 2.4), which is almost equal to the land area of Hawaii. This is somewhat higher than in 2020, when defoliation across 1.54 million ha was attributed to 59 defoliating agents (Potter and Paschke 2022), although only about half as much area was surveyed in 2020. Spongy moth was the most widely detected defoliation agent in 2021, found on 1.02 million ha or 61.2 percent of the total defoliation area. This was a change from the previous 3 years, during which eastern spruce budworm was the most widely detected

[1] *This ecoregion section appears as 313B–Navaho Canyonlands in Cleland and others (2007).*

defoliation agent (Potter and Paschke 2022; Potter and others 2020b, 2021). In 2021, eastern spruce budworm was identified on about 183 000 ha, or 10.9 percent of the total. This was followed by western spruce budworm (*C. freemani*) on 172 000 ha (10.3 percent of the total). No other agents were detected on >100 000 ha, but browntail moth (*Euproctis chrysorrhoea*) (80 000 ha, 4.8 percent), which is currently only a problem in the coastal region of the Northeast, and Gelechiid moths/needleminers (*Coleotechnites* spp.) (41 000 ha, 2.4 percent) were relatively widespread.

The Eastern FHM megaregion had by far the largest area on which defoliation was detected in 2021, 1.36 million ha (table 2.5). Surveyors identified 33 defoliation agents in the surveyed area, with three-quarters of the defoliation area attributed to spongy moth (1.02 million ha). Other major defoliators were eastern spruce budworm (183 000 ha, 13.4 percent), browntail moth (80 000 ha, 5.8 percent), and locust leafminer (*Odontota dorsalis*) (21 000 ha, 1.6 percent).

As in 2020, two ecoregion sections in the Great Lakes area exceeded 5-percent defoliation of surveyed canopy cover (fig. 2.4): 212H–Northern Lower Peninsula of Michigan and 212L–Northern Superior Uplands in northeastern Minnesota. The defoliation in the Lower Peninsula was caused by spongy moth in hardwood forests, while the Northern Superior Uplands mortality was the result of eastern spruce budworm in fir and spruce forests. These ecoregions encompassed three hot spots of very high defoliation density (fig. 2.5).

Table 2.4—Defoliation agents and complexes affecting >5000 ha in the conterminous United States in 2021

Agents/complexes causing defoliation, 2021	Area (ha)[a]
Spongy moth	1 024 902
Eastern spruce budworm	183 159
Western spruce budworm	171 926
Browntail moth	79 587
Gelechiid moths/needleminers	40 509
Pinyon needle scale	22 587
Locust leafminer	21 168
Unknown	17 180
Balsam woolly adelgid	14 432
Unknown defoliator	14 073
Maple leafcutter	10 541
Douglas-fir tussock moth	10 390
Other defoliator, known (code pending)	8937
Fall cankerworm	8447
Large aspen tortrix	8079
Forest tent caterpillar	8014
Larch casebearer	5300
Other (39)	25 816
Total, all defoliation agents	1 673 020

[a] All values are "footprint" areas for each agent or complex. The sum of the individual agents is not equal to the total for all agents due to the reporting of multiple agents per polygon.

Table 2.5—The top five defoliation agents or complexes for each Forest Health Monitoring megaregion and for Alaska and Hawaii in 2021

Defoliation agents and complexes, 2021	Area (ha)[a]
Eastern	
Spongy moth	1 017 414
Eastern spruce budworm	183 159
Browntail moth	79 587
Locust leafminer	21 168
Maple leafcutter	10 541
Other defoliation agents (28)	51 102
Total, all defoliation agents and complexes	1 362 419
Interior West	
Western spruce budworm	171 926
Gelechiid moths/needleminers	40 509
Pinyon needle scale	22 587
Unknown defoliator	13 647
Douglas-fir tussock moth	5549
Other defoliation agents (6)	7215
Total, all defoliation agents and complexes	261 059
Southern	
Spongy moth	7487
Loblolly pine sawfly	3425
Other defoliator	458
Dothistroma needle blight (*D. pini*)	454
Unknown	27
Total, all defoliation agents and complexes	11 852

Defoliation agents and complexes, 2021	Area (ha)[a]
West Coast	
Balsam woolly adelgid	14 432
Unknown	10 900
Douglas-fir tussock moth	4841
Lodgepole needleminer	3440
Lodgepole sawfly	1290
Other defoliation agents (13)	3888
Total, all defoliation agents and complexes	37 690
Alaska	
Western blackheaded budworm	210 412
Aspen leafminer	59 163
Birch leafminer	19 307
Rusty tussock moth	17 855
Unknown defoliator	6917
Other defoliation agents (37)	5800
Total, all defoliation agents and complexes	314 219
Hawaii	
ʻŌhiʻa/guava rust	0
Total, all defoliation agents and complexes	0

[a] The total area affected by other agents is listed at the end of each section. All values are "footprint" areas for each agent or complex. The sum of the individual agents is not equal to the total for all agents due to the reporting of multiple agents per polygon.

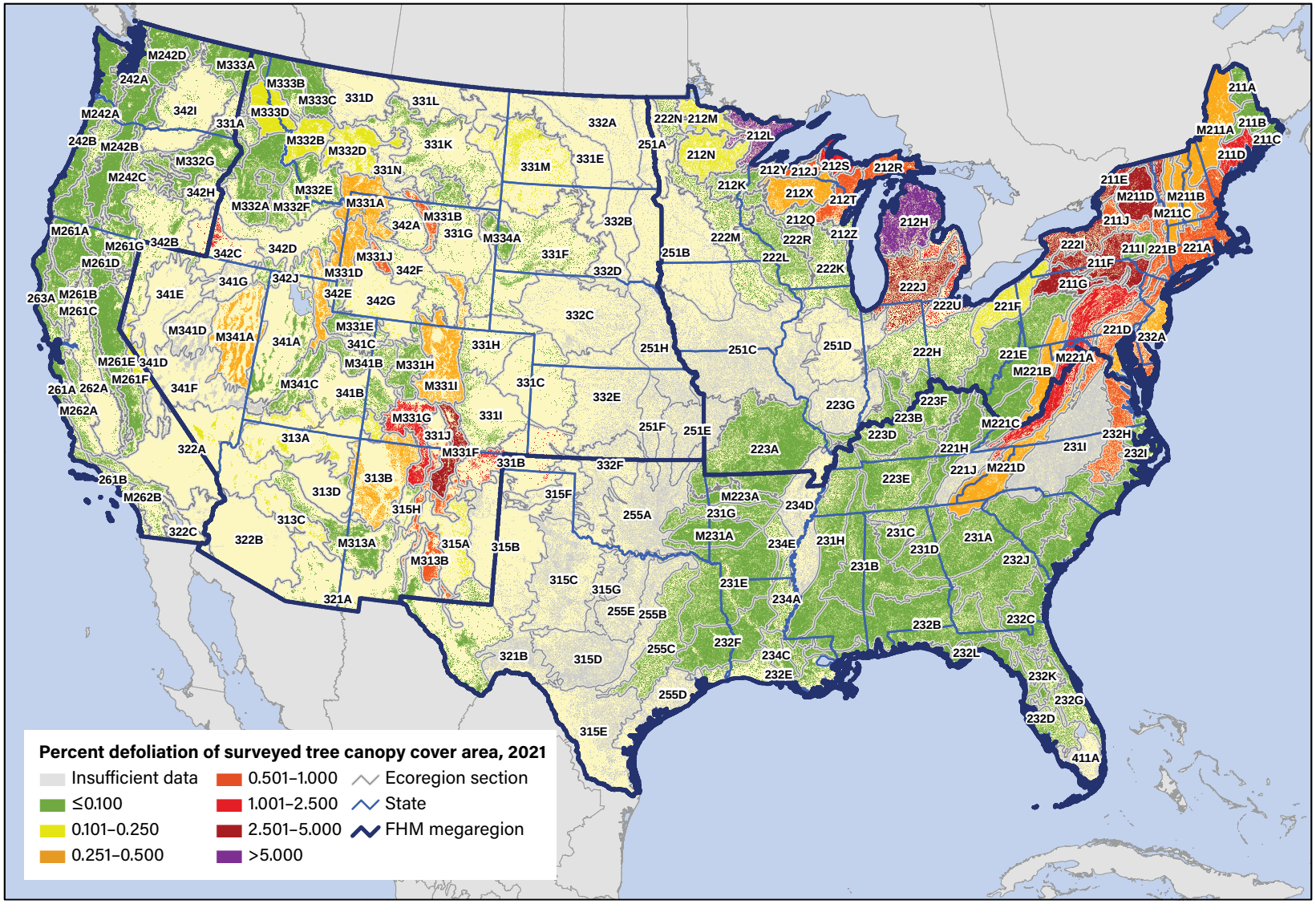

Figure 2.4—The percentage of surveyed tree canopy cover area with insect and disease defoliation, by ecoregion section within the conterminous United States, for 2021. The gray lines delineate ecoregion sections (Cleland and others 2007), and blue lines delineate Forest Health Monitoring megaregions. The 240-m tree canopy cover is based on data from a cooperative project between the Multi-Resolution Land Characteristics Consortium (Coulston and others 2012) and the Forest Service Geospatial Technology and Applications Center using the 2011 National Land Cover Database. (Data source: U.S. Department of Agriculture, Forest Service, Forest Health Protection)

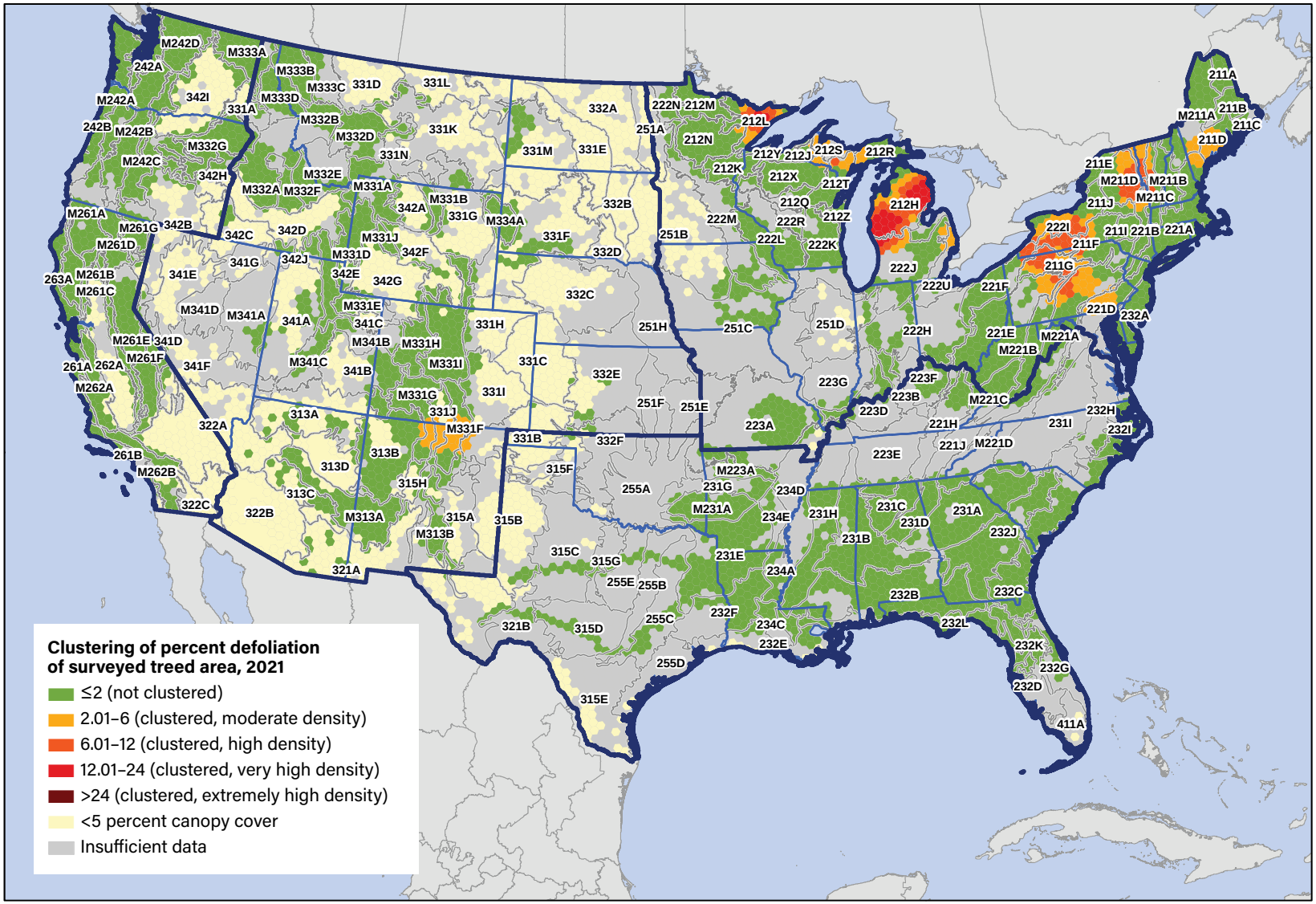

Figure 2.5—Hot spots of percentage of surveyed tree canopy cover area with insect and disease defoliation in 2021 for the conterminous United States by hexagons containing >5-percent tree canopy cover. Values are Getis-Ord Gi scores, with values >2 representing significant clustering of high defoliation occurrence densities. (No areas of significant clustering of low densities, <-2, were detected.) The gray lines delineate ecoregion sections (Cleland and others 2007), and blue lines delineate Forest Health Monitoring megaregions. Tree canopy cover is based on data from a cooperative project between the Multi-Resolution Land Characteristics Consortium (Coulston and others 2012) and the Forest Service Geospatial Technology and Applications Center using the 2011 National Land Cover Database. (Data source: U.S. Department of Agriculture, Forest Service, Forest Health Protection)*

The Eastern megaregion encompassed several other areas of high defoliation (>2.5 percent of surveyed canopy area). Several in New York and northern Pennsylvania were the result of spongy moth infestations (fig. 2.4):

- M211D–Adirondack Highlands (4.91-percent defoliation of surveyed canopy area)
- 211G–Northern Unglaciated Allegheny Plateau (4.85 percent)
- 211F–Northern Glaciated Allegheny Plateau (4.06 percent)
- 222I–Erie and Ontario Lake Plain (2.67 percent)
- 211E–St. Lawrence and Champlain Valley (2.66 percent)

These ecoregion sections were also the location of three hot spot areas of high defoliation density (fig. 2.5).

Farther west in the Great Lakes region, 2.88-percent defoliation in 222J–South Central Great Lakes on the Lower Peninsula of Michigan was caused by spongy moth, while the 2.75-percent defoliation of 212Y–Southwest Lake Superior Clay Plain (in northern Minnesota and Wisconsin and the Upper Peninsula of Michigan) was caused by large aspen tortrix (*Choristoneura conflictana*). Elsewhere, moderate levels of defoliation (1–2.5 percent) occurred in 212S–Northern Upper Peninsula (1.89 percent) because of an eastern spruce budworm outbreak, in 211D–Central Maine Coastal and Embayment (1.74 percent) because of a browntail moth infestation in northern red oak (*Quercus rubra*) stands, and in 222U–Lake Whittlesey Glaciolacustrine Plain (1.68 percent) and M221A–Northern Ridge and Valley (1.11 percent) because of spongy moth. All these areas had hot spots of at least moderate defoliation density (fig. 2.5).

In the Interior West FHM megaregion, 261 000 ha of damage in the surveyed area was attributed to 11 defoliators (table 2.5). As in recent years (Potter and Paschke 2022; Potter and others 2020b, 2021), western spruce budworm (172 000 ha) encompassed most of this area (65.9 percent). Gelechiid moths/needleminers were identified on 41 000 ha (15.5 percent), pinyon needle scale (*Matsucoccus acalyptus*) on 23 000 ha (8.7 percent), and Douglas-fir tussock moth (*Orgyia pseudotsugata*) on 6000 ha (2.1 percent).

The Interior West ecoregion section with the highest percent defoliation of surveyed canopy area (3.57 percent) was M331F–Southern Parks and Rocky Mountain Range, where outbreaks of Gelechiid moths/needleminers in ponderosa pine, western spruce budworm in fir and spruce, and an unknown defoliator in quaking aspen (*Populus tremuloides*) were detected (fig. 2.4). Meanwhile, western spruce budworm was the primary defoliation agent in the nearby M331G–South-Central Highlands ecoregion section (2.10-percent defoliation). Together, this damage caused a hot spot of moderate defoliation density in north-central New Mexico and south-central Colorado (fig. 2.5). Defoliation was also relatively high in M313B–Sacramento-Manzano Mountains to the south (0.77 percent), mostly because of pinyon needle scale.

Farther north, an outbreak of Douglas-fir tussock moth resulted in relatively high

defoliation (1.52 percent of surveyed canopy area) in 342C–Owyhee Highlands, while western spruce budworm was detected in M331J–Wind River Mountains (0.89 percent) and M331B–Bighorn Mountains (0.79 percent).

Meanwhile, 18 defoliating agents were recorded as affecting about 38 000 ha of surveyed area in the West Coast FHM megaregion during 2021 (table 2.5). Balsam woolly adelgid (*Adelges piceae*) was the most commonly detected, on 14 000 ha or 38.2 percent of all defoliation. An additional 11 000 ha of defoliation was attributed to an unknown defoliating agent (28.9 percent), while Douglas-fir tussock moth was detected on 4800 ha (12.8 percent) and lodgepole needleminer (*Coleotechnites milleri*) was found on 3400 ha (9.1 percent). No West Coast ecoregion section exceeded 1-percent defoliation of surveyed canopy area (fig. 2.4), and the megaregion did not encompass any defoliation hot spots (fig. 2.5).

In the Southern FHM megaregion, spongy moth (7500 ha, 63.1 percent of the total) was the most widely detected of five defoliation agents across 12 000 ha (table 2.5) within the surveyed area. Loblolly pine sawfly (*Neodiprion taedae linearis*) and Dothistroma needle blight (*Dothistroma pini*) were the other two identified defoliation agents, on 3400 ha and 500 ha, respectively (28.9 percent and 3.8 percent of defoliation area in the region). M221A–Northern Ridge and Valley in northern Virginia had 1.11-percent defoliation of the surveyed area (fig. 2.4) because of spongy moth detections. There were no defoliation hot spots in the megaregion (fig. 2.5).

Alaska and Hawaii

Surveyors detected 90 000 ha of mortality in Alaska in 2021 associated with nine agents (table 2.3), a slight increase in area from 2020. Spruce beetle, as in previous years, was the most widely detected mortality agent, representing 86.8 percent of the total for the State, across 78 000 ha. Two other mortality agents had a relatively extensive footprint, hemlock sawfly (*Neodiprion tsugae*), detected on 8500 ha (9.4 percent of the total), and yellow-cedar decline, identified on 3300 ha or 3.7 percent of the total.

As in 2020 (Potter and Paschke 2022), spruce beetle mortality was high in stands of white spruce (*Picea glauca*) in south-central Alaska (fig. 2.6), with extremely high 10.31-percent mortality across surveyed forest and shrubland in M133B–Alaska Range and a relatively high 2.58 percent in 133A–Cook Inlet Basin. M241C–Chugach-St. Elias Mountains also experienced spruce beetle mortality (0.31 percent). Meanwhile, mortality from hemlock sawfly in western hemlock (*Tsuga heterophylla*) stands and from yellow-cedar decline resulted in 0.15-percent mortality of the surveyed forest and shrubland of M241D–Alexander Archipelago in the Alaska panhandle.

Alaska experienced 314 000 ha of defoliation in 2021 (table 2.5), a considerable increase from the 68 000 ha detected in 2020 (Potter and Paschke 2022). This area was greater than any of the FHM regions in the CONUS except the Eastern, which experienced an extensive spongy moth outbreak. Of the 42 defoliating agents, western blackheaded budworm (*Acleris gloverana*) was the most

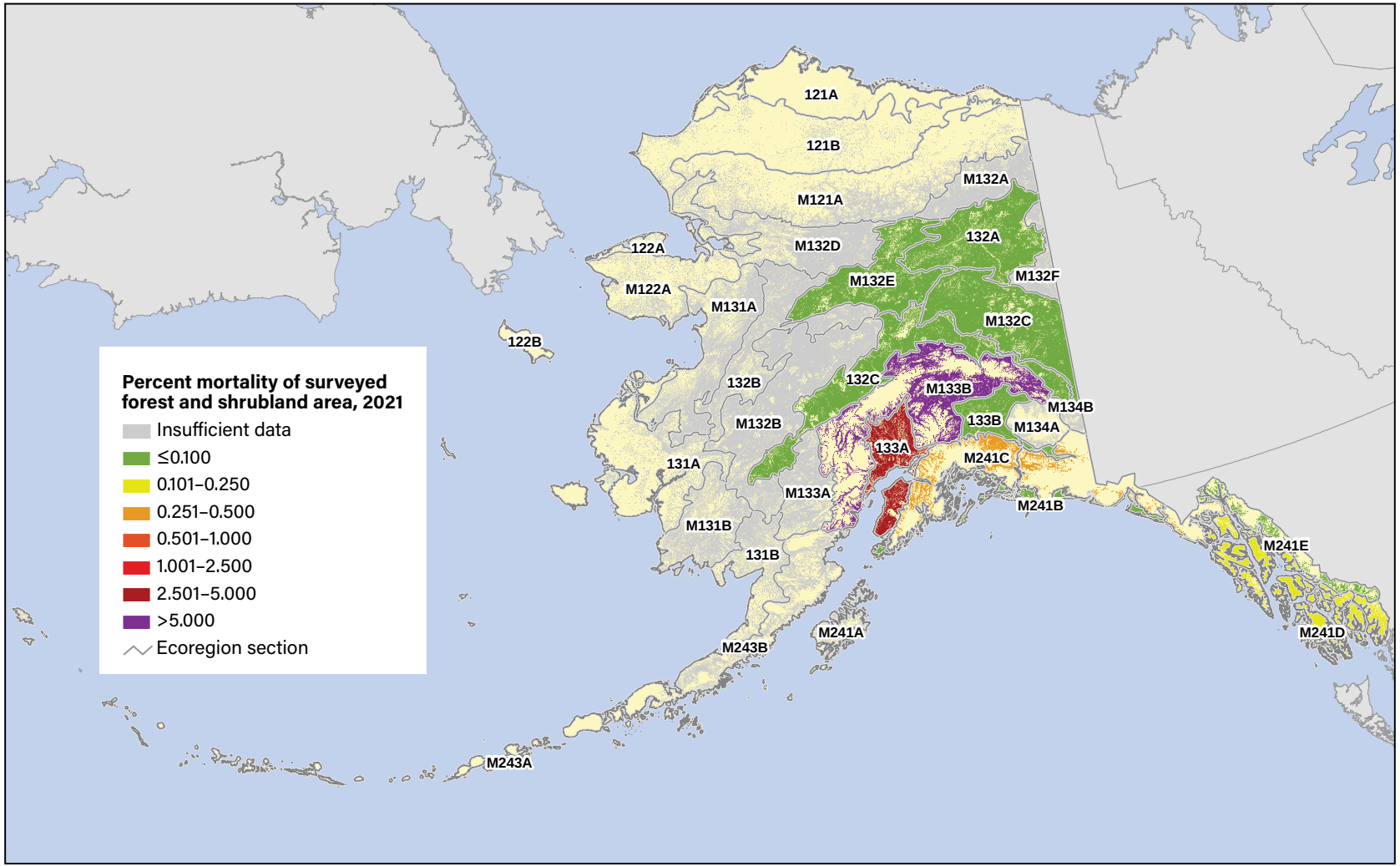

Figure 2.6—Percentage of 2021 surveyed Alaska forest and shrubland area within ecoregions with mortality caused by insects and diseases. The gray lines delineate ecoregion sections (Spencer and others 2002). Forest and shrub cover is derived from the 2011 National Land Cover Database. (Data source: U.S. Department of Agriculture, Forest Service, Forest Health Protection)

widely detected, on 210 000 ha, or 66.9 percent of the total defoliation area. Other widespread defoliators were aspen leafminer (*Phyllocnistis populiella*) on 59 000 ha (18.8 percent of the total), birch leafminer (*Fenusa pusilla*) on 19 000 ha (6.1 percent), and rusty tussock moth (*Orgyia antiqua*) on 18 000 ha (5.7 percent).

The highest levels of defoliation (5.03 percent of surveyed forest and shrubland) occurred in M241D–Alexander Archipelago in the Alaska panhandle, the location of a western blackheaded budworm outbreak in western hemlock (fig. 2.7). Four ecoregion sections in east-central Alaska had relatively high defoliation (>1 percent) because of activity by aspen leafminer, birch leafminer, and willow leaf blotchminer (*Micrurapteryx salicifoliella*):

- M132C–Yukon-Tanana Uplands (1.94 percent of surveyed forest and shrubland)
- M132E–Ray Mountains (1.49 percent)
- 132A–Yukon-Old Crow Basin (1.24 percent)
- 132C–Tanana-Kuskokwim Lowlands (1.15 percent).

Rusty tussock moth was the primary defoliator in M133B–Alaska Range (0.85-percent defoliation), while birch leafminer was detected in 133A–Cook Inlet Basin (0.35 percent).

Meanwhile, surveyors detected approximately 36 000 ha of mortality in Hawaii during 2021 (table 2.3), compared to 32 000 ha in 2020 (Potter and Paschke 2022) and 27 000 ha in 2019 (Potter and others 2021). While the mortality was not attributed to a specific agent, at least some of the damage was likely the result of rapid ʻōhiʻa death. This wilt disease is caused by two fungal pathogens, the more aggressive *Ceratocystis lukuohia* and the less aggressive *C. huliohia*, which both can kill ʻōhiʻa lehua (*Metrosideros polymorpha*) (Barnes and others 2018). This endemic species is the most abundant native tree in Hawaii, where it is deeply woven into Hawaiian culture (University of Hawaiʻi 2022). Both pathogens have been confirmed on Hawaiʻi Island, where most detections are of the more aggressive *C. lukuohia,* and on the island of Kauaʻi (University of Hawaiʻi 2022). In 2019, a small number of trees infected with *C. huliohia* were detected on Oʻahu and Maui, but it has not been detected on Maui since then (University of Hawaiʻi 2022).

Mortality was high across most of the montane wet ecoregions of Hawaiʻi Island, with extremely high mortality in Montane Wet-Hawaiʻi-Kaʻū (MWh-ka), where mortality was identified on 6.47 percent of the surveyed tree canopy area (fig. 2.8). Montane Wet-Hawaiʻi-Kona (MWh-ko) had 2.80-percent mortality, followed by Montane Wet-Hawaiʻi-Hilo-Puna (MWh-hp) (2.17 percent) and Montane Wet-Hawaiʻi-Kohala-Hāmākua (MWh-kh) (1.27 percent). There was 0.62-percent mortality of surveyed canopy area in the Mesic-Hawaiʻi ecoregion. High to moderate levels of mortality were also detected in three ecoregions on the island of Kauaʻi: Lowland Wet-Kauaʻi (LWk) (1.35 percent of surveyed tree canopy area), Montane Wet-Kauaʻi (MWk) (0.61 percent), and Mesic-Kauaʻi (MEk) (0.37 percent).

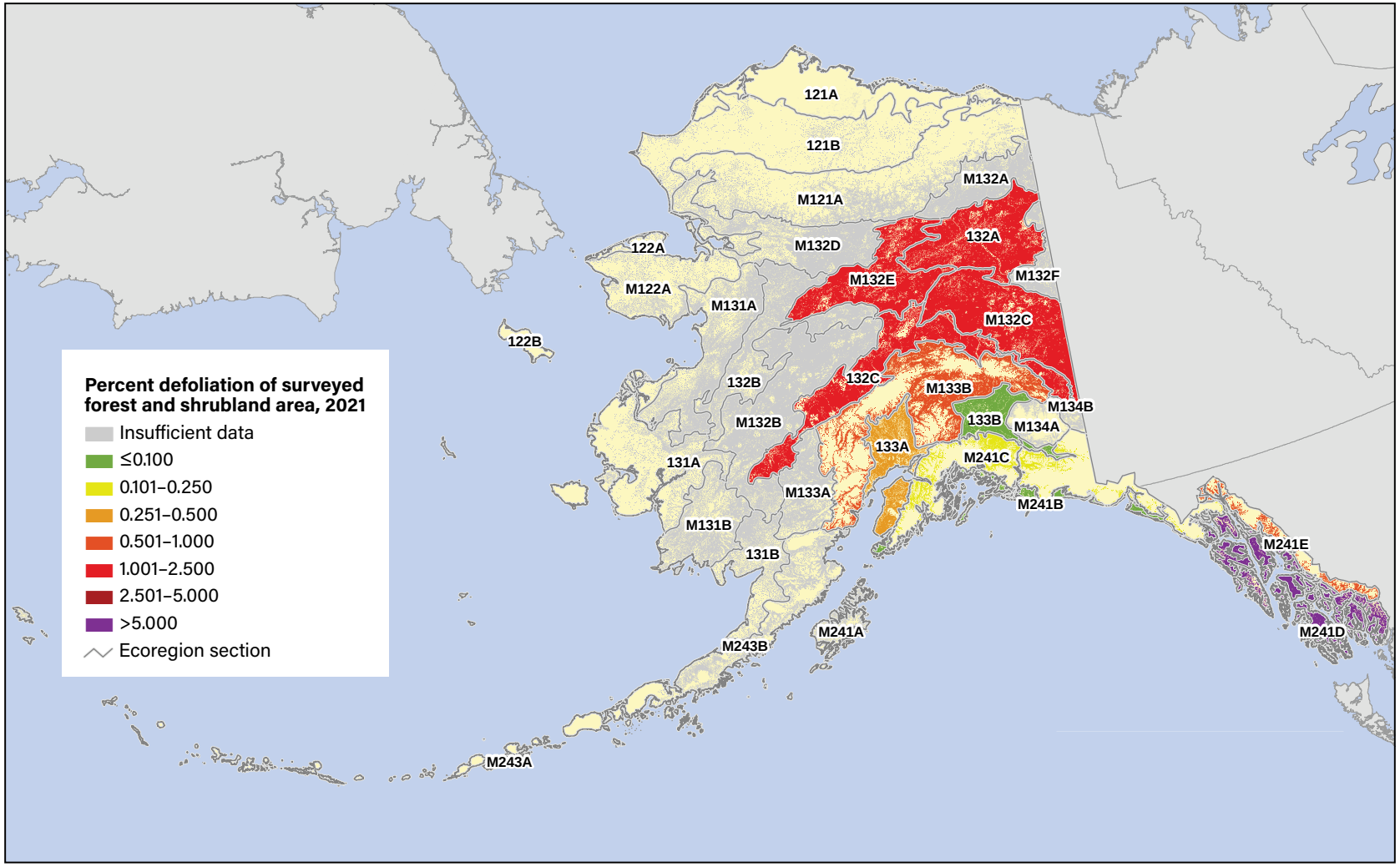

Figure 2.7—Percentage of 2021 surveyed Alaska forest and shrubland area within ecoregions with defoliation caused by insects and diseases. The gray lines delineate ecoregion sections (Spencer and others 2002). Forest and shrub cover is derived from the 2011 National Land Cover Database. (Data source: U.S. Department of Agriculture, Forest Service, Forest Health Protection)

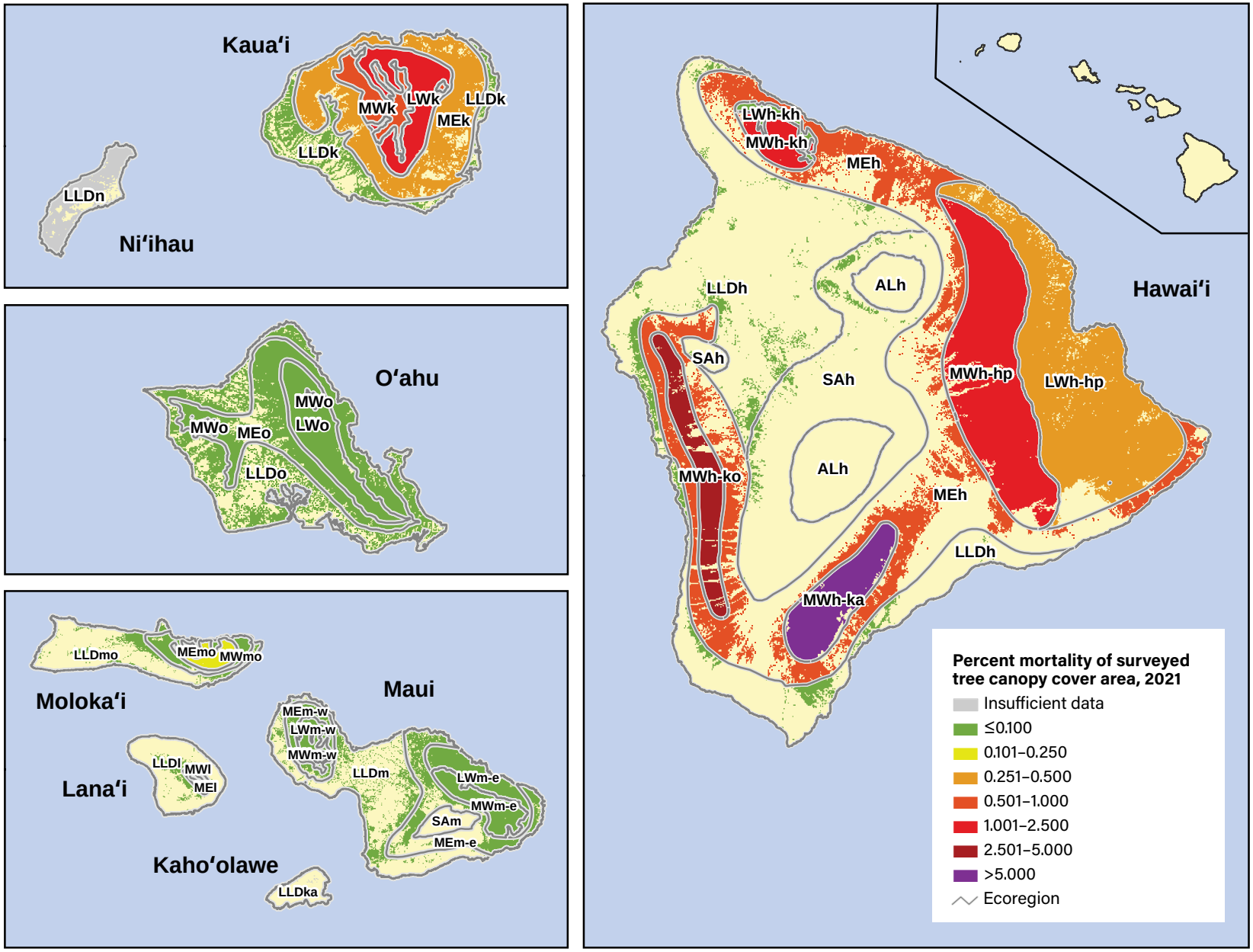

Figure 2.8—Percentage of 2021 surveyed Hawaii tree canopy area within island/ecoregion combinations with mortality caused by insects and diseases. Tree canopy cover is based on data from a cooperative project between the Multi-Resolution Land Characteristics Consortium (Coulston and others 2012) and the Forest Service Geospatial Technology and Applications Center using the 2011 National Land Cover Database. See table 1.1 for ecoregion identification. (Data source: U.S. Department of Agriculture, Forest Service, Forest Health Protection)

CONCLUSIONS

In 2021, forest health surveyors identified 60 mortality-causing agents and complexes across the CONUS on approximately 2.21 million ha, an area slightly less than the land area of New Hampshire. Emerald ash borer was the most widely detected mortality agent, identified on about 878 000 ha across the Eastern FHM megaregion, though mortality caused by this insect agent is challenging to map given the low density of ash in northern forests and other agents that also can cause ash mortality. This is consistent with recent years. Fir engraver caused extensive mortality in parts of the West, but the area of its impact has declined from recent years (e.g., Potter and others 2020b, 2021). As in recent years, Alaska experienced extensive mortality from spruce beetle, while much of the mortality in Hawaii may be associated with rapid ʻōhiʻa death.

Meanwhile, the national IDS reported damage in 2021 from 56 defoliation agents and complexes affecting approximately 1.67 million ha across the CONUS, almost equal to the land area of Hawaii. The majority of this defoliation was the result of a spongy moth outbreak, primarily in the Eastern FHM megaregion but in the Southern megaregion as well. Alaska had extensive defoliation, caused mostly by western blackheaded budworm in the Alexander Archipelago in the panhandle, as well as by aspen leafminer, birch leafminer, and rusty tussock moth in the interior of the State.

Continued monitoring of insect and disease outbreaks across the United States can guide appropriate follow-up investigation and management activities. Due to limitations of survey efforts to detect certain important forest insects and diseases, pests and pathogens discussed in this chapter do not include all the biotic forest health threats that are important to consider when making management decisions and budget allocations. However, large-scale assessments of mortality and defoliation severity represent a useful approach for identifying geographic areas where concentrations of monitoring and management activities might be most effective.

LITERATURE CITED

Abdulridha, J.; Ampatzidis, Y.; Ehsani, R.; de Castro, A. I. 2018. Evaluating the performance of spectral features and multivariate analysis tools to detect laurel wilt disease and nutritional deficiency in avocado. Computers and Electronics in Agriculture. 155: 203–211. https://doi.org/10.1016/j.compag.2018.10.016.

Anselin, L. 1992. Spatial data analysis with GIS: an introduction to application in the social sciences. Tech. Rep. 92-10. Santa Barbara, CA: National Center for Geographic Information and Analysis. 53 p.

Barnes, I.; Fourie, A.; Wingfield, M.J. [and others]. 2018. New Ceratocystis species associated with rapid death of *Metrosideros polymorpha* in Hawaii. Persoonia-Molecular Phylogeny and Evolution of Fungi. 40(1): 154–181. https://doi.org/10.3767/persoonia.2018.40.07.

Berryman, E.; McMahan, A. 2019. Using tree canopy cover data to help estimate acres of damage. In: Potter, K.M.; Conkling, B.L., eds. Forest Health Monitoring: national status, trends, and analysis 2018. Gen. Tech. Rep. SRS-239. Asheville, NC: U.S. Department of Agriculture, Forest Service, Southern Research Station: 125–141.

Brockerhoff, E.G.; Liebhold, A.M.; Jactel, H. 2006. The ecology of forest insect invasions and advances in their management. Canadian Journal of Forest Research. 36(2): 263–268. https://doi.org/10.1139/x06-013.

Castello, J.D.; Leopold, D.J.; Smallidge, P.J. 1995. Pathogens, patterns, and processes in forest ecosystems. BioScience. 45(1): 16–24. https://doi.org/10.2307/1312531.

Cleland, D.T.; Freeouf, J.A.; Keys, J.E. [and others]. 2007. Ecological subregions: sections and subsections for the conterminous United States. Gen. Tech. Rep. WO-76D. Washington, DC: U.S. Department of Agriculture, Forest Service. Map; Sloan, A.M., cartographer; presentation scale 1:3,500,000; colored. https://doi.org/10.2737/WO-GTR-76D.

Coleman, T.W.; Graves, A.D.; Heath, Z. [and others]. 2018. Accuracy of aerial detection surveys for mapping insect and disease disturbances in the United States. Forest Ecology and Management. 430: 321–336. https://doi.org/10.1016/j.foreco.2018.08.020.

Coulston, J.W.; Moisen, G.G.; Wilson, B.T. [and others]. 2012. Modeling percent tree canopy cover: a pilot study. Photogrammetric Engineering and Remote Sensing. 78(7): 715–727. https://doi.org/10.14358/PERS.78.7.715.

Edmonds, R.L.; Agee, J.K.; Gara, R.I. 2011. Forest health and protection. Long Grove, IL: Waveland Press, Inc. 667 p.

ESRI. 2017. ArcMap® 10.5.1. Redlands, CA: Environmental Systems Research Institute.

Forest Health Protection (FHP). 2019. Digital Mobile Sketch Mapping user's manual 2.1. Fort Collins, CO: U.S. Department of Agriculture, Forest Service, Forest Health Assessment and Applied Sciences Team. https://www.fs.usda.gov/foresthealth/technology/docs/DMSM_Tutorial/story_content/external_files/DMSM_User_Guide.pdf. [Date accessed: August 10, 2022].

Forest Health Protection (FHP). 2022. Insect and Disease Detection Survey (IDS) data downloads. Fort Collins, CO: U.S. Department of Agriculture, Forest Service, Forest Health Technology Enterprise Team. https://www.fs.usda.gov/foresthealth/applied-sciences/mapping-reporting/detection-surveys.shtml. [Date accessed: August 10, 2022].

Getis, A.; Ord, J.K. 1992. The analysis of spatial association by use of distance statistics. Geographical Analysis. 24(3): 189–206. https://doi.org/10.1111/j.1538-4632.1992.tb00261.x.

Hanavan, R.P.; Pontius, J.; Hallett, R. 2015. A 10-year assessment of hemlock decline in the Catskill Mountain region of New York State using hyperspectral remote sensing techniques. Journal of Economic Entomology. 108(1): 339–349. https://doi.org/10.1093/jee/tou015.

Hanavan, R.P.; Kamoske, A.G.; Schaaf, A.N. [and others]. 2021. Supplementing the Forest Health National Aerial Survey Program with remote sensing during the COVID-19 pandemic: lessons learned from a collaborative approach. Journal of Forestry. 2021: 1–8. https://doi.org/10.1093/jofore/fvab056.

Holdenrieder, O.; Pautasso, M.; Weisberg, P.J.; Lonsdale, D. 2004. Tree diseases and landscape processes: the challenge of landscape pathology. Trends in Ecology & Evolution. 19(8): 446–452. https://doi.org/10.1016/j.tree.2004.06.003.

Homer, C.G.; Dewitz, J.A.; Yang, L. [and others]. 2015. Completion of the 2011 National Land Cover Database for the conterminous United States: representing a decade of land cover change information. Photogrammetric Engineering and Remote Sensing. 81(5): 345–354.

Laffan, S.W. 2006. Assessing regional scale weed distributions, with an Australian example using *Nassella trichotoma*. Weed Research. 46(3): 194–206. https://doi.org/10.1111/j.1365-3180.2006.00491.x.

Liebhold, A.M.; McCullough, D.G.; Blackburn, L.M. [and others]. 2013. A highly aggregated geographical distribution of forest pest invasions in the USA. Diversity and Distributions. 19: 1208–1216. https://doi.org/10.1111/ddi.12112.

Logan, J.A.; Regniere, J.; Powell, J.A. 2003. Assessing the impacts of global warming on forest pest dynamics. Frontiers in Ecology and the Envionment. 1: 130–137. https://doi.org/10.1890/1540-9295(2003)001[0130:ATIOGW]2.0.CO;2.

Lovett, G.M.; Weiss, M.; Liebhold, A.M. [and others]. 2016. Nonnative forest insects and pathogens in the United States: impacts and policy options. Ecological Applications. 26: 1437–1455. https://doi.org/10.1890/15-1176.

Mack, R.N.; Simberloff, D.; Lonsdale, W.M. [and others]. 2000. Biotic invasions: causes, epidemiology, global consequences, and control. Ecological Applications. 10(3): 689–710. https://doi.org/10.1890/1051-0761(2000)010[0689:BICEGC]2.0.CO;2.

Manion, P.D. 2003. Evolution of concepts in forest pathology. Phytopathology. 93: 1052–1055. https://doi.org/10.1094/PHYTO.2003.93.8.1052.

Parry, D.; Teale, S.A. 2011. Alien invasions: the effects of introduced species on forest structure and function. In: Castello, J.D.; Teale, S.A., eds. Forest health: an integrated perspective. New York: Cambridge University Press: 115–162. https://doi.org/10.1017/CBO9780511974977.006.

Pontius, J.; Hanavan, R.P.; Hallett, R.A. [and others]. 2017. High spatial resolution spectral unmixing for mapping ash species across a complex urban environment. Remote Sensing of Environment. 199: 360–369. https://doi.org/10.1016/j.rse.2017.07.027.

Potter, K.M. 2012. Large-scale patterns of insect and disease activity in the conterminous United States and Alaska from the national Insect and Disease Detection Survey database, 2007 and 2008. In: Potter, K.M.; Conkling, B.L., eds. Forest Health Monitoring 2009 national technical report. Gen. Tech. Rep. SRS-167. Asheville, NC: U.S. Department of Agriculture, Forest Service, Southern Research Station: 63–78.

Potter, K.M. 2013. Large-scale patterns of insect and disease activity in the conterminous United States and Alaska from the national Insect and Disease Detection Survey, 2009. In: Potter, K.M.; Conkling, B.L., eds. Forest Health Monitoring: national status, trends, and analysis 2010. Gen. Tech. Rep. SRS-176. Asheville, NC: U.S. Department of Agriculture, Forest Service, Southern Research Station: 15–29.

Potter, K.M. 2023. Ecological regions of Hawai'i. Fort Collins, CO: Forest Service Research Data Archive. https://doi.org/10.2737/RDS-2023-0018. [Date accessed: July 31, 2023].

Potter, K.M.; Canavin, J.C.; Koch, F.H. 2020a. A forest health retrospective: national and regional results from 20 years of Insect and Disease Survey data. In: Potter, K.M.; Conkling, B.L., eds. Forest Health Monitoring: national status, trends, and analysis 2019. Gen. Tech. Rep. SRS-250. Asheville, NC: U.S. Department of Agriculture, Forest Service, Southern Research Station: 125–149.

Potter, K.M.; Escanferla, M.E.; Jetton, R.M.; Man, G. 2019a. Important insect and disease threats to United States tree species and geographic patterns of their potential impacts. Forests. 10(4): 304. https://doi.org/10.3390/f10040304.

Potter, K.M.; Escanferla, M.E.; Jetton, R.M. [and others]. 2019b. Prioritizing the conservation needs of United States tree species: evaluating vulnerability to forest insect and disease threats. Global Ecology and Conservation. 18: e00622. https://doi.org/10.1016/j.gecco.2019.e00622.

Potter, K.M.; Koch, F.H. 2012. Large-scale patterns of insect and disease activity in the conterminous United States and Alaska, 2006. In: Potter, K.M.; Conkling, B.L., eds. Forest Health Monitoring 2008 national technical report. Gen. Tech. Rep. SRS-158. Asheville, NC: U.S. Department of Agriculture, Forest Service, Southern Research Station: 63–72.

Potter, K.M.; Koch, F.H.; Oswalt, C.M.; Iannone, B.V. 2016. Data, data everywhere: detecting spatial patterns in fine-scale ecological information collected across a continent. Landscape Ecology. 31: 67–84. https://doi.org/10.1007/s10980-015-0295-0.

Potter, K.M.; Paschke, J.L. 2013. Large-scale patterns of insect and disease activity in the conterminous United States and Alaska from the national Insect and Disease Detection Survey database, 2010. In: Potter, K.M.; Conkling, B.L., eds. Forest Health Monitoring: national status, trends, and analysis 2011. Gen. Tech. Rep. SRS-185. Asheville, NC: U.S. Department of Agriculture, Forest Service, Southern Research Station: 15–28.

Potter, K.M.; Paschke, J.L. 2014. Large-scale patterns of insect and disease activity in the conterminous United States and Alaska from the national Insect and Disease Survey database, 2011. In: Potter, K.M.; Conkling, B.L., eds. Forest Health Monitoring: national status, trends, and analysis 2012. Gen. Tech. Rep. SRS-198. Asheville, NC: U.S. Department of Agriculture, Forest Service, Southern Research Station: 19–34.

Potter, K.M.; Paschke, J.L. 2015a. Large-scale patterns of insect and disease activity in the conterminous United States and Alaska from the national Insect and Disease Survey, 2012. In: Potter, K.M.; Conkling, B.L., eds. Forest Health Monitoring: national status, trends, and analysis 2013. Gen. Tech. Rep. SRS-207. Asheville, NC: U.S. Department of Agriculture, Forest Service, Southern Research Station: 19–36.

Potter, K.M.; Paschke, J.L. 2015b. Large-scale patterns of insect and disease activity in the conterminous United States, Alaska, and Hawaii from the national Insect and Disease Survey, 2013. In: Potter, K.M.; Conkling, B.L., eds. Forest Health Monitoring: national status, trends, and analysis 2014. Gen. Tech. Rep. SRS-209. Asheville, NC: U.S. Department of Agriculture, Forest Service, Southern Research Station: 19–38.

Potter, K.M.; Paschke, J.L. 2016. Large-scale patterns of insect and disease activity in the conterminous United States and Alaska from the national Insect and Disease Survey, 2014. In: Potter, K.M.; Conkling, B.L., eds. Forest Health Monitoring: national status, trends, and analysis 2015. Gen. Tech. Rep. SRS-213. Asheville, NC: U.S. Department of Agriculture, Forest Service, Southern Research Station: 21–40.

Potter, K.M.; Paschke, J.L. 2017. Large-scale patterns of insect and disease activity in the conterminous United States and Alaska from the national Insect and Disease Survey, 2015. In: Potter, K.M.; Conkling, B.L., eds. Forest Health Monitoring: national status, trends, and analysis 2016. Gen. Tech. Rep. SRS-222. Asheville, NC: U.S. Department of Agriculture, Forest Service, Southern Research Station: 21–42.

Potter, K.M.; Paschke, J.L. 2022. Broad-scale patterns of insect and disease activity across the 50 United States from the national Insect and Disease Survey, 2020. In: Potter, K.M.; Conkling, B.L., eds. Forest Health Monitoring: national status, trends, and analysis, 2021. Gen. Tech. Rep. SRS-266. Asheville, NC: U.S. Department of Agriculture, Forest Service, Southern Research Station: 25–49. https://doi.org/10.2737/SRS-GTR-266-Chap2.

Potter, K.M.; Paschke, J.L.; Koch, F.H.; Berryman, E.M. 2020b. Large-scale patterns of insect and disease activity in the conterminous United States, Alaska, and Hawaii from the national Insect and Disease Survey, 2018. In: Potter, K.M.; Conkling, B.L., eds. Forest Health Monitoring: national status, trends, and analysis 2019. Gen. Tech. Rep. SRS-250. Asheville, NC: U.S. Department of Agriculture, Forest Service, Southern Research Station: 27–55.

Potter, K.M.; Paschke, J.L.; Koch, F.H.; Zweifler, M. 2019c. Large-scale patterns of insect and disease activity in the conterminous United States, Alaska, and Hawaii from the national Insect and Disease Survey, 2017. In: Potter, K.M.; Conkling, B.L., eds. Forest Health Monitoring: national status, trends, and analysis 2018. Gen. Tech. Rep. SRS-239. Asheville, NC: U.S. Department of Agriculture, Forest Service, Southern Research Station: 21–49.

Potter, K.M.; Paschke, J.L.; Berryman, E.M. 2021. Large-scale patterns of insect and disease activity in the conterminous United States, Alaska, and Hawaii from the national Insect and Disease Survey, 2019. In: Potter, K.M.; Conkling, B.L., eds. Forest Health Monitoring: national status, trends, and analysis 2020. Gen. Tech. Rep. SRS-261. Asheville, NC: U.S. Department of Agriculture, Forest Service, Southern Research Station: 27–57.

Potter, K.M.; Paschke, J.L.; Zweifler, M. 2018. Large-scale patterns of insect and disease activity in the conterminous United States, Alaska, and Hawaii from the national Insect and Disease Survey, 2016. In: Potter, K.M.; Conkling, B.L., eds. Forest Health Monitoring: national status, trends, and analysis 2017. Gen. Tech. Rep. SRS-233. Asheville, NC: U.S. Department of Agriculture, Forest Service, Southern Research Station: 23–44.

Reams, G.A.; Smith, W.D.; Hansen, M.H. [and others]. 2005. The Forest Inventory and Analysis sampling frame. In: Bechtold, W.A.; Patterson, P.L., eds. The enhanced Forest Inventory and Analysis program—national sampling design and estimation procedures. Asheville, NC: U.S. Department of Agriculture, Forest Service, Southern Research Station: 11–26.

Shima, T.; Sugimoto, S.; Okutomi, M. 2010. Comparison of image alignment on hexagonal and square lattices. In: 2010 IEEE international conference on image processing. [Place of publication unknown]: Institute of Electrical and Electronics Engineers, Inc.: 141–144. https://doi.org/10.1109/icip.2010.5654351.

Slaton, M.R.; Warren, K.; Koltunov, A.; Smith, S. 2021. Accuracy assessment of Insect and Disease Survey and eDART for monitoring forest health. In: Potter, K.M.; Conkling, B.L., eds. Forest Health Monitoring: national status, trends, and analysis 2020. Gen. Tech. Rep. SRS-261. Asheville, NC: U.S. Department of Agriculture, Forest Service, Southern Research Station: 187–195.

Spencer, P.; Nowacki, G.; Fleming, M. [and others]. 2002. Home is where the habitat is: an ecosystem foundation for wildlife distribution and behavior. Arctic Research of the United States. 16: 6–17.

Teale, S.A.; Castello, J.D. 2011. Regulators and terminators: the importance of biotic factors to a healthy forest. In: Castello, J.D.; Teale, S.A., eds. Forest health: an integrated perspective. New York: Cambridge University Press: 81–114. https://doi.org/10.1017/CBO9780511974977.005.

Tobin, P.C. 2015. Ecological consequences of pathogen and insect invasions. Current Forestry Reports. 1: 25–32. https://doi.org/10.1007/s40725-015-0008-6.

University of Hawai'i, College of Tropical Agriculture and Human Resources. 2022. Rapid 'ōhi'a death. http://rapidohiadeath.org. [Date accessed: July 12, 2022].

White, D.; Kimerling, A.J.; Overton, W.S. 1992. Cartographic and geometric components of a global sampling design for environmental monitoring. Cartography and Geographic Information Systems. 19(1): 5–22. https://doi.org/10.1559/152304092783786636.

Zhang, L.; Rubin, B.D.; Manion, P.D. 2011. Mortality: the essence of a healthy forest. In: Castello, J.D.; Teale, S.A., eds. Forest health: an integrated perspective. New York: Cambridge University Press: 17–49. https://doi.org/10.1017/CBO9780511974977.003.

CHAPTER 3

Broad-Scale Patterns of Forest Fire Occurrence Across the United States and the Caribbean Territories, 2021

Kevin M. Potter

INTRODUCTION

Wildland fire is a pervasive disturbance agent in many forest ecosystems across the United States, causing widespread tree damage and mortality and impacting forest health both positively and negatively (Agee 1998, Thom and Seidl 2016, Wade and others 2000). Some forest types and tree species are adapted to fire under certain intensities and return intervals (Hanberry and others 2018, Jeronimo and others 2019). In some ecosystems, wildland fire has been essential for regulating processes that maintain forest health (Lundquist and others 2011). For example, it is an important ecological mechanism that shapes the distributions of species, maintains the structure and function of fire-prone communities, and acts as a significant evolutionary force (Bond and Keeley 2005, Pausas and Keeley 2019).

At the same time, wildland fires have created forest health and sustainability problems in some ecosystems (Edmonds and others 2011). Fires in some regions and ecosystems have become larger, more intense, and more damaging because of the accumulation of fuels from prolonged fire suppression (Pyne 2010). Robust research indicates that climate change, via more common drought conditions and higher temperatures, has already played a role in increased wildfire activity (Abatzoglou and Williams 2016, Higuera and Abatzoglou 2021). Current fire regimes on more than half the forested area in the conterminous United States (CONUS) have been moderately or significantly altered from historical regimes (Barbour and others 1999), potentially altering key ecosystem components, such as species composition, structural stage, stand age, canopy closure, and fuel loadings (Schmidt and others 2002, Stephens and others 2018). Evidence, in fact, suggests that few entirely natural fire regimes remain in North America (Parisien and others 2016). Such changes in fire intensity and recurrence could result in decreased forest resilience and persistence (Lundquist and others 2011), with plant communities in some regions undergoing rapid compositional and structural changes following fire suppression (Coop and others 2020, Nowacki and Abrams 2008).

In addition to their ecological and forest health consequences, large wildland fires also can have long-lasting social and economic consequences, including the loss of human life and property, smoke-related human health impacts, and the economic cost and dangers of fighting the fires themselves (Gill and others 2013, Richardson and others 2012). These impacts are particularly intense within the wildland-urban interface, the zone in which human development mixes with forest (Calkin and others 2015, Radeloff and others 2018). Additionally, exposure to wildfire smoke may have increased SARS-CoV-2 positivity rates among the public and thereby exacerbated the COVID-19 pandemic (Kiser and others 2021), while inhalation of wildfire smoke may have exposed firefighters to increased likelihood of SARS-CoV-2 infection and increased COVID-19 disease severity (Navarro and others 2021).

This chapter presents analyses of daily satellite-based fire occurrence data that map and quantify the locations and intensities of fire occurrences spatially across the CONUS, Alaska, Hawaii, and

How to cite this chapter:

Potter, Kevin M. 2023. Broad-scale patterns of forest fire occurrence across the United States and the Caribbean territories, 2021. In: Potter, Kevin M.; Conkling, Barbara L., eds. Forest Health Monitoring: national status, trends, and analysis 2022. Gen. Tech. Rep. SRS-273. Asheville, NC: U.S. Department of Agriculture, Forest Service, Southern Research Station: 55–81. https://doi.org/10.2737/SRS-GTR-273-Chap3.

the Caribbean territories in 2021. It also compares 2021 fire occurrences, within a geographic context, to all the recent years for which such data are available. Quantifying and monitoring such large-scale patterns of fire occurrence across the United States, as described in this chapter, can help improve our understanding of the ecological and economic impacts of fire. Specifically, large-scale assessments of fire occurrence can help identify areas where specific management activities may be needed, or where research into the ecological and socioeconomic impacts of fires would be beneficial.

METHODS

Data

The Moderate Resolution Imaging Spectroradiometer (MODIS) Rapid Response System (Justice and others 2002, 2011) extracts fire location and intensity information from the thermal infrared bands of imagery collected daily by two satellites at a resolution of 1 km, with the center of a pixel recorded as a fire occurrence (NASA Fire Information for Resource Management System 2022a). The MODIS Active Fire Detections for the United States database (NASA Fire Information for Resource Management System 2022b) allows analysts to spatially display and summarize fire occurrences across broad geographic regions for monitoring and reporting of wildland fire events (Coulston and others 2005; Potter 2012a, 2012b, 2013a, 2013b, 2014, 2015a, 2015b, 2016, 2017, 2018, 2019, 2020, 2021, 2022). The Terra and Aqua satellites' MODIS sensors identify the presence of a fire at the time of image collection by using a contextual algorithm that exploits the strong emission of mid-infrared radiation from fires (Giglio and others 2003). A fire occurrence is defined as one daily satellite detection of wildland fire in an approximately 1-km pixel, with multiple fire occurrences possible on a pixel across multiple days resulting from a single wildland fire that lasts more than 1 day. The resulting fire occurrence data represent only whether a fire was active because the MODIS data bands may not differentiate between a hot fire in a relatively small area (0.01 km^2, for example) and a cooler fire over a larger area (1 km^2, for example) if the foreground-to-background temperature contrast is not sufficiently high. The MODIS Active Fire database does well at capturing large fires during cloud-free conditions but may underrepresent rapidly burning, small, and low-intensity fires, as well as fires in areas with frequent cloud cover (Hawbaker and others 2008). The likelihood of detecting a fire beneath a tree canopy is probably low given the smaller general size of such fires and the fact that they are obscured by the canopy (Giglio and others 2018). For large-scale assessments, the dataset represents a good alternative to the use of ignition point information, which can be difficult to obtain or may not exist for many fires (Tonini and others 2009). The fire occurrence data additionally do not distinguish fires intentionally set for management purposes (controlled burns), which are common in some parts of the United States, such as the South, where many prescribed fires are smaller and/or lower severity and thus not detected by satellite sensors (Nowell and others 2018).

More information about the performance of this product is provided by Justice and others (2011).

It is important to underscore that estimates of burned area (e.g., Monitoring Trends in Burn Severity data [Eidenshink and others 2007, Picotte and others 2020]) and calculations of MODIS-detected fire occurrences are two different metrics for quantifying fire activity within a given year. Most importantly, the MODIS data contain both spatial and temporal components because persistent fire will be detected repeatedly over several days on a given 1-km pixel. In other words, a location can have a fire occurrence multiple times, once for each day a fire is detected at the location. Analyses of the MODIS-detected fire occurrences, therefore, measure the total number of daily 1-km pixels with fire during a year, as opposed to quantifying only the area on which fire occurred at some point during that timeframe. A fire detected on a single pixel every day for a week, for example, would be equivalent to seven fire occurrences.

The Terra and Aqua satellites that carry the MODIS sensors were launched in 1999 and 2002, respectively, and will be decommissioned eventually. An alternative fire occurrence data source is the Visible Infrared Imaging Radiometer Suite (VIIRS) sensors on board the Suomi National Polar-orbiting Partnership (Suomi NPP) and NOAA-20 weather satellites. The transition to VIIRS data for national and regional fire occurrence monitoring will require a comparison of fire occurrence detections between it and MODIS. This is because science-ready VIIRS fire data are available from 2015 onward (NASA Fire Information for Resource Management System 2022a) compared to more than 20 years for the MODIS data. It would be ideal for assessments of fire occurrence trends to analyze as long a temporal window as possible (i.e., from near the beginning of MODIS data availability), encompassing the combination of older MODIS data with newer VIIRS data.

Analyses

Using ArcMap® (ESRI 2017), I processed these MODIS products for 2021 and for the 20 preceding full years of data (beginning in 2001 because of issues with data collection and processing from the Terra satellite in 2000) to determine forest fire occurrence density for (1) ecoregion sections in the CONUS (Cleland and others 2007), (2) ecoregions on each of the major islands of Hawaii (Potter 2023), and (3) the islands of the Caribbean territories of Puerto Rico and the U.S. Virgin Islands. Fire occurrence density is the number of fire occurrences per 100 km^2 (10 000 ha) of tree canopy cover area. I calculated forest fire occurrence density metrics for the CONUS, Hawaii, and the Caribbean territories for each year after screening out wildland fires that did not intersect with tree canopy data. The tree canopy data had been resampled to 240 m from a 30-m raster dataset that estimates percentage of tree canopy cover (from 0 to 100 percent) for each grid cell. This dataset was generated from the 2011 National Land Cover Database (NLCD) (Homer and others 2015) through a cooperative project between the Multi-Resolution Land Characteristics Consortium and the U.S. Department of Agriculture, Forest Service,

Geospatial Technology and Applications Center (GTAC) (Coulston and others 2012). I treated any cell with >0-percent tree canopy cover as forest. Comparable tree canopy cover data were not available for Alaska, so I instead created a 240-m-resolution layer of forest and shrub cover from the 2011 NLCD. I then intersected the MODIS fire occurrence detection data with this layer and with ecoregion sections (Spencer and others 2002) to calculate the number of fire occurrences per 100 km^2 of forest and shrub cover within each ecoregion section in Alaska.

I also separately determined the total numbers of forest fire occurrences for the CONUS, Alaska, Hawaii, and the Caribbean territories after clipping the MODIS fire occurrences by the tree canopy cover or tree and shrub cover data.

I compared the fire occurrence density value for each of the ecoregions of the States and for the Caribbean territories in 2021 with the mean fire density values for the first 20 full years of MODIS Active Fire data collection (2001–2020). Specifically, I divided the difference of the 2021 value and the previous 20-year mean for the area by the standard deviation across the previous 20-year period, assuming a normal distribution of fire density over time. The result for each ecoregion was a standardized z-score, which is a dimensionless quantity describing the degree to which the fire occurrence density in the area in 2021 was higher, lower, or the same relative to all the previous years for which data have been collected, accounting for the variability in the previous years. The z-score is the number of standard deviations between the observation and the mean of the historic observations in the previous years. Approximately 68 percent of observations would be expected within one standard deviation of the mean, and 95 percent within two standard deviations. Near-normal conditions are those within a single standard deviation of the mean, although such a threshold is somewhat arbitrary. Conditions between about one and two standard deviations of the mean are moderately different from mean conditions but are not significantly different statistically. Those outside about two standard deviations would be considered statistically greater than or less than the long-term mean (p <0.025 at each tail of the distribution).

Additionally, I used the Spatial Association of Scalable Hexagons (SASH) analytical approach to identify forested areas in the CONUS with higher than expected fire occurrence density in 2021. This method identifies locations where ecological phenomena occur at greater or lower occurrences than expected by random chance and is based on a sampling frame optimized for spatial neighborhood analysis, adjustable to the appropriate spatial resolution, and applicable to multiple data types (Potter and others 2016). Specifically, it consists of dividing an analysis area into scalable equal-area hexagonal cells within which data are aggregated, followed by identifying statistically significant geographic clusters of hexagonal cells within which mean values are greater or less than those expected by chance. To identify these clusters, I employed a Getis-Ord G_i^* hot spot analysis (Getis and Ord 1992) in ArcMap® 10.5.1 (ESRI 2017).

The spatial units of analysis were 9,810 hexagonal cells, each approximately 834 km^2 in

area, generated in a lattice across the CONUS using intensification of the Environmental Monitoring and Assessment Program (EMAP) North American hexagon coordinates (White and others 1992). These coordinates are the foundation of a sampling frame in which a hexagonal lattice was projected onto the CONUS by centering a large base hexagon over the region (Reams and others 2005, White and others 1992). The hexagons are compact and uniform in their distance to the centroids of neighboring hexagons, meaning that a hexagonal lattice has a higher degree of isotropy (uniformity in all directions) than does a square grid (Shima and others 2010). These attributes are highly useful for spatial neighborhood analyses. Importantly, these scalable hexagons also are independent of geopolitical and ecological boundaries, avoiding the possibility of different sample units (such as counties, States, or watersheds) encompassing vastly different areas (Potter and others 2016). I selected hexagons 834 km^2 in area because this is a manageable size for making monitoring and management decisions in analyses across the CONUS (Potter and others 2016).

Fire occurrence density values were calculated as the number of forest fire occurrences per 100 km^2 of tree canopy cover area within a hexagon. I used the Getis-Ord G_i^* statistic to identify clusters of hexagonal cells with fire occurrence density values higher than expected by chance. This statistic allows for the decomposition of a global measure of spatial association into its contributing factors, by location, and is therefore particularly suitable for detecting outlier assemblages of similar conditions in a dataset, such as when spatial clustering is concentrated in one subregion of the data (Anselin 1992).

Briefly, G_i^* sums the differences between the mean values in a local sample, determined in this case by a moving window of each hexagon and its 18 first- and second-order neighbors (the 6 adjacent hexagons and the 12 additional hexagons contiguous to those 6) and the global mean of the 9,644 hexagonal cells with tree canopy cover (of the total 9,810) in the CONUS. As described in Laffan (2006), it is calculated as:

$$G_i^*(\boldsymbol{d}) = \frac{\sum_j w_{ij}(d)x_j - W_i^*\bar{x}^*}{s^*\sqrt{\frac{(ns_{1i}^*) - W_i^{*2}}{n-1}}}$$

where

G_i^* = the local clustering statistic (in this case, for the target hexagon)

i = the center of local neighborhood (the target hexagon)

d = the width of local sample window (the target hexagon and its first- and second-order neighbors)

x_j = the value of neighbor j

w_{ij} = the weight of neighbor j from location i (all the neighboring hexagons in the moving window were given an equal weight of 1)

n = the number of samples in the dataset (the 9,644 hexagons containing >5-percent tree cover and with at least 1 percent of the canopy cover surveyed)

W_i^* = the sum of the weights

s^*_{1i} = the number of samples within d of the central location (19: the focal hexagon and its 18 first- and second-order neighbors)

$\bar{x}^*$ = mean of whole dataset (in this case, the 9,644 hexagons)

s^* = the standard deviation of whole dataset (for the 9,644 hexagons)

G_i^* is standardized as a z-score with a mean of 0 and a standard deviation of 1, with values >1.96 representing significant local clustering of higher fire occurrence densities (p <0.025) and values <-1.96 representing significant clustering of lower fire occurrence densities (p <0.025), because 95 percent of the observations under a normal distribution should be within approximately two standard deviations of the mean (Laffan 2006). Values between -1.96 and 1.96 have no statistically significant concentration of high or low values. In other words, a hexagon and its 18 neighbors have a normal range of both high and low numbers of fire occurrences per 100 km^2 of tree canopy cover area. The threshold values are not exact because the correlation of spatial data violates the assumption of independence required for statistical significance (Laffan 2006). In addition, the Getis-Ord approach does not require that the input data be normally distributed, because the local G_i^* values are computed under a randomization assumption, with G_i^* equating to a standardized z-score that asymptotically tends to a normal distribution (Anselin 1992). The z-scores are reliable, even with skewed data, as long as the local neighborhood encompasses several observations (ESRI 2017): in this case, via the target hexagon and its 18 first- and second-order neighbors.

RESULTS AND DISCUSSION

Trends in Forest Fire Occurrence Detections for 2021

In 2021, the MODIS Active Fire database recorded 111,416 forest fire occurrences across the CONUS. This was the fourth highest in 21 full years of data collection but a 9-percent decrease in fire activity from 2020 (122,938 fire occurrences) (fig. 3.1). It was also 53 percent higher than the mean of the previous 20 years of data. At the same time, Alaska saw a 281-percent increase in fire occurrences (1,806) from 2020 (474) but a 93-percent decrease from the extremely high fire year of 2019 (26,493). The number of fire occurrences in 2021 was about 80 percent less than the mean for the preceding 2 decades. Also in 2021, 43 fire occurrences were detected in the State of Hawaii, an increase of 95 percent from 22 in 2020 but 84 percent below the 2001–2020 average of about 273 a year. Finally, Puerto Rico and the U.S. Virgin Islands experienced 13 fire occurrences, which was a 225-percent increase from 4 in 2020 and 44 percent above the average of about 9 per year.

These results are largely consistent with official national wildland fire statistics that track the numbers of wildfires reported and area burned (National Interagency Coordination Center 2022). The area burned in 2021 decreased to 2 883 645 ha from 4 096 364 ha in 2020, about 30 percent less. The number of reported wildfires, meanwhile, stayed approximately the same: 58,985

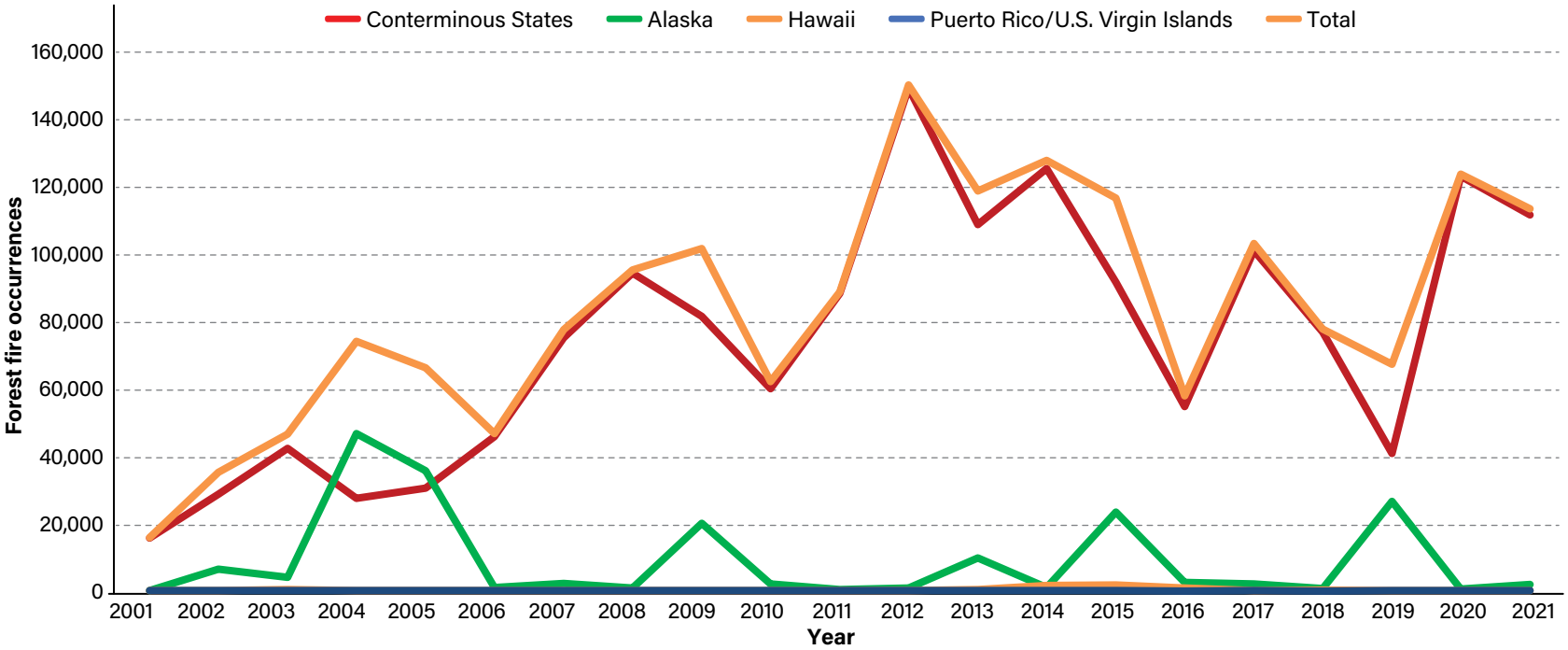

Figure 3.1—Forest fire occurrences detected by Moderate Resolution Imaging Spectroradiometer (MODIS) from 2001 through 2021 for the conterminous United States, Alaska, Hawaii, and Puerto Rico and the U.S. Virgin Islands, and for the entire Nation combined. (Data source: U.S. Department of Agriculture, Forest Service, Geospatial Technology and Applications Center, in conjunction with the NASA MODIS Rapid Response group)

compared to 58,950 the year before. Both area burned and number of fires in 2021 were similar to the 10-year average nationally but with more active years than normal for northern California, the Northern Rockies, the Pacific Northwest, and the northeastern quarter of the country (National Interagency Coordination Center 2022).

The National Interagency Coordination Center uses a benchmark threshold of 16 187 ha (40,000 acres) for tracking very large wildland fires and fire complexes. In 2021, 38 fires exceeded this threshold, compared to 50 in 2020 and 27 in 2019 (National Interagency Coordination Center 2020, 2021, 2022). Estimates of area burned and reported fires may be correlated with calculations of MODIS-detected fire occurrences, but as noted above, they are different metrics for quantifying fire activity.

The analysis of the 2021 MODIS wildland fire occurrence data indicates that, like 2020 (Potter 2022), the highest (extremely high) fire occurrence densities were present in the northwestern and Sierra Nevada regions of California, along with central Oregon and Washington (fig. 3.2). One ecoregion section in the Pacific Northwest had a very high fire occurrence density, while high densities were detected in the Pacific Northwest, the Northern Rockies, central Arizona and west-central New Mexico, and eastern Kansas.

Also as in 2020, the three specific ecoregion sections with the highest fire occurrence densities in 2021 were in California: M261D–Southern Cascades (52.2 fire occurrences/100 km^2 of tree canopy cover), M261E–Sierra Nevada (43.2 fire occurrences), and M261A–Klamath Mountains (36.8 fire occurrences) (table 3.1). Other ecoregion sections of the Pacific Northwest, Northern Rockies, and California were among those with the highest fire occurrence densities: M242C–Eastern Cascades (26.5), M242D–Northern Cascades (13.6), M332A–Idaho Batholith (10.9), M332E–Beaverhead Mountains (10.7), and M261C–Northern California Interior Coast Ranges (10.6). This geographic pattern was associated at least in part with the most expansive and intense drought throughout the West in the 21st century, with more than 95 percent of the region experiencing drought conditions through August and more than half of the region in extreme or exceptional drought (National Interagency Coordination Center 2022). A heat wave of unprecedented intensity also affected the Pacific Northwest, Northern Rockies, and the Great Basin in June.

Meanwhile, Alaska had snowpack that was near or above normal during the spring but experienced high levels of lightning activity during the summer (National Interagency Coordination Center 2022). Fire occurrence densities across Alaska in 2021 were low (fig. 3.3), with only two ecoregions in the east-central part of the State exceeding 1 fire occurrence/100 km^2 of forest and shrub cover: M132F–North Ogilvie Mountains (1.2) and M132C–Yukon-Tanana Uplands (1.1).

Hawaii ecoregions also had low fire occurrence densities in 2021, with only the Mesic (MEh, 2.1) and Montane Wet-Hawai‘i-Hilo-Puna (MWh-hp, 1.1.) regions on Hawai‘i Island exceeding 1 fire occurrence/100 km^2 of canopy cover (fig. 3.4). The 16 187-ha Mana Road Fire located in the Lowland/Leeward Dry ecoregion

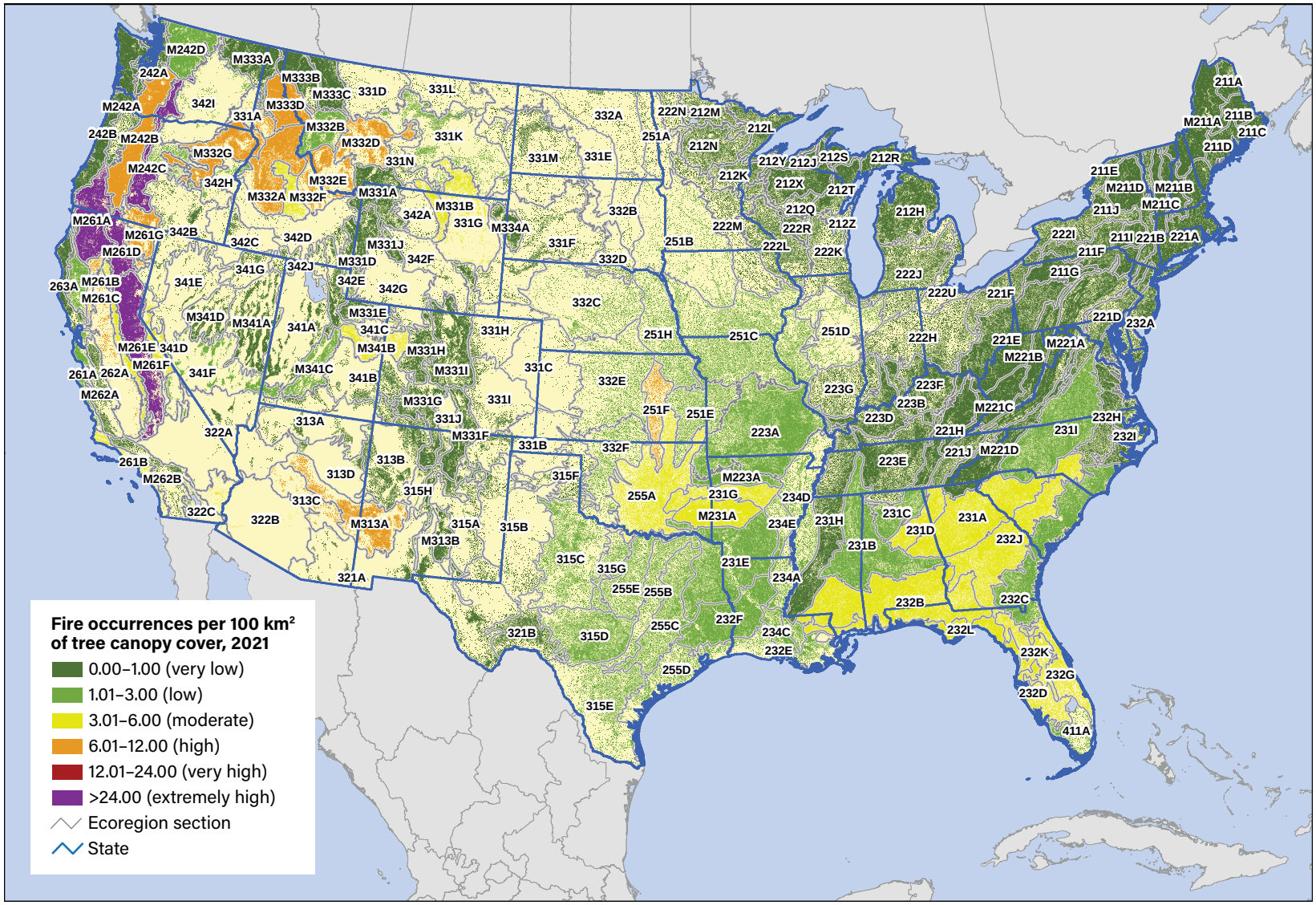

Figure 3.2—The number of forest fire occurrences per 100 km² (10 000 ha) of tree canopy coverage area, by ecoregion section within the conterminous United States, for 2021. The gray lines delineate ecoregion sections (Cleland and others 2007). Tree canopy cover is based on data from a cooperative project between the Multi-Resolution Land Characteristics Consortium (Coulston and others 2012) and the Forest Service Geospatial Technology and Applications Center using the 2011 National Land Cover Database. See figure 1.1A for ecoregion identification. (Source of fire data: U.S. Department of Agriculture, Forest Service, Geospatial Technology and Applications Center, in conjunction with the NASA Moderate Resolution Imaging Spectroradiometer Rapid Response group)

Table 3.1—The 15 ecoregion sections in the conterminous United States with the highest fire occurrence densities in 2021

Section	Name	Tree canopy area (100 km^2)	Fire occurrences (number)	Density[a]
M261D	Southern Cascades	150.6	7,862	52.2
M261E	Sierra Nevada	427.8	18,485	43.2
M261A	Klamath Mountains	338.5	12,465	36.8
M242C	Eastern Cascades	219.4	5,825	26.5
M242D	Northern Cascades	251.1	3, 421	13.6
M332A	Idaho Batholith	338.9	3,680	10.9
M332E	Beaverhead Mountains	147.1	1,573	10.7
M261C	Northern California Interior Coast Ranges	18.2	193	10.6
M333A	Okanogan Highland	247.9	2, 595	10.5
M332G	Blue Mountains	309.7	3,038	9.8
M332D	Belt Mountains	166.5	1,598	9.6
262A	Great Valley	19.4	185	9.5
331A	Palouse Prairie	33.4	301	9.0
M333D	Bitterroot Mountains	235.3	2,095	8.9
M242B	Western Cascades	427.9	3,591	8.4

[a] Density = fire occurrences per 100 km^2 of tree canopy coverage area.

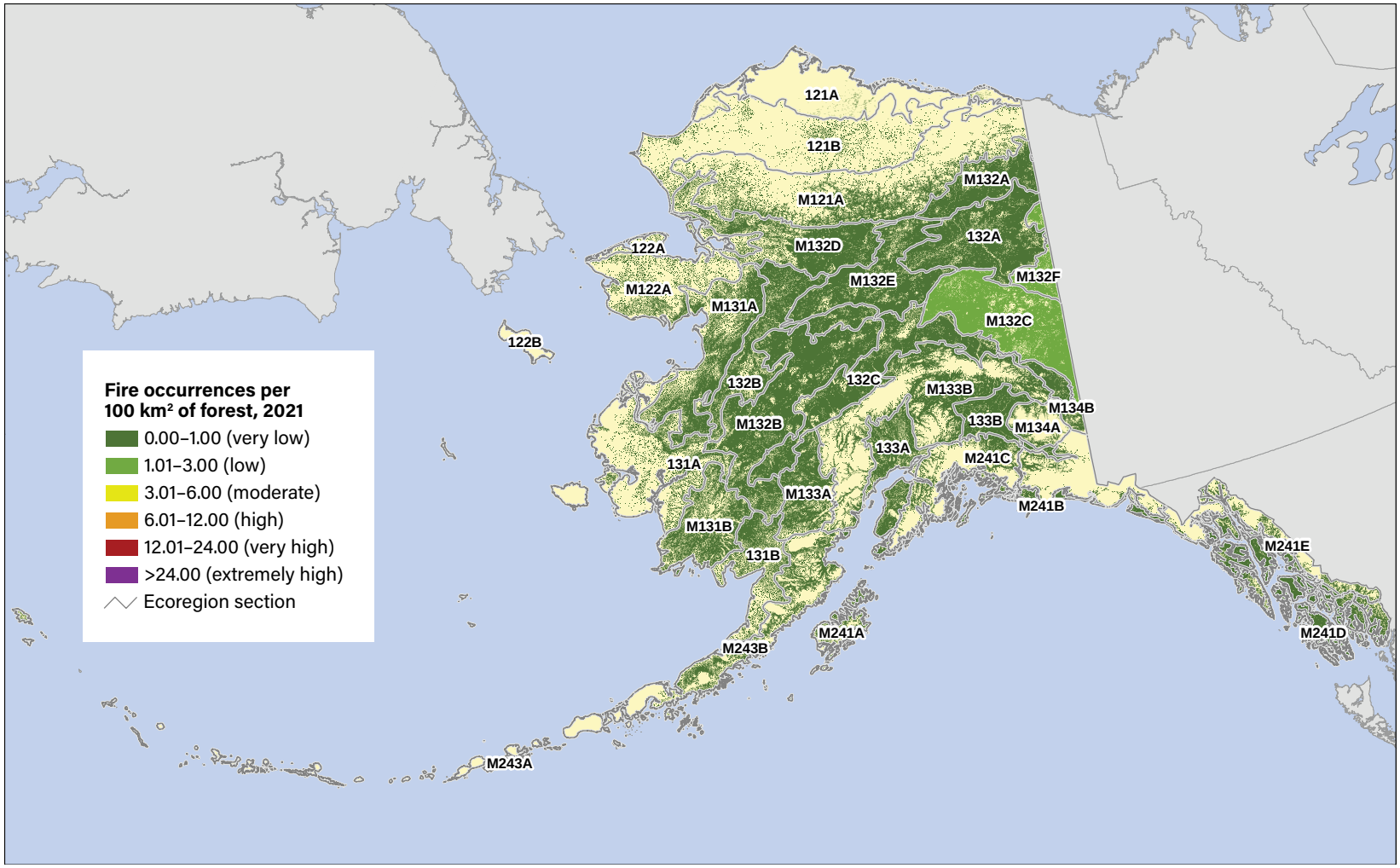

Figure 3.3—The number of forest fire occurrences per 100 km² (10 000 ha) of forest and shrub cover, by ecoregion section within Alaska, for 2021. The gray lines delineate ecoregion sections (Spencer and others 2002). Forest and shrub cover are derived from the 2011 National Land Cover Database. See figure 1.1B for ecoregion identification. (Source of fire data: U.S. Department of Agriculture, Forest Service, Geospatial Technology and Applications Center, in conjunction with the NASA Moderate Resolution Imaging Spectroradiometer Rapid Response group)

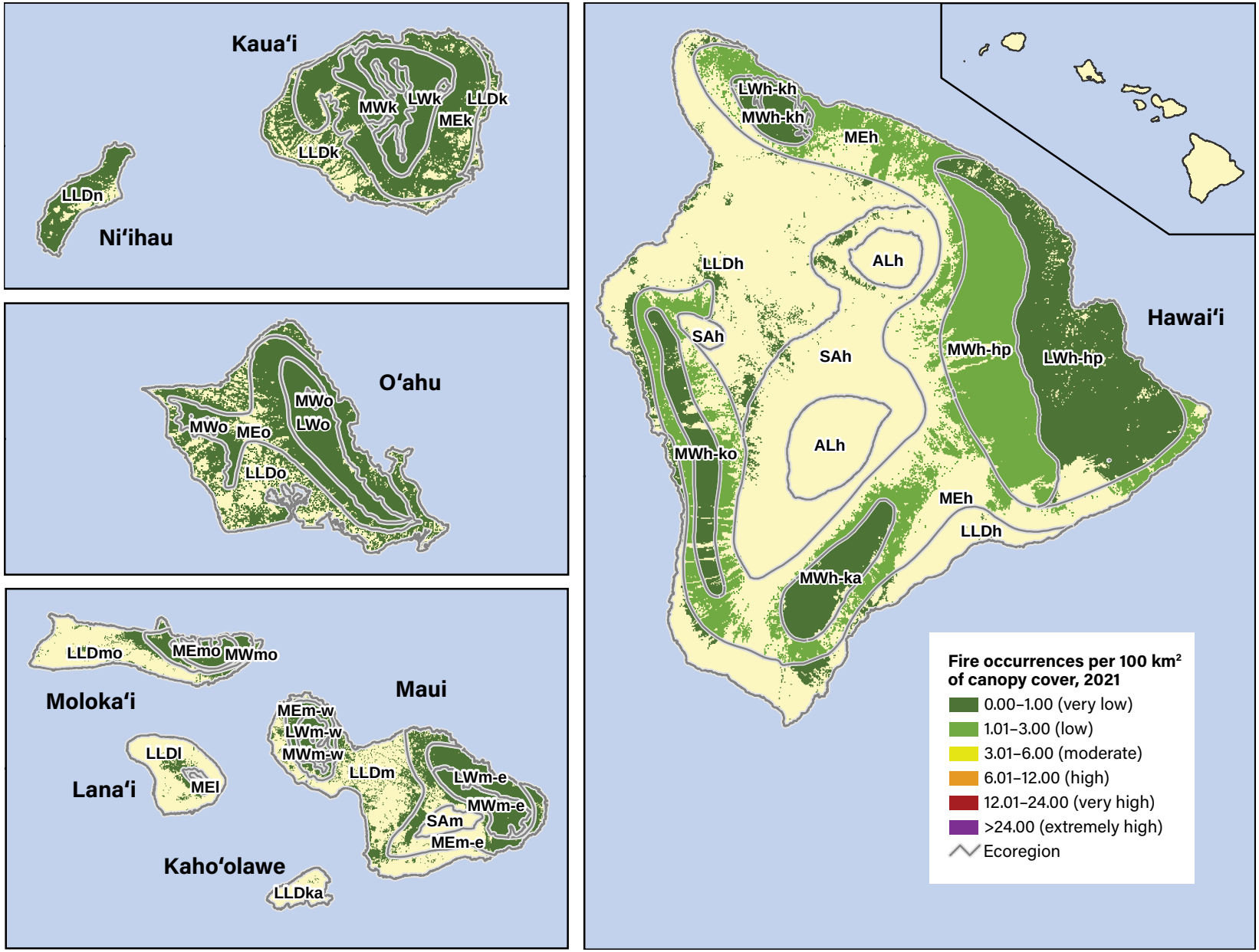

Figure 3.4—The number of forest fire occurrences per 100 km² (10 000 ha) of tree canopy coverage area, by island/ecoregion combination in Hawaii, for 2021. Tree canopy cover is based on data from a cooperative project between the Multi-Resolution Land Characteristics Consortium (Coulston and others 2012) and the Forest Service Geospatial Technology and Applications Center using the 2011 National Land Cover Database. See table 1.1 for ecoregion identification. (Source of fire data: U.S. Department of Agriculture, Forest Service, Geospatial Technology and Applications Center, in conjunction with the NASA Moderate Resolution Imaging Spectroradiometer Rapid Response group)

of Hawai‘i Island (LLDh), which was one of the largest in the State's history (National Interagency Coordination Center 2022), was not reflected in the Hawaii statistics because it occurred almost entirely in brush.

Finally, fire occurrence densities in 2021 were ≤1 fire occurrence/100 km^2 of tree canopy cover for most islands of the U.S. Caribbean territories (Puerto Rico and the U.S. Virgin Islands) except for Isla de Vieques (2.2) and Saint Croix (1.8) (fig. 3.5).

Comparison to Longer Term Trends

The long-term collection of MODIS Active Fire data (more than 2 decades) makes it possible to contrast annual (2021) forest fire occurrence densities with longer term trends (2001–2020) for ecoregions in the CONUS, Alaska, and Hawaii, and for Caribbean territories. During that 2-decade period, the highest mean annual fire occurrence density (12.5 fire occurrences/100 km^2 of tree canopy cover annually) was in M261B–Northern California Coast Ranges (table 3.2), while several other ecoregion sections in the Pacific Coast States, Idaho, and Arizona/New Mexico, and along the Gulf Coast in the Southeast, exceeded 6 fire occurrences/100 km^2 of tree canopy cover (fig. 3.6A). Other ecoregion sections with high average annual fire occurrence densities included M332A–Idaho Batholith in central Idaho (11.8), M261A–Klamath Mountains of northwestern California and southeastern Oregon (10.8), M261E–Sierra Nevada in California (9.8), and M262B–Southern California Mountain and Valley near the southern California coast (9.7) (table 3.2). Elsewhere in the West and the Southeast, ecoregion sections experienced ≤3–6 fire occurrences/100 km^2 of tree canopy cover annually, while much of the Midwest and all the Northeast experienced ≤1.

The M261B–Northern California Coast Ranges and M332A–Idaho Batholith ecoregion sections also had the greatest annual variation in fire occurrence densities from 2001 through 2020 (fig. 3.6B). High variation was also present in other mountainous ecoregion sections of California and the Pacific Northwest, while more moderate variation existed in other parts of the West, including central Oregon and Washington, northwestern Montana, and central Arizona and west-central New Mexico. These are regions with relatively high mean annual fire occurrence densities (fig. 3.6A). Other areas—including in north-central Colorado and west-central Wyoming—have relatively high variation with low mean annual fire occurrence densities, suggesting low numbers of fire occurrences most years with high numbers in others. Ecoregion sections of the Midwest and Northeast and in coastal areas of Oregon and Washington had the lowest interannual variation (standard deviation <1), while slightly higher variation (standard deviation 1–5) was apparent across the Southeast, the central Rocky Mountains, and the Great Basin. Parts of the Southeast, especially along the Gulf Coast, had low annual variation but relatively high mean annual fire occurrence densities, suggesting consistently high numbers of fire occurrences over time.

Compared to the previous 20-year mean and accounting for temporal variability, nine ecoregion

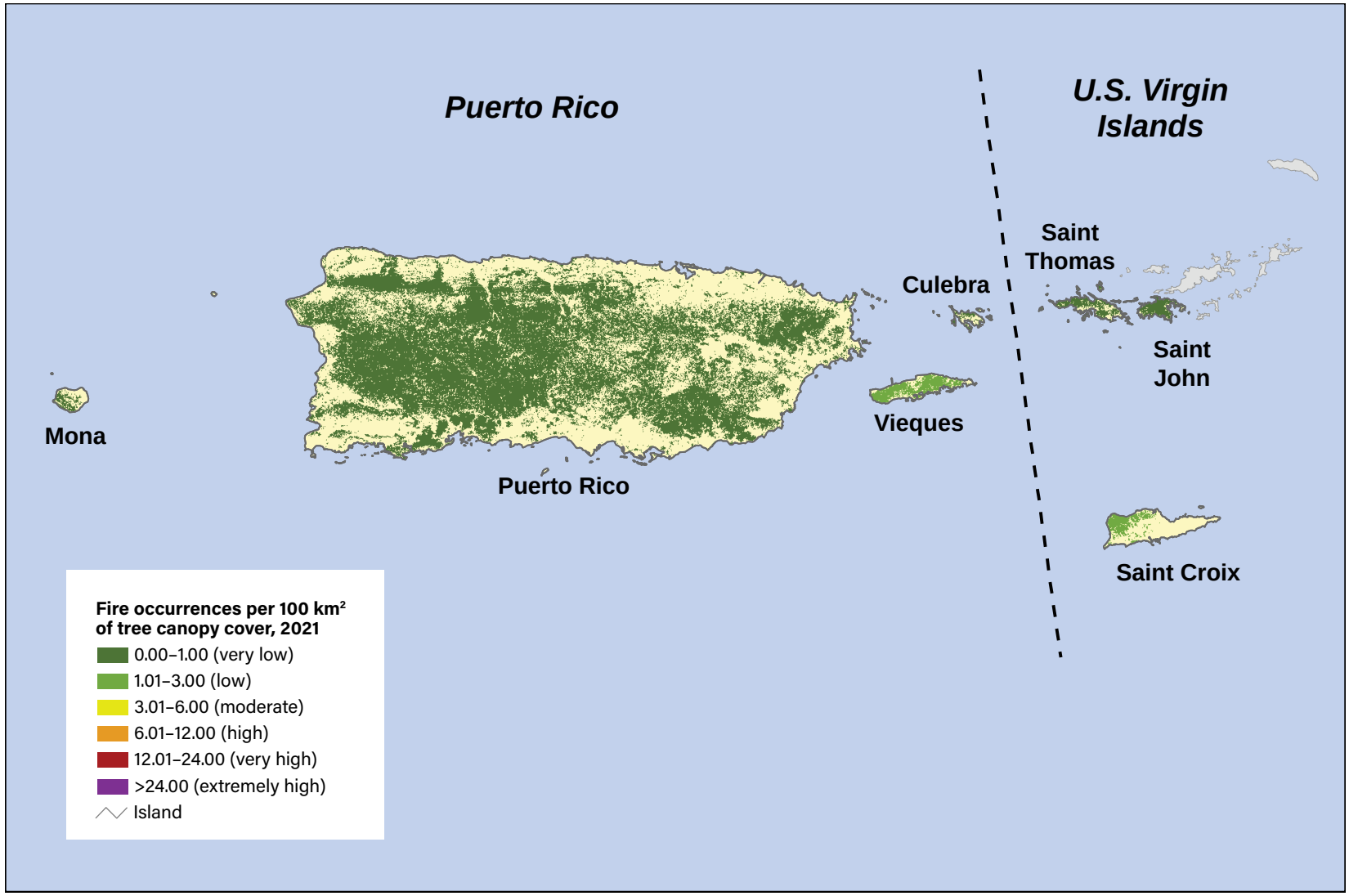

Figure 3.5—The number of forest fire occurrences per 100 km² (10 000 ha) of tree canopy coverage area, by island in Puerto Rico and the U.S. Virgin Islands, for 2021. Tree canopy cover is based on data from a cooperative project between the Multi-Resolution Land Characteristics Consortium (Coulston and others 2012) and the Forest Service Geospatial Technology and Applications Center using the 2011 National Land Cover Database. (Source of fire data: U.S. Department of Agriculture, Forest Service, Geospatial Technology and Applications Center, in conjunction with the NASA Moderate Resolution Imaging Spectroradiometer Rapid Response group)

Table 3.2—The 15 ecoregion sections in the conterminous United States with the highest mean annual fire occurrence densities from 2001 through 2020

Section	Name	Tree canopy area (100 km^2)	Mean annual fire occurrence density[a]
M261B	Northern California Coast Ranges	114.1	12.5
M332A	Idaho Batholith	338.9	11.8
M261A	Klamath Mountains	338.5	10.8
M261E	Sierra Nevada	427.8	9.8
M262B	Southern California Mountain and Valley	58.1	9.7
M313A	White Mountains-San Francisco Peaks-Mogollon Rim	202.5	7.4
313C	Tonto Transition	17.5	7.2
261A	Central California Coast	66.8	7.0
251F	Flint Hills	57.8	6.9
232B	Gulf Coastal Plains and Flatwoods	888.7	6.1
M242D	Northern Cascades	251.1	6.0
331A	Palouse Prairie	33.4	5.7
M332F	Challis Volcanics	72.2	5.6
M333C	Northern Rockies	176.3	5.4
232J	Southern Atlantic Coastal Plains and Flatwoods	604.0	5.3

[a] Mean annual fire occurrence density = fire occurrences per 100 km^2 of tree canopy coverage area.

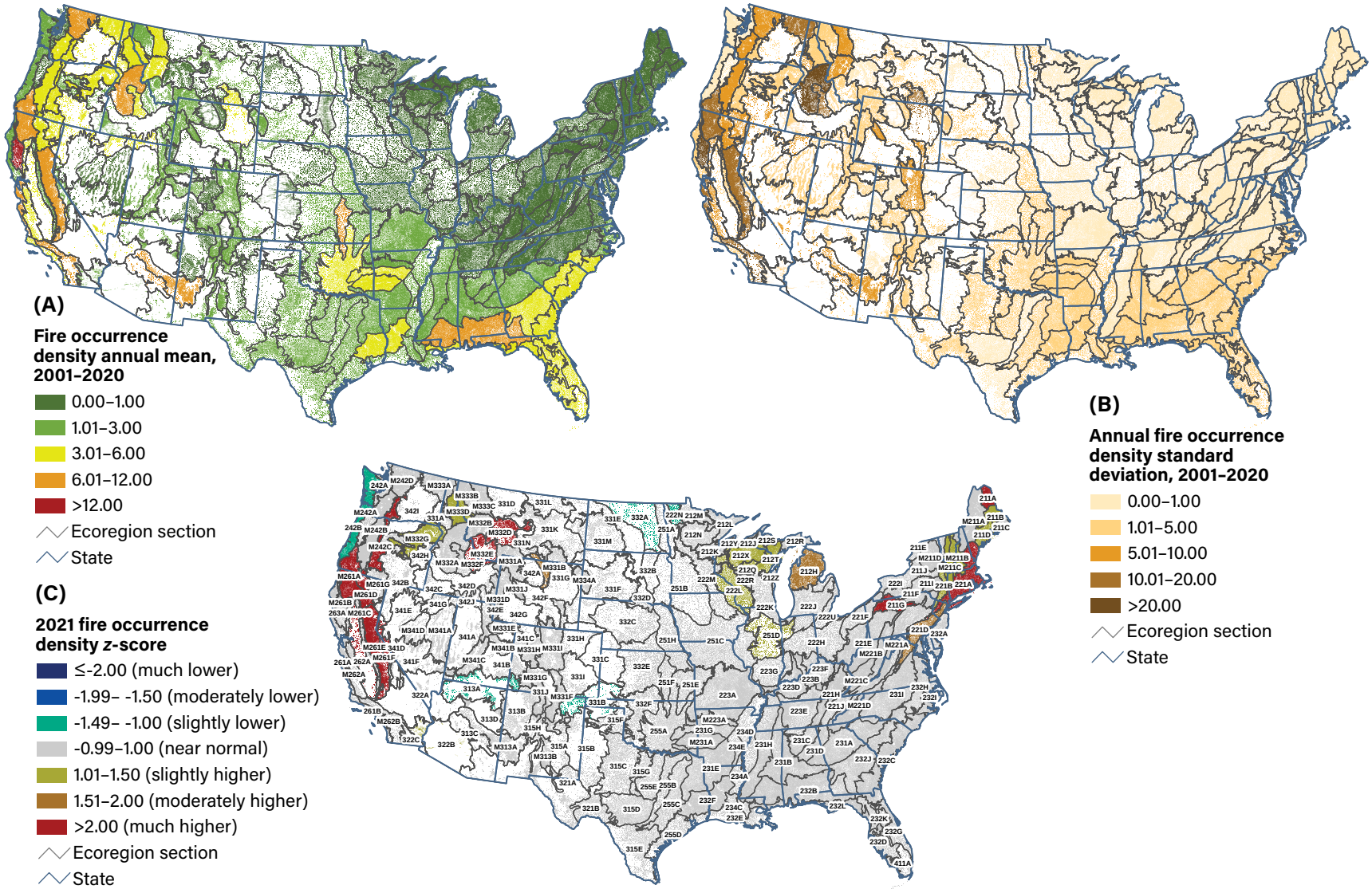

Figure 3.6—(A) Mean number and (B) standard deviation of forest fire occurrences per 100 km² (10 000 ha) of tree canopy coverage area from 2001 through 2020, by ecoregion section within the conterminous 48 States. (C) Degree of 2021 fire occurrence density excess or deficiency, by ecoregion section relative to 2001–2020 and accounting for variation over that period. The gray lines delineate ecoregion sections (Cleland and others 2007). Tree canopy cover is based on data from a cooperative project between the Multi-Resolution Land Characteristics Consortium (Coulston and others 2012) and the Forest Service Geospatial Technology and Applications Center using the 2011 National Land Cover Database. (Source of fire data: U.S. Department of Agriculture, Forest Service, Geospatial Technology and Applications Center, in conjunction with the NASA Moderate Resolution Imaging Spectroradiometer Rapid Response group)

sections in California, the Pacific Northwest, the Northern Rockies, and the Northeast had much higher fire occurrence densities in 2021 than normal (fig. 3.6C). Three of the California ecoregion sections (M261A–Klamath Mountains, M261D–Southern Cascades, and M261E–Sierra Nevada) had a high fire occurrence density in 2021 as well as a relatively high mean for the previous 2 decades. Other western ecoregion sections (M242D–Northern Cascades in northern Washington, M242C–Eastern Cascades in central Washington and Oregon, 341D–Mono in eastern California and western Nevada, and M332E–Beaverhead Mountains and M332D–Belt Mountains in southwestern Montana) had moderate average annual fire occurrence densities. Those in the Northeast, however, had much higher fire occurrence densities in 2021 relative to a very low long-term normal (211G–Northern Unglaciated Allegheny Plateau, 221A–Lower New England, and 211A–Aroostook Hills and Lowlands). In other words, these are areas that tend to have few fires in a typical year and therefore don't require many fire occurrences to be classified as having more than normal.

Meanwhile, a handful of ecoregion sections in the West and the Midwest had fire occurrence densities in 2021 that were lower than expected, as indicated by *z*-scores ≤-1. One was in the Pacific Northwest (M242A–Oregon and Washington Coast Ranges), and two were in the Southwestern States (313A–Grand Canyon and 331B–Southern Plains). All of these are areas that had low to moderate annual fire occurrence densities on average.

In Alaska, mean annual fire occurrence densities for 2001–2020 were relatively low except for moderate densities in the central and east-central parts of the State (M132E–Ray Mountains and 132A–Yukon-Old Crow Basin) (fig. 3.7A). These ecoregion sections, along with the neighboring M132C–Yukon-Tanana Uplands and M132F–North Ogilvie Mountains, exhibited the most variability over the 2-decade period preceding 2021 (fig. 3.7B). Only a single Alaska ecoregion section in 2021 had a fire occurrence density outside normal compared to the previous 20 years and controlling for variability: M241D–Alexander Archipelago, where there was a much higher fire occurrence density than normal (fig. 3.7C). This is an area that typically had very few fire occurrences.

In Hawaii, the area that exhibited the highest annual fire occurrence density mean (fig. 3.8A) and variability (fig. 3.8B) from 2001 through 2020 was the Lowland Wet-Hilo-Puna ecoregion (LWh-hp) on the eastern side of Hawai'i Island (18.7 fire occurrences/100 km^2 of tree canopy cover, standard deviation 41.1). Contained within this area are recently active portions of the lower east rift zone of Kīlauea volcano, where lava flows incinerated some forested areas (Andrews 2018). With one exception, all other ecoregions in the State had an annual mean fire occurrence density of ≤1 fire occurrence/100 km^2 of tree cover. The exception was the Mesic region on the Hawai'i Island (MEh), where it was 2.2. In 2021, no Hawaiian ecoregions had fire occurrence densities outside expectations (*z*-score >1), controlling for variability over the previous 2 decades (fig. 3.8C).

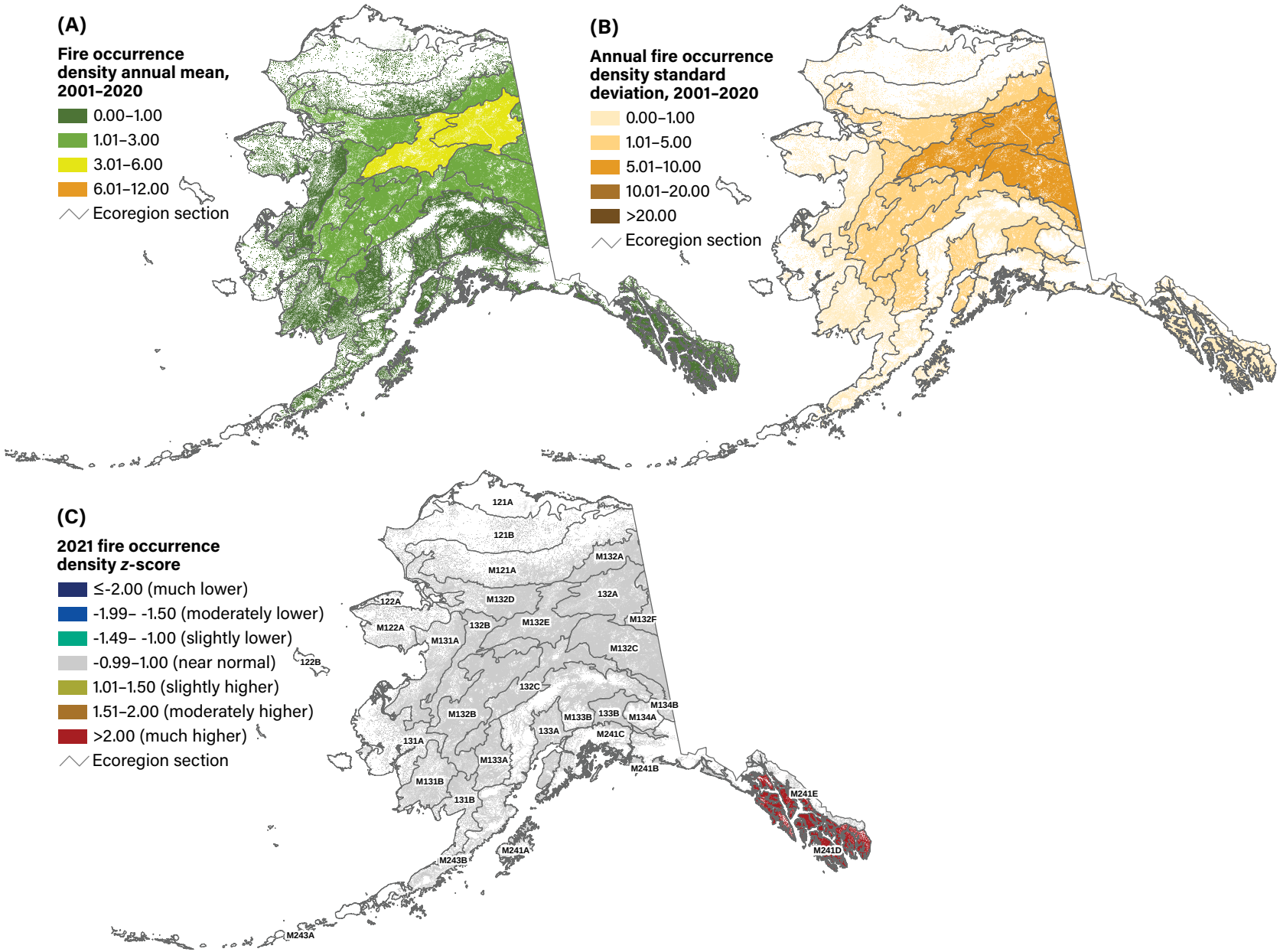

Figure 3.7—(A) Mean number and (B) standard deviation of forest fire occurrences per 100 km² (10 000 ha) of forest and shrub cover from 2001 through 2020, by ecoregion section in Alaska. (C) Degree of 2021 fire occurrence density excess or deficiency, by ecoregion section relative to 2001–2020 and accounting for variation over that period. The gray lines delineate ecoregion sections (Spencer and others 2002). Forest and shrub cover are derived from the 2011 National Land Cover Database. (Source of fire data: U.S. Department of Agriculture, Forest Service, Geospatial Technology and Applications Center, in conjunction with the NASA Moderate Resolution Imaging Spectroradiometer Rapid Response group)

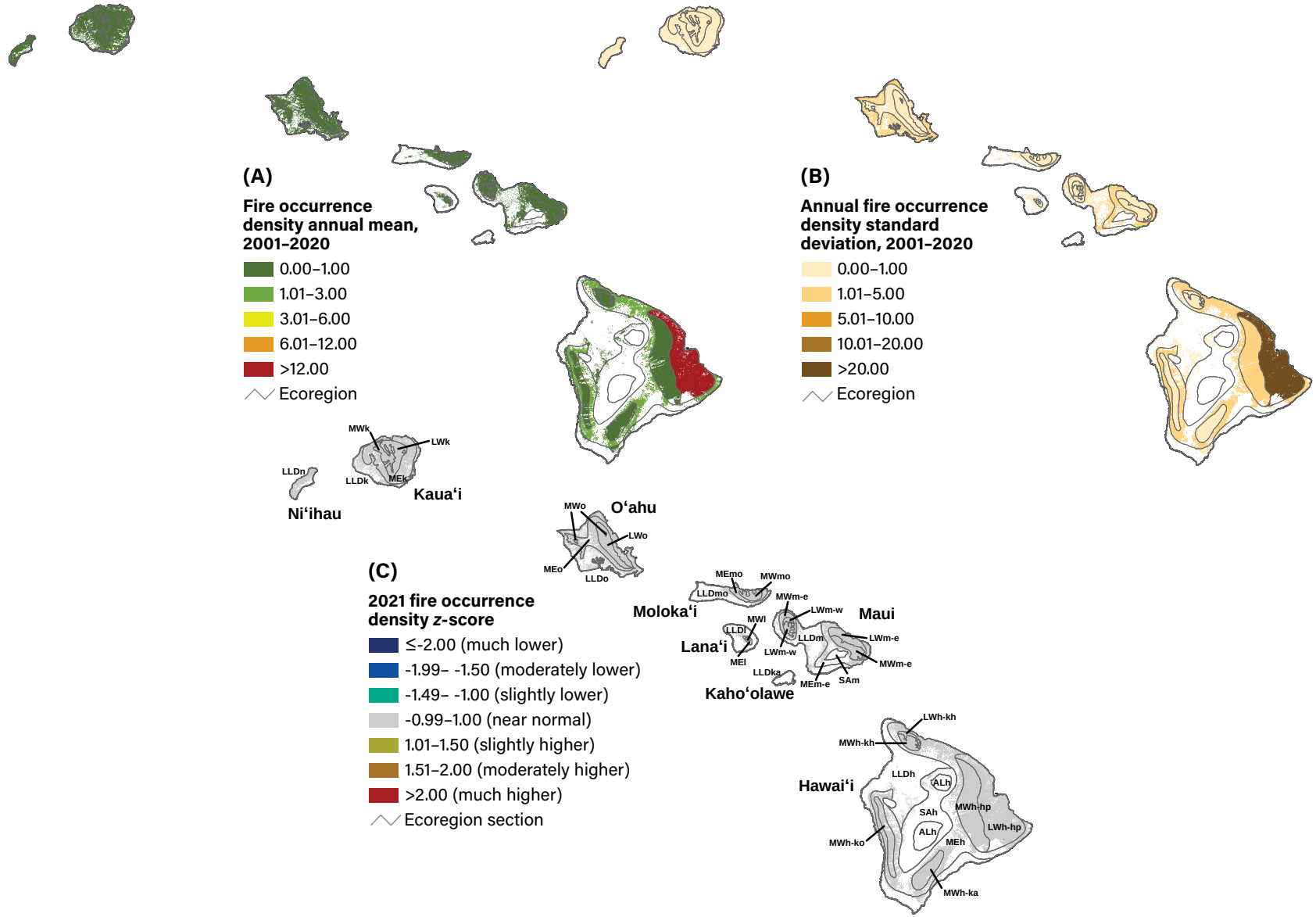

Figure 3.8—(A) Mean number and (B) standard deviation of forest fire occurrences per 100 km² (10 000 ha) of tree canopy coverage area from 2001 through 2020, by island/ecoregion combination in Hawaii. (C) Degree of 2021 fire occurrence density excess or deficiency, by island/ecoregion combination relative to 2001–2020 and accounting for variation over that period. Tree canopy cover is based on data from a cooperative project between the Multi-Resolution Land Characteristics Consortium (Coulston and others 2012) and the Forest Service Geospatial Technology and Applications Center using the 2011 National Land Cover Database. (Source of fire data: U.S. Department of Agriculture, Forest Service, Geospatial Technology and Applications Center, in conjunction with the NASA Moderate Resolution Imaging Spectroradiometer Rapid Response group)

Finally, all the islands encompassed by Puerto Rico and the U.S. Virgin Islands had fire occurrence means and standard deviations ≤1 from 2001–2020 (figs. 3.9A and 3.9B). Two islands had higher than expected fire occurrence densities in 2021 (z-score >1): Isla de Vieques in Puerto Rico and Saint Croix in the U.S. Virgin Islands (fig. 3.9C).

Geographic Hot Spots of Fire Occurrence Density

Geographic hot spot analyses using analysis units smaller than ecoregions (the main unit of analysis thus far in this chapter) can offer additional insights into where, statistically, fire occurrences are more concentrated than expected by chance during a given year. Specifically, this approach can identify areas across the CONUS with higher than expected fire occurrence densities compared to the entire study region. For 2021, the SASH method detected a geographic hot spot of extremely high fire occurrence density (G_i^* >24) in northern California as well as four hot spots of very high fire occurrence density (G_i^* >12 and ≤24) elsewhere in the West (fig. 3.10).

The single hot spot with extremely high fire occurrence density spanned M261E–Sierra Nevada and M261D–Southern Cascades. This is the region of the 2021 Dixie Fire, the largest single wildfire in California history, and exceeded in area only by the August Complex of fires the previous year (CALFIRE 2022). The Dixie Fire burned 389 837 ha and destroyed more than 1,300 buildings between July 13 and October 23; it cost approximately $637 million to contain (CALFIRE 2022, National Interagency Coordination Center 2022). Additionally, the 42 763-ha Beckwourth Complex, which was ignited July 3, reported as contained September 21, and cost approximately $543 million to contain, was also in this area (National Interagency Coordination Center 2022).

A very high fire occurrence density hot spot, centered in nearby M261A–Klamath Mountains of northwestern California, was caused in part by five large fires and fire complexes in 2021 (CALFIRE 2022, National Interagency Coordination Center 2022):

- Monument Fire, 90 295 ha, July 31–October 25; $164 million containment cost, 50 structures destroyed
- River Complex, 80 678 ha, July 30–October 24; $95 million containment cost, 122 structures destroyed
- Antelope Fire, 58 935 ha, August 1–October 14; $75 million containment cost
- McFarland Fire, 49 636 ha, July 30–September 15; $44 million containment cost
- McCash Fire, 38 430 ha, July 31–October 27; $53 million containment cost

Another hot spot of similar intensity was located in the M261E–Sierra Nevada, also in California. This one was caused by the Caldor Fire west of Lake Tahoe, which scorched 89 773 ha between its ignition on August 14 and its containment on October 20. This human-caused blaze cost an estimated $271 million to contain after burning 1,003 buildings (CALFIRE 2022, National Interagency Coordination Center 2022).

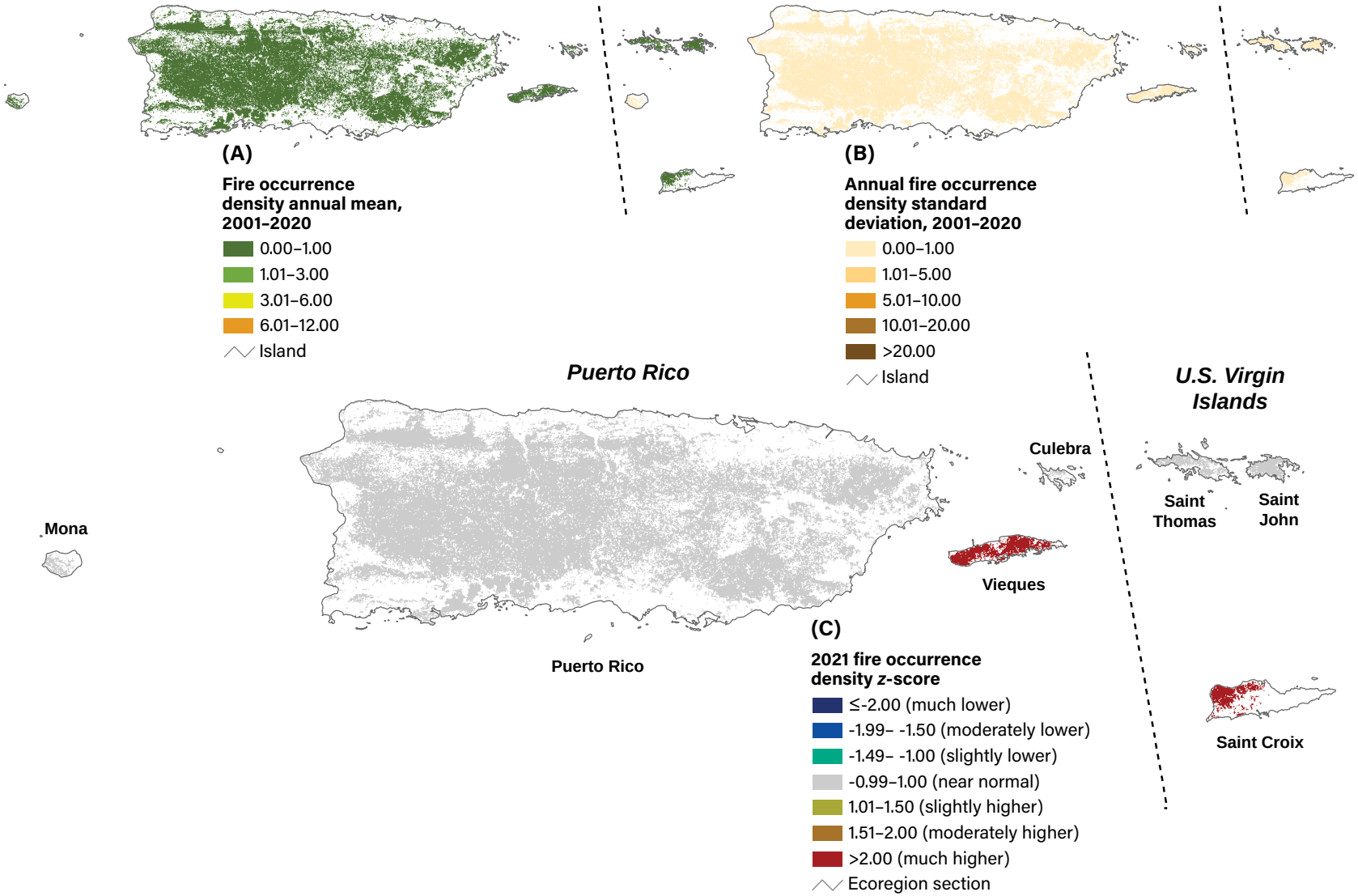

Figure 3.9—(A) Mean number and (B) standard deviation of forest fire occurrences per 100 km² (10 000 ha) of forested area from 2001 through 2020, by island in Puerto Rico and the U.S. Virgin Islands. (C) Degree of 2021 fire occurrence density excess or deficiency, by island relative to 2001–2020 and accounting for variation over that period. Tree canopy cover is based on data from a cooperative project between the Multi-Resolution Land Characteristics Consortium (Coulston and others 2012) and the U.S. Department of Agriculture, Forest Service, Geospatial Technology and Applications Center using the 2011 National Land Cover Database.

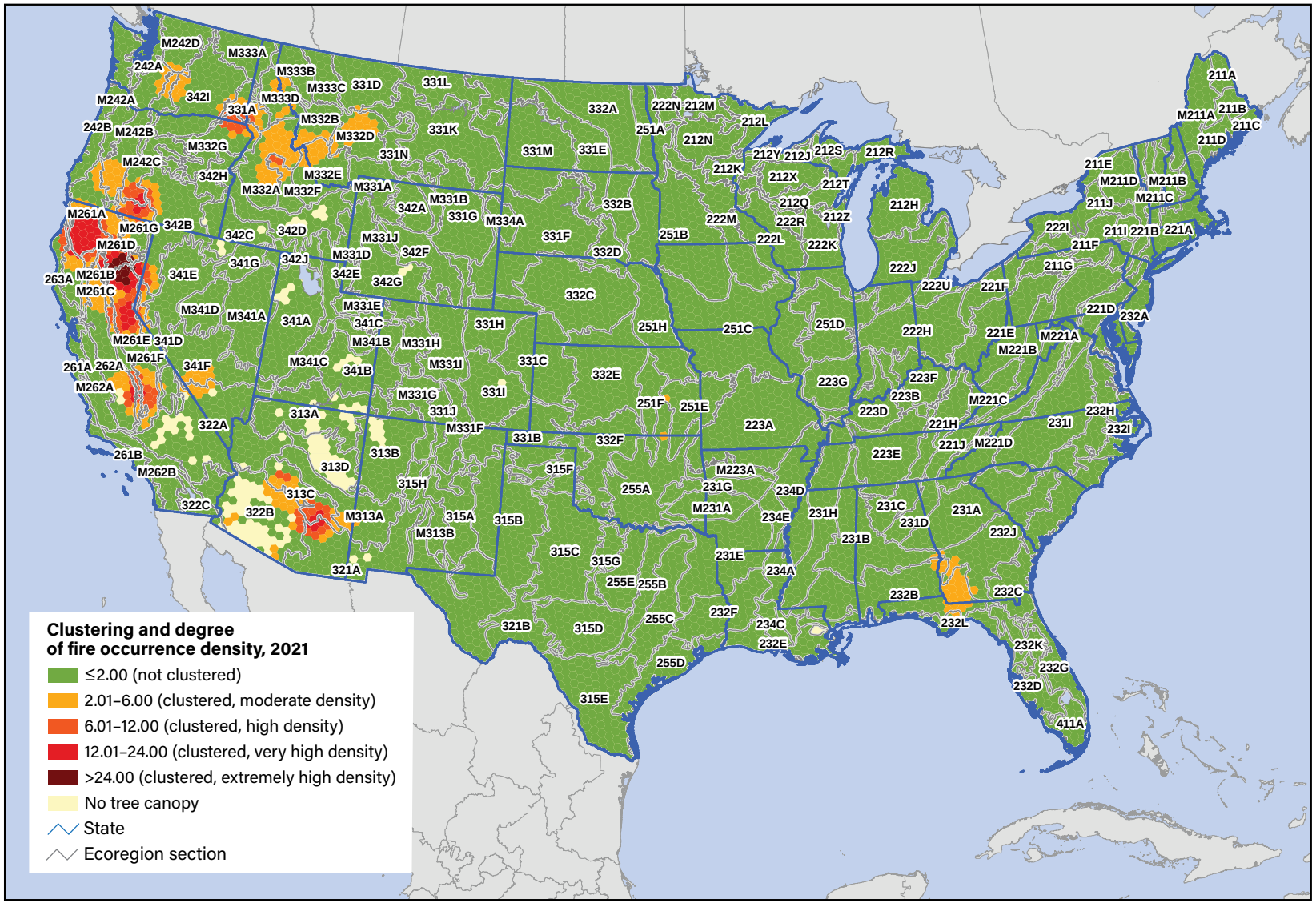

Figure 3.10—Hot spots of fire occurrence, by ecoregion section within the conterminous United States, for 2021. Values are Getis-Ord Gi scores, with values >2 representing significant clustering of high fire occurrence densities. (No areas of significant clustering of lower fire occurrence densities, <-2, were detected.) The gray lines delineate ecoregion sections (Cleland and others 2007).*

To the south, also in M261E–Sierra Nevada as well as in M261F–Sierra Nevada Foothills, a very high fire occurrence density hot spot was associated with the Windy Fire (39 468 ha, $78 million) and the KNP Complex (35 737 ha, $170 million), which burned from September through November and December, respectively (National Interagency Coordination Center 2022).

One additional hot spot of very high fire occurrence density in 2021 was detected outside of California (fig. 3.10) and was also associated with a megafire:

- 313C–Tonto Transition and 321A–Basin and Range of southeastern Arizona, location of the human-caused Telegraph Fire, which burned 73 150 ha between June 4 and July 2 and cost $36 million to contain, and the nearby human-caused Mescal Fire, which burned 29 239 ha (National Interagency Coordination Center 2022)

Additionally, four hot spots of high fire occurrence density (G_i^* >6 and ≤12) were identified in the West during 2021 (fig. 3.10):

- In south-central Oregon (M242C–Eastern Cascades and M261G–Modoc Plateau), where the Bootleg Fire—the third largest fire in recorded Oregon history (Sutton and others 2021)—burned 167 425 ha between July 6 and August 13, costing approximately $101 million to contain (National Interagency Coordination Center 2022) and destroying more than 400 structures (InciWeb 2021)
- In north-central Washington (M242D–Northern Cascade and M333A–Okanogan Highland)
- In southeastern Washington and northeastern Oregon (331A–Palouse Prairie)
- In central Idaho (M332F–Challis Volcanics)

A hot spot of moderate fire occurrence density (G_i^* >2 and ≤6) occurred in the southwestern corner of Georgia and the panhandle of Florida (232B–Gulf Coastal Plains and Flatwoods and 232L–Gulf Coastal Lowlands). One additional small moderate fire occurrence density hot spot was detected in southeastern Kansas (255A–Cross Timbers and Prairie).

CONCLUSIONS

In 2021, the number of MODIS satellite-detected forest fire occurrences in the CONUS was the fourth highest in 21 full years of data collection but still represented a 9-percent decrease in fire activity from the extremely active 2020 fire season. The year included the largest single fire event in California history as well as the third largest in Oregon's. Parts of California and the Pacific Northwest in 2021 had extremely high fire occurrence densities (fire occurrences per 100 km^2 of tree canopy cover area), while areas of the Northern Rockies, Pacific Northwest, and Southwest had very high or high densities. The extensive fire activity in these regions resulted in geographic hot spots of extremely high or very high fire occurrence density. Not surprisingly, these areas experienced fire occurrence densities that were much higher than normal in 2021 compared to the previous 20-year mean and

accounting for variability over time. Parts of the Northeast also had fire occurrence densities that exceeded normal, although these areas tend to have few fires in a typical year and therefore don't require many fire occurrences to be classified as outside expectations. At the same time, a few ecoregion sections in the Southwest and Pacific Northwest had significantly lower fire occurrence densities than normal.

Meanwhile, Alaska in 2021 experienced a 281-percent increase in fire occurrences from 2020, but this was a 93-percent decrease from the extremely high fire year of 2019 and about 80 percent less than the mean for the preceding 2 decades. An ecoregion section within the panhandle of Alaska was the only part of the State that had a higher than normal fire occurrence density. Hawaiian forests in 2021 also had fire occurrence densities that were low and within expectations. Parts of both Puerto Rico (Isla de Vieques) and the U.S. Virgin Islands (Saint Croix) had higher than expected fire occurrence densities in 2021.

The results of these geographic analyses are intended to offer insights into where fire occurrences have been concentrated spatially during a given year and compared to previous years; they are not intended to quantify the severity of a given fire season. Given the limits of MODIS active fire detection using 1-km-resolution data, these products may underrepresent the number of fire occurrences in some ecosystems where small and low-intensity fires are common, and where high cloud frequency can interfere with fire detection. These products can also have commission errors. At the same time, these high-temporal-fidelity products currently offer the best means for daily monitoring of forest fire occurrences.

Ecological and forest health impacts relating to fire and other abiotic disturbances are scale-dependent properties, which in turn are affected by management objectives (Lundquist and others 2011). Information about the concentration of fire occurrences may pinpoint areas of concern for aiding management activities and for investigations into the ecological and socioeconomic impacts of forest fire potentially outside the range of historic frequency. Given the potential for climate change and shifting species distributions to alter historic fire regimes, quantifying the location and frequency of forest fire occurrences across the United States can also help to better understand emerging spatiotemporal patterns of fire occurrence.

LITERATURE CITED

Abatzoglou, J.T.; Williams, A.P. 2016. Impact of anthropogenic climate change on wildfire across Western US forests. Proceedings of the National Academy of Sciences. 113(42): 11770–11775. https://doi.org/10.1073/pnas.1607171113.

Agee, J.K. 1998. The landscape ecology of western forest fire regimes. Northwest Science. 72: 24–34.

Andrews, R.G. 2018. America's most hazardous volcano erupted this year. Then it erupted and erupted. The New York Times. December 12. https://www.nytimes.com/2018/12/12/science/kilauea-hawaii-volcano-eruption.html. [Date accessed: July 15, 2019].

Anselin, L. 1992. Spatial data analysis with GIS: an introduction to application in the social sciences. Tech. Rep. 92-10. Santa Barbara, CA: University of California, National Center for Geographic Information and Analysis. 53 p.

Barbour, M.G.; Burk, J.H.; Pitts, W.D. [and others]. 1999. Terrestrial plant ecology. Menlo Park, CA: Addison Wesley Longman, Inc. 649 p.

Bond, W.J.; Keeley, J.E. 2005. Fire as a global "herbivore": the ecology and evolution of flammable ecosystems. Trends in Ecology & Evolution. 20(7): 387–394. https://doi.org/10.1016/j.tree.2005.04.025.

CALFIRE. 2022. Top 20 largest California wildfires. https://www.fire.ca.gov/media/4jandlhh/top20_acres.pdf/. [Date accessed: May 18, 2022].

Calkin, D.E.; Thompson, M.P.; Finney, M.A. 2015. Negative consequences of positive feedbacks in US wildfire management. Forest Ecosystems. 2: 9. https://doi.org/10.1186/s40663-015-0033-8.

Cleland, D.T.; Freeouf, J.A.; Keys, J.E. [and others]. 2007. Ecological subregions: sections and subsections for the conterminous United States. Gen. Tech. Rep. WO-76D. Washington, DC: U.S. Department of Agriculture, Forest Service. Map; Sloan, A.M., cartographer; presentation scale 1:3,500,000; colored. https://doi.org/10.2737/WO-GTR-76D.

Coop, J.D.; Parks, S.A.; Stevens-Rumann, C.S. [and others]. 2020. Wildfire-driven forest conversion in western North American landscapes. BioScience. 70(8): 659–673. https://doi.org/10.1093/biosci/biaa061.

Coulston, J.W.; Ambrose, M.J.; Riitters, K.H.; Conkling, B.L. 2005. Forest Health Monitoring 2004 national technical report. Gen. Tech. Rep. SRS-90. Asheville, NC: U.S. Department of Agriculture, Forest Service, Southern Research Station. 81 p. https://doi.org/10.2737/SRS-GTR-90.

Coulston, J.W.; Moisen, G.G.; Wilson, B.T. [and others]. 2012. Modeling percent tree canopy cover: a pilot study. Photogrammetric Engineering and Remote Sensing. 78(7): 715–727. https://doi.org/10.14358/PERS.78.7.715.

Edmonds, R.L.; Agee, J.K.; Gara, R.I. 2011. Forest health and protection. Long Grove, IL: Waveland Press, Inc. 667 p.

Eidenshink, J.; Schwind, B.; Brewer, K. [and others]. 2007. A project for monitoring trends in burn severity. Fire Ecology. 3(1): 3–21. https://doi.org/10.4996/fireecology.0301003.

ESRI. 2017. ArcMap® 10.5.1. Redlands, CA: Environmental Systems Research Institute.

Getis, A.; Ord, J.K. 1992. The analysis of spatial association by use of distance statistics. Geographical Analysis. 24(3): 189–206. https://doi.org/10.1111/j.1538-4632.1992.tb00261.x.

Giglio, L.; Descloitres, J.; Justice, C.O.; Kaufman, Y.J. 2003. An enhanced contextual fire detection algorithm for MODIS. Remote Sensing of Environment. 87(2–3): 273–282. https://doi.org/10.1016/S0034-4257(03)00184-6.

Giglio, L.; Schroeder, W.; Hall, J.V.; Justice, C.O. 2018. MODIS Collection 6 active fire product user's guide: revision B. https://cdn.earthdata.nasa.gov/conduit/upload/10575/MODIS_C6_Fire_User_Guide_B.pdf. [Date accessed: May 16, 2022].

Gill, A.M.; Stephens, S.L.; Cary, G.J. 2013. The worldwide "wildfire" problem. Ecological Applications. 23(2): 438–454. https://doi.org/10.1890/10-2213.1.

Hanberry, B.B.; Bragg, D.C.; Hutchinson, T.F. 2018. A reconceptualization of open oak and pine ecosystems of eastern North America using a forest structure spectrum. Ecosphere. 9(10): e02431. https://doi.org/10.1002/ecs2.2431.

Hawbaker, T.J.; Radeloff, V.C.; Syphard, A.D. [and others]. 2008. Detection rates of the MODIS active fire product. Remote Sensing of Environment. 112: 2656–2664. https://doi.org/10.1016/j.rse.2007.12.008.

Higuera, P.E.; Abatzoglou, J.T. 2021. Record-setting climate enabled the extraordinary 2020 fire season in the Western United States. Global Change Biology. 27(1). https://doi.org/10.1111/gcb.15388.

Homer, C.G.; Dewitz, J.A.; Yang, L. [and others]. 2015. Completion of the 2011 National Land Cover Database for the conterminous United States: representing a decade of land cover change information. Photogrammetric Engineering and Remote Sensing. 81(5): 345–354.

InciWeb. 2021. Bootleg fire daily update July 27. https://inciweb.nwcg.gov/incident/article/7609/62069/. [Date accessed: May 19, 2022].

Jeronimo, S.M.; Kane, V.R.; Churchill, D.J. [and others]. 2019. Forest structure and pattern vary by climate and landform across active-fire landscapes in the montane Sierra Nevada. Forest Ecology and Management. 437: 70–86. https://doi.org/10.1016/j.foreco.2019.01.033.

Justice, C.O.; Giglio, L.; Korontzi, S. [and others]. 2002. The MODIS fire products. Remote Sensing of Environment. 83(1–2): 244–262. https://doi.org/10.1016/S0034-4257(02)00076-7.

Justice, C.O.; Giglio, L.; Roy, D. [and others]. 2011. MODIS-derived global fire products. In: Ramachandran, B.; Justice, C.O.; Abrams, M.J., eds. Land remote sensing and global environmental change: NASA's earth observing system and the science of ASTER and MODIS. New York: Springer: 661–679. https://doi.org/10.1007/978-1-4419-6749-7_29.

Kiser, D.; Elhanan, G.; Metcalf, W.J. [and others]. 2021. SARS-CoV-2 test positivity rate in Reno, Nevada: association with PM2.5 during the 2020 wildfire smoke events in the Western United States. Journal of Exposure Science and Environmental Epidemiology. 31: 797–803. https://doi.org/10.1038/s41370-021-00366-w.

Laffan, S.W. 2006. Assessing regional scale weed distributions, with an Australian example using *Nassella trichotoma*. Weed Research. 46(3): 194–206. https://doi.org/10.1111/j.1365-3180.2006.00491.x.

Lundquist, J.E.; Camp, A.E.; Tyrrell, M.L. [and others]. 2011. Earth, wind and fire: abiotic factors and the impacts of global environmental change on forest health. In: Castello, J.D.; Teale, S.A., eds. Forest health: an integrated perspective. New York: Cambridge University Press: 195–243. https://doi.org/10.1017/CBO9780511974977.008.

NASA Fire Information for Resource Management System. 2022a. FIRMS frequently asked questions. https://earthdata.nasa.gov/faq/firms-faq. [Date accessed: May 16, 2022].

NASA Fire Information for Resource Management System. 2022b. MODIS fire archive download tool. https://firms.modaps.eosdis.nasa.gov/download/. [Date accessed: April 26, 2022].

National Interagency Coordination Center. 2020. Wildland fire summary and statistics annual report: 2019. https://www.predictiveservices.nifc.gov/intelligence/2019_statssumm/intro_summary19.pdf. [Date accessed: April 3, 2020].

National Interagency Coordination Center. 2021. Wildland fire summary and statistics annual report: 2020. https://www.predictiveservices.nifc.gov/intelligence/2020_statssumm/intro_summary20.pdf. [Date accessed: May 20, 2021].

National Interagency Coordination Center. 2022. Wildland fire summary and statistics annual report: 2020. https://www.predictiveservices.nifc.gov/intelligence/2021_statssumm/intro_summary21.pdf. [Date accessed: May 11, 2022].

Navarro, K.M.; Clark, K.A.; Hardt, D.J. [and others]. 2021. Wildland firefighter exposure to smoke and COVID-19: a new risk on the fire line. Science of the Total Environment. 760: 144296. https://doi.org/10.1016/j.scitotenv.2020.144296.

Nowacki, G.J.; Abrams, M.D. 2008. The demise of fire and "mesophication" of forests in the Eastern United States. BioScience. 58(2): 123–138. https://doi.org/10.1641/B580207.

Nowell, H.K.; Holmes, C.D.; Robertson, K. [and others]. 2018. A new picture of fire extent, variability, and drought interaction in prescribed fire landscapes: insights from Florida government records. Geophysical Research Letters. 45(15): 7874–7884. https://doi.org/10.1029/2018GL078679.

Parisien, M.A.; Miller, C.; Parks, S.A. [and others]. 2016. The spatially varying influence of humans on fire probability in North America. Environmental Research Letters. 11(7): 1–18. https://doi.org/10.1088/1748-9326/11/7/075005.

Pausas, J.G.; Keeley, J.E. 2019. Wildfires as an ecosystem service. Frontiers in Ecology and the Environment. 17(5): 289–295. https://doi.org/10.1002/fee.2044.

Picotte, J.J.; Bhattarai, K.; Howard, D. [and others]. 2020. Changes to the Monitoring Trends in Burn Severity program mapping production procedures and data products. Fire Ecology. 16: 16. https://doi.org/10.1186/s42408-020-00076-y.

Potter, K.M. 2012a. Large-scale patterns of forest fire occurrence in the conterminous United States and Alaska, 2005–07. In: Potter, K.M.; Conkling, B.L., eds. Forest Health Monitoring 2008 national technical report. Gen. Tech. Rep. SRS-158. Asheville, NC: U.S. Department of Agriculture, Forest Service, Southern Research Station: 73–83.

Potter, K.M. 2012b. Large-scale patterns of forest fire occurrence in the conterminous United States and Alaska, 2001–08. In: Potter, K.M.; Conkling, B.L., eds. Forest Health Monitoring 2009 national technical report. Gen. Tech. Rep. SRS-167. Asheville, NC: U.S. Department of Agriculture, Forest Service, Southern Research Station: 151–161.

Potter, K.M. 2013a. Large-scale patterns of forest fire occurrence in the conterminous United States and Alaska, 2009. In: Potter, K.M.; Conkling, B.L., eds. Forest Health Monitoring: national status, trends, and analysis 2010. Gen. Tech. Rep. SRS-176. Asheville, NC: U.S. Department of Agriculture, Forest Service, Southern Research Station: 31–39.

Potter, K.M. 2013b. Large-scale patterns of forest fire occurrence in the conterminous United States and Alaska, 2010. In: Potter, K.M.; Conkling, B.L., eds. Forest Health Monitoring: national status, trends, and analysis 2011. Gen. Tech. Rep. SRS-185. Asheville, NC: U.S. Department of Agriculture, Forest Service, Southern Research Station: 29–40.

Potter, K.M. 2014. Large-scale patterns of forest fire occurrence in the conterminous United States and Alaska, 2011. In: Potter, K.M.; Conkling, B.L., eds. Forest Health Monitoring: national status, trends, and analysis 2012. Gen. Tech. Rep. SRS-198. Asheville, NC: U.S. Department of Agriculture, Forest Service, Southern Research Station: 35–48.

Potter, K.M. 2015a. Large-scale patterns of forest fire occurrence in the conterminous United States and Alaska, 2012. In: Potter, K.M.; Conkling, B.L., eds. Forest Health Monitoring: national status, trends, and analysis 2013. Gen. Tech. Rep. SRS-207. Asheville, NC: U.S. Department of Agriculture, Forest Service, Southern Research Station: 37–53.

Potter, K.M. 2015b. Large-scale patterns of forest fire occurrence in the conterminous United States and Alaska, 2013. In: Potter, K.M.; Conkling, B.L., eds. Forest Health Monitoring: national status, trends, and analysis 2014. Gen. Tech. Rep. SRS-209. Asheville, NC: U.S. Department of Agriculture, Forest Service, Southern Research Station: 39–55.

Potter, K.M. 2016. Large-scale patterns of forest fire occurrence in the conterminous United States, Alaska, and Hawaii, 2014. In: Potter, K.M.; Conkling, B.L., eds. Forest Health Monitoring: national status, trends, and analysis 2015. Gen. Tech. Rep. SRS-213. Asheville, NC: U.S. Department of Agriculture, Forest Service, Southern Research Station: 41–60.

Potter, K.M. 2017. Large-scale patterns of forest fire occurrence in the conterminous United States, Alaska, and Hawaii, 2015. In: Potter, K.M.; Conkling, B.L., eds. Forest Health Monitoring: national status, trends, and analysis 2016. Gen. Tech. Rep. SRS-222. Asheville, NC: U.S. Department of Agriculture, Forest Service, Southern Research Station: 43–62.

Potter, K.M. 2018. Large-scale patterns of forest fire occurrence in the conterminous United States, Alaska, and Hawaii, 2016. In: Potter, K.M.; Conkling, B.L., eds. Forest Health Monitoring: national status, trends, and analysis 2017. Gen. Tech. Rep. SRS-233. Asheville, NC: U.S. Department of Agriculture, Forest Service, Southern Research Station: 45–64.

Potter, K.M. 2019. Large-scale patterns of forest fire occurrence across the 50 United States and the Caribbean territories, 2017. In: Potter, K.M.; Conkling, B.L., eds. Forest Health Monitoring: national status, trends, and analysis 2018. Gen. Tech. Rep. SRS-239. Asheville, NC: U.S. Department of Agriculture, Forest Service, Southern Research Station: 51–76.

Potter, K.M. 2020. Large-scale patterns of forest fire occurrence across the 50 United States and the Caribbean territories, 2018. In: Potter, K.M.; Conkling, B.L., eds. Forest Health Monitoring: national status, trends, and analysis 2019. Gen. Tech. Rep. SRS-250. Asheville, NC: U.S. Department of Agriculture, Forest Service, Southern Research Station: 57–82.

Potter, K.M. 2023. Ecological regions of Hawai'i. Fort Collins, CO: Forest Service Research Data Archive. https://doi.org/10.2737/RDS-2023-0018. [Date accessed: July 31, 2023].

Potter, K.M. 2021. Broad-scale patterns of forest fire occurrence across the 50 United States and the Caribbean territories, 2019. In: Potter, K.M.; Conkling, B.L., eds. Forest Health Monitoring: national status, trends, and analysis 2020. Gen. Tech. Rep. SRS-261. Asheville, NC: U.S. Department of Agriculture, Forest Service, Southern Research Station: 59–84.

Potter, K.M. 2022. Broad-scale patterns of forest fire occurrence across the 50 United States and the Caribbean territories, 2020. In: Potter, K.M.; Conkling, B.L., eds. Forest Health Monitoring: national status, trends, and analysis 2021. Gen. Tech. Rep. SRS-266. Asheville, NC: U.S. Department of Agriculture, Forest Service, Southern Research Station: 51–78. https://doi.org/10.2737/SRS-GTR-266-Chap3.

Potter, K.M.; Koch, F.H.; Oswalt, C.M.; Iannone, B.V. 2016. Data, data everywhere: detecting spatial patterns in fine-scale ecological information collected across a continent. Landscape Ecology. 31: 67–84. https://doi.org/10.1007/s10980-015-0295-0.

Pyne, S.J. 2010. America's fires: a historical context for policy and practice. Durham, NC: Forest History Society. 91 p.

Radeloff, V.C.; Helmers, D.P.; Anu Kramer, H. [and others]. 2018. Rapid growth of the US wildland-urban interface raises wildfire risk. Proceedings of the National Academy of Sciences. 115(13): 3314–3319. https://doi.org/10.1073/pnas.1718850115.

Reams, G.A.; Smith, W.D.; Hansen, M.H. [and others]. 2005. The Forest Inventory and Analysis sampling frame. In: Bechtold, W.A.; Patterson, P.L., eds. The enhanced Forest Inventory and Analysis program—national sampling design and estimation procedures. Gen. Tech. Rep. SRS-80. Asheville, NC: U.S. Department of Agriculture, Forest Service, Southern Research Station: 11–26.

Richardson, L.A.; Champ, P.A.; Loomis, J.B. 2012. The hidden cost of wildfires: economic valuation of health effects of wildfire smoke exposure in southern California. Journal of Forest Economics. 18(1): 14–35. https://doi.org/10.1016/j.jfe.2011.05.002.

Schmidt, K.M.; Menakis, J.P.; Hardy, C.C. [and others]. 2002. Development of coarse-scale spatial data for wildland fire and fuel management. Gen. Tech. Rep. RMRS-87. Fort Collins, CO: U.S. Department of Agriculture, Forest Service, Rocky Mountain Research Station. 41 p. https://doi.org/10.2737/RMRS-GTR-87.

Shima, T.; Sugimoto, S.; Okutomi, M. 2010. Comparison of image alignment on hexagonal and square lattices. In: 2010 IEEE international conference on image processing. [Place of publication unknown]: Institute of Electrical and Electronics Engineers, Inc.: 141–144. https://doi.org/10.1109/ICIP.2010.5654351.

Spencer, P.; Nowacki, G.; Fleming, M. [and others]. 2002. Home is where the habitat is: an ecosystem foundation for wildlife distribution and behavior. Arctic Research of the United States. 16: 6–17.

Stephens, S.L.; Collins, B.M.; Fettig, C.J. [and others]. 2018. Drought, tree mortality, and wildfire in forests adapted to frequent fire. BioScience. 68(2): 77–88. https://doi.org/10.1093/biosci/bix146.

Sutton, J.; Guy, M.; Silverman, H. 2021. The Bootleg Fire in Oregon is so large, it's creating its own weather. July 20. https://www.cnn.com/2021/07/20/weather/us-western-wildfires-tuesday/index.html. [Date accessed: May 20, 2022].

Thom, D.; Seidl, R. 2016. Natural disturbance impacts on ecosystem services and biodiversity in temperate and boreal forests. Biological Reviews. 91(3): 760–781. https://doi.org/10.1111/brv.12193.

Tonini, M.; Tuia, D.; Ratle, F. 2009. Detection of clusters using space-time scan statistics. International Journal of Wildland Fire. 18(7): 830–836. https://doi.org/10.1071/WF07167.

Wade, D.D.; Brock, B.L.; Brose, P. [and others]. 2000. Fire in eastern ecosystems. In: Brown, J.K.; Kapler, J., eds. Wildland fire in ecosystems: effects of fire on flora. Gen. Tech. Rep. RMRS-42-vol. 2. Ogden, UT: U.S. Department of Agriculture, Forest Service, Rocky Mountain Research Station: 53–96.

White, D.; Kimerling, A.J.; Overton, W.S. 1992. Cartographic and geometric components of a global sampling design for environmental monitoring. Cartography and Geographic Information Systems. 19(1): 5–22. https://doi.org/10.1559/152304092783786636.

CHAPTER 4

Satellite Observations of Forest Disturbances for the Conterminous United States During the 2021 Growing Season

Steven P. Norman and
William M. Christie

INTRODUCTION

Accurate forest disturbance mapping is a critical aspect of forest monitoring, but efforts have been inconsistent over landscapes and time (Coleman and others 2018, Housman and others 2018, Potter and Paschke 2022). Remote sensing is particularly adept at monitoring change in canopy cover from patch mortality or defoliation at scale, but it struggles to resolve dispersed tree impacts common to mixed species forests, gradual declines, delayed mortality, and cumulative impacts. As our need for precise mapping and understanding of disturbance grows, technology has provided invaluable solutions, but efficient causal attribution and impact assessment remain obstacles at broad scales. Recent advances in high-spatial-resolution imagery and high-speed computation have revolutionized forest canopy monitoring. With more efficient use of higher resolution imagery, our capacity to understand the mechanisms of forest change and precise disturbance impacts at scale has grown (Norman and Christie 2022).

Coordinated use of remote sensing datasets of different temporal and spatial resolution can satisfy a range of forest monitoring needs. For example, imagery is often of sufficiently high spatial resolution to resolve change in the canopy status of tree clusters if not that of individual trees. While such high-resolution imagery can also be generalized to map change in forest patches, coarser 250-m-resolution imagery from the Moderate Resolution Imaging Spectroradiometer (MODIS) (i.e., Terra and Aqua satellites) and the 300-m-resolution European Space Agency's Sentinel-3 satellites can often satisfy this need as well but do so more efficiently at scale due in part to their high pass-over frequency. Such spatially coarse but frequent imagery tracks large canopy disturbances at subseasonal temporal resolution in ways that distinguish persistent disturbance from ephemeral disturbance. Of particular concern in eastern deciduous forests are early season fire, wind, frost, or defoliation events, which may be detectable for just a few weeks or months of the growing season and yet be the target of forest monitoring efforts. Moreover, frequent observations give us more opportunities to acquire clear canopy views during the most optimal time of year for a given region. That is, with high-frequency streaming data, analysts can avoid issues related to seasonal weather-related differences in spring and fall timing and better target disturbances based on their optimal phenological characteristics.

This chapter provides a broad overview of disturbance during the 2021 growing season for the conterminous United States (CONUS) using spatially coarse but temporally frequent satellite imagery. We demonstrated the scalability of this general technique in an earlier publication, which described mapping of prominent disturbances for the United States at 10-m resolution (Norman and Christie 2022).

METHODS

We used Google Earth Engine (Gorelick and others 2017) to calculate the Normalized Difference Vegetation Index (NDVI) for the CONUS for a portion of the 2020 and 2021

How to cite this chapter:

Norman, Steven P.; Christie, William M. 2023. Satellite observations of forest disturbances for the conterminous United States during the 2021 growing season. In: Potter, Kevin M.; Conkling, Barbara L., eds. Forest Health Monitoring: national status, trends, and analysis 2022. Gen. Tech. Rep. SRS-273. Asheville, NC: U.S. Department of Agriculture, Forest Service, Southern Research Station: 83–90. https://doi.org/10.2737/SRS-GTR-273-Chap4.

growing seasons using surface-corrected MODIS 8-day composite NDVI from the Terra and Aqua satellites (MOD09Q1 and MYD09Q1, respectively) at 250-m resolution. We calculated the maximum value of these 8-day NDVI values over regionally adaptive 1–2-month windows. This regional modification of date windows lets us avoid months with heavy clouds and strong seasonal phenological change, while letting us capture key ephemeral disturbances during the growing season. For areas west of the 100th meridian, the NDVI composite window was July 15 to August 31 during the warm season; for the Northeast above the 36.5° N parallel, it was June 15 to July 15 to capture the effects of early summer defoliators; for the South, we used June 1 to July 15 given the region's early growing season and patchy persistent cloud cover; for peninsular Florida south of the 29° N parallel, we used September 1 to October 31 when clouds were less frequent compared to earlier in the summer. Comparison of NDVI values for 2021 with 2020 provided a regionally mosaiced map of 1-year change in NDVI.

We filtered the MODIS grid cells to only include those having majority forest cover based on the 30-m classification of the North American Land Change Monitoring System (NALCMS) for 2015 for a portion of Canada (http://www.cec.org/north-american-land-change-monitoring-system/) (Latifovic and others 2012) and the National Land Cover Dataset for 2016 for the United States (https://www.mrlc.gov/) (Jin and others 2019). Forests included evergreen, deciduous, mixed forest, and woody wetland types.

We thresholded NDVI departure at -0.05 and used values lower than that to define departure. We summed the majority-forest MODIS cells with NDVI departures and the total number of forest cells overall by 834-km^2 hexagons to provide landscape-scale insights useful for broad-scale monitoring (Norman and Christie 2022, Potter and others 2016). This gave us the percentage of majority-forest MODIS cells with NDVI departures for each hexagon. Where tree cover was sparse or absent, such as across the Great Plains, we imposed a minimum forest area requirement of 1500 ha (3,700 acres) for a hexagon.

RESULTS AND DISCUSSION

At a broad scale, the pattern of prominent forest disturbances across the CONUS for 2021 reflected that of prior years (fig. 4.1) (Norman and Christie 2020, 2022). The strongest NDVI departures occurred in the West, followed by the South, then the Northeast. States or ecoregions having these large anomalies often shift, however, in response to specific regional disturbances, such as drought, and more local disturbances, such as fire, insect outbreaks, and hurricanes.

West

The major disturbance detected for the West during 2021 was drought. According to the U.S. Drought Monitor (USDM), by August 2021, severe to exceptional drought was widespread and affecting every State west of the 100th meridian except for the southern Great Plains (https://droughtmonitor.unl.edu/). Other

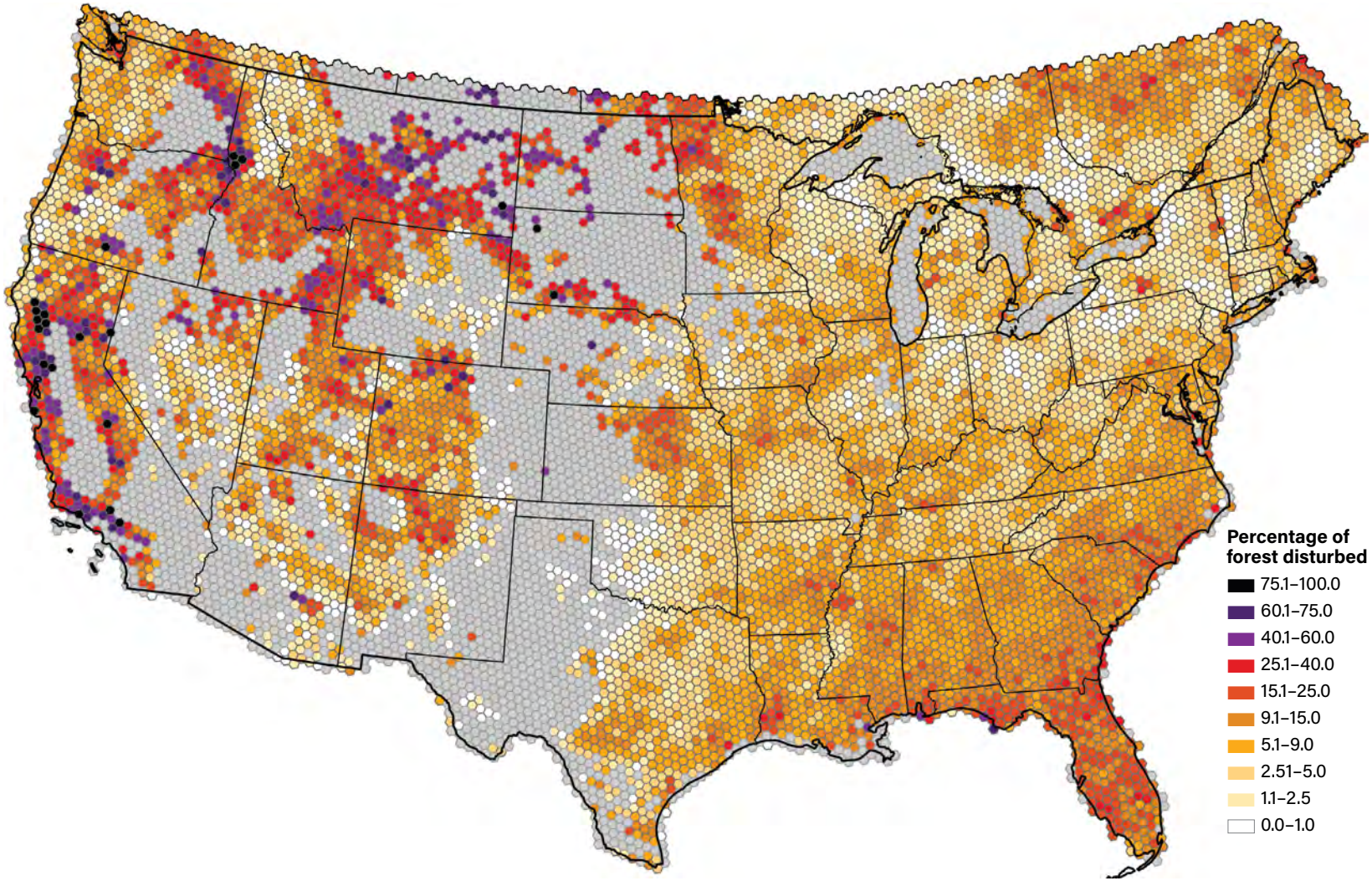

Figure 4.1—Percentage of majority-forest 250-m Moderate Resolution Imaging Spectroradiometer grid cells with disturbance in 2021 compared to 2020 using a Normalized Difference Vegetation Index departure threshold of ≤-0.05 summarized by 834-km² hexagons for the conterminous United States and southern Canada. Gray hexagons had too little forest cover to reliably map.

regional exceptions where drought was minor or absent included the Cascades and coastal forests of western Washington, coastal Oregon, northwestern Montana, the Black Hills of South Dakota, and central Colorado. Through summer, the USDM showed severe to exceptional drought building northward, with Southwestern States experiencing summer drought of longer duration than the Northwestern States. Figure 4.1 reflects more NDVI anomalies in California and in the Northwestern States than for Arizona, New Mexico, Colorado, and Utah, so the general pattern seen in figure 4.1 does not reflect differences in summer drought duration. It may, however, reflect differences in the baseline NDVI values from 2020 as there was more drought in the Southwest in 2020. The 1-year NDVI departure for those areas may reflect a less reliable expectation of "normal."

Known limitations of tracking evergreen tree stress associated with drought in the West from coarse remote sensing and NDVI are within-grid-cell mixed vegetation cover and the relative insensitivity of conifer NDVI to drought stress. From an optical remote sensing perspective, grass is highly sensitive to drought stress compared to evergreen trees, so 13-ha MODIS grid cells with a mixed grass and evergreen tree cover may be overwhelmed by variation in grass productivity or phenological responses more than any direct tree response to drought (Norman and others 2016). Spatial patterns of NDVI departure may then be a function of the fraction of the MODIS cell that supports the sensitive (grass) cover type rather than a meaningful measure of tree stress. Adding to the assessment challenge, extensive western forests have recently lost their conifer cover to fire, drought, or insects, but these remain classified as "forest" by NLCD. As disturbance and mortality become more widespread, this is a growing problem that can only be resolved by a more accurate or current forest mask or through use of finer resolution imagery, such as Sentinel-2 that reduces the mixed cover-type problem (Norman and Christie 2022).

Large local anomalies are readily seen across the West in figure 4.1, and these usually related to large wildfires that occurred between the fall of 2020 and early 2021. The most prominent nondrought disturbance that is evident on figure 4.1 is the million-acre (418 000 ha) August Complex that burned a large part of the Mendocino National Forest and adjacent areas in northwestern California during late 2020. Based on perimeters from the Monitoring Trends in Burn Severity (MTBS) project (https://www.mtbs.gov/) and satellite-detected thermal hot spots, wildfires from late 2020 or early 2021 also explain most isolated hexagon anomalies elsewhere in California, Oregon, Idaho, Colorado, and Arizona. In less treed areas, such as northern Nevada, eastern Montana, and the Dakotas, however, figure 4.1 shows forest disturbances not associated with wildfires. These areas could have been responding to drought, which is likely given their tendency to occur in riparian zones that include considerable edge with drought-sensitive grass. These areas experienced moderate to exceptional drought during the 2021 growing season.

Insect and Disease Survey (IDS) maps, coordinated by the U.S. Department of Agriculture, Forest Service, Forest Health Protection program,

showed extensive tree defoliation or mortality across forest areas of all Western States, including areas experiencing drought in 2021, but not exclusively. Wherever the 2021 insect damage exceeded that of 2020, it would add to the fraction of the hexagon measured as disturbed. However, as the COVID-19 pandemic may have impacted the extent of mapping in 2020 (Potter and Paschke 2022), the influence of a single-year baseline in 2020 cannot be easily resolved. In 2020, IDS maps showed large areas of canopy damage in Colorado, New Mexico, Montana, Idaho, Washington, and Oregon. In California, however, COVID-19 precautions prevented aerial survey flights from occurring in 2020, making comparisons impossible.

Northeast

The USDM showed severe to exceptional drought in Minnesota and Iowa and minor drought in northernmost New England and central Appalachia during the summer of 2021. Low to severe drought was also a factor in New England in 2020. Figure 4.1 shows strong forest NDVI departure in central and western Minnesota that is consistent with the extreme drought of midsummer, but there was not a clear association with drought for northern New England nor the central Appalachians.

Moderate forest NDVI decline was evident over broad portions of many Midwestern States where tree cover is fragmented or limited to riparian zones. The IDS maps were incomplete for most of these areas with limited forest, so the cause of this decline was difficult to interpret from the available data. A portion of this decline may be from emerald ash borer (*Agrilus planipennis*) mortality. When ash (*Fraxinus* spp.) occurs in mixed stands and declines gradually over several years, it can be challenging to accurately map these declines based on anything other than aerial flights or very high-resolution remote sensing.

During early summer 2021, spongy moth (*Lymantria dispar*) caused large patches of tree defoliation in Michigan, Pennsylvania, New Jersey, New York, Connecticut, New Hampshire, Maine, and Ontario, Canada. These show up well on figure 4.1 and agree with the raw maps of NDVI change and with IDS maps of spongy moth defoliation (fig. 4.2). The spongy moth outbreak in Michigan was especially notable and follows a similar large outbreak there in 2020. Elsewhere in the Northeast, extensive patches of eastern spruce budworm (*Choristoneura fumiferana*) defoliation were mapped in northeastern Minnesota, and Lophodermium needle cast of pines was mapped in Cape Cod, MA. Also detected were emerald ash borer damage in southeastern Pennsylvania, and in the South, winter ice storm damage in eastern Kentucky. Other than the spongy moth defoliation, none of these other damage agents is indicated in the hexagons on figure 4.1. This is either because they were of low impact or limited extent, or their mapped impacts were relatively minor when taken as a percentage of the available forest in that hexagon. As shown on figure 4.2, MODIS has no problem mapping large patches of spongy moth defoliations at 250-m resolution (Spruce and others 2011). Detection of smaller patches often requires higher resolution imagery, such as Sentinel-2 (Norman and Christie 2022).

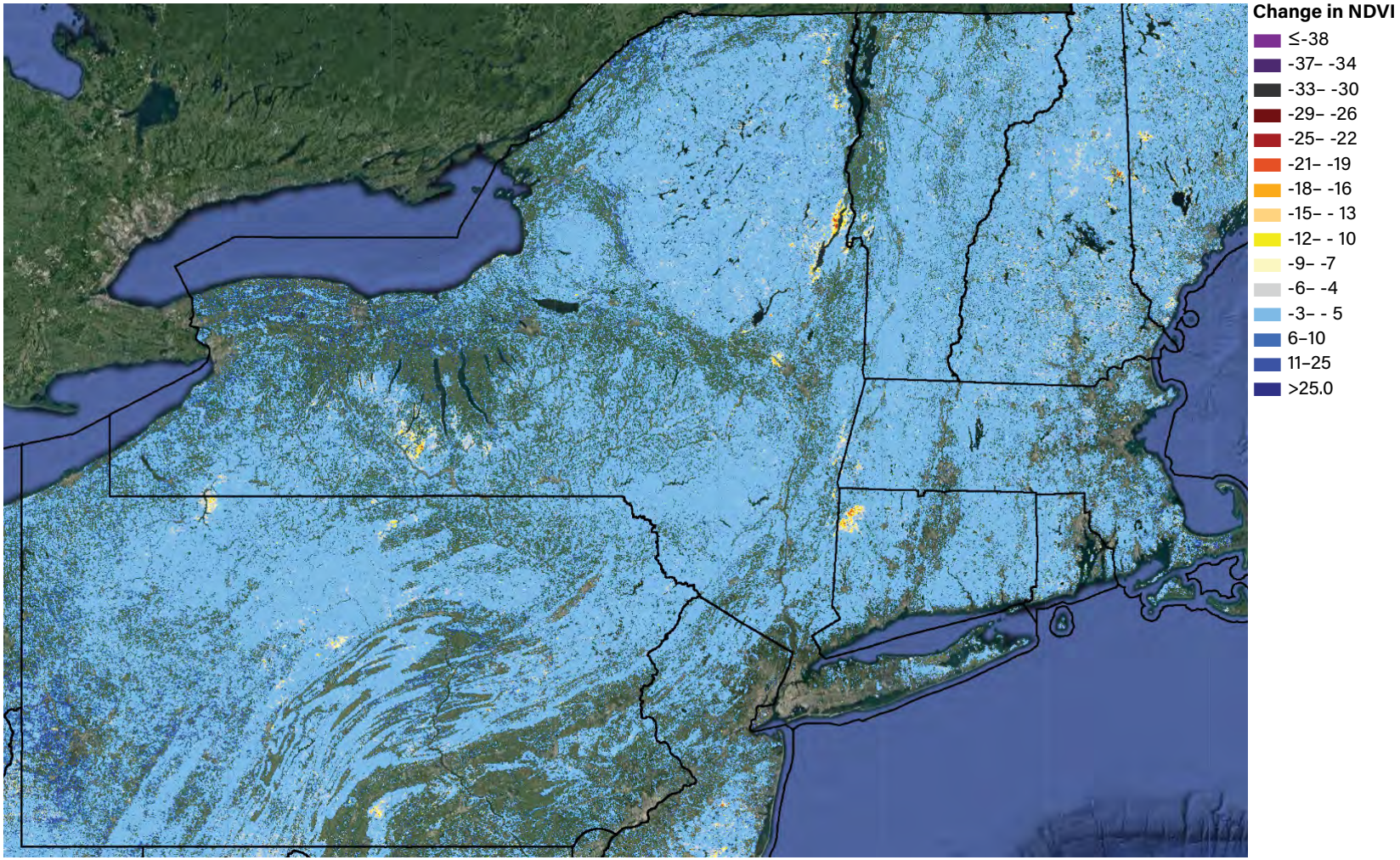

*Figure 4.2—A comparison of absolute 1-year change in Normalized Difference Vegetation Index (NDVI) at 250 m from the Moderate Resolution Imaging Spectroradiometer showing the regional occurrence of insect defoliation, mostly from spongy moth (*Lymantria dispar*) in the Northeast (6/15 to 7/15 composites for 2021 versus 2020).*

South

As has been observed recurrently, the leading cause of forest disturbance in the South has been commercial logging operations, and much of the NDVI departure seen in the Southeast's Coastal Plain on figure 4.1 reflects this cause (Hansen and others 2013; Norman and Christie 2020, 2022). It is common for hexagons of the Southeast to exhibit 5 to 15 percent of their forest as departed from NDVI values of the prior year.

There are numerous hot spots of disturbance activity shown on figure 4.1 that can be attributed to other or more complex causes. Damage from Hurricane Laura in southwestern Louisiana and from Hurricane Sally in southern Alabama are evident. A subsequent increase in logging compared to the prior baseline year may have also contributed to these patterns there. Florida also shows spotty NDVI departures; which relates to the variable rate of logging in places. The rate of logging may have increased in the wake of Hurricane Michael in Florida's panhandle, but most areas shown in red for Florida on figure 4.1 are not directly or indirectly associated with storm damage. This may be a combination of fire and logging operations and, in some places, lingering atmospheric problems not fully removed by this analysis.

CONCLUSIONS

Remote sensing has a proven record of mapping and tracking large patch disturbances at coarse scales (Hansen and others 2013, Kennedy and others 2018, Spruce and others 2011). The patterns shown on figure 4.1 represent those more prominent disturbances while contextualizing them within the forested landscape in which they occur. The research frontier lies with precise mapping of disturbances at much finer resolution (i.e., with sufficient detail to capture the status of individual canopy trees); similar techniques have been, and can be, used with 10-m-resolution Sentinel-2 imagery or finer using Google Earth Engine (Norman and Christie 2022). This finer resolution is useful for mapping tree mortality in mixed stands, which are common in areas of the Eastern United States, in addition to resolving cause when multiple drivers of forest change co-occur. For example, mapping emerald ash borer mortality has been resolved by integrating Landsat with Sentinel-2 and lidar height data in Minnesota (Host and others 2020). In the Southern Appalachians, gradual tree mortality from the nonnative hemlock woolly adelgid (*Adelges tsugae*) could be partially distinguished from fire regime mortality using Landsat over a longer period than the 1-year analysis used in this current study (Khodaee and others 2020). Regional or national analyses provide a coarse-filter perspective on forest disturbance, but a full understanding requires landscape or site analysis that involves multiple years of context and regional expertise.

LITERATURE CITED

Coleman, T.W.; Graves, A.D.; Heath, Z. [and others] 2018. Accuracy of aerial detection surveys for mapping insect and disease disturbances in the United States. Forest Ecology and Management. 430: 321–336. https://doi.org/10.1016/j.foreco.2018.08.020.

Gorelick, N.; Hancher, M.; Dixon, M. [and others]. 2017. Google Earth Engine: planetary-scale geospatial analysis for everyone. Remote Sensing of Environment. 202: 18–27. https://doi.org/10.1016/j.rse.2017.06.031.

Hansen, M.C.; Potapov, P.V.; Moore, R. [and others]. 2013. High resolution global maps of 21st-century forest cover change. Science. 342: 850–853. https://doi.org/10.1126/science.1244693.

Host, T.K.; Russell, M.B.; Windmuller-Campione, M.A. [and others]. 2020. Ash presence and abundance derived from composite Landsat and Sentinel-2 time series and lidar surface models in Minnesota, USA. Remote Sensing. 12(8): 1341. https://doi.org/10.3390/RS12081341.

Housman, I.W.; Chastain, R.A.; Finco, M.V. 2018. An evaluation of forest health Insect and Disease Survey data and satellite-based remote sensing forest change detection methods: case studies in the United States. Remote Sensing. 10(8): 1184. https://doi.org/10.3390/rs10081184.

Jin, S.; Homer, C.; Yang, L. [and others]. 2019. Overall methodology design for the United States National Land Cover Database 2016 products. Remote Sensing. 11(24). https://doi.org/10.3390/rs11242971.

Kennedy, R.E.; Yang, Z.; Gorelick, N. [and others]. 2018. Implementation of the LandTrendr algorithm on Google Earth Engine. Remote Sensing. 10: 691. https://doi.org/10.3390/rs10050691.

Khodaee, M.; Hwang, T.; Kin, J. [and others]. 2020. Monitoring forest infestation and fire disturbance in the Southern Appalachian using a times series analysis of Landsat imagery. Remote Sensing. 12(15): 2412. https://doi.org/10.3390/rs12152412.

Latifovic, R.; Homer, C.; Ressl, R. [and others]. 2012. North American Land Change Monitoring System. In: Giri, C.P., ed.. Remote sensing of land use and land cover. Boca Raton, FL: CRC Press: 303–323. https://www.researchgate.net/publication/281545328_North_American_Land_Change_Monitoring_System. [Date last accessed: December 21, 2022].

Norman, S.P.; Christie, W.M. 2020. Satellite-based evidence of forest stress and decline across the conterminous United States for 2016, 2017, and 2018. In: Potter, K.M.; Conkling, B.L., eds. Forest Health Monitoring: national status, trends, and analysis 2019. Gen. Tech. Rep. SRS-250. Asheville, NC: U.S. Department of Agriculture, Forest Service, Southern Research Station: 151–166.

Norman, S.P.; Christie, W.M. 2022. Precise mapping of disturbance impacts to U.S. forests using high-resolution satellite imagery. In: Potter, K.M.; Conkling, B.L., eds. Forest Health Monitoring: national status, trends, and analysis 2021. Gen. Tech. Rep. SRS-266. Asheville, NC: U.S. Department of Agriculture, Forest Service, Southern Research Station: 119–133. https://doi.org/10.2737/SRS-GTR-266-Chap6.

Norman, S.P.; Koch, F.H.; Hargrove, W.W. 2016. Review of broad-scale drought monitoring of forests: toward an integrated data mining approach. Forest Ecology and Management. 380: 346–358. https://doi.org/10.1016/j.foreco.2016.06.027.

Potter, K.M.; Koch, F.H.; Oswalt, C.M.; Iannone, B.V. 2016. Data, data everywhere: detecting spatial patterns in fine-scale ecological information collected across a continent. Landscape Ecology. 31: 67–84. https://doi.org/10.1007/s10980-015-0295-0.

Potter, K.M.; Paschke, J.L. 2022. Broad-scale patterns of insect and disease activity across the 50 United States from the national Insect and Disease Survey, 2020. In: Potter, K.M.; Conkling, B.L., eds. Forest Health Monitoring: national status, trends, and analysis 2021. Gen. Tech. Rep. SRS-266. Asheville, NC: U.S. Department of Agriculture, Forest Service, Southern Research Station: 25–49. https://doi.org/10.2737/SRS-GTR-266-Chap2.

Spruce, J.P.; Sader, S.; Ryan, R.E. [and others]. 2011. Assessment of MODIS NDVI time series data products for detecting forest defoliation by gypsy moth outbreaks. Remote Sensing of Environment. 1152: 427–437. https://doi.org/10.1016/j.rse.2010.09.013.

CHAPTER 5

Tree Mortality

Mark J. Ambrose

INTRODUCTION

Tree mortality is a natural process in all forest ecosystems. High mortality can be an indicator of forest health problems. On a regional scale, high mortality levels may indicate widespread insect or disease impacts. Regionally high mortality may also occur if a large proportion of the forest in a particular region is made up of older, senescent stands. I present an approach that seeks to detect mortality patterns that might reflect changes to ecosystem processes at large scales. In many cases, the proximate cause of mortality may be discernable. Understanding proximate causes of mortality *may* provide insight into whether the mortality is within the range of natural variation or reflects more fundamental changes to ecological processes.

DATA

I used the U.S. Department of Agriculture, Forest Service, Forest Inventory and Analysis (FIA) Phase 2 (P2) data as the basis of the mortality analysis. The FIA P2 data are collected across forested land throughout the United States, with approximately one plot per 6,000 acres of forest, using a rotating panel sample design (Bechtold and Patterson 2005). Field plots are divided into spatially balanced panels, with one panel being measured each year. A single cycle of measurements consists of measuring all panels. This "annualized" method of inventory was adopted, State by State, beginning in 1999. The cycle length (i.e., number of years required to measure all plot panels) ranges from 5 to 10 years.

An analysis of mortality requires data collected at a minimum of two points in time. Therefore, mortality analysis was possible for areas where data from repeated plot measurements using consistent sampling protocols were available (i.e., where one cycle of measurements had been completed and at least one panel of the next cycle had been measured, and where there had been no changes to the protocols affecting measurements of trees or saplings). In this analysis, I used the most recent cycle of remeasurements for each State and omitted ecoregion sections if there were not at least 50 remeasured plots in the dataset.

Due to the COVID-19 pandemic, FIA data collection slowed during 2020 and 2021. Therefore, although mortality analyses were possible for all of the conterminous United States, no new data were available from any Western States (i.e., the available datasets are the same as those used for the Forest Health Monitoring: National Status, Trends, and Analysis 2021 report). Therefore, for this report, I limited the analysis to States in the Eastern and Central United States. Figure 5.1 shows the States included in the analysis as well as the forested area in those States.[1]

METHODS

The FIA program calculates tree growth, mortality, and removal volume on each plot over the interval between repeated measurements. These values are stored in the FIA Database (version 9.0.1) (Burrill and others 2021). EVALIDator (ver. 1.8.0.01) is FIA's online tool for querying the FIA Database

[1] *For the latest analysis of mortality that includes Western States, see Ambrose and others 2022.*

How to cite this chapter:

Ambrose, Mark J. 2023. Tree mortality. In: Potter, Kevin M.; Conkling, Barbara L., eds. Forest Health Monitoring: national status, trends, and analysis 2022. Gen. Tech. Rep. SRS-273. Asheville, NC: U.S. Department of Agriculture, Forest Service, Southern Research Station: 91–101. https://doi.org/10.2737/SRS-GTR-273-Chap5.

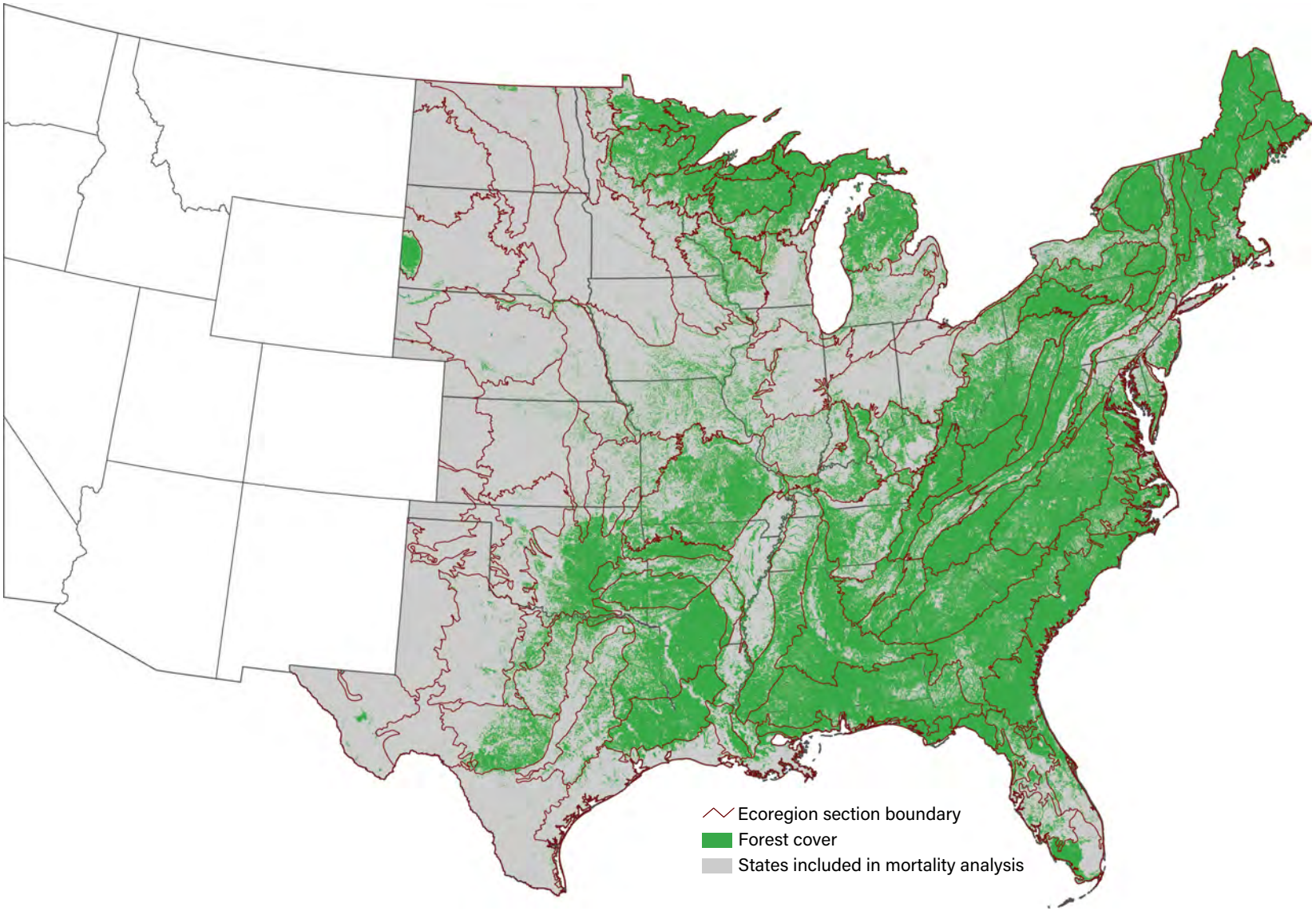

Figure 5.1—Forest cover in the States where mortality was analyzed by ecoregion section (Cleland and others 2007). Forest cover was derived from Moderate Resolution Imaging Spectrometer (MODIS) satellite imagery (USDA Forest Service 2008).

and generating area-based reports on forest characteristics (USDA Forest Service FIA 2019). EVALIDator was used to obtain net growth rates and mortality rates over the most recent measurement cycle for each of 113 ecoregion sections (Cleland and others 2007, McNab and others 2007) covering the Eastern and Central United States. For most States, the most recent cycle of available data ran through 2020[2] (e.g., data collected from 2014 through 2020).

To compare mortality across forest types and climate zones, I used the ratio of annual mortality to gross growth (MRATIO) as a standardized mortality indicator (Coulston and others 2005). The MRATIO has proven to be a useful indicator of forest health, but it can be a problematic indicator, especially when growth rates are very low. The MRATIO can also be difficult to interpret when there is high uncertainty associated with growth estimates.

To identify causal agents for the observed mortality, I also used EVALIDator to summarize mortality by the reported "cause of death" associated with the observed mortality. FIA records causes of death as general categories (e.g., insects, fire, weather). For each ecoregion with a high MRATIO, I used EVALIDator to generate a table of annual mortality volume by FIA species group (Burrill and others 2018) and cause of death. From these tables, it is possible to make reasonable assumptions about the particular insects or diseases that may be affecting certain regions. Care must be used in interpreting these causes because tree mortality may actually be caused by a combination of factors, such as drought and insects. Further information about the causes of mortality is provided by the aerial survey of insects and disease (see ch. 2 in this report). It is difficult to directly match aerial survey data to mortality observed on FIA plots due to both the difference in timing when mortality is recorded and difficulty matching plot locations with aerial survey mortality polygons. However, I have incorporated aerial survey information into the discussion by referencing State Forest Health Highlights, which reflect in large part the results of aerial surveys.

RESULTS AND DISCUSSION

The MRATIO values are shown in figure 5.2. The MRATIO can be large if an overmature forest is senescing and losing a cohort of older trees. If forests are not naturally senescing, a high MRATIO (>0.6) may indicate high mortality due to some acute cause (e.g., insects or diseases) or due to generally deteriorating forest health conditions. The ecoregion sections with the highest MRATIOs are labeled on the map in figure 5.2. In the discussion that follows, I focus on the ecoregion sections having MRATIOs >0.6.

The highest MRATIO occurred in ecoregion section M334A–Black Hills (MRATIO = 1.29). The MRATIO was also extremely high in adjacent 331F–Western Great Plains (MRATIO = 0.92) in South Dakota and Nebraska. Other areas of high mortality relative to growth on the Great Plains were in 332A–Northeastern Glaciated Plains (MRATIO = 0.64) in North

[2] *Overall, the most recent data available for any State ranged from 2018 to 2021.*

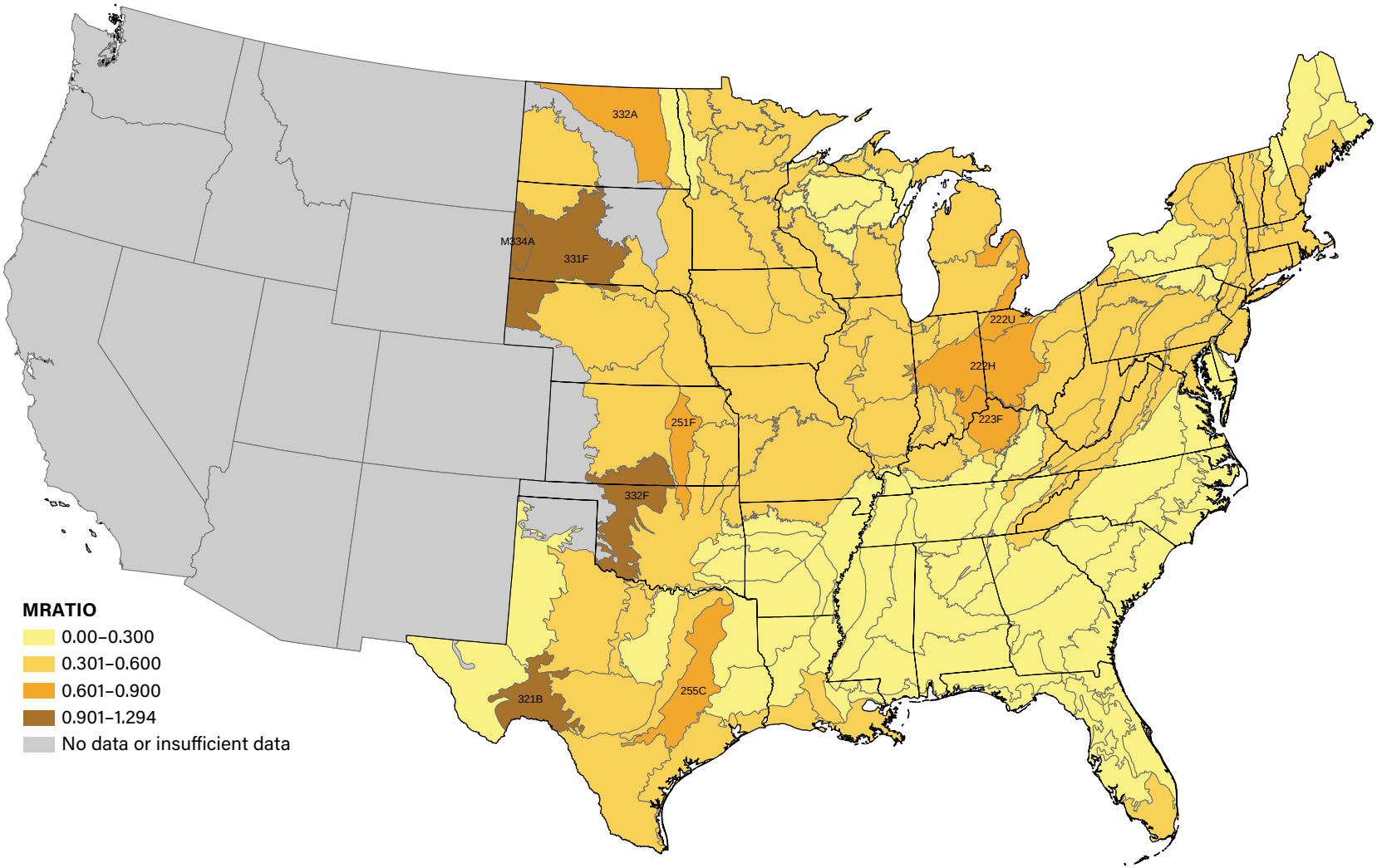

Figure 5.2—Tree mortality expressed as the ratio of annual mortality volume to gross annual growth volume (MRATIO), by ecoregion section (Cleland and others 2007). (Data source: U.S. Department of Agriculture, Forest Service Forest Inventory and Analysis program)

Dakota. In these Great Plains ecoregion sections where mortality is high relative to growth, the predominant vegetation is grassland. Although the ecoregions are quite large, there was relatively little forest land to measure. In the Great Plains, tree growth is generally slow because of naturally dry conditions. Where the number of sample plots is small and tree growth is naturally slow, care must be taken in interpreting mortality relative to growth.

In ecoregion section M334A–Black Hills (MRATIO = 1.29), the vast majority (94 percent) of mortality occurred in the ponderosa and Jeffrey pines species group. For the entire ecoregion section, 75 percent of mortality was caused by insects, while 14 percent was caused by fire (table 5.1); for the ponderosa and Jeffrey pine species group, insects and fire were responsible for 78 percent and 14 percent of mortality, respectively. Mortality in this ecoregion section is most likely related to mountain pine beetle (*Dendroctonus ponderosae*). There had been an ongoing mountain pine beetle outbreak in the Black Hills region (Ball and others 2015, 2016; South Dakota Department of Agriculture 2011, 2012, 2013, 2014). Mountain pine beetle activity has declined dramatically in the region since 2015 (Ball and others 2017, Wyoming State Forestry Division 2017). The pine beetle outbreak has ended, but reported mortality remains high because results reported, based on the most recent cycles of FIA data, reflect mortality over the period that includes the peak of the outbreak in 2015.

In ecoregion section 331F–Western Great Plains (MRATIO = 0.92), fire caused 61 percent of mortality; another 20 percent of mortality was weather-related (table 5.1). In this ecoregion section, most of the mortality (about 87 percent) occurred in the ponderosa and Jeffrey pines species group. In this species group, 62 percent of mortality was due to fire and 22 percent was due to adverse weather; only 8 percent of mortality was related to insects.

The majority of the mortality in ecoregion section 332A–Northeastern Glaciated Plains (MRATIO = 0.64) of North Dakota was split between the cottonwood and aspen (69 percent) and select white oaks (19 percent) species groups. About 30 percent of the mortality overall (table 5.1), 39 percent of mortality in the select white oaks species group, and 26 percent of mortality in the cottonwood and aspen species group was related to adverse weather. North Dakota experienced both drought (North Dakota Forest Service 2017) and heavy precipitation that waterlogged tree root systems (North Dakota Forest Service 2020) during the monitoring period, both of which severely stressed trees. In addition, North Dakota experienced numerous storm events over the past several years, including 435 hail events and 66 tornadoes during the 2015 and 2016 growing seasons. Damage due to hailstorms can make trees susceptible to a number of fungal diseases (North Dakota Forest Service 2015, 2016). Cottonwood canker fungi have been identified as a problem throughout North Dakota (North Dakota Forest Service 2014, 2015); these fungi may be contributing to the observed mortality in the cottonwood and aspen species group. About 18 percent of mortality was attributed to animals; almost all of this occurred in the cottonwood and aspen species group.

Table 5.1—Ecoregion sections in the Eastern and Central United States having the highest mortality relative to growth (MRATIO), annual mortality and growth rates, species groups having the greatest mortality relative to growth, and associated causes of mortality

Ecoregion section	Average annual mortality	Average annual gross growth	MRATIO	Species groups[a] having the highest mortality[b]	Major causes of mortality[c]
	--- cubic feet per year ---				
M334A–Black Hills	47,840,846	36,971,471	1.29	Ponderosa and Jeffrey pines (94%)	Insects (75%), fire (14%)
332F–South Central and Red Bed Plains	18,476,189	19,195,108	0.96	Other eastern soft hardwoods (38%), other eastern softwoods (25%), other eastern hard hardwoods (13%)	Fire (54%), disease (23%), weather-related (23%)
321B–Stockton Plateau	8,830,859	9,587,071	0.92	Western woodland softwoods (92%)	Weather-related (68%), fire (30%)
331F–Western Great Plains	11,539,479	12,592,299	0.92	Ponderosa and Jeffrey pines (87%)	Fire (61%), weather-related (20%)
255C–Oak Woods and Prairie	118,181,937	150,755,567	0.78	Oaksd (46%), loblolly and shortleaf pines (13%)	Weather-related (64%), disease (23%)
223F–Interior Low Plateau-Bluegrass	104,017,750	156,580,166	0.66	Ash (59%), other eastern soft hardwoods (15%)	Insects (55%), vegetation (13%)[e]
222U–Lake Whittlesey Glaciolacustrine Plain	44,342,544	67,606,692	0.66	Ash (65%), other eastern soft hardwoods (13%)	Insects (66%)
332A–Northeastern Glaciated Plains	5,877,224	9,133,469	0.64	Cottonwood and aspen (69%), select white oaks (19%)	Weather-related (30%), animals (18%)
251F–Flint Hills	11,607,118	18,076,691	0.64	Oaks[d] (44%), other eastern soft hardwoods (33%)	Weather-related (39%), insects (14%), disease (14%)
222H–Central Till Plains-Beech-Maple	111,213,566	175,798,966	0.63	Ash (57%), other eastern soft hardwoods (16%)	Insects (55%)

[a] For the species included in each species group, see Appendices E and F in Burrill and others 2018.
[b] The value in parentheses is the proportion of average annual mortality volume in the ecoregion section occurring in the species group.
[c] The value in parentheses is the proportion of average annual mortality volume in the ecoregion section attributed to the causal agent.
[d] Overall mortality has been combined for the Forest Inventory and Analysis select red oaks, select white oaks, other red oaks, and other white oaks species groups.
[e] Mortality caused by suppression, Competition, vines/kudzu (Burrill and others 2018).

Ecoregion section 332F–South Central and Red Bed Plains in Kansas and Oklahoma had the second highest observed MRATIO (0.96). Fifty-four percent of mortality was due to fire, while 23 percent of mortality was attributed to disease and another 23 percent to adverse weather (table 5.1). The region was affected by a severe drought in 2011 as well as additional droughty periods in years that followed (Kansas Forest Service 2012, 2013, 2014; Oklahoma Forestry Services 2014, 2015, 2016, 2020). The species groups in which most of the mortality occurred (other eastern soft hardwoods, other eastern softwoods, and other eastern hard hardwoods) include a large number of unrelated species. Thus, understanding the specific impacts of weather and disease on particular species in this ecoregion would require a more detailed analysis beyond the scope of this report.

In ecoregion section 251F–Flint Hills (MRATIO = 0.64), also in Kansas and Oklahoma, 39 percent of mortality was weather-related, while insects and disease were each responsible for about 14 percent of mortality (table 5.1). The region frequently experiences adverse weather events. In addition to drought, these include hail, tornadoes, high winds, and ice storms (Kansas Forest Service 2020). The highest mortality occurred in the combined oaks species groups (44 percent of the ecoregion section's mortality). Eighty-two percent of mortality in this species group was attributed to adverse weather.

Ecoregion section 255C–Oak Woods and Prairie in Texas also had relatively high mortality (MRATIO = 0.78). About 46 percent of the mortality occurred in the combined oaks species groups, and another 13 percent occurred in the loblolly and shortleaf pines species group. The majority (64 percent) of mortality in this ecoregion section was identified as weather-related (table 5.1). Weather was responsible for 60 and 36 percent of mortality in the combined oaks and loblolly and shortleaf pines species groups, respectively. A record-setting drought in 2011 affected Oklahoma and Texas, and additional droughty periods occurred in following years (Oklahoma Forestry Services 2014, 2015, 2016, 2020). Drought was reported as weakening both pines (*Pinus* spp.) and hardwoods in Texas, making them susceptible to a variety of pests and pathogens (Smith 2013, 2014). Disease was the reported cause of another 23 percent of mortality (table 5.1). Disease was reported as responsible for 36 percent of mortality in the combined oaks species groups; fire was responsible for 57 percent of pine mortality. Oak wilt has been a major problem in oak woodlands in central Texas (Smith 2014; Texas A&M Forest Service 2015, 2016, 2019) and probably contributed to the red and white oak (*Quercus* spp.) mortality in the combined oak species group. Pine engraver beetle (*Ips* spp.) has been a problem in Texas' pine forests and may have contributed to mortality in the loblolly and shortleaf pines species group (Smith 2014; Texas A&M Forest Service 2015, 2016, 2017).

Ecoregion section 321B–Stockton Plateau (MRATIO = 0.92) is a region of extremely low forest cover (fig. 5.1). There, about 68 percent of mortality was related to adverse weather and another 30 percent was due to fire (table 5.1). About 92 percent of mortality occurred in the

western woodland softwoods species group; about 70 percent of mortality in this species group was due to weather and 29 percent was due to fire. Most of this mortality probably was related to the previously discussed drought that affected Texas beginning in 2011.

Mortality relative to growth was also rather high (MRATIO = 0.66) in ecoregion section 222U–Lake Whittlesey Glaciolacustrine Plain. There, the majority of the mortality (65 percent) was in the ash species group. About 66 percent of mortality in that ecoregion section was caused by insects (table 5.1), and insects were responsible for 98 percent of ash (*Fraxinus* spp.) mortality. Most of this mortality was due to emerald ash borer (*Agrilus planipennis*), which has produced extremely high ash mortality throughout Ohio and Michigan (Michigan Department of Natural Resources 2014, 2015, 2016, 2017; Ohio Department of Natural Resources, Division of Forestry 2014, 2015, 2020). Indeed, emerald ash borer has been "the most devastating forest pest in Ohio in recent years" (Ohio Department of Natural Resources, Division of Forestry 2020) and has caused the death of the "vast majority" of native ash in northwestern Ohio (Ohio Department of Natural Resources, Division of Forestry 2016, 2017).

Similarly, in the adjacent ecoregion section 222H–Central Till Plains-Beech-Maple (MRATIO = 0.63) in Ohio and Indiana, much of the mortality (57 percent) was in the ash species group and 97 percent of ash mortality was due to emerald ash borer[3] (table 5.1). Indeed, emerald ash borer has been confirmed throughout the ecoregion as well as throughout Indiana (Marshall 2017, 2018, 2020; Ohio Department of Natural Resources, Division of Forestry 2016, 2017).

The situation is similar in ecoregion section 223F–Interior Low Plateau-Bluegrass (MRATIO = 0.66) in southern Indiana and Ohio and north-central Kentucky. There, about 54 percent of mortality was in the ash species group. Fifty-five percent of overall mortality in the ecoregion section was attributed to insects, but almost all (94 percent) of ash mortality was due to emerald ash borer.[4] Emerald ash borer has been confirmed throughout the portion of the ecoregion section that is in Kentucky at least since 2016 (Kentucky Division of Forestry 2016).

CONCLUSIONS

This analysis shows that in most of the Eastern and Central United States, mortality is low relative to tree growth. The areas of highest mortality occur in the forests and woodlands of the Great Plains ecoregions. A common

[3] *Personal communication. 2022. Philip Marshall, Forest Health Specialist and Director of the Division of Entomology & Plant Pathology, Indiana Division of Forestry, 402 W. Washington St., Indianapolis, IN 46204; Tom Macy, Forest Health Program Manager, Ohio Division of Forestry, 2045 Morse Road Building H1, Columbus, OH 43229.*

[4] *Personal communication. 2022. Philip Marshall, Forest Health Specialist and Director of the Division of Entomology & Plant Pathology, Indiana Division of Forestry, 402 W. Washington St., Indianapolis, IN 46204; Tom Macy, Forest Health Program Manager, Ohio Division of Forestry, 2045 Morse Road Building H1, Columbus, OH 43229; Alexandra Blevins, Forest Health Specialist, Kentucky Division of Forestry, 300 Sower Blvd, Frankfort, KY 40601.*

characteristic of most of the ecoregions having high mortality is that they are on the margins of land suitable for forest growth, being very dry. Thus, they tend to be extremely vulnerable to changes in weather patterns that might produce prolonged and/or extreme drought. Drought, combined with a variety of other biotic and/or abiotic stressors, is responsible for much of the mortality observed.

One insect pest issue, however, does stand out in the East. In ecoregion sections 222H–Central Till Plains-Beech-Maple, 222U–Lake Whittlesey Glaciolacustrine Plain, and 223F–Interior Low Plateau-Bluegrass, ash mortality due to emerald ash borer is extremely high.

It is also important to realize that the analyses presented in this chapter alone cannot tell the complete story regarding tree mortality. Mortality concentrated in highly fragmented forest or nonforest areas adjacent to human development may not be detected because the available FIA data do not cover most urban areas or other places not defined as forest by FIA. Also, these analyses are unlikely to detect a pest or pathogen attacking a particular tree species in a mixed-species forest where other species are growing vigorously. This is especially true of species (e.g., ash) that make up a relatively small proportion of many eastern forests. For example, it is known that emerald ash borer has been causing very high ash mortality in many Eastern and Central States in recent years (Ohio Department of Natural Resources, Division of Forestry 2016; USDA APHIS 2018). Yet, this mortality stands out only in ecoregion sections 222H–Central Till Plains-Beech-Maple, 222U–Lake Whittlesey Glaciolacustrine Plain, and 223F–Interior Low Plateau-Bluegrass. Elsewhere in the East, though ash mortality is known to be extremely high, the mortality currently is masked because ash is a relatively minor component of the forest.

To gain a more complete understanding of mortality, it is important to consider the results of this analysis together with other indicators of forest health. Forest Inventory and Analysis tree damage data (Burrill and others 2021), as well as Evaluation Monitoring projects that focus on particular mortality-causing agents (ch. 8, 10, and 11), can provide insight into smaller scale or species-specific mortality issues. Large-scale analyses of forest-damaging events, including insect and disease activity (ch. 2) and fire (ch. 3), are also important for understanding mortality patterns. This can be especially important in the West, where mortality data are limited.

LITERATURE CITED

Ambrose, M.J.; Hanavan, R.; Smith, T. 2022. Tree mortality. In: Potter, K.M.; Conkling, B.L., eds. Forest Health Monitoring: national status, trends, and analysis 2021. Gen. Tech. Rep. SRS-266. Asheville, NC: U.S. Department of Agriculture, Forest Service, Southern Research Station: 101–115. https://doi.org/10.2737/SRS-GTR-266-Chap5.

Ball, J.; Pyser, N.; Warnke, M. 2016. Forest health highlights in South Dakota 2016. Pierre: South Dakota Department of Agriculture, Division of Resource Conservation and Forestry. 6 p. https://www.fs.usda.gov/foresthealth/docs/fhh/SD_FHH_2016.pdf. [Date accessed: August 18, 2022].

Ball, J.; Seidl, A.; Warnke, M. 2017. State of South Dakota forest health highlights. Pierre: South Dakota Department of Agriculture, Division of Resource Conservation and Forestry. 8 p. https://sdda.sd.gov/conservation-forestry/forest-health/SDHighlights_2017-2.pdf. [Date accessed: July 23, 2019].

Ball, J.; Seidl, A.; Warnke, M. 2018. State of South Dakota forest health highlights. Pierre: South Dakota Department of Agriculture, Division of Resource Conservation and Forestry. 12 p. https://sdda.sd.gov/conservation-forestry/forest-health/SDHighlights_2018.pdf. [Date accessed: July 1, 2019].

Ball, J.; Warnke, M.; Garbisch, B. 2015. Forest health highlights in South Dakota 2015. Pierre: South Dakota Department of Agriculture, Division of Resource Conservation and Forestry. 9 p. https://www.fs.usda.gov/foresthealth/docs/fhh/SD_FHH_2015.pdf. [Date accessed: August 18, 2022].

Bechtold, W.A.; Patterson, P.L., eds. 2005. The enhanced Forest Inventory and Analysis program—national sampling design and estimation procedures. Gen. Tech. Rep. SRS-80. Asheville, NC: U.S. Department of Agriculture, Forest Service, Southern Research Station. 85 p. https://doi.org/10.2737/SRS-GTR-80.

Burrill, E.A.; DiTommaso, A.M.; Turner, J.A. [and others]. 2021. The Forest Inventory and Analysis Database: database description and user guide for Phase 2 (version 9.0.1). Washington, DC: U.S. Department of Agriculture, Forest Service. 1026 p. https://www.fia.fs.usda.gov/library/database-documentation/. [Date last accessed: December 22, 2022].

Burrill, E.A.; Wilson, A.M.; Turner, J.A. [and others]. 2018. The Forest Inventory and Analysis Database: database description and user guide for Phase 2 (version 8.0). Washington, DC: U.S. Department of Agriculture, Forest Service. 946 p. https://www.fia.fs.usda.gov/library/database-documentation/. [Date last accessed: December 22, 2022].

Cleland, D.T.; Freeouf, J.A.; Keys, J.E. [and others]. 2007. Ecological subregions: sections and subsections for the conterminous United States. Gen. Tech. Rep. WO-76D. Washington, DC: U.S. Department of Agriculture, Forest Service. Map; Sloan, A.M., cartographer; presentation scale 1:3,500,000; colored. https://doi.org/10.2737/WO-GTR-76D.

Coulston, J.W.; Ambrose, M.J.; Stolte. K.S. [and others]. 2005. Criterion 3 – health and vitality. In: Conkling, B.L.; Coulston, J.W.; Ambrose, M.J., eds. Forest Health Monitoring 2001 national technical report. Gen. Tech. Rep. SRS-81. Asheville, NC: U.S. Department of Agriculture, Forest Service, Southern Research Station. 204 p.

Kansas Forest Service. 2012. Kansas forest health highlights 2012. 5 p. https://www.fs.usda.gov/foresthealth/docs/fhh/KS_FHH_2012.pdf. [Date accessed: August 18, 2022].

Kansas Forest Service. 2013. Kansas forest health highlights 2013. 6 p. https://www.fs.usda.gov/foresthealth/docs/fhh/KS_FHH_2013.pdf. [Date accessed: August 18, 2022].

Kansas Forest Service. 2014. Kansas forest health highlights 2014. 6 p. https://www.fs.usda.gov/foresthealth/docs/fhh/KS_FHH_2014.pdf. [Date accessed: August 18, 2022].

Kansas Forest Service. 2020. Kansas forest health highlights 2020. 21 p. https://www.fs.usda.gov/foresthealth/docs/fhh/KS_FHH_2020.pdf. [Date accessed: August 18, 2022].

Kentucky Division of Forestry. 2016. Kentucky forest health highlights 2016. 12 p. https://www.fs.usda.gov/foresthealth/docs/fhh/KY_FHH_2016.pdf. [Date accessed: August 18, 2022].

Marshall, P.T. 2017. 2017 Indiana forest health highlights. Vallonia, IN: Indiana Department of Natural Resources. 17 p. https://www.in.gov/dnr/forestry/files/fo-Forest_Health_Highlights_2017.pdf. [Date accessed: June 20, 2019].

Marshall, P.T. 2018. 2018 Indiana forest health highlights. Vallonia, IN: Indiana Department of Natural Resources. 17 p. https://www.in.gov/dnr/forestry/files/fo-Forest_Health_Highlights_2018.pdf. [Date accessed: June 20, 2019].

Marshall, P.T. 2020. 2020 Indiana forest health highlights. Vallonia, IN: Indiana Department of Natural Resources. 17 p. https://www.fs.usda.gov/foresthealth/docs/fhh/IN_FHH_2020.pdf. [Date accessed: August 18, 2022].

McNab, W.H.; Cleland, D.T.; Freeouf, J.A. [and others], comps. 2007. Description of ecological subregions: sections of the conterminous United States. [CD-ROM]. Gen. Tech. Rep. WO-76B. Washington, DC: U.S. Department of Agriculture, Forest Service. 80 p. https://doi.org/10.2737/WO-GTR-76B.

Michigan Department of Natural Resources. 2014. 2014 forest health highlights. 51 p. https://www.fs.usda.gov/foresthealth/docs/fhh/MI_FHH_2014.pdf. [Date accessed August 18, 2022].

Michigan Department of Natural Resources. 2015. 2015 forest health highlights. 50 p. https://www.fs.usda.gov/foresthealth/docs/fhh/MI_FHH_2015.pdf. [Date accessed August 18, 2022].

Michigan Department of Natural Resources. 2016. 2016 forest health highlights. 52 p. https://www.fs.usda.gov/foresthealth/docs/fhh/MI_FHH_2016.pdf. [Date accessed: August 18, 2022].

Michigan Department of Natural Resources. 2017. 2017 forest health highlights. 31 p. https://www.fs.usda.gov/foresthealth/docs/fhh/MI_FHH_2017.pdf. [Date accessed: August 18, 2022].

North Dakota Forest Service. 2014. North Dakota forest health highlights 2014. 24 p. https://www.ag.ndsu.edu/ndfs/documents/north-dakota-forest-health-highlights-2014.pdf. [Date accessed: August 18, 2022].

North Dakota Forest Service. 2015. North Dakota forest health highlights 2015. 24 p. https://www.ag.ndsu.edu/ndfs/documents/north-dakota-forest-health-highlights-2015-web.pdf. [Date accessed: August 18, 2022].

North Dakota Forest Service. 2016. Forest health highlights: North Dakota 2016. 4 p. https://www.ag.ndsu.edu/ndfs/documents/north-dakota-forest-health-highlights-2016.pdf. [Date accessed: August 18, 2022].

North Dakota Forest Service. 2017. Forest health highlights: North Dakota 2017. 12 p. https://www.ag.ndsu.edu/ndfs/documents/north-dakota-forest-health-highlights-2017.pdf. [Date accessed: August 18, 2022].

North Dakota Forest Service. 2020. Forest health highlights: North Dakota 2020. 8 p. https://www.fs.usda.gov/foresthealth/docs/fhh/ND_FHH_2020.pdf.[Date accessed: August 18, 2022].

Ohio Department of Natural Resources, Division of Forestry. 2014. 2014 Ohio forest health highlights. 7 p. Columbus, OH: Ohio Department of Natural Resources, Division of Forestry. https://www.fs.usda.gov/foresthealth/docs/fhh/OH_FHH_2014.pdf. [Date accessed August 18, 2022].

Ohio Department of Natural Resources, Division of Forestry. 2015. 2015 Ohio forest health highlights. 8 p. Columbus, OH: Ohio Department of Natural Resources, Division of Forestry. https://www.fs.usda.gov/foresthealth/docs/fhh/OH_FHH_2015.pdf. [Date accessed: August 18, 2022].

Ohio Department of Natural Resources, Division of Forestry. 2016. 2016 Ohio forest health highlights. 8 p. Columbus, OH: Ohio Department of Natural Resources, Division of Forestry. https://www.fs.usda.gov/foresthealth/docs/fhh/OH_FHH_2016.pdf. [Date accessed: August 18, 2022].

Ohio Department of Natural Resources, Division of Forestry. 2017. 2017 Ohio Forest Health Highlights. 7 p. Columbus, OH: Ohio Department of Natural Resources, Division of Forestry. https://www.fs.usda.gov/foresthealth/docs/fhh/OH_FHH_2017.pdf. [Date accessed: July 7, 2019].

Ohio Department of Natural Resources, Division of Forestry. 2020. Ohio Forest Health Highlights 2020. 8 p. Columbus, OH: Ohio Department of Natural Resources, Division of Forestry. https://www.fs.usda.gov/foresthealth/docs/fhh/OH_FHH_2020.pdf. [Date accessed: August 18, 2022].

Oklahoma Forestry Services. 2014. Oklahoma forest health highlights 2014. 5 p. https://www.fs.usda.gov/foresthealth/protecting-forest/forest-health-monitoring/monitoring-forest-highlights.shtml. [Date accessed: August 18, 2022].

Oklahoma Forestry Services. 2015. Oklahoma forest health highlights 2015. 6 p. https://www.fs.usda.gov/foresthealth/docs/fhh/OK_FHH_2015.pdf. [Date accessed: August 18, 2022].

Oklahoma Forestry Services. 2016. Oklahoma forest health highlights 2016. 6 p. https://www.fs.usda.gov/foresthealth/docs/fhh/OK_FHH_2016.pdf. [Date accessed: August 18, 2022].

Oklahoma Forestry Services. 2020. Oklahoma forest health highlights 2020. 9 p. https://www.fs.usda.gov/foresthealth/docs/fhh/OK_FHH_2020.pdf. [Date accessed: August 18, 2022].

Smith, L.A. 2013. Forest health insects and diseases conditions Texas 2013. Longview, TX: Texas A & M Forest Service. 5 p. https://www.fs.usda.gov/foresthealth/docs/fhh/TX_FHH_2013.pdf. [Date accessed: August 18, 2022].

Smith, L.A. 2014. Forest health highlights in Texas 2014. Longview, TX: Texas A & M Forest Service. 1 p. https://www.fs.usda.gov/foresthealth/docs/fhh/TX_FHH_2014.pdf. [Date accessed: August 18, 2022].

South Dakota Department of Agriculture. 2011. South Dakota forest health highlights 2011. Pierre: South Dakota Department of Agriculture, Division of Resource Conservation and Forestry. 4 p. https://www.fs.usda.gov/foresthealth/docs/fhh/SD_FHH_2011.pdf. [Date accessed: August 18, 2022].

South Dakota Department of Agriculture. 2012. South Dakota 2012 forest health highlights. Pierre: South Dakota Department of Agriculture, Division of Resource Conservation and Forestry. 5 p. https://www.fs.usda.gov/foresthealth/docs/fhh/SD_FHH_2012.pdf. [Date accessed: August 18, 2022].

South Dakota Department of Agriculture. 2013. South Dakota 2013 forest health highlights. Pierre: South Dakota Department of Agriculture, Division of Resource Conservation and Forestry. 5 p. https://www.fs.usda.gov/foresthealth/docs/fhh/SD_FHH_2013. [Date accessed: August 18, 2022].

South Dakota Department of Agriculture. 2014. South Dakota 2014 forest health highlights. Pierre: South Dakota Department of Agriculture, Division of Resource Conservation and Forestry. 7 p. https://www.fs.usda.gov/foresthealth/docs/fhh/SD_FHH_2014.pdf. [Date accessed: August 18, 2022].

Texas A & M Forest Service. 2015. Forest health highlights in Texas 2015. Longview, TX. 1 p. https://www.fs.usda.gov/foresthealth/docs/fhh/TX_FHH_2015.pdf. [Date accessed: August 18, 2022].

Texas A & M Forest Service. 2016. Forest health highlights in Texas 2016. Longview, TX. 1 p. https://www.fs.usda.gov/foresthealth/docs/fhh/TX_FHH_2016.pdf. [Date accessed: August 18, 2022].

Texas A & M Forest Service. 2017. Forest health highlights 2017. Longview, TX. 2 p. https://www.fs.usda.gov/foresthealth/docs/fhh/TX_FHH_2017.pdf. [Date accessed: August 18, 2022].

Texas A & M Forest Service. 2019. Forest health highlights 2019. Longview, TX. 2 p. https://www.fs.usda.gov/foresthealth/docs/fhh/TX_FHH_2019.pdf. [Date accessed: August 18, 2022].

U.S. Department of Agriculture (USDA) Animal and Plant Health Inspection Service (APHIS). 2018. Emerald ash borer. https://www.aphis.usda.gov/aphis/resources/pests-diseases/hungry-pests/the-threat/emerald-ash-borer/emerald-ash-borer-beetle. [Date accessed: August 31, 2018].

U.S. Department of Agriculture (USDA) Forest Service. 2008. National forest type dataset. http://data.fs.usda.gov/geodata//rastergateway/forest_type/index.php. [Date accessed: September 13, 2021].

U.S. Department of Agriculture (USDA) Forest Service, Forest Inventory and Analysis (FIA). 2019. Forest Inventory EVALIDator web-application. Version 1.8.0.01. St. Paul, MN: U.S. Department of Agriculture, Forest Service, Northern Research Station. http://apps.fs.fed.us/Evalidator/evalidator.jsp. [Date accessed: June 9, 2022].

Wyoming State Forestry Division. 2017. 2017 Wyoming forest health highlights. 17 p. https://www.fs.usda.gov/foresthealth/docs/fhh/WY_FHH_2017.pdf. [Date accessed March 6, 2022].

SECTION 2

Analyses of Long-Term Forest Health Trends and Presentations of New Techniques

CHAPTER 6

Crown Dieback and Damages in the Eastern United States

KaDonna C. Randolph

INTRODUCTION

The Forest Inventory and Analysis (FIA) program of the Forest Service, U.S. Department of Agriculture, visually assesses tree crown conditions as an indicator of forest health. These assessments are useful because individual tree photosynthetic capacity is dependent upon the size and condition of the crown. In general, trees with full, vigorous crowns are associated with more vigorous growth rates (Zarnoch and others 2004); when trees undergo stress, e.g., from an insect attack or extreme weather event, the first symptoms are often visible in the crown. Furthermore, tree crowns form the overstory structure of the forest and directly influence the composition and structure of the understory thereby making them an integral component of the forest ecosystem.

Initially implemented by the Forest Health Monitoring (FHM) program, crown conditions have been measured in the United States since 1990 (Randolph 2013). After a series of field tests and reviews in the early 1990s, the crown condition indicator was formalized to include a set of eight variables: vigor class, uncompacted live crown ratio, crown light exposure, crown position, crown density, crown dieback, foliage transparency, and crown diameter (Schomaker and others 2007). When the FHM detection monitoring plots were incorporated into FIA in the year 2000, assessment of these variables was continued by FIA (Woodall and others 2011). Over time, the crown assessment protocols have been refined to address client needs, field logistics, and budgetary demands (USDA Forest Service 2016). Presently, FIA assesses uncompacted live crown ratio and crown dieback as the primary crown condition metrics.

This chapter represents the fourth national summary of crown condition in the United States. Previous summaries were included in Forest Health Monitoring: 2006 National Technical Report (Randolph 2009), Forest Health Monitoring: National Status, Trends, and Analysis 2013 (Randolph 2015), and Forest Health Monitoring: National Status, Trends, and Analysis 2017 (Randolph 2018). In like manner, the objective of this report is to summarize current crown dieback, current crown-damaging agents, and 20-year crown dieback trends for the most common genera and species ("species groups") in the Eastern United States (fig. 6.1) with the goal of identifying species in decline and geographical areas of concern, e.g., Randolph and others (2012).

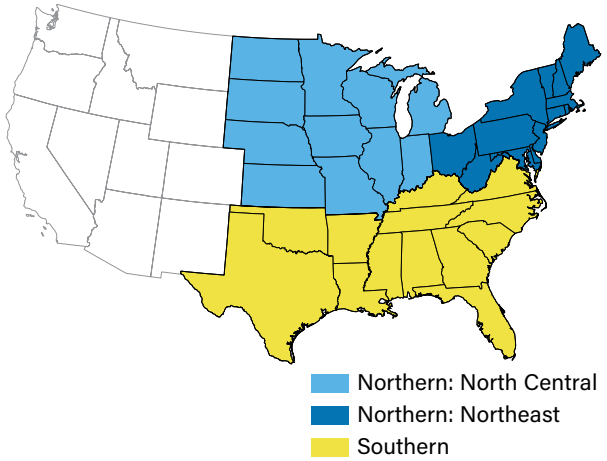

Figure 6.1—Regional breakdown of the Eastern United States for the crown condition analysis.

How to cite this chapter:

Randolph, KaDonna C. 2023. Crown dieback and damages in the Eastern United States. In: Potter, Kevin M.; Conkling, Barbara L., eds. Forest Health Monitoring: national status, trends, and analysis 2022. Gen. Tech. Rep. SRS-273. Asheville, NC: U.S. Department of Agriculture, Forest Service, Southern Research Station: 105–126. https://doi.org/10.2737/SRS-GTR-273-Chap6.

METHODS

Data

The FIA program assesses crown dieback and damage on live trees with diameter at breast height (d.b.h.) ≥12.7 cm on its network of nationwide plots (Bechtold and Patterson 2005). Crown dieback is defined as the recent mortality of branches with fine twigs, which begins at the terminal portion of a branch and proceeds toward the trunk (Schomaker and others 2007). Crown dieback is measured by means of ocular estimation and coded as 0, 05, 10, … 95, 99, where the code represents the upper limit of the class, e.g., 1–5-percent crown dieback is code 05. Crown dieback for live trees with complete defoliation, i.e., 100-percent crown dieback, is coded as 99. Biotic and abiotic agents causing tree damage above specific thresholds are observed by means of visual inspection successively from the bottom of the tree to the top, i.e., roots, bole, branches, and foliage. Up to three damage agents can be recorded per tree. Damage agents fall into one of 23 classes and may be recorded generally, e.g., abiotic agent, or specifically, e.g., wind. Typically, damage to the crown must meet or exceed 20 percent of the branches, stems, or foliage in order for a damage agent to be noted. However, any damage to the terminal leader or any evidence of a successful attack is sufficient for other agents (USDA Forest Service 2015). When trees have died or been cut since the previous inventory, FIA field crews assign a single cause of death from a list of eight possible agents: insect, disease, fire, animal, weather, vegetation (suppression, competition, vines), silvicultural or land clearing activity, and unknown.

The FIA plot network consists of permanently monumented plots located at a sampling intensity of approximately one plot per 6,000 acres (2428 ha) across the country. Plots are divided into spatially balanced panels and one panel of plots is measured each year on a rotating and ongoing basis. The time it takes to measure all panels within a State is referred to as a cycle. The majority of States in the Eastern United States are on 5- or 7-year cycles. Exceptions are Oklahoma and Texas, which have 5-year cycles in their eastern regions and 10-year cycles in their central and western regions. The FIA program dates its inventories according to the year of the most recently collected panel of plots. For example, the 2021 inventory for Arkansas, which is on a 5-year cycle, includes data collected in FIA inventory years 2017 through 2021.

To summarize current crown conditions in the Eastern United States, I utilized various subsets of the crown dieback, damage agent, and cause of death data collected by FIA in the Northern and Southern regions (fig. 6.1, table 6.1) (Burrill and others 2021). Data collection during 2020 and 2021 was sporadic and imbalanced across the country due to the COVID-19 pandemic. Therefore, the most recent data included in this summary were from the 2019 inventory for most States (table 6.1). I calculated changes in crown dieback over time by pairing the most recent observations with those made on the same trees in the previous measurement cycle. I also incorporated crown dieback estimates for prior years as reported previously by Randolph (2006, 2018) and Randolph and others (2010a, 2010b).

Table 6.1—Most recent Forest Inventory and Analysis inventory year for data included in the crown condition summary, by region and State

Region	Inventory year	State
Northern	2019	Connecticut, Delaware, Illinois, Indiana, Iowa, Kansas, Maine, Maryland, Massachusetts, Michigan, Minnesota, Missouri, Nebraska, New Hampshire, New Jersey, New York, North Dakota, Ohio, Pennsylvania, Rhode Island, South Dakota, Vermont, West Virginia, Wisconsin
Southern	2018	Florida, Louisiana, Kentucky, Tennessee, Texas
Southern	2019	Alabama, Arkansas, Georgia, Mississippi, North Carolina, Oklahoma, South Carolina, Virginia

Analyses

Survivorship—I evaluated the relationship between past crown dieback and current tree status, i.e., survivorship, by matching individual tree observations made with the most recent data, i.e., the 2018 or 2019 inventory year (table 6.1) (current assessment) with those made in the immediately preceding inventory. Measurement intervals for individual trees assessed during these time periods ranged from 4.2 to 7.4 years (mean = 5.6, SD = 0.7) in the Northern region and from 3.0 to 12.2 years (mean = 6.1, SD = 1.5) in the Southern region; however, to reduce variation, I only included trees with a remeasurement period within one standard deviation of their respective regional mean in the survivorship analysis. I calculated the proportion of trees by previous crown dieback class (0 percent, >0–10 percent, >11–20 percent, and >20 percent) and current tree status (live or dead) for each region. In addition, I calculated the proportion of mortality, i.e., trees with current tree status = dead, among trees with 0-percent crown dieback at the previous inventory for each species group by region. This calculation exposed species groups potentially affected by the occurrence of acute stressors between the previous and current assessments.

The FIA damage collection protocol is crafted in such a way that damage agents are recorded only when symptoms exceed predefined thresholds that indicate the tree is likely to (1) die within 1 to 2 years, (2) have reduced growth in the near term, or (3) have diminished marketability (USDA Forest Service 2015). Therefore, to identify damage agents that may contribute to imminent tree mortality, I calculated the frequency of each general damage agent by region and species class (softwood, hardwood) for trees in the >20-percent dieback class.

Current crown dieback and damage—I summarized current crown dieback conditions by region for all trees combined, species class (softwood, hardwood), and species groups measured on at least 100 plots by region. I calculated mean crown dieback using the ratio of means estimator (Cochran 1977, Woodall and others 2011). I also calculated the frequency of trees in each crown dieback class (0 percent, >0–10 percent, >10–20 percent, and >20 percent). In the past, crown dieback has been more prevalent in the Northern region than in the Southern region (Randolph 2015, 2018). Therefore, to compare species groups present in both regions,

I ranked the species groups according to mean crown dieback, proportion of trees in the 0-percent dieback class, and proportion of trees in the >20-percent dieback class within each region. I based cross-regional comparisons of crown condition by species group on the average of the three rankings.

To identify geographical areas with excessive crown dieback, I calculated the proportion of trees with >20-percent crown dieback for each FIA plot condition[1] by species class, species group, and for all species combined. I mapped the proportions according to the approximate plot locations provided by FIA and examined the proportions visually. I only mapped conditions with at least three tally trees. For plot locations with multiple conditions, the greatest proportion of trees with >20-percent crown dieback among the conditions was displayed.

I calculated the frequency of each general damage agent by region and species group. For each plot condition, I calculated the proportion of trees with damage agents considered especially injurious to tree crowns by damage agent and species class. I mapped the condition-level proportions according to the approximate plot locations provided by FIA and examined the proportions visually. I only mapped conditions with at least three tally trees. For plot locations with multiple conditions, the greatest proportion of damaged trees among the conditions was displayed. The damage agents included in the spatial analysis were defoliating insects; sucking insects; chewing insects; decline complexes/dieback/wilts; foliage diseases; wind, snow, and ice; and parasitic/epiphytic plants (USDA Forest Service 2015). All these agents except wind, snow, and ice are general categories and include multiple specific agents.

Crown dieback trends—Using graphs, I compared current mean crown dieback to mean crown dieback from four prior time periods (1996–1999, 2001–2005, 2006–2010, and 2011–2015), by region, for all species combined and by species group. In addition, I compared current crown dieback (d_2) to previous crown dieback (d_1) by region and species group for all trees measured during both assessments. The hypothesis that the average ratio between d_2 and d_1 equaled 1 was tested with a paired t-test under a log transformation:

$$H_0: \bar{\delta} = 0 \text{ versus } H_A: \bar{\delta} \neq 0$$

where

$\bar{\delta}$ is the mean of $\log(d_{ij2} + c) - \log(d_{ij1} + c)$

where

c is a constant equal to 0.1

d_{ij2} is current crown dieback on tree i on plot j

d_{ij1} is previous crown dieback on tree i on plot j

The log transformation was necessary to accommodate crown dieback's severely skewed distribution and the addition of c was needed to adjust 0-percent crown dieback to a log transformable value. I used the R package SURVEY (Lumley 2004, R Core Team 2022)

[1] *An FIA plot is stratified into homogeneous condition classes based on ownership, forest type, stand size, stand density, stand origin, and reserved status (USDA Forest Service 2015).*

to accommodate the inventory design in which trees are nested on plots. I performed the hypothesis test for surviving trees only and for surviving trees plus mortality trees. Crown dieback is not assessed for dead trees; therefore, d_2 for mortality trees was set to the maximum possible dieback, i.e., 99 percent. I did not include harvested trees because it was not known if the trees were alive or dead at the time they were cut. As with the survivorship analysis, I only included trees with a remeasurement period within one standard deviation of their respective regional mean remeasurement period in this analysis. I considered crown dieback between the current and previous assessments to be statistically significantly different if the 95-percent confidence interval for $\bar{\delta}$ did not include zero. I back transformed results and present them under the original hypothesis such that 95-percent confidence intervals including 1 indicate no statistical difference; intervals with an upper confidence limit <1 indicate a statistically significant decline in crown dieback; and intervals with a lower confidence limit >1 indicate a statistically significant increase in crown dieback.

RESULTS AND DISCUSSION

Relationship Between Crown Dieback and Survivorship

Crown dieback is strongly correlated with tree survivorship such that trees with greater amounts of dieback are more likely to die within 5 years than those with little or no dieback (Morin and others 2015, Steinman 2000). Therefore, as expected, the likelihood of mortality tended to increase with increasing crown dieback in both regions (fig. 6.2). Although high levels of crown dieback are a good indicator of impending mortality, there are instances when trees with no crown dieback die before they are remeasured. This is most likely to happen when trees die quickly as the result of an acute stressor, e.g., wildfire, or when the effects of less acute stressors coincide with a lengthy remeasurement period. Overall, mortality among the trees with 0-percent crown dieback at the previous inventory was low (5.2 percent in the Northern region; 7.8 percent in the Southern region). Such was the case for most individual species groups except ash (*Fraxinus* spp.) and elm (*Ulmus* spp.) in the Northern region and ash, black cherry (*Prunus serotina*), and Virginia pine (*Pinus virginiana*) in the Southern region (fig. 6.3). An inspection of reported causes of death indicated that insects, most likely emerald ash borer (*Agrilus planipennis*) (Morin and others 2017), and diseases, most likely Dutch elm disease (*Ophiostoma novo-ulmi)* (Karnosky 1979, USDA Forest Service 2011), were the most frequently reported agents for northern ash and elm, respectively. Though no single agent dominated the causes of death recorded for ash and black cherry in the Southern region, insects, diseases, weather, and vegetation (suppression, competition, vines) were recorded frequently. Vegetation was the most frequently reported cause of death among the Virginia pines.

Damage agents observed on trees with >20-percent crown dieback suggest possible causes of death for trees most at risk of mortality. Stem decay, defined as rot occurring in the tree bole or stems above the roots and stump and recorded by

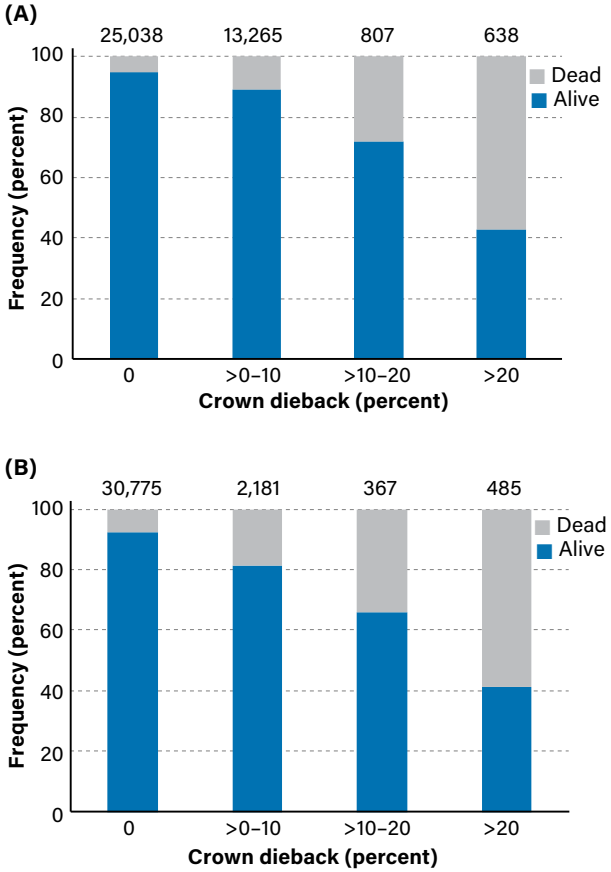

Figure 6.2—Proportion of remeasured trees in the (A) Northern and (B) Southern regions of the Eastern United States, by previous crown dieback and current tree status. The number of trees in each dieback class is listed above the column. (Data source: U.S. Department of Agriculture, Forest Service, Forest Inventory and Analysis program)

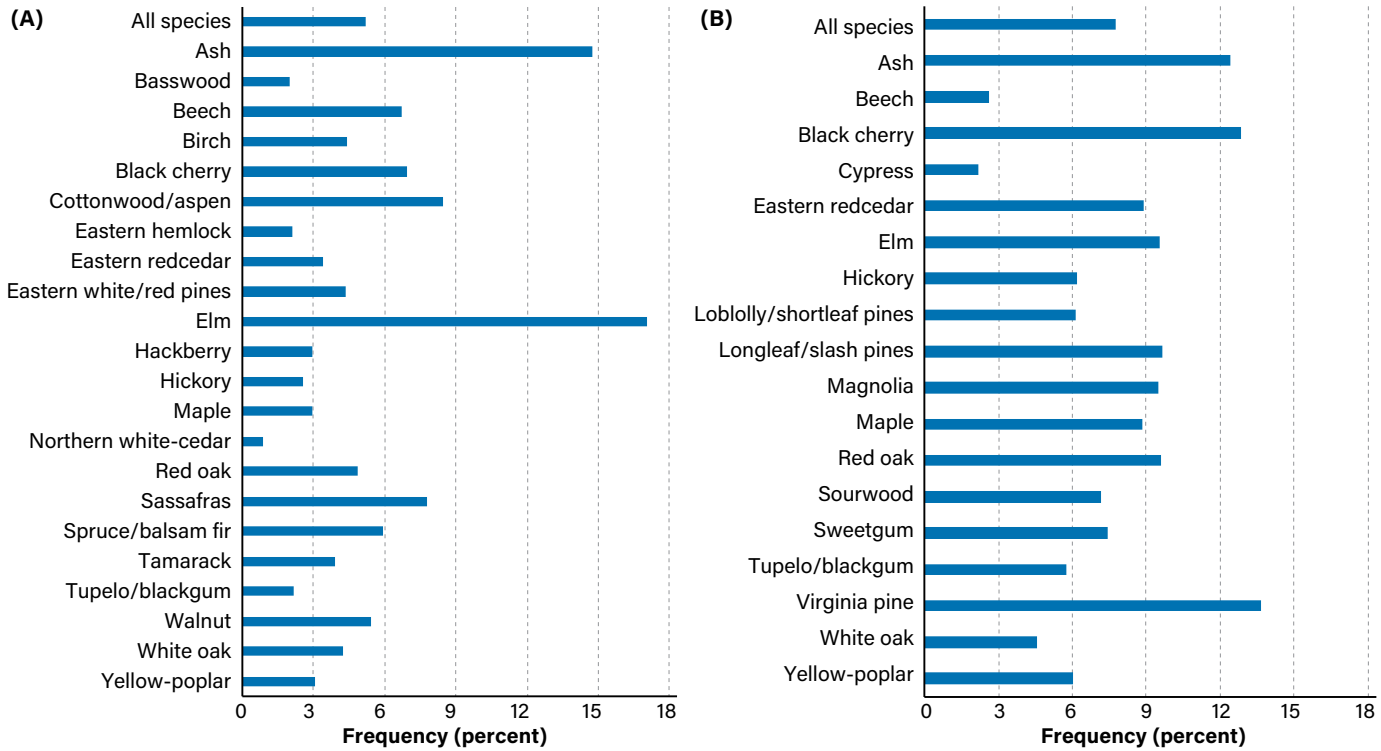

Figure 6.3—Proportion of trees with 0-percent crown dieback during the previous assessment that were dead upon remeasurement during the current assessment in the (A) Northern and (B) Southern regions of the Eastern United States, by species group. All species groups shown are based on at least 200 observations. (Data source: U.S. Department of Agriculture, Forest Service, Forest Inventory and Analysis program)

FIA when there is any evidence of rotten wood, conks, or fungal fruiting bodies (USDA Forest Service 2015), is the most frequently recorded damage agent in the Eastern United States (Randolph and others 2021). As such, it was no surprise that stem decay was the most frequently recorded damage agent among trees with >20-percent crown dieback in both the Northern region (25.7 percent for softwoods; 42.5 percent for hardwoods) and Southern region (66.2 percent for softwoods; 72.6 percent for hardwoods). Other damage agents frequently associated with >20-percent crown dieback were boring insects in the Northern region and cankers and decline complexes/dieback/wilts in the Southern region (fig. 6.4).

Current Crown Dieback and Damage

The expectations that hardwoods typically have more crown dieback than softwoods and that crown dieback is more prevalent in the Northern region than in the Southern region held true (tables 6.2 and 6.3). Among the softwood species groups, the overall best crown conditions were observed for eastern white and red pines (*P. strobus, P. resinosa*) in the Northern region and loblolly and shortleaf pines (*P. taeda, P. echinata*) in the Southern region. Likewise, the overall best crown conditions among the hardwood species groups were observed for tupelo and blackgum (*Nyssa* spp.), basswood (*Tilia americana*), birch (*Betula* spp.), cottonwood and aspen (*Populus* spp.) in the Northern region, and birch, yellow-poplar (*Liriodendron tulipifera*), beech (*Fagus grandifolia*), and tupelo and blackgum in the Southern region. The overall poorest crown conditions in the

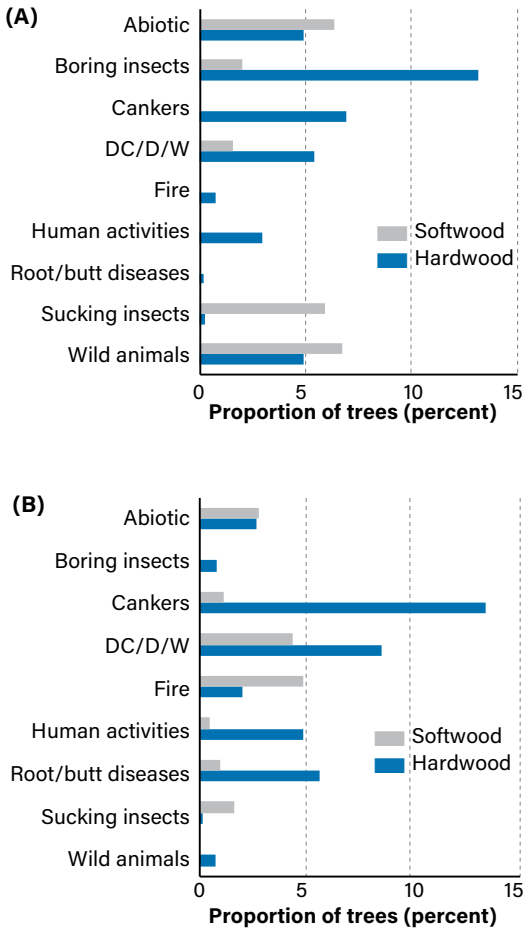

Figure 6.4—Frequency of common damage agents among trees with crown dieback >20 percent in the (A) Northern and (B) Southern regions of the Eastern United States, by species class. DC/D/W = decline complexes/dieback/wilts. (Data source: U.S. Department of Agriculture, Forest Service, Forest Inventory and Analysis program)

Table 6.2—Current mean crown dieback and proportion of trees by dieback class for species groups in the Northern region

Species group	Number of plots	Number of trees	Mean	SEM	Dieback class			
					0	>0–10	>10–20	>20
			percent		- - - - - - - - - - - *percent* - - - - - - - - - - -			
Softwood	1,909	26,064	1.4	0.1	84.7	13.1	1.2	1.0
Eastern hemlock	428	3,077	1.0	0.1	90.4	8.1	0.7	0.8
Eastern redcedar	223	1,192	1.8	0.2	71.3	27.1	1.2	0.4
Eastern white and red pines	617	4,442	0.6	0.1	93.2	6.2	0.3	0.3
Northern white-cedar	285	4,092	3.6	0.4	68.4	24.4	4.2	3.1
Spruce and balsam fir	883	9,603	1.1	0.1	87.2	11.4	0.7	0.6
Tamarack	127	741	1.1	0.3	88.3	9.4	1.6	0.7
Hardwood	3,569	60,930	3.3	0.1	65.1	31.0	1.7	2.1
Ash	984	3,811	6.9	0.9	59.1	30.5	3.6	6.8
Basswood	353	1,325	1.7	0.2	77.0	21.7	0.5	0.8
Beech	629	2,700	3.3	0.2	66.8	28.0	2.9	2.3
Birch	1,159	5,159	2.2	0.1	72.8	24.8	1.3	1.2
Black cherry	711	2,206	4.0	0.3	59.5	35.6	2.4	2.5
Cottonwood and aspen	749	4,984	2.2	0.2	80.5	16.6	1.1	1.9
Elm	744	1,907	6.3	0.4	44.0	48.1	2.8	5.0
Hackberry	239	715	3.8	0.4	48.7	48.3	1.1	2.0
Hickory	755	2,619	2.3	0.2	65.0	33.9	0.4	0.6
Maple	2,364	18,581	2.5	0.1	72.8	24.0	1.7	1.6
Red oak[a]	1,301	5,129	3.6	0.2	53.1	43.6	1.7	1.6
Sassafras	201	616	4.9	0.7	51.5	43.3	2.1	3.1
Tupelo and blackgum	239	559	1.6	0.3	75.5	24.0	0.2	0.4
Walnut	327	740	3.8	0.4	52.3	44.7	1.4	1.6
White oak[b]	1,023	5,334	3.6	0.2	48.3	49.3	1.1	1.3
Yellow-poplar	250	1,089	2.8	0.4	69.5	28.0	0.9	1.6

SEM = standard error of the mean.

[a] *Quercus* section *Lobatae*.

[b] *Quercus* section *Quercus*.

Table 6.3—Current mean crown dieback and proportion of trees by dieback class for species groups in the Southern region

Species group	Number of plots	Number of trees	Mean	SEM	Dieback class			
					0	>0–10	>10–20	>20
			percent		percent			
Softwood	4,194	57,963	0.9	0.1	94.9	3.6	0.5	1.1
Cypress	138	1,048	0.3	0.1	98.9	0.4	0.2	0.6
Eastern redcedar	589	2,226	0.9	0.2	96.7	1.4	0.6	1.2
Loblolly and shortleaf pines	2,339	37,769	0.1	0.0	99.6	0.3	0.0[a]	0.1
Longleaf and slash pines	309	3,912	0.3	0.1	98.0	1.4	0.3	0.3
Pinyon-juniper	1,102	11,405	3.7	0.3	77.4	16.3	2.1	4.3
Virginia pine	156	783	0.6	0.3	98.0	1.1	0.4	0.5
Hardwood	6,511	71,206	2.1	0.1	84.8	11.6	1.6	2.0
Ash	662	2,135	3.0	0.5	88.5	6.2	1.6	3.7
Beech	219	468	0.7	0.3	97.9	1.1	0.0	1.1
Birch	137	418	0.4	0.2	97.6	1.9	0.0	0.5
Black cherry	434	829	1.6	0.3	91.6	5.2	1.7	1.6
Elm	1,544	4,521	1.4	0.1	89.5	8.1	0.9	1.4
Hickory	1,066	2,908	1.0	0.1	93.9	4.0	1.0	1.1
Honey mesquite	1,817	10,530	4.6	0.4	61.9	31.4	2.8	3.8
Magnolia	221	629	1.3	0.4	95.5	1.9	0.6	1.9
Maple	1,153	3,976	1.4	0.2	94.1	2.8	1.2	1.9
Red oak[b]	2,631	10,398	1.4	0.1	91.5	5.9	1.1	1.5
Sourwood	234	655	1.4	0.4	93.1	4.7	0.8	1.4
Sugarberry	486	1,539	1.1	0.2	90.1	8.2	0.6	1.1
Sweetgum	1,750	6,865	1.2	0.1	94.8	2.4	1.4	1.5
Tupelo and blackgum	888	3,001	0.7	0.1	96.3	2.0	0.9	0.8
Walnut	136	288	3.9	1.3	77.4	14.6	4.5	3.5
White oak[c]	2,531	13,176	2.6	0.2	76.2	19.3	2.4	2.1
Yellow-poplar	556	2,296	0.6	0.1	97.5	1.3	0.6	0.6

SEM = standard error of the mean.
[a] Value is >0.0 but <0.1.
[b] *Quercus* section *Lobatae*.
[c] *Quercus* section *Quercus*.

Northern region were observed for northern white-cedar (*Thuja occidentalis*), elm, ash, and sassafras (*Sassafras albidum*). In the Southern region, the overall poorest crown conditions were observed for pinyon-juniper,[2] honey mesquite (*Prosopis glandulosa*), walnut (*Juglans* spp.), and ash.

Potential causes for the poor crown conditions varied by species group. Reported damage agents on ash and elm support the effect of known stressors, i.e., emerald ash borer and Dutch elm disease, respectively. Northern white-cedar trees often grow in areas inundated by water (Boulfroy and others 2012), and pinyon-juniper trees typically grow in environments where moisture is scarce (Shaw and others 2005). Both water-related stresses can lead to crown dieback (Bréda and others 2006, Kozlowski 1986). In addition, reported damage agents suggest wild animals, possibly beaver (*Castor canadensis*), may have contributed to northern white-cedar crown dieback and fire may have contributed to pinyon-juniper crown dieback. Root/butt and other general diseases were commonly reported damage agents on honey mesquite and are likely contributors to its crown dieback. Similarly, root/butt diseases and heart rot were common among walnut. In addition to stem decay, damage by cankers, wild animals, and vines was commonly reported for sassafras.

Though crown dieback was more prevalent in the Northern region than in the Southern region, most of the species groups found throughout the Eastern United States ranked similarly within the two regions. On average, birch, tupelo/blackgum, and hickory (*Carya* spp.) ranked among the species groups with the best crown conditions. Ash, black cherry, and eastern redcedar (*Juniperus virginiana*) ranked among the species groups with the poorest crown conditions, and maple (*Acer* spp.) and red oak (*Quercus* section *Lobatae*) ranked in the middle. Crown conditions for beech, elm, walnut, white oak (*Quercus* section *Quercus*), yellow-poplar and two *Celtis* species, hackberry (*C. accidentalis*) and sugarberry (*C. laevigata*), ranked differently within the two regions. For best crown conditions, beech and yellow-poplar ranked in the top third among species groups in the Southern region and in the middle third among species groups in the Northern region. Elm ranked in the middle third among species groups in the Southern region and in the bottom third among species groups in the Northern region. Sugarberry ranked in the middle third among species groups in the Southern region and hackberry ranked in the bottom third among species groups in the Northern region. Walnut and white oak ranked in the bottom third among species groups in the Southern region and in the middle third among species groups in the Northern region. No species groups ranked in the top third in one region and bottom third in the other region.

Spatially, FIA plot locations where >25 percent of the trees had >20-percent crown dieback were scattered throughout the Northern region, whereas in the Southern region, they were concentrated primarily in Texas (fig. 6.5). Further

[2] *Woodland pinyon pines (* Pinus cembroides, P. edulis, P. remota*) and woodland junipers (* Juniperus ashei, J. coahuilensis, J. deppeana, J. flaccida, J. monosperma, J. pinchotii, J. scopulorum*).*

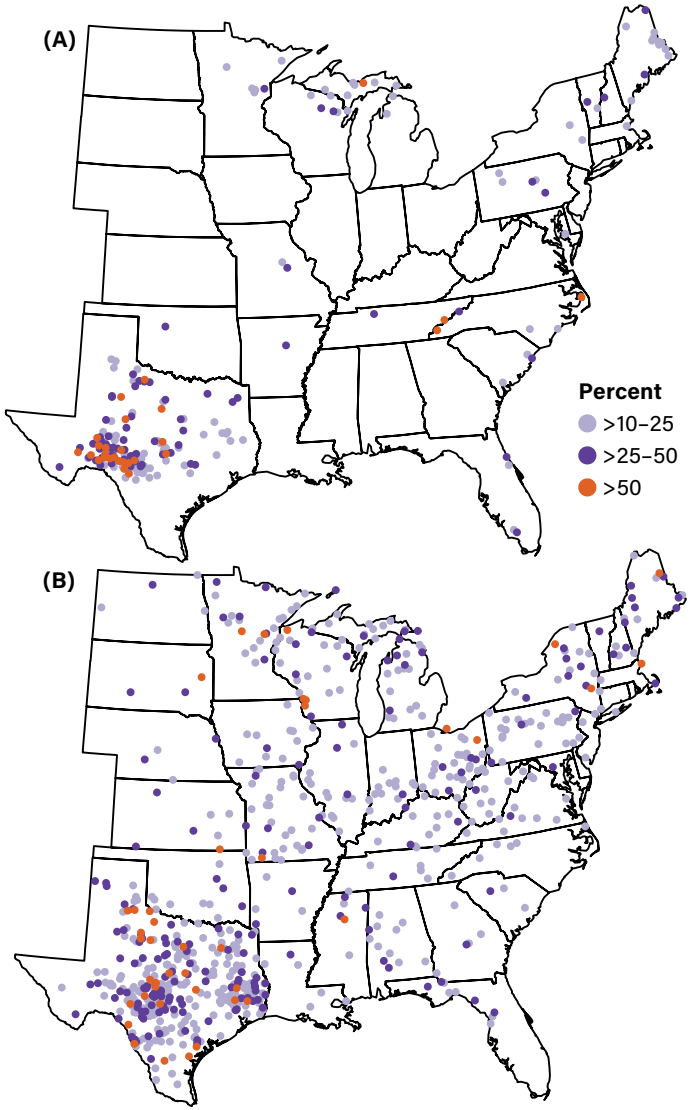

Figure 6.5—Proportion of (A) softwood and (B) hardwood trees with crown dieback >20 percent, by Forest Inventory and Analysis (FIA) plot location. Plot locations are approximate. (Data source: U.S. Department of Agriculture, Forest Service, FIA program)

examination indicated that the Texas plots where >25 percent of the trees had >20-percent crown dieback were composed of Ashe juniper (*J. ashei*), Pinchot juniper (*J. pinchotii*), honey mesquite, and live oak (*Q. virginiana*) and had evidence of weather- and fire-related disturbances. Other than ubiquitous stem decay, the most frequently recorded damage agents among trees with >20-percent crown dieback in Texas were heart rot and decline complexes/dieback/wilts.

Four agents stood out among those considered especially damaging to tree crowns: defoliators, chewing/sucking insects, parasitic/epiphytic plants, and wind. Plots with defoliating insect damage to >25 percent of the trees were concentrated in the Northeast and the Lake States (fig. 6.6). Eastern spruce budworm (*Choristoneura fumiferana*) was the most common insect recorded in the Lake States, and spongy moth (*Lymantria dispar*), primarily, and eastern tent caterpillar (*Malacosoma americanum*), secondarily, were the predominant specific insects recorded in the Northeast. Sucking insects and chewing insects were combined because only a few instances of chewing insect damage were observed. Though some sucking insect damage was noted on hardwood trees, e.g., beech scale (*Cryptococcus fagisuga*), the majority of sucking insect damage was observed on softwood trees throughout Appalachia and New England (fig. 6.7) for which balsam woolly adelgid (*Adelges piceae*) and hemlock woolly adelgid (*A. tsugae*) were the most frequently cited culprits. Parasitic/epiphytic plant damage was scattered across the Northern region and consisted primarily of vine damage on hardwood trees (fig. 6.8). Vine damage was distributed throughout the canopy in

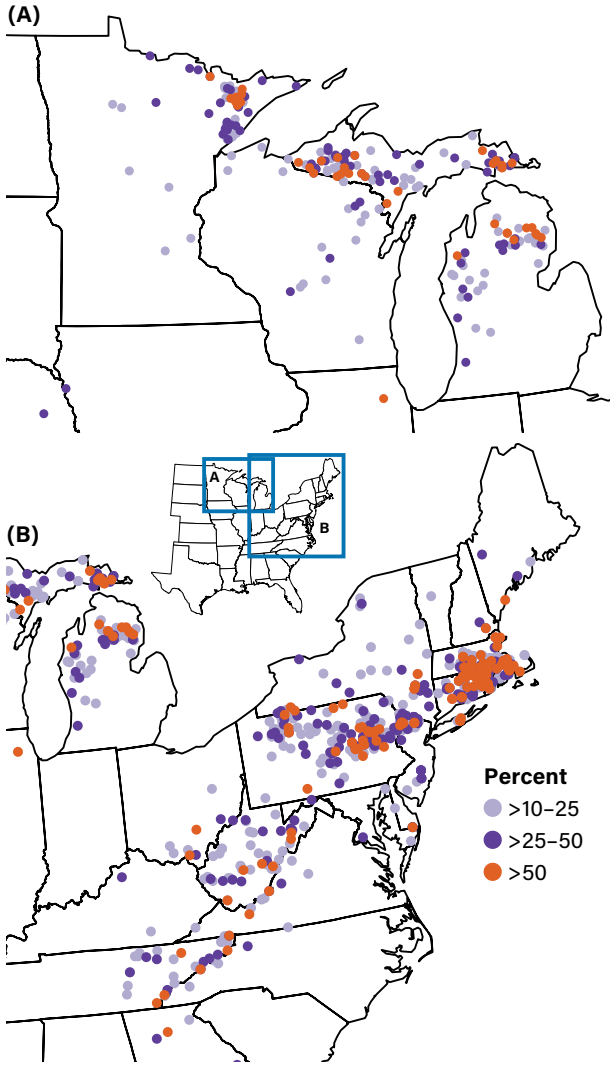

Figure 6.6—Forest Inventory and Analysis (FIA) plot locations in the (A) Lake States and (B) Northeastern regions of the Eastern United States where trees were frequently damaged by defoliating insects, by proportion of trees affected. Plot locations are approximate. (Data source: U.S. Department of Agriculture, Forest Service, FIA program)

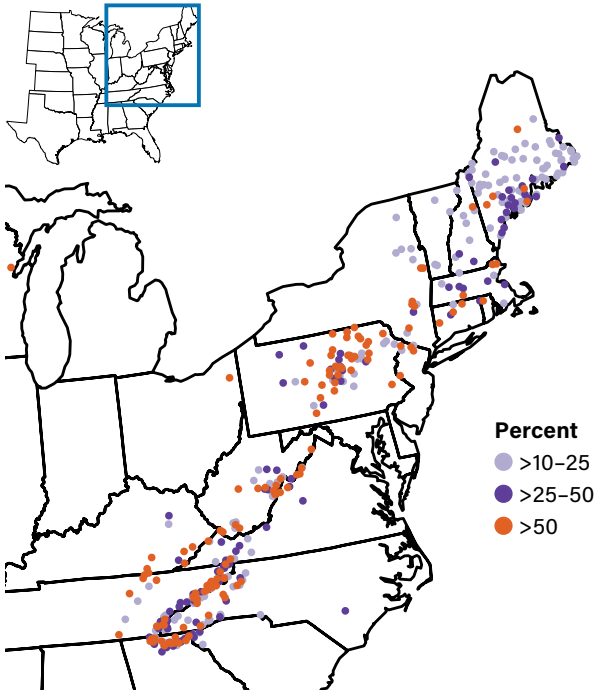

Figure 6.7—Forest Inventory and Analysis (FIA) plot locations in the Eastern United States where softwood trees were frequently damaged by chewing or sucking insects, by proportion of trees affected. Plot locations are approximate. (Data source: U.S. Department of Agriculture, Forest Service, FIA program)

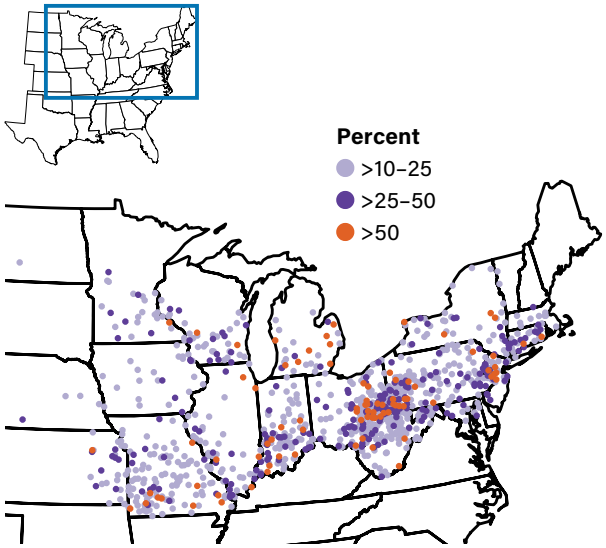

Figure 6.8—Forest Inventory and Analysis (FIA) plot locations in the Eastern United States where hardwood trees were frequently damaged by vines, by proportion of trees affected. Plot locations are approximate. (Data source: U.S. Department of Agriculture, Forest Service, FIA program)

a manner consistent with the distribution of trees. That is, the majority of trees tallied were in the codominant crown class and the majority of all vine-damaged trees were in the codominant crown class. However, the proportion of vine-damaged trees within each crown class was greatest for the intermediate crown class. Except for wind damage in the Lake States (fig. 6.9), most likely due to major storm events in the summer of 2016 (Minnesota Department of Natural Resources 2016, Wisconsin Department of Natural Resources 2016), there were no concentrations of damage from the other agents considered especially damaging to tree crowns.

I did not include a comparison of mean crown dieback between damaged and undamaged trees because up to three damage agents are allowed to be recorded for an individual tree, which confounds the effect of any particular damage agent. Sample sizes of damaged and undamaged trees became increasingly imbalanced once the subset of trees with only one damage agent was further divided by those for which crown dieback was assessed, and even more so when trees were classed by species group.

Trends in Crown Dieback

Tree crown dieback may be caused by agents acting directly on the crown or by agents affecting the movement of water and nutrients to the crown, or both. In some cases, crown dieback may be ephemeral such that tree growth returns to normal once the causal agent is no longer present (Smith and Conkling 2004). In other cases, crown dieback may continually worsen if the causal

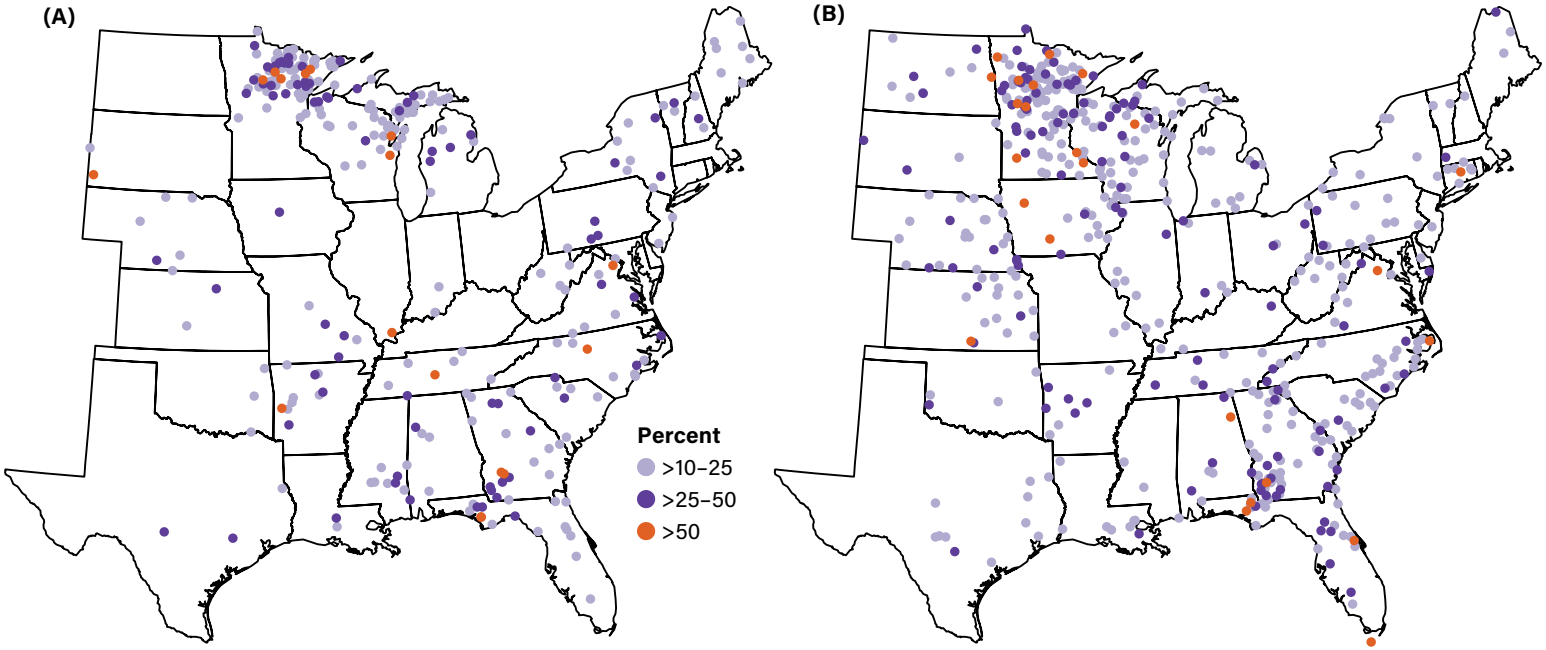

Figure 6.9—Forest Inventory and Analysis (FIA) plot locations in the Eastern United States where (A) softwood and (B) hardwood trees were frequently damaged by wind, by proportion of trees affected. Plot locations are approximate. (Data source: U.S. Department of Agriculture, Forest Service, FIA program)

agent persists. Some fluctuation in average crown dieback is expected over time; however, increasing or ongoing high levels of crown dieback are cause for concern, especially for individual species groups with no known stressors.

There has been an overall downward trend in mean crown dieback for all species combined in both the Northern and Southern regions since the late 1990s (fig. 6.10). Yet the degree to which average crown dieback changed varied by species group. Mean crown dieback for most species groups either declined or exhibited no change. This was true for all softwood species groups examined in the Northern and Southern regions (fig. 6.11). The same was also true for almost all hardwood species groups considered in the Southern region (fig. 6.12). The only hardwood species group in the Southern region with a ratio of current mean crown dieback to mean crown dieback in 1999 that was >1 was ash (ratio = 1.1). This is likely due to emerald ash borer, which was detected in the Southern region (Fairfax County, VA) in 2008 and in all Southern States except Florida and Mississippi by the end of 2020 (Emerald Ash Borer Information Network 2022). Among the hardwood species groups in the Northern region, mean crown dieback during the current inventory period was at least 1.2 times greater than it was during the earliest inventory period for ash, elm, sassafras, walnut, yellow-poplar, and hackberry (fig. 6.13). Despite the overall increases for these groups, current mean crown dieback was less than mean crown dieback observed during previous years for some species groups. For example, mean crown dieback peaked for sassafras in 2010 and in 2015 for hackberry. In contrast, declines in mean crown dieback in the Northern region have been steady since 1999 (fig. 6.13A).

The test comparing the ratio of d^2 to d^1 indicated that, on average, crown dieback on surviving trees either declined or remained steady for all species groups in the Northern (table 6.4) and Southern (table 6.5) regions. This may be because trees with crown dieback dropped out of the population due to mortality or because crown dieback was either not present or no longer recordable by definition, i.e., the dieback was no longer "recent" and consisting of fine twigs (Schomaker and others 2007). Including mortality trees in the comparison of d^2 to d^1 indicated that most of the species groups with declines in mean crown dieback from 2015 to 2019 in the Southern region (figs. 6.11B and 6.12) may have been due, at least in part, to trees dropping out of the inventory because of mortality (table 6.5). Likewise in the Northern region, declines in mean crown dieback from 2015 to 2019 for birch and cottonwood and aspen (*Populus* spp.) (fig. 6.13) may also have been due, at least in part, to mortality (table 6.4).

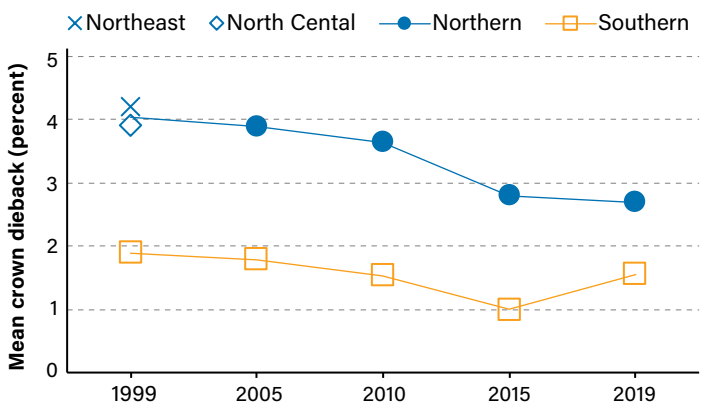

Figure 6.10—Mean crown dieback for trees ≥5.0 inches diameter at breast height in the Eastern United States, by region and year. Crown dieback in the 1990s was collected by the Forest Service Forest Health Monitoring program and reported by Randolph (2006) and Randolph and others (2010a, 2010b). NC = North Central; NE = Northeastern. (Additional data source: U.S. Department of Agriculture, Forest Service, Forest Inventory and Analysis program)

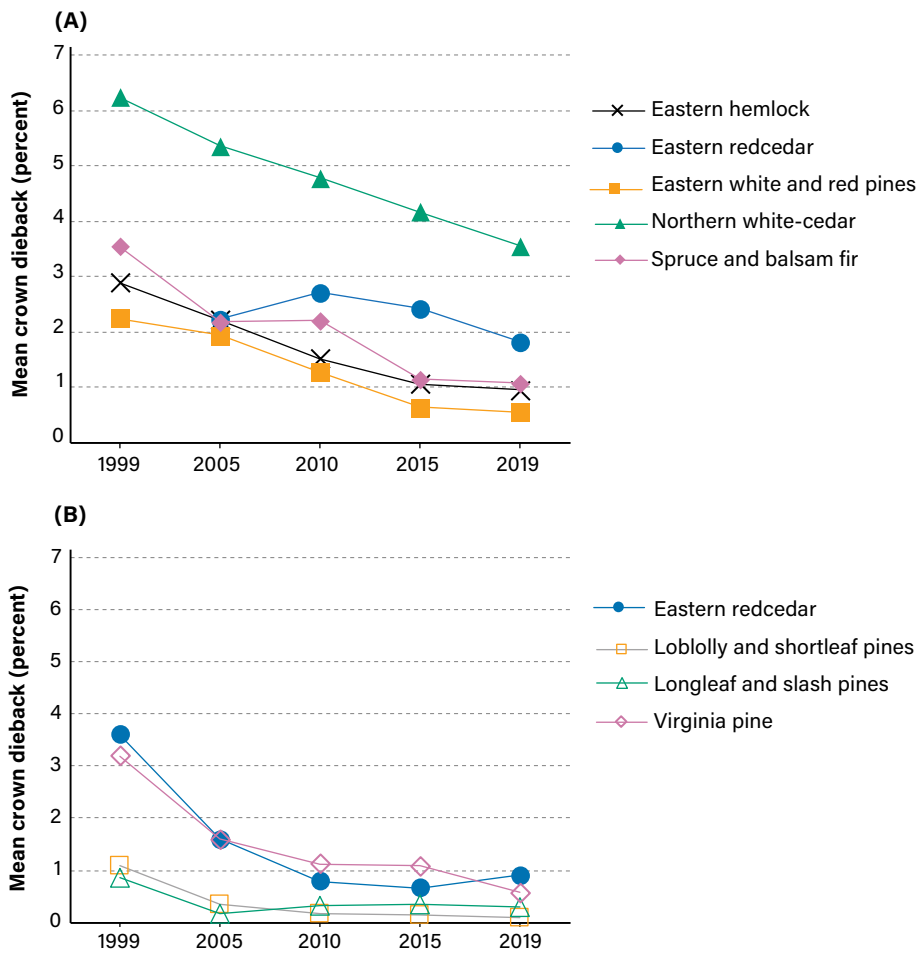

Figure 6.11—Mean crown dieback for softwood species groups in the (A) Northern and (B) Southern regions of the Eastern United States, by species group and year. (Data Source: U.S. Department of Agriculture, Forest Service, Forest Inventory and Analysis program)

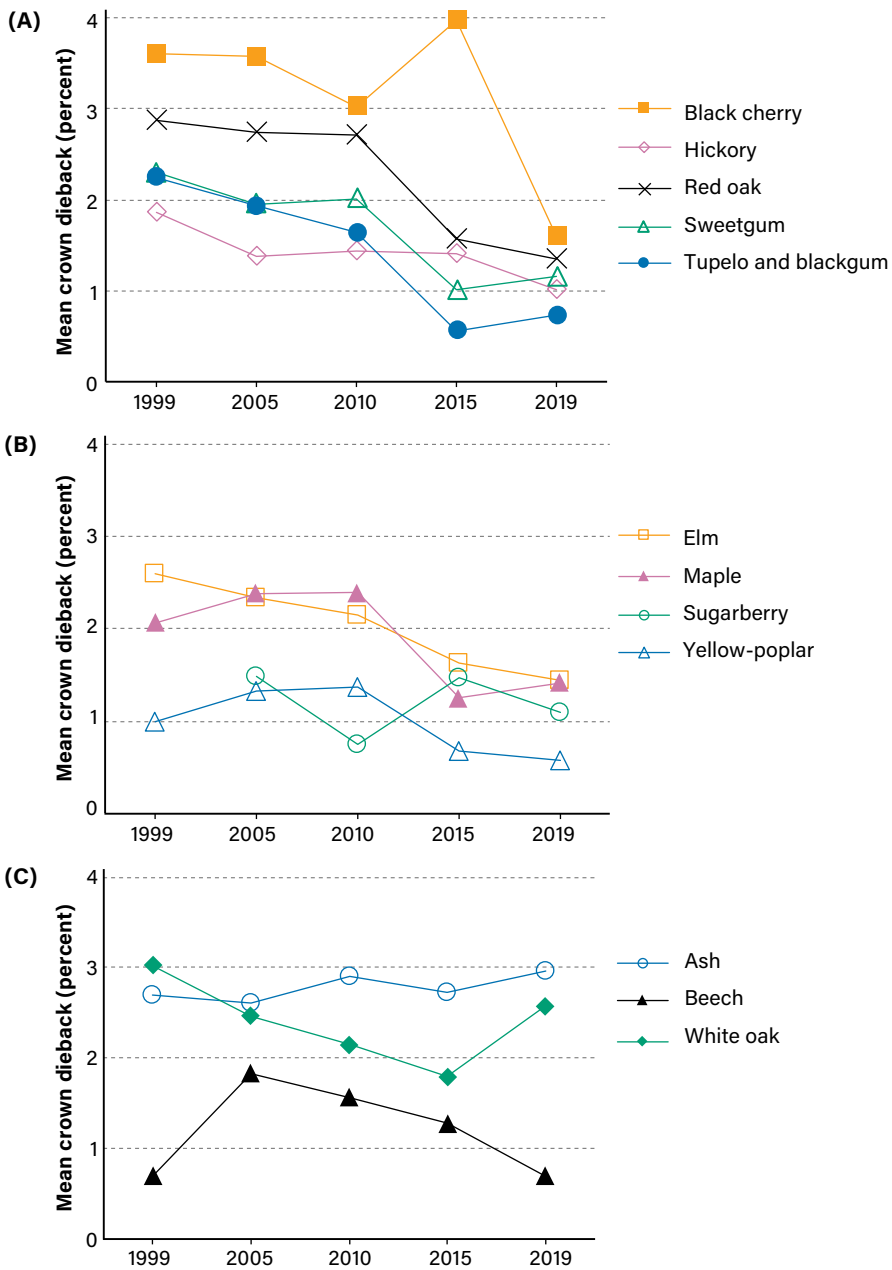

Figure 6.12—Mean crown dieback for hardwood species groups in the Southern region of the Eastern United States for which the ratio between current mean crown dieback and the earliest mean crown dieback was (A) ≤0.5, (B) >0.5 and <0.8, and (C) ≥0.8. (Data Source: U.S. Department of Agriculture, Forest Service, Forest Inventory and Analysis program)

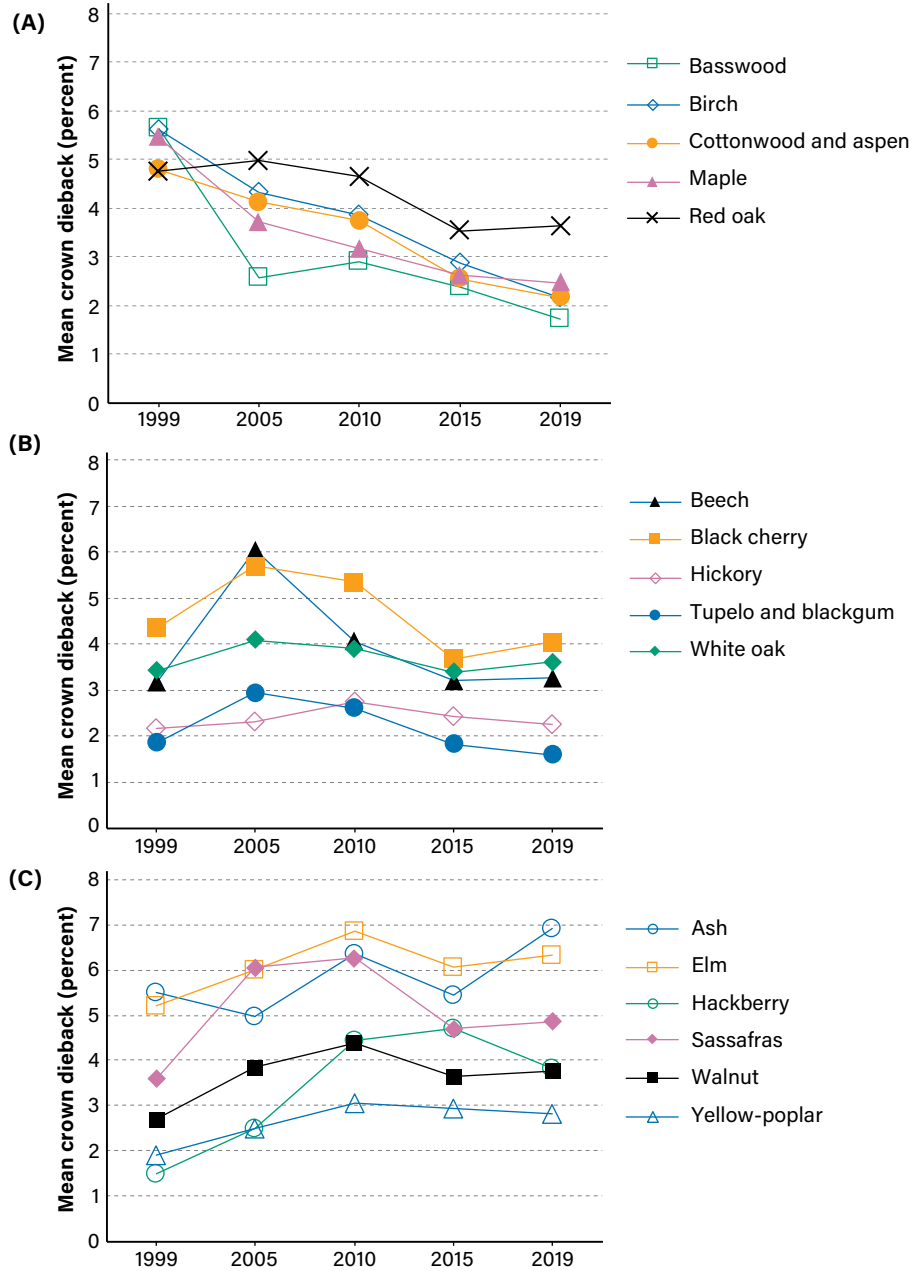

Figure 6.13—Mean crown dieback for hardwood species groups in the Northern region of the Eastern United States for which the ratio between current mean crown dieback and the earliest mean crown dieback was (A) <0.8, (B) ≥0.8 and <1.2, and (C) ≥1.2. (Data Source: U.S. Department of Agriculture, Forest Service, Forest Inventory and Analysis program)

Table 6.4—Mean ratio between current and previous crown dieback, and 95-percent upper (UCL) and lower (LCL) confidence limits, for paired trees in the Northern region, by species group

	Surviving trees and mortality trees					Surviving trees only				
Species group	Number of plots	Number of trees	Mean	LCL	UCL	Number of plots	Number of trees	Mean	LCL	UCL
Softwood	888	12,033	1.2	1.1	1.3	866	11,231	0.9	0.8	1.0
Eastern hemlock	190	1,321	1.1	0.9	1.4	188	1,288	0.9	0.8	1.2
Eastern redcedar	86	458	1.2	0.7	1.9	82	431	0.9	0.5	1.5
Eastern white and red pines	266	2,087	1.1	0.9	1.2	264	1,984	0.8	0.7	0.9
Northern white-cedar	155	2,062	0.9	0.7	1.3	154	2,001	0.9	0.6	1.2
Spruce and balsam fir	451	4,487	1.3	1.1	1.6	440	4,088	0.9	0.7	1.0
Tamarack	67	399	1.1	0.6	1.9	66	382	0.8	0.6	1.2
Hardwood	1,644	26,113	1.2	1.1	1.3	1,574	23,652	0.8	0.8	0.9
Ash	459	1,797	2.4	1.8	3.2	394	1,463	1.12	0.9	1.4
Basswood	156	576	0.6	0.4	0.8	152	559	0.5	0.4	0.7
Beech	282	1,137	1.5	1.1	2.1	273	1,030	1.0	0.8	1.3
Birch	534	2,267	1.2	1.0	1.4	515	2,064	0.8	0.7	1.0
Black cherry	294	961	1.4	1.1	1.8	273	858	0.9	0.7	1.2
Cottonwood and aspen	354	2,164	1.5	1.2	1.8	330	1,870	0.8	0.7	1.0
Elm	336	887	2.1	1.6	2.8	288	695	1.0	0.8	1.2
Hackberry	94	250	0.9	0.5	1.6	88	228	0.7	0.4	1.2
Hickory	299	1,040	1.2	0.9	1.5	287	985	0.9	0.7	1.2
Maple	1,056	8,037	0.9	0.8	1.0	1,036	7,579	0.7	0.6	0.8
Red oak[a]	565	2,234	1.1	0.9	1.4	530	2,032	0.8	0.7	1.0
Sassafras	94	268	1.5	0.8	2.8	82	228	0.9	0.5	1.6
Tupelo and blackgum	107	235	1.1	0.8	1.6	104	230	1.0	0.7	1.4
Walnut	132	292	1.0	0.7	1.6	119	269	0.8	0.5	1.1
White oak[b]	427	2,298	1.4	1.1	1.9	404	2,111	1.1	0.8	1.4
Yellow-poplar	97	401	1.2	0.8	1.7	92	365	0.9	0.6	1.3

[a] *Quercus* Section *Lobatae*.
[b] *Quercus* Section *Quercus*.

Table 6.5—Mean ratio between current and previous crown dieback, and 95-percent upper (UCL) and lower (LCL) confidence limits, for paired trees in the Southern region, by species group

	Surviving trees and mortality trees					Surviving trees only				
Species group	Number of plots	Number of trees	Mean	LCL	UCL	Number of plots	Number of trees	Mean	LCL	UCL
Softwood	986	12,020	1.6	1.5	1.7	920	11,097	1.0	0.9	1.0
Cypress	59	387	1.1	0.9	1.3	58	378	0.9	0.8	1.0
Eastern redcedar	150	548	1.7	1.3	2.2	140	497	1.0	0.9	1.1
Loblolly and shortleaf pines	668	8,347	1.5	1.4	1.6	630	7,795	1.0	1.0	1.0
Longleaf and slash pines	163	1,697	1.9	1.5	2.6	148	1,518	1.0	0.8	1.2
Virginia pine	95	523	2.1	1.4	3.3	87	444	0.8	0.7	1.0
Hardwood	1,350	17,296	1.5	1.4	1.6	1,202	15,403	0.8	0.8	0.9
Ash	192	575	1.9	1.4	2.6	162	482	0.8	0.6	1.1
Beech	76	176	0.8	0.6	1.1	74	166	0.7	0.5	0.9
Black cherry	196	386	1.5	1.0	2.2	166	322	0.6	0.5	0.9
Elm	287	613	1.5	1.2	1.9	259	534	0.8	0.7	0.9
Hickory	405	1,237	1.2	1.0	1.5	379	1,129	0.8	0.7	0.9
Maple	512	1,889	1.7	1.4	1.9	463	1,665	0.9	0.8	1.0
Red oak[a]	803	3,041	1.6	1.4	1.8	737	2,664	0.8	0.8	0.9
Sourwood	133	358	1.3	0.9	1.7	118	317	0.8	0.6	1.0
Sugarberry	52	161	1.7	1.0	2.6	48	145	0.9	0.7	1.2
Sweetgum	483	1,801	1.4	1.2	1.7	459	1,638	0.9	0.8	0.9
Tupelo and blackgum	317	1,058	1.2	1.0	1.4	294	989	0.8	0.7	0.9
White oak[b]	620	2,706	1.0	0.8	1.1	585	2,516	0.7	0.6	0.8
Yellow-poplar	284	1,096	1.3	1.1	1.5	272	1,019	0.9	0.8	1.0

[a] *Quercus* Section *Lobatae*.
[b] *Quercus* Section *Quercus*.

CONCLUSIONS

In general, crown conditions were as expected for most species groups and overall exemplified the presence of known stressors in the Eastern United States, such as beech bark disease, emerald ash borer, hemlock woolly adelgid, spongy moth, and eastern spruce budworm. Damage by wind and vines was also common; however, damage by foliage diseases, decline complexes/dieback/wilts, and snow and ice was less frequent. With only a few exceptions, average crown dieback has remained stable or declined over the last 20 years. Among the softwood species groups included in this summary, crown dieback was greatest among northern white-cedar trees in the Northern region and pinyon-juniper trees in the Southern region. Among the hardwood species groups, crown dieback was greatest among ash and elm trees in the Northern region and honey mesquite trees in the Southern region. Favorably, a downward trend in crown dieback was observed for northern white-cedar over the last 20 years and within the last 10 years for elm; however, crown dieback continued to trend upward for ash. The first remeasurement of trees in central and western Texas is only partially complete; therefore, it is unclear if the high levels of crown dieback for pinyon-juniper and honey mesquite are characteristic for these species groups or trending in one direction or the other.

LITERATURE CITED

Bechtold, W.A.; Patterson, P.L., eds. 2005. The enhanced Forest Inventory and Analysis program—national sampling design and estimation procedures. Gen. Tech. Rep. SRS-80. Asheville, NC: U.S. Department of Agriculture, Forest Service, Southern Research Station. 85 p. https://doi.org/10.2737/SRS-GTR-80.

Boulfroy, E.; Forget, E.; Hofmeyer, P.V. [and others]. 2012. Silvicultural guide for northern white-cedar (eastern white cedar). Gen. Tech. Rep. NRS-98. Newtown Square, PA: U.S. Department of Agriculture, Forest Service, Northern Research Station. 74 p. https://doi.org/10.2737/NRS-GTR-98.

Bréda, N.; Huc, R.; Granier, A.; Dreyer, E. 2006. Temperate forest trees and stands under severe drought: a review of ecophysiological responses, adaptation processes and long-term consequences. Annals of Forest Science. 63: 625–644. https://doi.org/10.1051/forest:2006042.

Burrill, E.A.; DiTommaso, A.M.; Turner, J.A. [and others]. 2021. The Forest Inventory and Analysis Database: database description and user guide for Phase 2 (version 9.0). [Place of publication unknown]: U.S. Department of Agriculture, Forest Service. 1024 p. http://www.fia.fs.usda.gov/library/database-documentation. [Date accessed: August 10, 2022].

Cochran, W.G. 1977. Sampling techniques. 3d ed. New York: John Wiley. 428 p.

Emerald Ash Borer Information Network. 2022. State & county detection table. http://www.emeraldashborer.info/state-dectection-table.php. [Date accessed: June 24, 2022].

Karnosky, D.F. 1979. Dutch elm disease: a review of the history, environmental implications, control, and research needs. Environmental Conservation. 6(4): 311–322. https://doi.org/10.1017/S037689290000357X.

Kozlowski, T.T. 1986. Soil aeration and growth of forest trees (review article). Scandinavian Journal of Forest Research. 1: 113–126. https://doi.org/10.1080/02827588609382405.

Lumley, T. 2004. Analysis of complex survey samples. Journal of Statistical Software. 9(1): 1–19. https://doi.org/10.18637/jss.v009.i08.

Minnesota Department of Natural Resources. 2016. 2016 Forest health highlights. St. Paul, MN: Minnesota Department of Natural Resources, Division of Forestry, Forest Health Unit. 59 p.

Morin, R.S.; Liebhold, A.M.; Pugh, S.A.; Crocker, S.J. 2017. Regional assessment of emerald ash borer, *Agrilus planipennis*, impacts in forests of the Eastern United States. Biological Invasions. 19: 703–711. https://doi.org/10.1007/s10530-016-1296-x.

Morin, R.S.; Randolph, K.C.; Steinman, J. 2015. Mortality rates associated with crown health for eastern forest tree species. Environmental Monitoring and Assessment. 187(3): 87. https://doi.org/10.1007/s10661-015-4332-x.

R Core Team. 2022. R: a language and environment for statistical computing. R Foundation for Statistical Computing. Vienna, Austria.

Randolph, K. 2015. Crown condition. In: Potter, K.M.; Conkling, B.L., eds. Gen. Tech. Rep. SRS-207. Forest Health Monitoring: national status, trends, and analysis 2013. Asheville, NC: U.S. Department of Agriculture, Forest Service, Southern Research Station: 135–151.

Randolph, K.; Bechtold, W.A.; Morin, R.S.; Zarnoch, S.J. 2012. Evaluating elevated levels of crown dieback among northern white-cedar (*Thuja occidentalis* L.) trees in Maine and Michigan: a summary of evaluation monitoring. In: Potter, K.M.; Conkling, B.L., eds. Gen. Tech. Rep. SRS-167. Forest Health Monitoring: 2009 national technical report. Asheville, NC: U.S. Department of Agriculture, Forest Service, Southern Research Station: 219–223.

Randolph, K.C. 2006. Descriptive statistics of tree crown condition in the Southern United States and impacts on data analysis and interpretation. Gen. Tech. Rep. SRS-94. Asheville, NC: U.S. Department of Agriculture, Forest Service, Southern Research Station. 17 p. https://doi.org/10.2737/SRS-GTR-94.

Randolph, K.C. 2009. Crown condition. In: Ambrose, M.J.; Conkling, B.L., eds. Gen Tech. Rep. SRS-117. Forest Health Monitoring: 2006 national technical report. Asheville, NC: U.S. Department of Agriculture, Forest Service, Southern Research Station: 65–110.

Randolph, K.C. 2013. Development history and bibliography of the U.S. Forest Service crown-condition indicator for forest health monitoring. Environmental Monitoring and Assessment. 185(6): 4977–4993. https://doi.org/10.1007/s10661-012-2919-z.

Randolph, K.C. 2018. Crown condition. In: Potter, K.M.; Conkling, B.L., eds. Gen Tech. Rep. SRS-233. Forest Health Monitoring: national status, trends, and analysis 2017. Asheville, NC: U.S. Department of Agriculture, Forest Service, Southern Research Station: 115–132.

Randolph, K.C.; Dooley, K.; Shaw, J.D. [and others]. 2021. Past and present individual-tree damage assessments of the US national forest inventory. Environmental Monitoring and Assessment. 193: 116. https://doi.org/10.1007/s10661-020-08796-z.

Randolph, K.C.; Morin, R.S.; Steinman, J. 2010a. Descriptive statistics of tree crown condition in the North Central United States. Gen. Tech. Rep. SRS-125. Asheville, NC: U.S. Department of Agriculture, Forest Service, Southern Research Station. 21 p. https://doi.org/10.2737/SRS-GTR-125.

Randolph, K.C.; Morin, R.S.; Steinman, J. 2010b. Descriptive statistics of tree crown condition in the Northeastern United States. Gen. Tech. Rep. SRS-124. Asheville, NC: U.S. Department of Agriculture, Forest Service, Southern Research Station. 21 p. https://doi.org/10.2737/SRS-GTR-124.

Schomaker, M.E.; Zarnoch, S.J.; Bechtold, W.A. [and others]. 2007. Crown-condition classification: a guide to data collection and analysis. Gen. Tech. Rep. SRS-102. Asheville, NC: U.S. Department of Agriculture, Forest Service, Southern Research Station. 78 p. https://doi.org/10.2737/SRS-GTR-102.

Shaw, J.D.; Steed, B.E.; DeBlander, L.T. 2005. Forest Inventory and Analysis (FIA) annual inventory answers the question: what is happening to pinyon-juniper woodlands? Journal of Forestry. 10(36): 280–286.

Smith, W.D.; Conkling, B.L. 2004. Analyzing forest health data. Gen. Tech. Rep. SRS-77. Asheville, NC: U.S. Department of Agriculture, Forest Service, Southern Research Station. 33 p. https://doi.org/10.2737/SRS-GTR-77.

Steinman, J. 2000. Tracking the health of trees over time on forest health monitoring plots. In: Hansen, M.; Burk, T., eds. Gen. Tech. Rep. NC-212. Integrated tools for natural resources inventories in the 21st century, proceedings of the IUFRO conference; 1998 August 16–20; Boise, ID. St. Paul, MN: U.S. Department of Agriculture, Forest Service, North Central Research Station: 334–339.

U.S. Department of Agriculture (USDA) Forest Service. 2011. Dutch elm disease. Factsheet. Forest Health Protection, Rocky Mountain Region. 2 p. https://www.fs.usda.gov/Internet/FSE_DOCUMENTS/stelprdb5342693.pdf. [Date accessed: February 28, 2023].

U.S. Department of Agriculture (USDA) Forest Service. 2015. Forest Inventory and Analysis national core field guide. Volume 1: field data collection procedures for Phase 2 plots. Version 7.0. [Place of publication unknown]. 431 p. https://www.fia.fs.usda.gov/library/field-guides-methods-proc/docs/2015/Core-FIA-FG-7.pdf. [Date accessed: August 10, 2022].

U.S. Department of Agriculture (USDA) Forest Service. 2016. Forest Inventory and Analysis strategic plan. A document fulfilling requirements of Section 8301 of the Agriculture Act of 2014. FS-1079. [Place of publication unknown]. 49 p. https://www.fia.fs.usda.gov/library/bus-org-documents/docs/strategic-plan-docs/FIA%20Strategic%20Plan%20FS-1079.pdf. [Date accessed: August 10, 2022].

Wisconsin Department of Natural Resources. 2016. Wisconsin DNR forest health 2016 annual report. [Place of publication unknown]. 25 p.

Woodall, C.W.; Amacher, M.C.; Bechtold, W.A. [and others]. 2011. Status and future of the forest health indicators program of the USA. Environmental Monitoring and Assessment. 177: 419–436. https://doi.org/10.1007/s10661-010-1644-8.

Zarnoch, S.J.; Bechtold, W.A.; Stolte, K.W. 2004. Using crown condition variables as indicators of forest health. Canadian Journal of Forest Research. 34: 1057–1070. https://doi.org/10.1139/x03-277.

CHAPTER 7

The National Lichen Atlas: Summarizing 23 Years of Epiphytic Lichen Community Data

Sarah Jovan and
Susan Will-Wolf

INTRODUCTION

Since its inception in 1989 to the present, nearly 10,000 standardized surveys of epiphytic (tree-dwelling) lichen communities have been conducted as part of the National Lichen Indicator ("Indicator" hereafter), making it the single most extensive lichen community monitoring program in the world. These surveys, used widely by Federal Land Managers (FLMs) and researchers alike, provide valuable information on air quality, climate, biodiversity, and lichen floristics in U.S. forests. Many surveys were conducted on the U.S. Department of Agriculture, Forest Service, Forest Inventory and Analysis (FIA) plot network and thus link to numerous co-located measurements of forest structure collected by FIA field crews. Moreover, the systematic nature of the data, which also provides information about where lichen species *do not* occur, is highly valuable to ecologists, biogeographers, and taxonomists seeking to understand species' distributions and habitat preferences.

Three Forest Service programs played central roles in collecting Indicator data. The earliest surveys collected in the late 1980s were part of various pilot studies conducted "off grid" by the Forest Health Monitoring (FHM) program and the National Forest System's Air Resource Management (ARM) program. In 1993, the FHM program initiated large-scale data collection on the FIA grid (Stolte and others 1993), with the FIA program taking over management of the Indicator around 2003. The ARM program, using their own funding, field crews, and sampling schedule, also conducts many of their surveys on the FIA plot network.

Field and data processing protocols were consistent across participating programs. However, the format of collected data, its accessibility, taxonomic treatment of lichen species, and the availability of other co-located datasets, varied widely. Thus, our goal was to package together Indicator data across parent programs, for the first time, using a consistent, user-friendly format. To do so, we built a comprehensive database called the National FIA Lichen Database (NFLD) and used it to create a National Lichen Atlas to illustrate the breadth of the combined Indicator datasets (Jovan and others 2020, 2021b). These products cover the first 23 years of Indicator data, up through 2012 when FIA ceased large-scale collection of lichen surveys. Data collection since then has been more sporadic and geographically targeted, often using the 23 years of data in the NFLD as a baseline.

METHODS

Field

In brief, Indicator data come from timed surveys (up to 2 hours) aiming to capture all epiphytic noncrustose lichen species encountered within a 0.94-acre area. A voucher specimen is collected and abundance code assigned to every species suspected to be unique (Jovan and others 2020). Surveyors are specially trained and certified in the Indicator protocol, with their performance assessed by professional lichenologists usually at least once per season. Voucher specimens are identified by lichenologists and later deposited in herbaria to make them available for further study.

How to cite this chapter:

Jovan, Sarah; Will-Wolf, Susan. 2023. The National Lichen Atlas: summarizing 23 years of epiphytic lichen community data. In: Potter, Kevin M.; Conkling, Barbara L., eds. Forest Health Monitoring: national status, trends, and analysis 2022. Gen. Tech. Rep. SRS-273. Asheville, NC: U.S. Department of Agriculture, Forest Service, Southern Research Station: 127–136. https://doi.org/10.2737/SRS-GTR-273-Chap7.

Data

For the NFLD, we built six linkable core tables to house all FHM and FIA data using a structure similar to the "LICHEN-…" tables in the Forest Inventory and Analysis Database (FIADB), one of several parent databases to the NFLD. We integrated all ARM data collected through 2012 into a seventh table, [LICHEN_ATLAS], which we used to generate the species distribution maps for the National Lichen Atlas. The [LICHEN_ATLAS] table serves as a user-friendly starting place for analysts because it integrates all data, including relevant geographic and the most commonly used environmental variables, into a single table. For more information, the NFLD version 1.0 is available along with a detailed user guide (Jovan and others 2020) at https://www.fia.fs.usda.gov/program-features/indicators/lichen/.

RESULTS AND DISCUSSION

For the comprehensive [LICHEN_ATLAS] table, we were able to collate approximately 115,500 lichen records across the three participating Forest Service programs. Records represent about 8,300 lichen community surveys covering 6,000 unique forested locations from 1989 to 2012 (fig. 7.1). The NFLD makes more than one-third of these Indicator surveys available to the public for the first time. The FHM program collected 2,311 surveys; FIA collected an additional 3,061; ARM added an additional 2,970 surveys to [LICHEN_ATLAS] over the same time period.

More than 85 percent of all surveys were collected on the FIA grid (and are identified as such in the NFLD), which means extensive co-located forest structure data may be available for these plots. The user guide (Jovan and others 2020) provides instructions for accessing the NFLD's parent databases to help users obtain environmental variables not included in the [LICHEN_ATLAS] table. The remaining surveys, classified as "off-grid" plots, were located in areas of special interest to support specific research or management objectives not otherwise served by the on-grid dataset. Requests for additional data for off-grid sites can be sent to this chapter's authors.

Indicator surveys detected roughly 440 distinct taxa as identified under program criteria. The evolutionary history of lichens is poorly understood compared to vascular plants, making the field of lichen taxonomy highly dynamic. Thus, to compare "apples to apples," users of Indicator data must first assess the need to reconcile the taxonomy of lichen names in their dataset. More than 350 taxonomic name changes were adopted by the Indicator programs over the course of data collection. Each change in name or species concept is recorded in the core NFLD table named [REF_LICHEN_SPP_COMMENTS]. This table provides detailed rationales for each name change, along with relevant literature citations and suggested actions for users to take depending upon the geographic region and timespan their dataset covers. Alternatively, we have already applied a consistent taxonomic treatment to the [LICHEN_ATLAS] table, making it a user-friendly starting point with the main downside being that we needed to lump a few cryptic species and several newer species

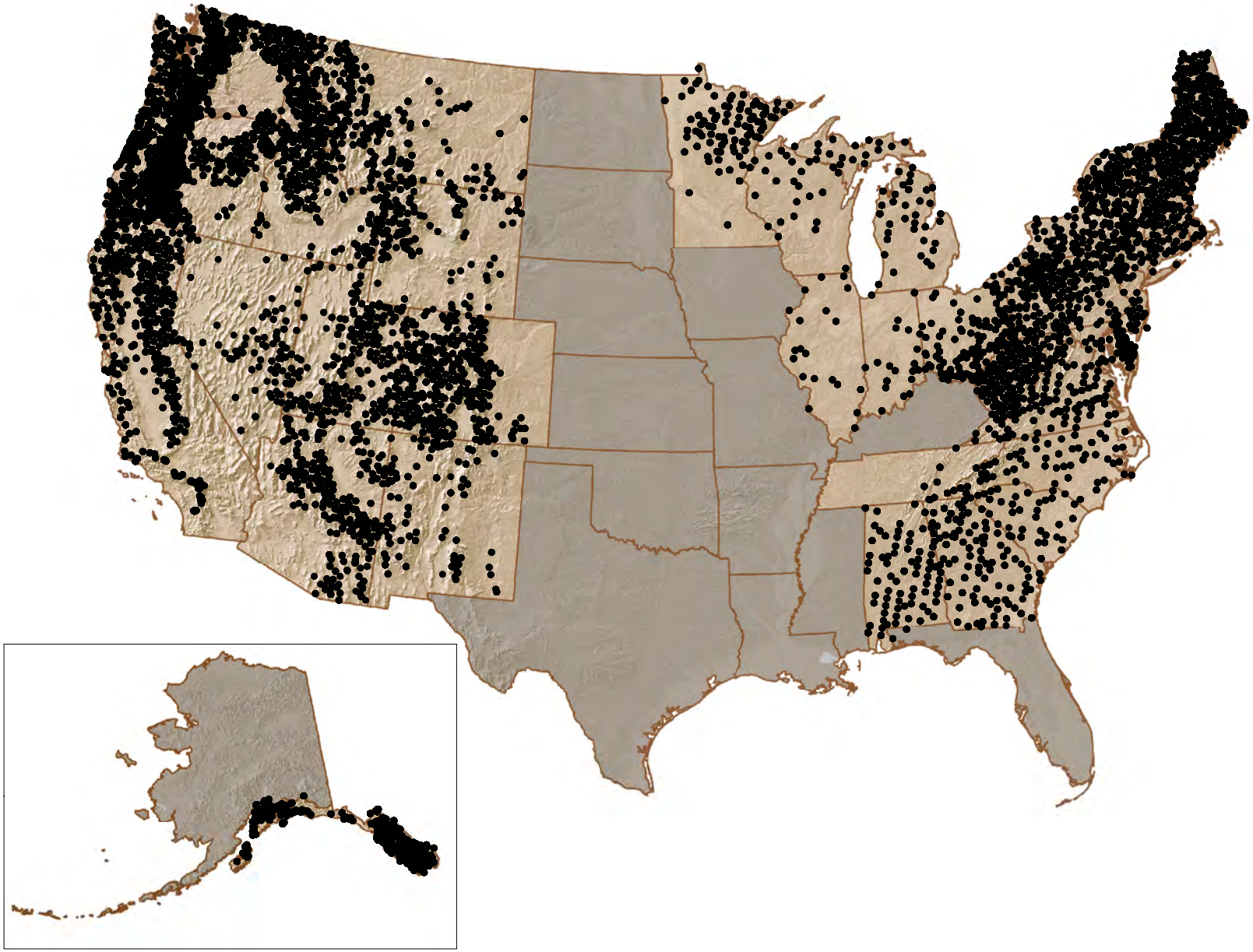

Figure 7.1—Map of lichen survey sites in the National Lichen Atlas (Jovan and others 2021b). Each site was visited one to four times. Site locations are approximate.

names together due to the long time period covered by the dataset. Older specimens are not routinely revisited to update species names although many are stored in herbaria and thus available to interested users for further study. This left us with about 400 taxa to feature with distribution maps and photos in the Atlas. The [LICHEN_ATLAS] table includes both the reconciled and original names determined for each lichen occurrence, so analysts wishing to use the table can make their own decisions about when and how to implement suggested actions in [REF_LICHEN_SPP_COMMENTS].

Atlas Examples: Distributions of Air Quality Indicator Species

More than 100 studies to date use the Indicator data as a baseline for investigating spatial and, increasingly, temporal trends in lichen community-based metrics (Jovan and others 2020). Many metrics have been developed to indicate air quality, climate, and other change on forest land in the United States, although air quality is by far the most common focus. Lichens are highly sensitive to pollution due to their reliance on atmospheric sources of water and nutrients, leading to the accumulation of many pollutants in their tissues as well as predictable shifts in species composition. Metrics describing these community shifts and assays measuring pollutant concentrations in lichen tissue are both common, inexpensive ways to better understand pollution patterns across the landscape.

For example, excess nitrogen (N) deposition is linked to a wide array of detrimental ecological effects in both the Eastern and Western United States (Jovan and others 2021a, Root and others 2021, Smith and others 2020). Lichens are extremely responsive to N; as levels begin exceeding natural background levels, lichen communities start to gain "eutrophic" (i.e., N-loving) species and lose native "oligotrophic" (N-sensitive) species. Eutrophs, like species of the brightly colored genera *Candelaria* (figs. 7.2A and 7.3), *Xanthoria,* and *Xanthomendoza*, tend to be relatively small in size with broad geographic distributions. Eutrophs occur in naturally N-enriched sites (e.g., under bird perches), although anthropogenic N sources like fertilizers, livestock enclosures, and motor vehicle emissions have allowed them to greatly expand their abundance. In contrast, oligotrophs may grow quite large, play important ecological roles in the forest system, and often have geographically restricted distributions even in the absence of pollution. One example, the iconic witch's hair lichen (*Alectoria sarmentosa*; figs. 7.2B, 7.2C, and fig. 7.4), grows abundantly on tree trunks and branches in wet montane forests of the Northwest and Alaska where it is used extensively by wildlife for forage and nest building. Ecological functions like these are thus impacted when elevated N reduces the health and abundance of *A. sarmentosa* and other oligotrophic species. Community shifts like this, i.e., where sensitive species are replaced by tolerant or pollution-loving species, are the basis of lichen-based "critical loads," a management tool FLMs use to determine where pollutant levels may be causing ecological harm (Geiser and others 2021).

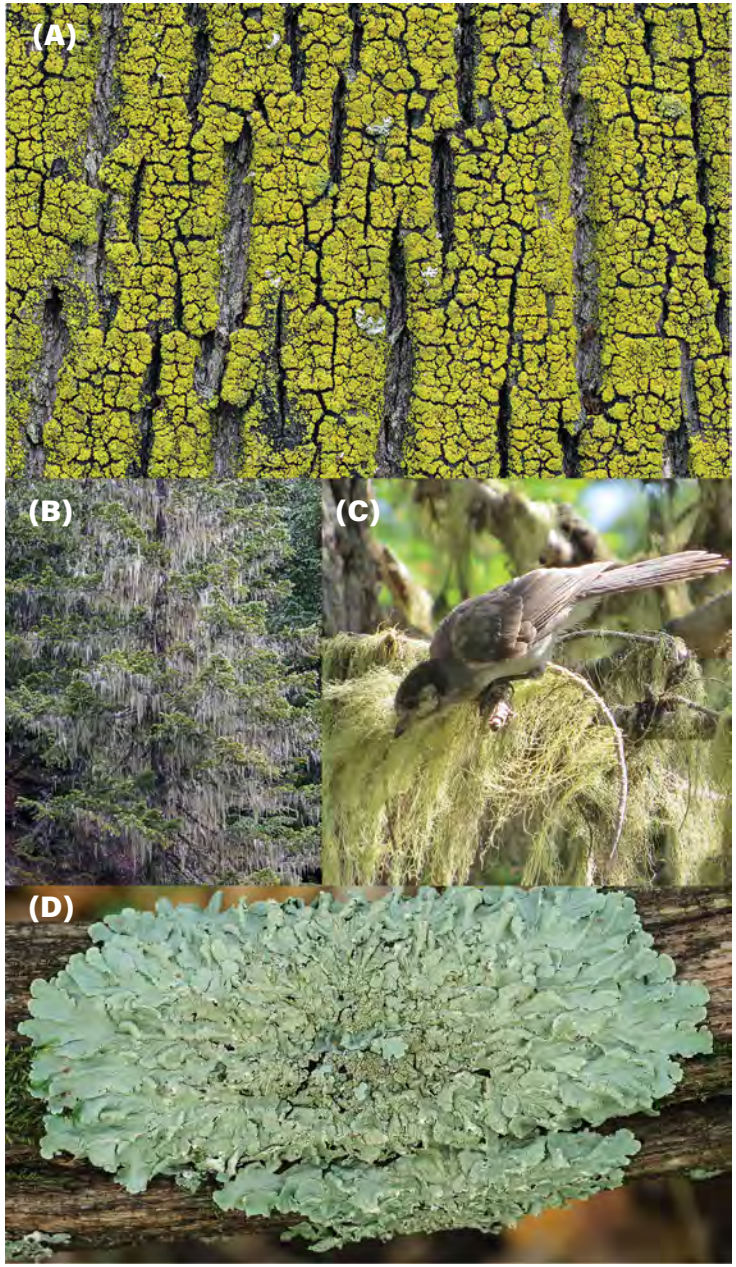

Other pollutants, like heavy metals and many air toxics, accumulate in lichens without causing observable community-level effects. The ARM program, which is most active in the Pacific Northwest and Alaska, pairs all Indicator community surveys with assays of heavy metals, N, and sulphur (S) in lichen tissue collected onsite. Witch's hair lichen (figs. 7.2B and 7.2C) grows in long luxurious "beards," making it a favorite target species of ARM surveyors. Tissue collection by FIA crews was never a routine part of the 23 years of "baseline" data, although most recent surveys include some assay data. One of the most common target species collected on FIA plots in the East, for instance, is the common greenshield lichen (*Flavoparmelia caperata*; figs. 7.2D and 7.5), valued for its widespread distribution and manageable size (Will-Wolf and others 2017).

Figure 7.2—Photos of common lichens used to indicate air quality: (A) Candelaria pacifica, *(B, C)* Alectoria sarmentosa, *and (D)* Flavoparmelia caperata. *(A, B, D: Courtesy photos by Richard Droker [Creative Commons license: https://creativecommons.org/licenses/by-nc-nd/2.0/]; C: Courtesy photo by Leppyone [Creative Commons license: https://creativecommons.org/licenses/by/2.0/])*

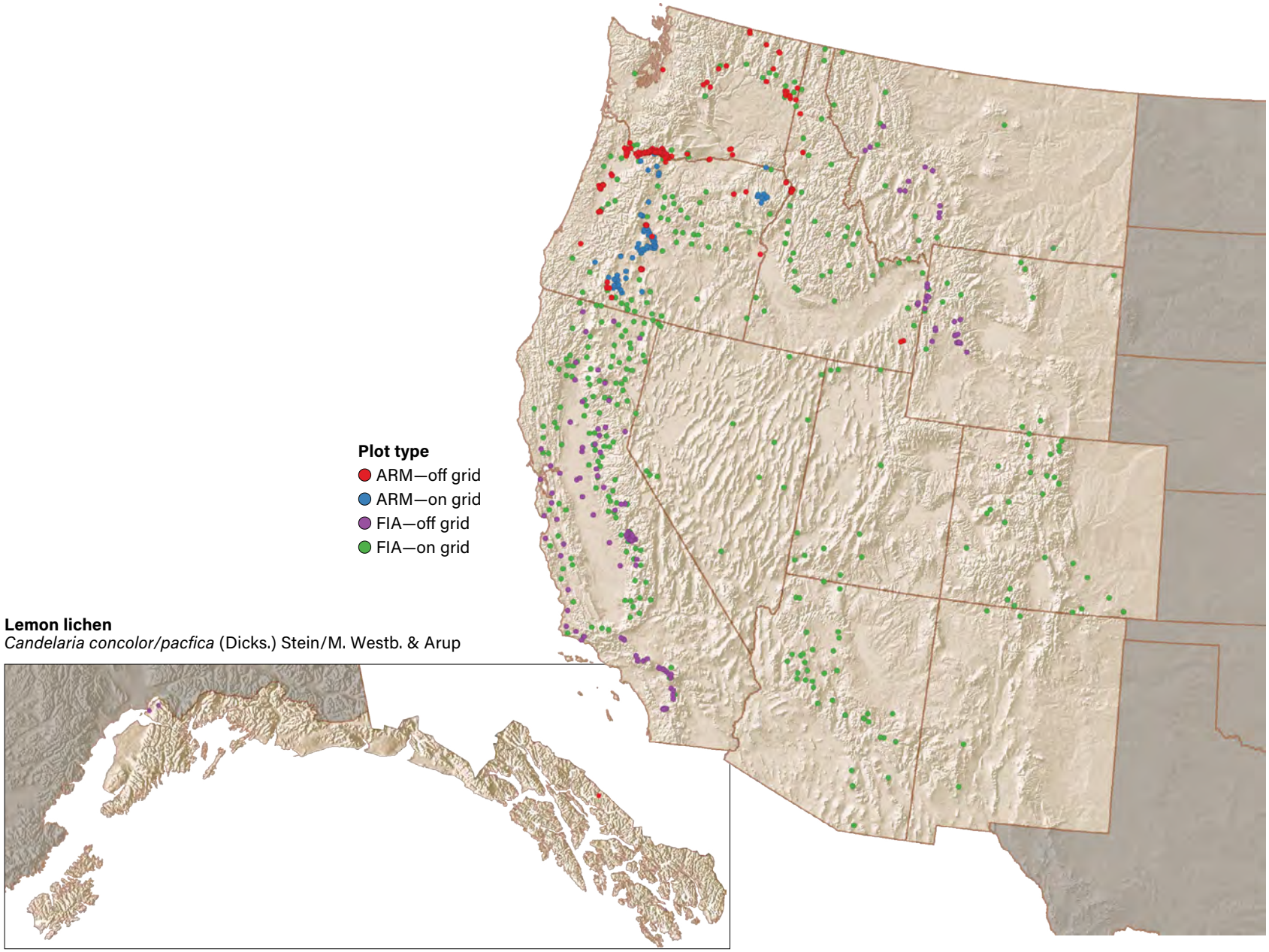

Figure 7.3—Map of Indicator surveys where Candelaria concolor *and* C. pacifica *were found on Air Resource Management (ARM) and Forest Inventory and Analysis (FIA) plots. These species are mapped together because their sterile forms are difficult to differentiate. Western records are likely* C. pacifica, *while eastern records are likely* C. concolor. *Plot locations are approximate.*

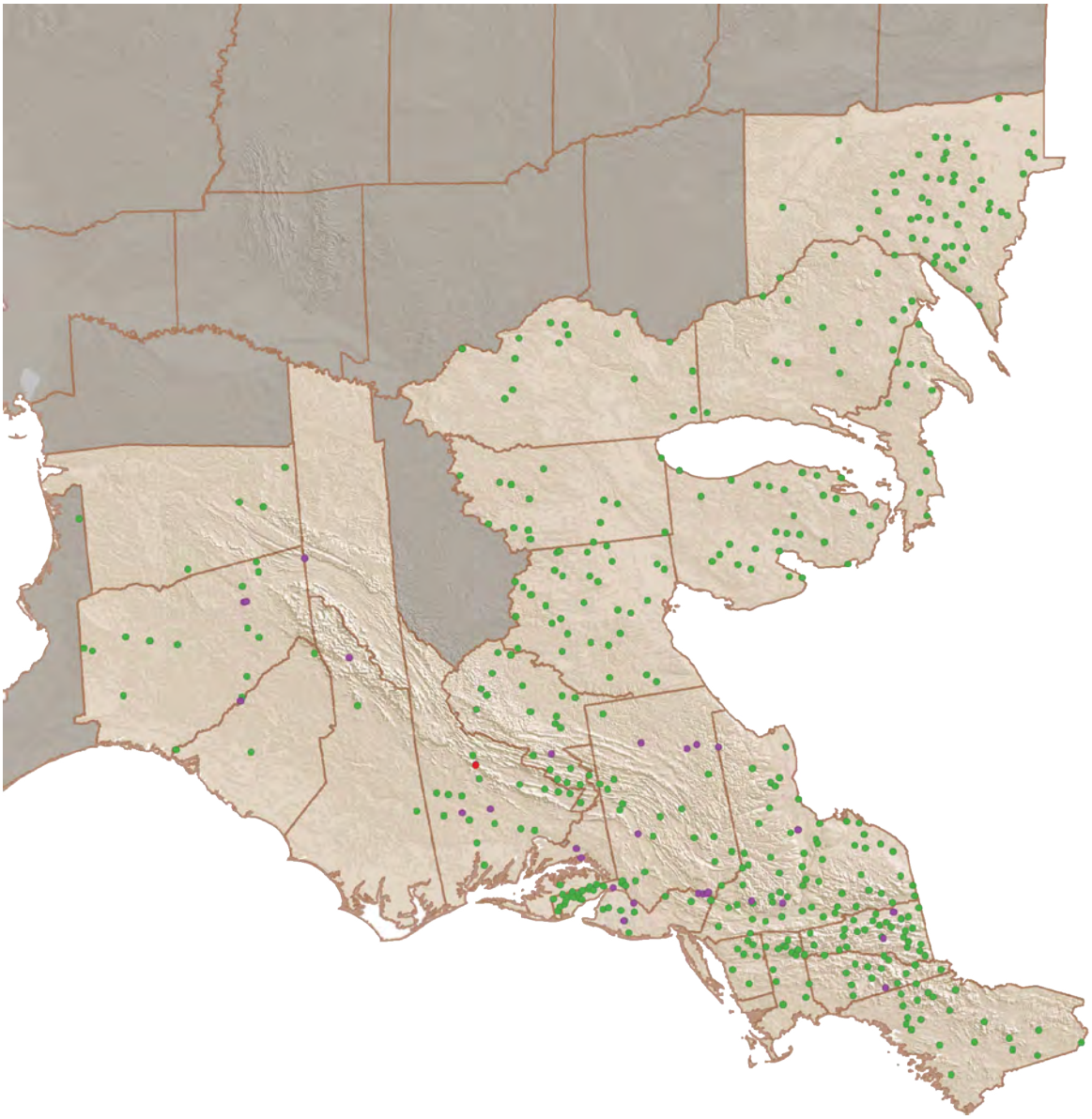

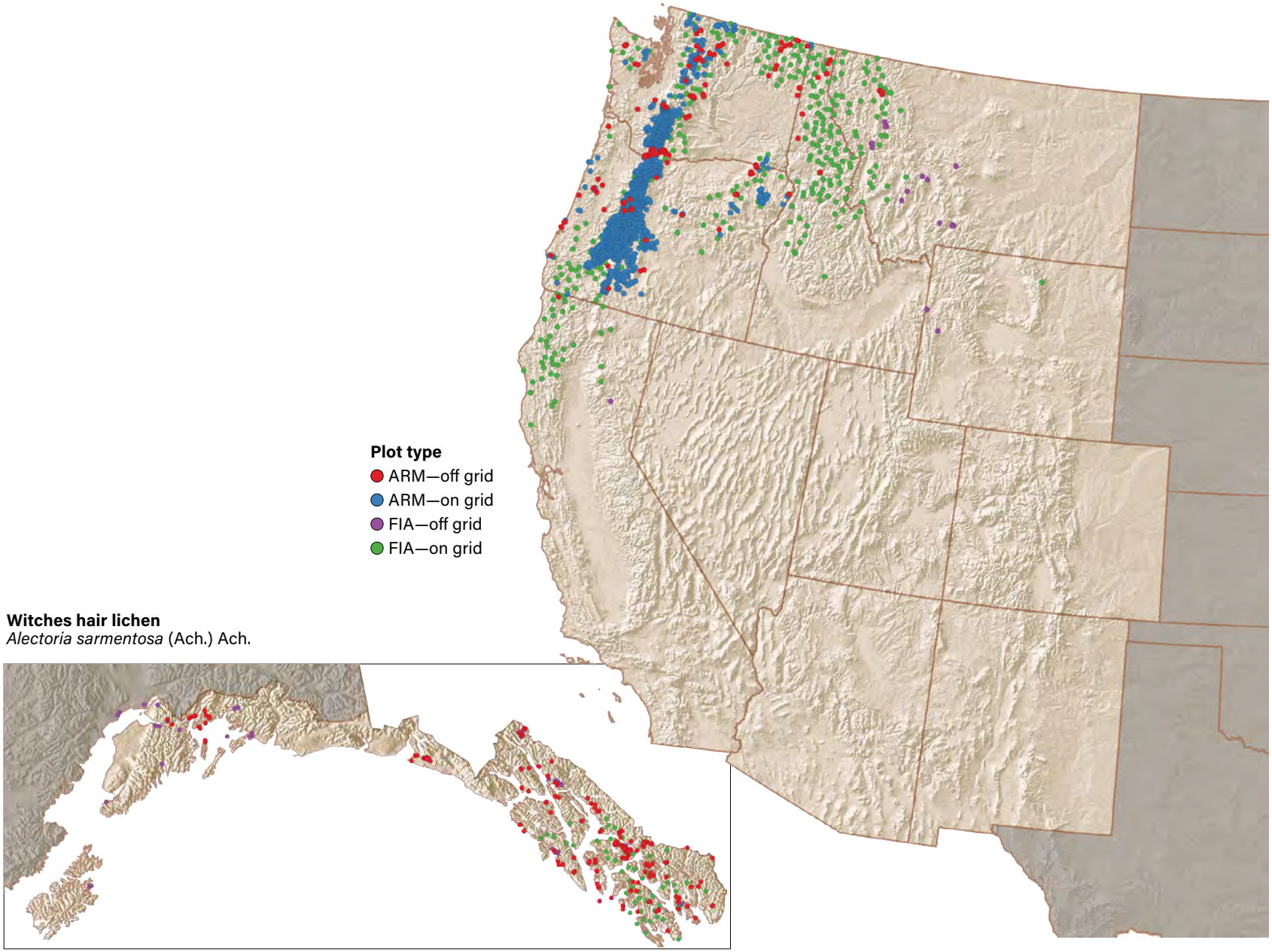

Figure 7.4—Map of Indicator surveys where Alectoria sarmentosa *was found on Air Resources Management (ARM) and Forest Inventory and Analysis (FIA) plots. Plot locations are approximate.*

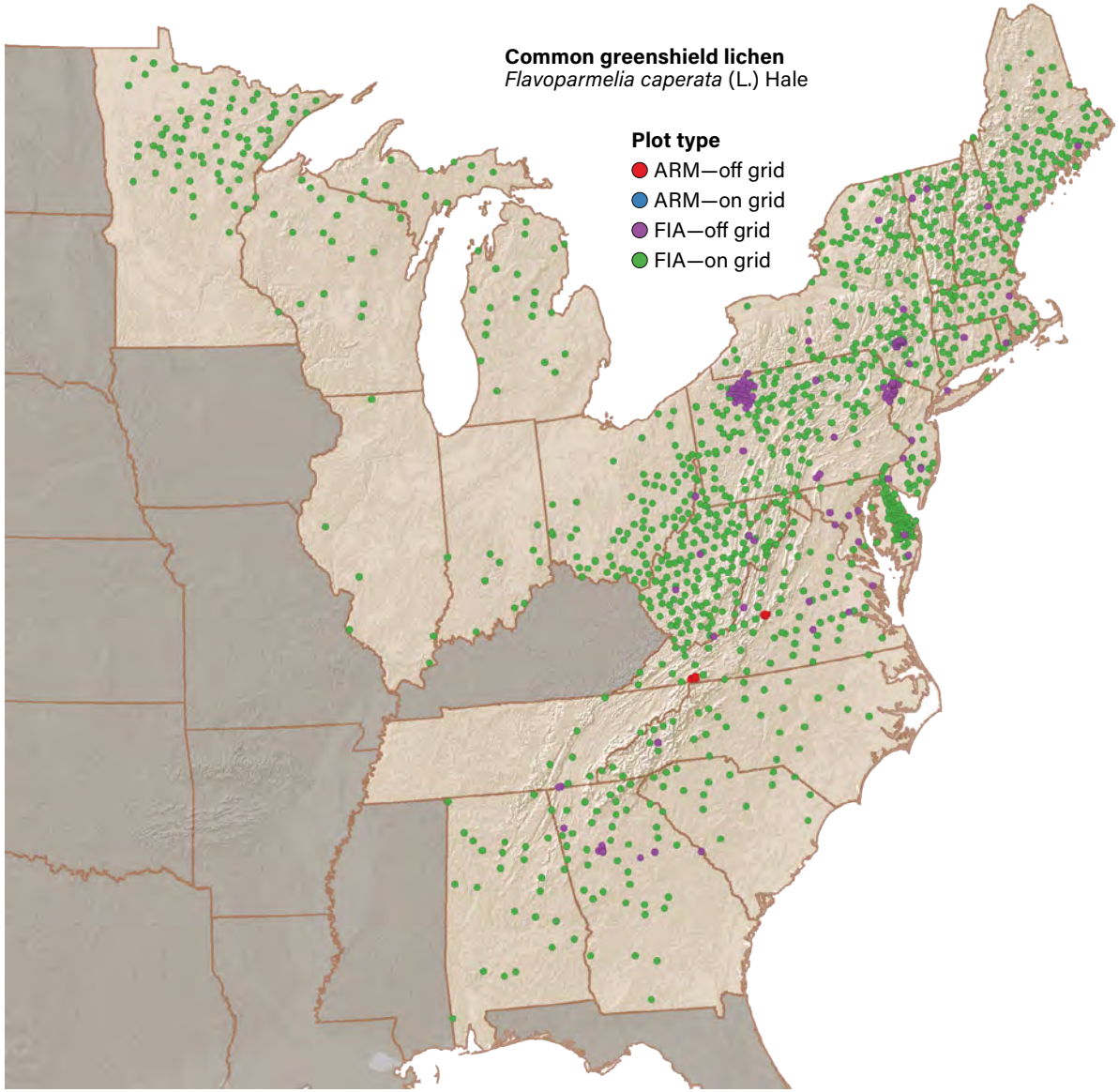

Figure 7.5—Map of Indicator surveys where Flavoparmelia caperata *was found on Air Resources Management (ARM) and Forest Inventory and Analysis (FIA) plots. Plot locations are approximate.*

CONCLUSIONS

Publication of the NFLD version 1.0 and National Lichen Atlas marks a significant milestone, making data from thousands of lichen surveys conducted from 1989 to 2012 available to the public for the first time. Despite reduced data collection since 2012, the ARM and FIA programs have maintained their long-term partnership to continue serving clients of the Indicator, making data more readily available and, when possible, supporting additional data collection to answer specific research or management questions. Future versions of the NFLD will incorporate these newer datasets, including assay data where available.

LITERATURE CITED

Geiser, L.H.; Root, H.; Smith, R.J. [and others]. 2021. Lichen-based critical loads for deposition of nitrogen and sulfur in US forests. Environmental Pollution. 291: 118187. https://doi.org/10.1016/j.envpol.2021.118187.

Jovan, S.; Fenn, M.E.; Buhler, M. [and others]. 2021a. Challenges characterizing N deposition to high elevation protected areas: a case study integrating instrument, simulated, and lichen inventory datasets for the Devils Postpile National Monument and surrounding region, USA. Ecological Indicators. 122: 107311. https://doi.org/10.1016/j.ecolind.2020.107311.

Jovan, S.; Haldeman, M.; Will-Wolf, S. [and others]. 2021b. National atlas of epiphytic lichens in forested habitats of the United States. Gen. Tech. Rep. PNW-986. Portland, OR: U.S. Department of Agriculture, Forest Service, Pacific Northwest Research Station. 96 p.

Jovan, S.; Will-Wolf, S.; Geiser, L. [and others]. 2020. User guide for the national Forest Inventory and Analysis lichen database (version 1.0). Gen. Tech. Rep. PNW-988. Portland, OR: U.S. Department of Agriculture, Forest Service, Pacific Northwest Research Station. 83 p.

Root, H.T.; Jovan, S.; Fenn, M. [and others]. 2021. Lichen bioindicators of nitrogen and sulfur deposition in dry forests of Utah and New Mexico, USA. Ecological Indicators. 127: 107727. https://doi.org/10.1016/j.ecolind.2021.107727.

Smith, R.J.; Jovan, S.; Stanton, D.; Will-Wolf, S. 2020. Epiphytic macrolichen communities indicate climate and air quality in the U.S. Midwest. The Bryologist. 123(3): 517–533. https://doi.org/10.1639/0007-2745-123.3.516.

Stolte, K.; Mangis, D.; Doty, R. [and others], eds. 1993. Lichens as bioindicators of air quality. Gen. Tech. Rep. RM-224. Fort Collins, CO: U.S. Department of Agriculture, Forest Service, Rocky Mountain Forest and Range Experiment Station. 131 p.

Will-Wolf, S.; Jovan, S.; Amacher, M.C. 2017. Lichen elements as pollution indicators: evaluation of methods for large monitoring programmes. The Lichenologist. 49(4): 415–424. https://doi.org/10.1017/S0024282917000299.

SECTION 3

Evaluation Monitoring Project Summaries

Each year, the Forest Health Monitoring (FHM) program funds a variety of Evaluation Monitoring (EM) projects, which are projects to determine the extent, severity, and causes of undesirable changes in forest health identified through Detection Monitoring (see the FHM website: https://www.fs.usda.gov/foresthealth/protecting-forest/forest-health-monitoring/index.shtml). In addition, EM projects can produce information about forest health improvements. The EM projects are submitted, reviewed, and selected through an established process. More detailed information about how EM projects are selected, the most recent call letter, and reporting responsibilities are listed on the Forest Health Protection Grants website (https://www.fs.usda.gov/foresthealth/working-with-us/index.shtml).

Beginning in 2008, each FHM National Status, Trends, and Analysis report contains summaries of recently completed EM projects. Each summary provides an overview of the project and results, citations for products and other relevant information, and a contact for questions or further information. The summaries provide an introduction to the kinds of monitoring projects supported by FHM and include enough information for readers to pursue specific interests. Four EM project summaries are included in this report.

CHAPTER 8

Ash Tree Decline and Mortality in Ohio and the Allegheny National Forest in Pennsylvania

Kathleen S. Knight,
Charles E. Flower,
Jason S. Kilgore,
Alejandro A. Royo,
Timothy D. Fox,
Rachel H. Kappler,
Brian M. Hoven,
Joshua S. Wigal,
Jordan D. Bernard,
and Robert P. Long

How to cite this chapter:

Knight, Kathleen S.; Flower, Charles E.; Kilgore, Jason S.; Royo, Alejandro A.; Fox, Timothy D.; Kappler, Rachel H.; Hoven, Brian M.; Wigal, Joshua S.; Bernard, Jordan D.; Long, Robert P. 2023. Ash tree decline and mortality in Ohio and the Allegheny National Forest in Pennsylvania. In: Potter, Kevin M.; Conkling, Barbara L., eds. Forest Health Monitoring: national status, trends, and analysis 2022. Gen. Tech. Rep. SRS-273. Asheville, NC: U.S. Department of Agriculture, Forest Service, Southern Research Station: 139–147 https://doi.org/10.2737/SRS-GTR-273-Chap8.

INTRODUCTION

The emerald ash borer (*Agrilus planipennis*) (EAB) is a wood-boring beetle from Asia that has killed billions of ash (*Fraxinus* spp.) trees in North America since its accidental introduction to southeastern Michigan in the mid-1990s. The EAB spread rapidly and has become one of the most costly/destructive pests in North America (Aukema and others 2011). It affects multiple ash species, driving several to be listed as endangered (Jerome and others 2017). Previous studies have shown substantial EAB-caused mortality of larger size classes of ash in forests (Flower and others 2013, Morin and others 2017); however, in some sites, ashes have survived as lingering survivor trees (Koch and others 2015), small seedlings (Klooster and others 2014), or trees from root sprouts (Kashian 2016).

The impacts of invasive pests on host trees vary by species and vary across the landscape based on geophysical characteristics and forest stand conditions (Flower and Gonzalez-Meler 2015). Earlier research has indicated differences in mortality from EAB among ash species (Anulewicz and others 2007, Rebek and others 2008, Tanis and McCullough 2012), which may be due to tree resistance to EAB, the preference of EAB adults, or both (Koch and others 2015). For example, adult EABs have been shown to prefer other native ash species over blue ash (*F. quadrangulata*) (Pureswaran and Poland 2009, Tanis and McCullough 2012). Understanding patterns of ash decline and mortality helps forest managers plan for and manage EAB impacts and also provides context for identification of lingering ash trees to test for EAB resistance.

METHODS

We studied the EAB impacts on ash in two very different landscape contexts in Ohio and Pennsylvania. The Ohio sites are typically smaller forested areas, including Federal and State lands, local parks, and privately owned land, completely surrounded by agricultural areas or suburban housing and retail. In contrast, the Pennsylvania sites are in the Allegheny National Forest (ANF), a heavily forested landscape with considerable geographic relief surrounded by and interspersed with forested State and private lands.

In Ohio, we set up three monitoring plots in each of 60 sites during 2005–2008 prior to ash mortality to include a range of ash densities, stand ages, and species: white ash (*F. americana*), green ash (*F. pennsylvanica*), pumpkin ash (*F. profunda*), black ash (*F. nigra*), and blue ash. Each of these five ash species has different habitat affinities, ranging from upland forests for white ash, to riparian areas for green ash, to limestone areas with high calcium soils for blue ash, to wet forests for black, pumpkin, and green ash. We used bark and twig morphology to identify blue ash, bark and sessile leaflets to identify black ash, and seed shape and calyx length to identify white, green, and pumpkin ash. We collected voucher specimens of ash seeds, leaves, and twigs and preserved them at the U.S. Department of Agriculture, Forest Service, Northern Research Station lab in Delaware, OH. In sites that contained a mix of white and green ash and hybrids, or green and pumpkin ash, it was difficult to distinguish among these tree species and so they were pooled.

In Ohio, we measured ash trees ≥10 cm diameter at breast height (d.b.h.) in three to five 11.3-m-radius circular plots per site and measured ash saplings and seedlings in smaller nested plots (see Knight and others 2014 for detailed methods). We tracked >3,000 individual trees and recorded ash canopy health condition on a 1–5 scale where 1 is healthy, 5 is dead, and 2, 3, and 4 are stages of decline. We also recorded EAB symptoms, d.b.h., mortality, and tree fall. Tree fall was defined as the main trunk of the tree on the ground, due to the lower trunk snapping or uprooting. We visited plots yearly 2005–2014 and again in 2019; we visited sites with remaining live trees in 2020 and 2021. From 2008–2021, in nine sites in central Ohio and five sites in northwestern Ohio, we measured EAB populations. We hung four purple prism traps coated with tanglefoot and baited with manuka oil lures in ash trees throughout the season when EAB adults are active (450–550 growing degree days [GDD] to late August) and counted EAB adults caught on the traps.

In northwestern Pennsylvania, we set up 190 monitoring plots in 2010 prior to ash mortality at the ANF. In contrast to the Ohio sites, the ANF is marked by considerable topography, creating upper slope areas where soil base cations may be depleted due to leaching and lower slope areas with richer soils. These soil differences have led to declines in ash health in upper slope areas prior to EAB impact (Royo and Knight 2012). We selected ash sites by superimposing a 700-ha grid throughout the ANF land base and used existing stand composition data to identify blocks containing ash and to select paired upper and lower slope plots. All ash trees in monitoring plots at the ANF are white ash, and very few ash saplings and seedlings existed in any of our sites. We used basal area factor (BAF) 10 prism plots to record ash canopy health condition, d.b.h., and mortality of ash trees in 2010, 2015, and 2018–2021.

RESULTS

Figures 8.1 and 8.2 depict the progression of ash mortality across the landscapes of Ohio and the ANF, respectively. In most sites, ash trees (≥10 cm d.b.h.) were relatively healthy at the beginning of the monitoring period and then progressed to substantial mortality. At the ANF, white ash had experienced 77-percent mortality by 2021. Mortality patterns differed markedly by species in Ohio (table 8.1), with blue ash exhibiting better survival rates than other species. In sites containing both white ash and blue ash, the white ash was attacked and killed first. Then, the blue ash began to decline, with some trees succumbing to EAB, but with >70 percent of the trees surviving. In contrast, < 5 percent of the white and green ash trees ≥10 cm d.b.h. originally present in all plots were still alive by 2019. In most sites, black ash had 100-percent mortality; however, at a few sites where nearby ash trees had been treated with systemic insecticide, black ash and pumpkin ash had greater survival. Ash trees fell rapidly after mortality, with 20 percent of the trees falling within 2 years and >80 percent falling within 8 years (fig. 8.3).

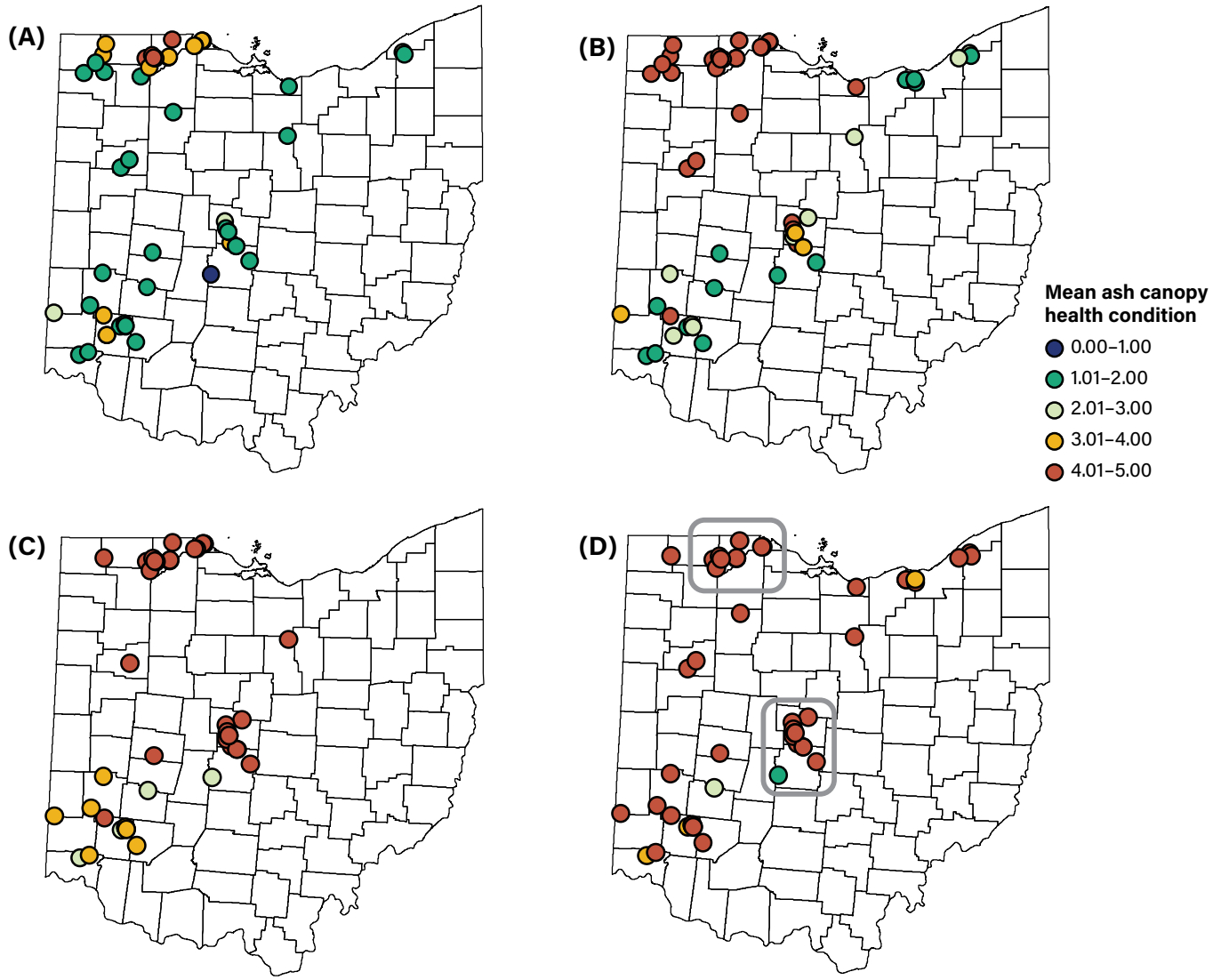

Figure 8.1—Ash canopy health condition of trees ≥10 cm diameter at breast height in Ohio in (A) 2008, (B) 2011, (C) 2014, and (D) 2019. Ash canopy health condition is a 1–5 rating, where 1 is a healthy canopy, 5 is a completely dead canopy, and 2, 3, and 4 are stages of decline. Sites in northwestern Ohio and central Ohio where emerald ash borer traps were used yearly are circled in panel D.

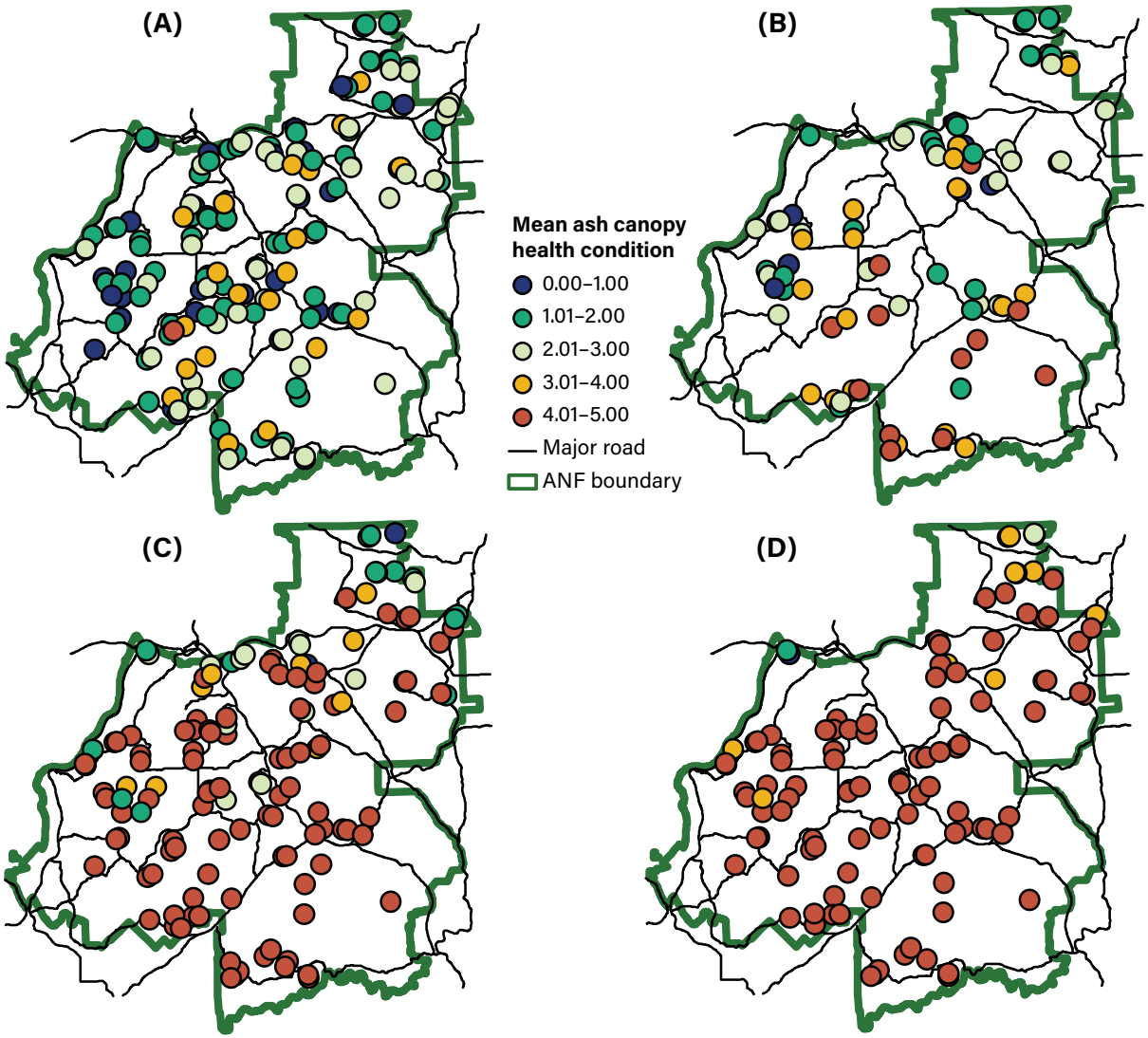

Figure 8.2—Ash canopy health condition from prism plots on the Allegheny National Forest (ANF) in (A) 2010, (B) 2015, (C) 2018, and (D) 2021.

Table 8.1—Differences in mortality and canopy health condition for ash trees ≥10 cm d.b.h. recorded in the Ohio monitoring plots, 2006–2019

Species	Number of trees	Mean initial d.b.h.	Mean canopy health rating, 2019[a]	Dead, 2019
		cm		*percent*
White ash (*Fraxinus americana*)	529	24.1	5.0	98.6
Black ash (*F. nigra*)	80	20.5	4.7	91.8
Green ash (*F. pennsylvanica*)	391	25.9	4.9	95.8
Pumpkin ash (*F. profunda*)	50	27.0	4.2	66.7
Blue ash (*F. quadrangulata*)	60	28.1	2.9	28.3
Green ash/white ash[b]	308	21.3	5.0	99.1
Green ash/pumpkin ash[b]	444	24.2	4.9	97.2

[a] Canopy health is rated on a 1–5 scale where 1 is healthy and 5 is dead.
b Species were lumped in sites with evidence of a mix of white and green ash and hybrids, or green and pumpkin ash.

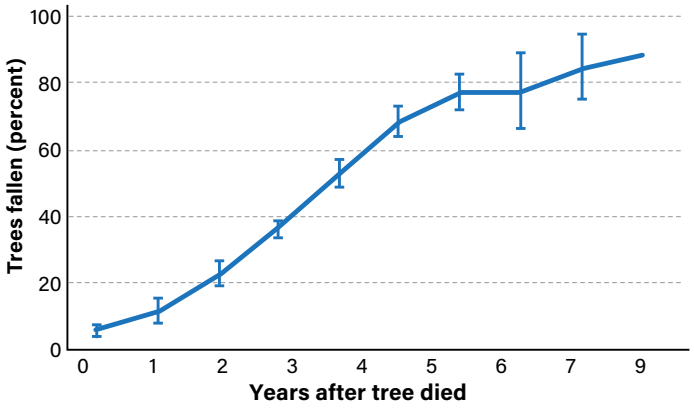

Figure 8.3—Percentage of fallen dead trees from 1,100 ash trees ≥10 cm diameter at breast height that died during 2006–2014 in Ohio.

In Ohio, the abundance of ash saplings (1.0–9.9 cm d.b.h.) was quite variable and did not show consistent changes in abundance from pre-EAB to post-EAB impact (table 8.2). The sapling size class is highly dynamic due to mortality and recruitment, with some of the larger saplings killed by EAB, other saplings dying from other causes, and recruitment occurring especially in areas where abundant ash seedlings grew rapidly as canopy gaps opened. In many Ohio sites, ash seedlings are abundant (data not shown). However, newly germinated seedlings are not present or very rare.

The EAB traps in Ohio showed similar patterns in each monitored site. Trap catch numbers increased slowly at first and then rapidly in an exponential pattern, with peak catches typically coinciding with 50-percent mortality of the ash trees at a site, then a rapid crash in EAB populations as the remaining ash trees died (fig. 8.4). However, EAB populations persisted at low levels and showed a small resurgence more recently in northwestern Ohio (fig. 8.5).

Table 8.2—Presence of live mature ash (≥10 cm d.b.h.) and presence and abundance of ash saplings (1.0–9.9 cm d.b.h.) in Ohio monitoring plots prior to emerald ash borer (EAB) impact (2006–2008) and after EAB impact (2019)

	pre-EAB				post-EAB	
Species	Number of plots with mature trees	Number of plots with saplings	Mean number of saplings per plot	Standard deviation saplings per plot	Mean number of saplings per plot	Standard deviation saplings per plot
White ash (*Fraxinus americana*)	68	15	1.2	3.9	0.2	0.6
Black ash (*F. nigra*)	26	12	4.5	10.5	4.0	7.4
Green ash (*F. pennsylvanica*)	35	12	5.9	18.4	3.2	9.6
Pumpkin ash (*F. profunda*)	9	0	0.0	0.0	2.0	2.3
Blue ash (*F. quadrangulata*)	22	12	8.7	20.8	4.1	8.4
Green ash/white ash[a]	36	11	3.7	9.9	1.7	4.6
Green ash/pumpkin ash[a]	39	12	0.9	1.8	1.9	4.2

[a] Species were lumped in sites with evidence of a mix of white and green ash and hybrids, or green and pumpkin ash.

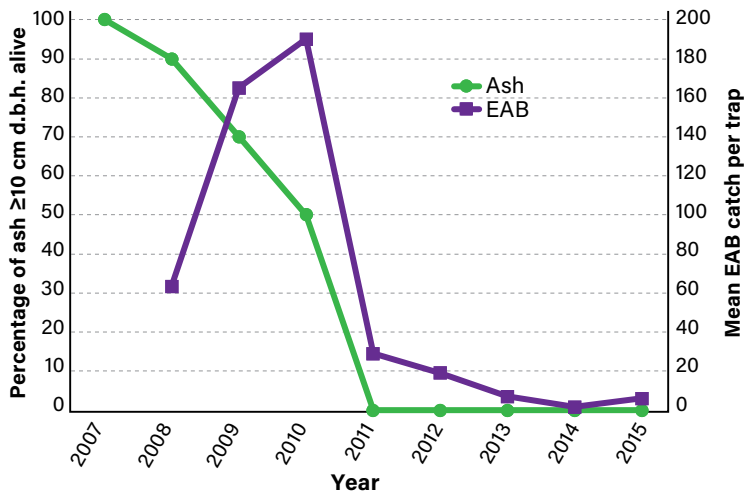

Figure 8.4—Emerald ash borer (EAB) trap catches and the percentage of live ash trees ≥10 cm diameter at breast height (d.b.h.) at a site in central Ohio showing the typical pattern of ash and EAB population dynamics.

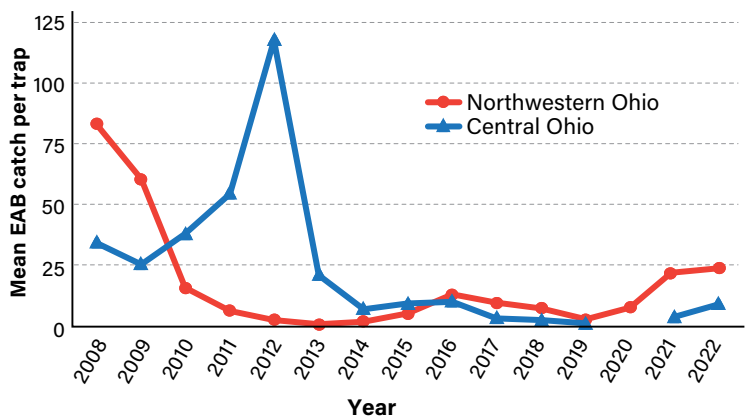

Figure 8.5—Emerald ash borer trap catches in northwestern and central Ohio monitoring sites. Note: Due to the COVID-19 pandemic, data were not collected from central Ohio sites in 2020.

CONCLUSIONS

Our data show nearly complete mortality of most species of ash ≥10 cm d.b.h. in two very different landscapes in Ohio and Pennsylvania. Tracking of individual trees on a yearly basis during a rapid mortality event allowed us to accurately quantify the effect of EAB. Because many trees die and fall in <4 years, estimates of mortality from one-time or longer interval surveys that only include standing trees likely underestimate mortality from EAB.

The survival of larger ash trees during the initial wave of EAB infestation may result from multiple mechanisms, including adult EAB feeding and landing preference, tree resistance (i.e., the tree's ability to kill the EAB larvae) (Koch and others 2015), and tree tolerance (i.e., the tree's ability to survive and grow while infested). The small percentage of large ash trees that have survived EAB infestation in Ohio and at the ANF are of considerable interest because they may be useful for breeding programs for resistance to EAB.

Consistent with research in Michigan showing blue ash to have generally higher survival than other ash species (Tanis and McCullough 2012), the survival of blue ash in the Ohio sites was much better than other species. This may be due to adult EAB having reduced preference for blue ash, as shown in feeding and landing studies (Pureswaran and Poland 2009). Long-term monitoring of blue ash sites will determine whether this higher survival rate will persist.

While the larger trees exhibit very high mortality rates, smaller ash saplings likely have less mortality caused by EAB, and seedlings <0.5 cm d.b.h. are not infested by EAB. We recorded abundant regeneration at some of the Ohio monitoring sites. The future dynamics of EAB populations and the surviving ash populations will determine the future of ash in Ohio. At the ANF, there is almost no ash regeneration at our monitoring sites, and white ash has simply disappeared from the landscape in only a decade.

For more information:
Kathleen Knight
kathleen.s.knight@usda.gov

ACKNOWLEDGMENTS

The U.S. Department of Agriculture's Animal and Plant Health Inspection Service (APHIS) Plant Protection and Quarantine, Forest Service Forest Health Monitoring, Forest Service Special Technology Development Program, Forest Service and APHIS Emerald Ash Borer Technology Development, Forest Service Targeted Allocation, and National Resources Inventory grant programs funded the monitoring work. We thank the Ohio Department of Natural Resources, Metroparks, and other public and private landowners of Ohio for access to study sites. Allegheny National Forest staff including Steve Forry, Andrea Hille, and Justin LaMountain have assisted with data sharing and study logistics. We thank the many student interns and Forest Service technicians who have assisted in data collection and entry on this project, including Stephanie Smith, Kyle Costilow, Lawrence Long, Ernie Wiltsie, Joshua Hanson, Grag Sanford, Eric Baxter, Stephanie Fluke, Jamie Himes, Ashley Will, Britton Flash, Bernadette Wiggin, Joel Throckmorton, Thomas Macy, Robert Ford, Sagar Jasani, Zak Morvay,

Sarah Starr, Mike Marshall, Ellie Monarch, Rachel Hefflinger, Sam Stroebel, Dane Weeks, Erik DeBurgomaster, Ben Gombash, Matt Higham, Scott Kelsey, Parker Jones, Eli Aubihl, Dawlton Nelson, Vikram Singh, Jesse Reardon, Emily Melnik, Sara Miller, Lillian Ostrander, Brandon Marcucci, Alexander Skowron, Ben Phillips, Beth Tull, Grace Gutierrez, Debilea Chapel, Grace Kirwin, Dean Kralic, Ed Vandever, Julia Zick, Joan Jolliff, Kirsten Lehtoma, and Danielle Kelley. We thank Bill Oldland for sponsoring the Evaluation Monitoring grant and providing input. We thank Susan Crocker and Toby Petrice for helpful comments on this manuscript.

LITERATURE CITED

Anulewicz, A.C.; McCullough, D.G.; Cappaert, D.L. 2007. Emerald ash borer (*Agrilus planipennis*) density and canopy dieback in three North American ash species. Arboriculture & Urban Forestry. 33(5): 338–349. https://doi.org/10.48044/jauf.2007.039.

Aukema, J.E.; Leung, B.; Kovacs, K. [and others]. 2011. Economic impacts of non-native forest insects in the continental United States. PLOS ONE. 6(9): e24587. https://doi.org/10.1371/journal.pone.0024587.

Flower, C.E.; Gonzalez-Meler, M.A. 2015. Responses of temperate forest productivity to insect and pathogen disturbances. Annual Review in Plant Biology. 66: 547–569. https://doi.org/10.1146/annurev-arplant-043014-115540.

Flower, C.E.; Knight, K.S.; Gonzalez-Meler, M.A. 2013. Impacts of the emerald ash borer (*Agrilus planipennis*) induced ash (*Fraxinus* spp.) mortality on forest carbon cycling and successional dynamics in the Eastern United States. Biological Invasions. 15(4): 931–944. https://doi.org/10.1007/s10530-012-0341-7.

Jerome, D.; Westwood, M.; Oldfield, S.; Romero-Severson, J. 2017. *Fraxinus americana*. The IUCN Red List of Threatened Species. https://www.iucnredlist.org/species/61918430/61918432. [Date accessed: May 11, 2022].

Kashian, D.M. 2016. Sprouting and seed production may promote persistence of green ash in the presence of the emerald ash borer. Ecosphere. 7(4): e01332. https://doi.org/10.1002/ecs2.1332.

Klooster, W.S.; Herms, D.A.; Knight, K.S. [and others]. 2014. Ash (*Fraxinus* spp.) mortality, regeneration, and seed bank dynamics in mixed hardwood forests following invasion by emerald ash borer (*Agrilus planipennis*). Biological Invasions. 16: 859–873. https://doi.org/10.1007/s10530-013-0543-7.

Knight, K.S.; Flash, B.P.; Kappler, R.H. [and others]. 2014. Monitoring ash (*Fraxinus* spp.) decline and emerald ash borer (*Agrilus planipennis*) symptoms in infested areas. Gen. Tech. Rep. NRS-139. Newtown Square, PA: U.S. Department of Agriculture, Forest Service, Northern Research Station. 18 p. https://doi.org/10.2737/NRS-GTR-139.

Koch, J.L.; Carey, D.W.; Mason, M.E. [and others]. 2015. Intraspecific variation in *Fraxinus pennsylvanica* responses to emerald ash borer (*Agrilus planipennis*). New Forests. 46: 995–1011. https://doi.org/10.1007/s11056-015-9494-4.

Morin, R.S.; Liebhold, A.M.; Pugh, S.A.; Crocker, S.J. 2017. Regional assessment of emerald ash borer, *Agrilus planipennis*, impacts in forests of the Eastern United States. Biological Invasions. 19: 703–711. https://doi.org/10.1007/s10530-016-1296-x.

Pureswaran, D.S.; Poland, T.M. 2009. Host selection and feeding preference of *Agrilus planipennis* (Coleoptera: Buprestidae) on ash (*Fraxinus* spp.). Environmental Entomology. 38: 757–765. https://doi.org/10.1603/022.038.0328.

Rebek, E.J.; Herms, D.A.; Smitley, D.R. 2008. Interspecific variation in resistance to emerald ash borer (Coleoptera: Buprestidae) among North American and Asian ash (*Fraxinus* spp.). Environmental Entomology. 37(1): 242–246. https://doi.org/10.1603/0046-225X(2008)37[242:IVIRTE]2.0.CO;2.

Royo, A.A.; Knight, K.S. 2012. White ash (*Fraxinus americana*) decline and mortality: the role of site nutrition and stress history. Forest Ecology and Management. 286: 8–15. https://doi.org/10.1016/j.foreco.2012.08.049.

Tanis, S.R.; McCullough, D.G. 2012. Differential persistence of blue ash and white ash following emerald ash borer invasion. Canadian Journal of Forest Research. 42: 1542–1550. https://doi.org/10.1139/x2012-103.

CHAPTER 9

Detecting Changes in Forest Condition at Landscape Scales Using a Landsat-Based Harmonic Modeling Approach

Valerie J. Pasquarella,
Randall S. Morin,
Andrew M. Liebhold,
Nathan W. Siegert,
Clare A. Rodenberg,
and Kyle J. Haynes

How to cite this chapter:

Pasquarella, Valerie J.; Morin, Randall S.; Liebhold, Andrew M.; Siegert, Nathan W.; Rodenberg, Clare A.; Haynes, Kyle J. 2023. Detecting changes in forest condition at landscape scales using a Landsat-based harmonic modeling approach. In: Potter, Kevin M.; Conkling, Barbara L., eds. Forest Health Monitoring: national status, trends, and analysis 2022. Gen. Tech. Rep. SRS-273. Asheville, NC: U.S. Department of Agriculture, Forest Service, Southern Research Station: 149–162. https://doi.org/10.2737/SRS-GTR-273-Chap9.

INTRODUCTION

The health and condition of forested ecosystems are increasingly affected by a variety of disturbances including forest harvests, fires, and pests and pathogens (Cohen and others 2016, Lovett and others 2006). The Insect and Disease Survey (IDS), coordinated by the U.S. Department of Agriculture, Forest Service, Forest Health Protection, has historically used annual aerial surveys to map and monitor pest damage (Coleman and others 2018). However, remote sensing instruments are uniquely poised to provide consistent, regularly updated monitoring over large areas, and numerous forest disturbance detection and condition monitoring approaches have been developed (Cohen and others 2017, Hall and others 2007, Koltunov and others 2020, Rullan-Silva and others 2013, Senf and others 2017). These automated approaches can be combined with field datasets including systematic plot measurements from the Forest Service's Forest Inventory and Analysis (FIA) program to build an improved understanding of how the spatial and temporal distribution of disturbances affects forest structure, composition, and resilience (Lister and others 2020, Schroeder and others 2014, Vogt and Koch 2016). Yet monitoring short-duration changes, such as those associated with defoliating insect outbreaks, and characterizing the longer term effects of defoliator outbreaks remain an ongoing challenge.

Detecting changes in forest health and condition requires a formally designed baseline against which comparisons can be made (Norman and Christie 2020). In the context of spectral measurements, baselines are typically defined in terms of seasonally similar values from different years or other aggregate statistics (e.g., Chastain and others 2015, Norman and others 2013), but comparing individual observations from different years and/or times of year can be problematic due to potential differences in foliar phenology and other confounding factors, such as missed clouds and shadows and other uncorrected atmospheric effects. Given that forest ecosystems tend to have relatively stable and persistent phenological signals (Pasquarella and others 2016), cyclic patterns in the reflectance of forest ecosystems are typically well represented by regression models with harmonic terms that characterize seasonal variability while remaining robust to noisy observations (Wilson 2015; Wilson and others 2012, 2018; Zhu and others 2012). Thus, a harmonic baseline monitoring approach enables more direct comparison of observed and predicted values for specific dates.

Previous efforts to map the 2016–2018 forest defoliation caused by outbreak populations of the spongy moth (*Lymantria dispar*) in southern New England using a Landsat-based harmonic monitoring approach (Pasquarella and others 2017, 2018) relied on a single harmonic model to represent long periods of relative stability as a baseline for comparison. Although this fixed-baseline approach facilitated pre- and post-outbreak comparisons, the designated baseline period was highly dependent on the specific study area and disturbance of interest, and we found notable variations in the magnitude of disturbance for vegetation condition scores calculated using different baseline years (Pasquarella and others

2021). The fixed-baseline approach also posed a challenge in terms of generating historic assessments (since baseline fitting might overlap with monitoring dates) as well as when the baseline period is increasingly far into the past relative to the period being monitored (since the baseline becomes less representative of current conditions as time since fitting increases).

As a key deliverable of our Evaluation Monitoring project, we introduce a more flexible moving-window approach for Landsat-based harmonic condition monitoring (HCM) that considers both spatial and temporal variability in forest disturbance dynamics and improves our ability to estimate uncertainties in both near-real-time and aggregated seasonal assessments. In this summary, we briefly describe our method and efforts to operationalize our workflow for the northern portion of Forest Service Region 9 (Eastern Region) using the Google Earth Engine platform. We compare results generated using the new moving-window workflow with comparable fixed-baseline results for a set of field sites in central Massachusetts. We then tested the utility of HCM-generated vegetation condition scores for assessing relationships between defoliation and growth and mortality rates of oaks (*Quercus* spp.) in Pennsylvania using FIA plot measurements, building on previous work by Morin and Liebhold (2016) that relied on aerial survey data.

METHODS

Our HCM approach is based on the assumption that univariate time series of reflectance observations for a band or index of interest can be relatively well characterized by a harmonic regression model (Sellers and others 1996). This approach is particularly suited for condition monitoring using vegetation indices in regions/ecosystems with strong phenological signals. Although our methods could be adapted to other sensors, we currently rely on Landsat time series due to the length of the Landsat observation record (1985 to present) as well as moderate spatial (30-m) and temporal (8- to 16-day) resolutions. We use the following model to estimate baseline reflectance:

$$y(\mathrm{x}) = \mathrm{a} + bx + \sum_{j \in N} \left(\mathrm{c}_j \cos\left(\frac{2\pi j}{T}\mathrm{x}\right) + d_j \sin\left(\frac{2\pi j}{T}\mathrm{x}\right) \right) + \varepsilon$$

where

y = the predicted vegetation index, e.g., Tasseled Cap Greenness (TCG) (Crist 1985; Crist and Kauth 1986)

x = the ordinal date of each observation

a = the modeled intercept

b = the modeled slope

N = a set of integers specifying the frequency, j, of the Fourier series harmonics (e.g., $N = \{1, 3\}$, corresponding to 12-month and 4-month harmonics)

c_j = the cosine coefficients

d_j = the sine coefficients estimated at each frequency

T = the number of days in a year ($T = 365.25$)

ε = the residual error term for each observation

The use of a 4-month harmonic was preferred over a 6-month harmonic to characterize higher

frequency asymmetry in the seasonal reflectance profile without adding an additional set of harmonic terms.

Once baseline reflectance models have been estimated, vegetation condition scores are calculated as the difference between the observed and predicted reflectance values for a given acquisition date, and are normalized by the root mean square error (RMSE) of the baseline model used to generate the predicted value, i.e.:

$$\text{score} = \frac{y - y_{pred}}{RMSE}$$

Thus, vegetation condition scores are a normalized anomaly metric that estimates the magnitude of change in reflectance relative to the uncertainty in baseline model fit.

Previous implementations of our HCM workflow that relied on a single baseline model for prediction and monitoring calculated a single vegetation condition score for each acquisition date during a specified monitoring period. However, selection of a suitable baseline period may be challenging in frequently disturbed landscapes. Furthermore, noise in reflectance observations may impact the quality of models fit to different time periods. Therefore, the latest version of our workflow utilizes an ensemble approach that combines vegetation condition score estimates from multiple baseline models (see Pasquarella 2021 for code). Baseline models are fit to Landsat time series using a moving window such that each model is fit to a unique time period in 1-year increments and the n models preceding the specified monitoring period are used to generate a set of n vegetation condition score estimates for each acquired image during the specified monitoring period. These scores can then be averaged across all dates within the monitoring period to produce a more robust estimate of potential condition change for each pixel in the specified study area. Although baseline length (in years) is an adjustable parameter in our workflow, we use a baseline period of 5 years (e.g., models are generated for 1985–1989, 1986–1990, 1987–1991, and so on), which provides a sufficient number of observations for fitting a six-term harmonic model while remaining responsive to temporally localized changes in reflectance patterns and approximating the FIA remeasurement cycle.

RESULTS AND DISCUSSION

Condition Monitoring Workflow and Visualization Tools

To demonstrate our ability to monitor changes in vegetation condition over large spatial extents, we piloted our improved HCM workflow for nine States in the northern portion of Forest Service Region 9, specifically Maine, New Hampshire, Vermont, New York, Massachusetts, Connecticut, Rhode Island, New Jersey, and Pennsylvania. We used time series of Landsat 5, 7, and 8 observations to generate annual maps of condition change assessments for the years 1995 to present using a May 1 through September 30 monitoring period. We applied the TCG coefficients for surface reflectance data (Crist 1985, Crist and Kauth 1986) to observations from all three Landsat sensors, assuming that observations are relatively well calibrated across

sensors with any differences characterized in the error term. We selected the monitoring period to generally characterize vegetation change during the Northern Hemisphere growing season including spongy moth defoliation, which typically peaks in June. The monitoring period, however, is a user-specified input in our workflow and can range from single-date predictions, which provide the most precise estimates of timing but may include gaps due to masking cloud and shadow artifacts, to longer monitoring periods that average over multiple observations to provide more robust estimates and improve spatial coverage. Our final assessment products combine results across Landsat orbital paths and include per-pixel mean and standard deviation of scores, mean and standard deviation of observed TCG, and number of observations. The use of multiple shorter baselines eliminates the need to specify a single longer baseline *a priori* and enables characterization of uncertainty in condition score across models.

We developed a Condition Monitoring Explorer application (app) to facilitate interactive exploration of annual results. The tool displays a series of annual vegetation condition assessment maps as well as time series of results for clicked points (fig. 9.1). Pre-cached results for more than 2 decades load quickly, and condition change patterns can be compared through time at a variety of spatial extents and using different disturbance severity thresholds. The app along with its code and workflow are publicly available (Pasquarella 2021) and can be updated, extended, and modified as needed. Users can also request access to baseline model and condition assessment assets, which are updated periodically to reflect changes in Landsat collections and other processing improvements.

The mapped results characterize expected patterns, such as severe defoliation by spongy moth across Rhode Island and eastern Connecticut in 2016 (fig. 9.1). Because the approach is currently based purely on spectral change, we also detect TCG anomalies associated with other types of change, such as human development (e.g., vegetation clearing for construction) and extreme weather events like the 2011 tornado in Springfield, MA. Given that the series of baseline models are fit to observations from years immediately preceding the target monitoring year, some baseline periods for sites experiencing multiyear disturbances will include years with decreased TCG. When vegetation does not recover, i.e., in the case of permanent clearing or development, we would expect baselines to adjust to the new normal, with vegetation condition scores returning to near-zero values. In cases where post-disturbance regrowth or other increases in vegetation cover and vigor are observed, we expect to see positive anomalies, i.e., above-baseline TCG values, indicating that TCG in the monitoring year is higher than the predicted values estimated from baselines including disturbed states.

Comparisons with Previous Implementations

The HCM workflow was initially developed to characterize defoliation events, and assessments generated using fixed-baseline versions have been

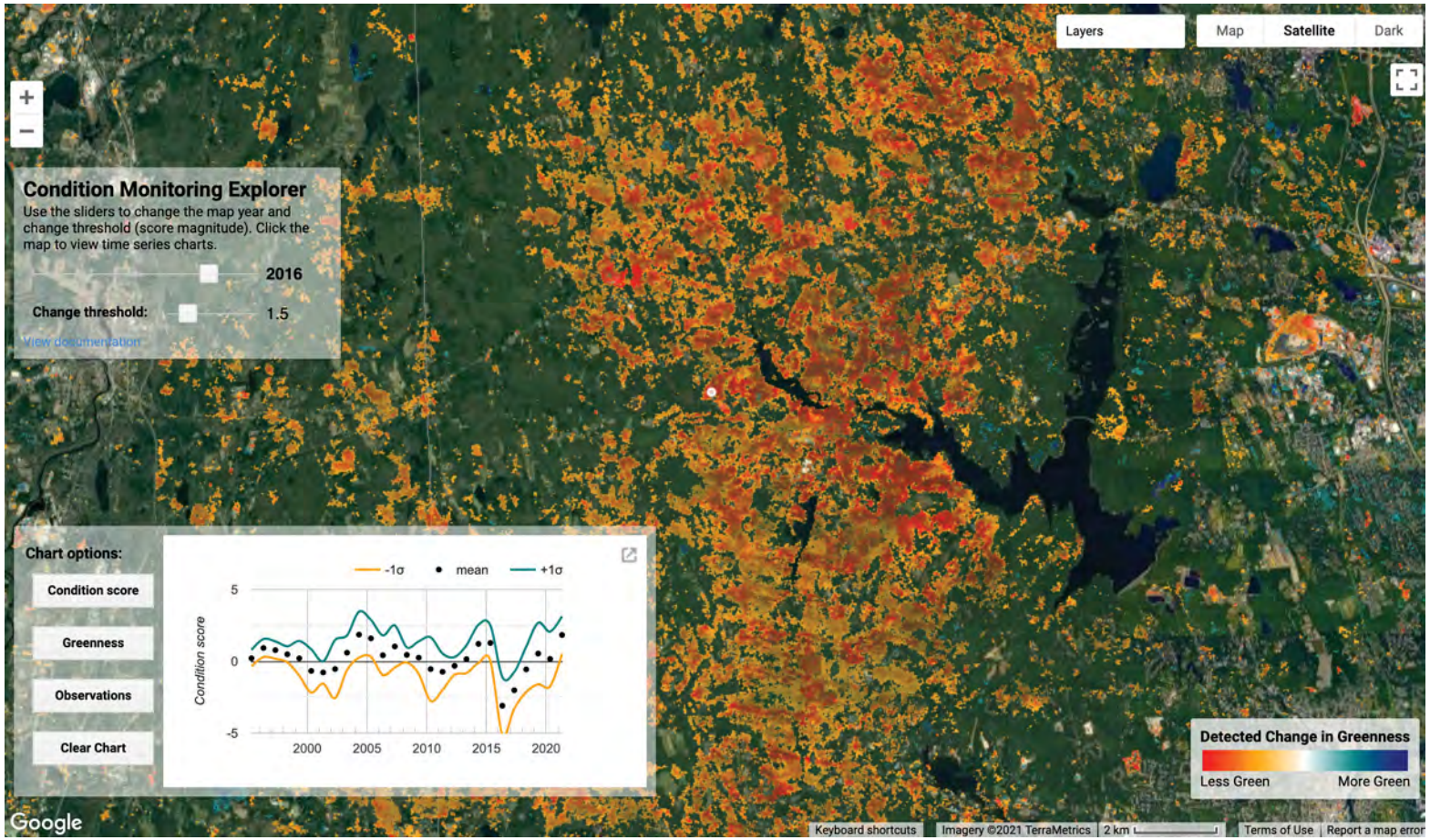

Figure 9.1—Severe defoliation by spongy moth across Rhode Island and eastern Connecticut in 2016 as seen in the Condition Monitoring Explorer app in Google Earth Engine (https://valeriepasquarella.users.earthengine.app/view/condition-monitoring-explorer). This tool allows users to visualize annual condition change estimates for 1995 to present. Adjusting the year slider changes the map year displayed, and the change threshold slider adjusts a mask on the magnitude of change ranging from 0 (all changes) to 4 (four or more times the estimated baseline root mean square error). Clicking a point on the mapped area displays time series of condition scores, Tasseled Cap Greenness, and number of observations for the corresponding 30-m Landsat pixel.

used in studies examining the distribution of the fungus *Entomophaga maimaiga* (Elkinton and others 2019), spongy moth outbreaks (Pasquarella and others 2021), runoff (Smith-Tripp and others 2021), nonstructural carbohydrates and mortality (Barker Plotkin and others 2021), and soil nitrogen dynamics (Conrad-Rooney and others 2020). To place our moving-window ensemble results in the context of previous implementations, we compared results generated using this new version of the workflow with three different assessments using the following fixed time period baselines: 2000–2010 and 2005–2015 from the baseline comparison study (Pasquarella and others 2021) and 2000–2010 from the 2018 southern New England reanalysis study (Pasquarella and others 2018). We extracted condition scores from each of these assessments for a set of 486 plots sampled from six 350-ha "hot spots" representing a range of forest types and defoliation severity in the Quabbin Reservoir Watershed in central Massachusetts. These plots generally experienced little if any defoliation during the 2016 spongy moth outbreak event with more significant impacts in 2017 and were surveyed in late summer/early fall of 2017 to characterize post-defoliation canopy recovery (see MacLean and others 2021 for details).

We used a series of scatterplots of results for the years 2016 and 2017 to compare scores generated using different baseline periods and workflows (fig. 9.2). We found that scores for the year 2016 generated using a fixed 2005–2015 baseline were most strongly correlated with those generated using our new approach that used baseline models fit to data from 5-year moving windows across 2005–2015 (R^2 = 0.91). The HCM-generated vegetation condition scores were less comparable across older baseline periods, with 2016 results calculated using 2000–2010 baselines showing weaker correlation with the 2016 HCM results calculated using moving-window models fit to the 10 years prior, with R^2 values ranging from 0.62 to 0.70.

As expected, 2017 scores for these sites were generally more negative, reflecting more widespread and significant defoliation. Again, vegetation condition scores generated using the 2005–2015 fixed baseline were most strongly correlated with the HCM approach (R^2 = 0.80), where models would be fit to observations from 2006–2016 to generate 2017 results, and less correlated with scores generated using older 2000–2010 baselines (R^2 = 0.30 and 0.29). In both years, results from the reanalysis products appear somewhat less correlated with HCM results than the Google Earth Engine implementation for the same baseline period. The results of these exploratory comparisons are in line with previous findings that selection of a baseline period has notable effects on condition score values (Pasquarella and others 2021).

Comparisons with Forest Inventory and Analysis Plot Data/Mortality

We also use our HCM results to investigate relationships between estimated defoliation and tree mortality and growth in FIA plots in Pennsylvania. Morin and Liebhold (2016) found increases in spongy moth host-tree mortality rates and decreases in growth rates in areas where

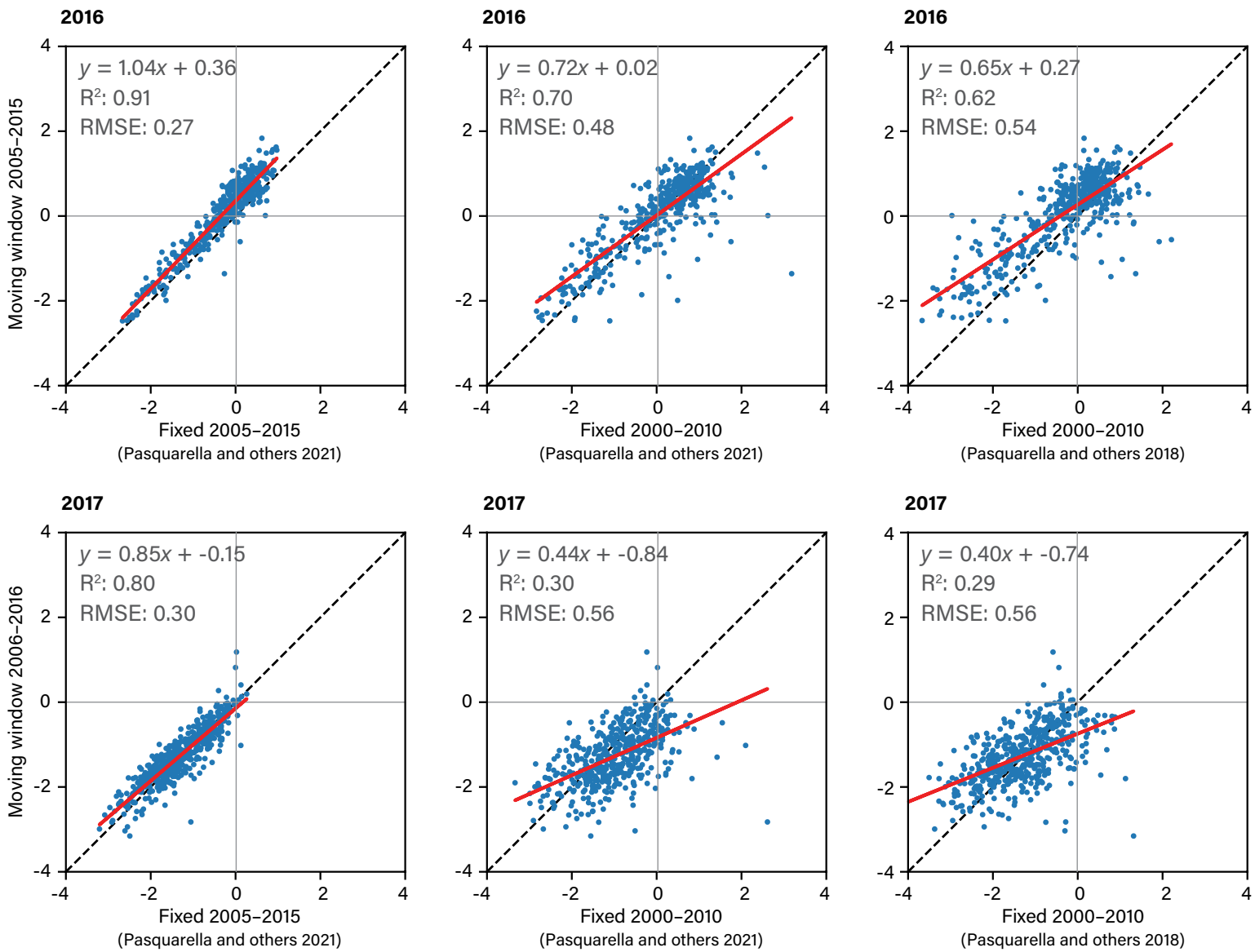

Figure 9.2—Comparison of results for 486 plots sampled from six clusters of plots (hot spots) across the Quabbin Reservoir Watershed in central Massachusetts for the years 2016 and 2017. Condition monitoring scores based on a new moving-window approach are compared with results from previous studies using fixed harmonic baselines, specifically 2005–2015 (left) and 2000–2010 (center) baselines from the baseline comparison study (Pasquarella and others 2021) and the southern New England reanalysis product (right) (Pasquarella and others 2018), which is analogous to the 2000–2010 results generated using Google Earth Engine. All baseline models are fit using Tasseled Cap Greenness using annual and 4-month harmonics and all available Landsat 5, 7, and 8 observations.

multiple years of repeated defoliation within the previous 10 years were observed through aerial sketch-mapping surveys. We conducted a similar analysis using vegetation condition scores from the newly developed procedure in place of sketch-map survey data.

Given FIA plot data must be processed locally, we exported series of annual condition score rasters for our Pennsylvania study area from Google Earth Engine. Although the condition monitoring tool displays assessments for a monitoring period of May through September (05-01 to 10-01), we also tested a more constrained period of June through August (06-01 to 09-01) to better correspond to the expected timing of peak spongy moth defoliation. To account for spatial coherence in defoliated patches and reduce any high-frequency noise, we applied a 3- x 3-pixel (90- x 90-m) smoothing kernel to our outputs.

Following Morin and Liebhold (2016), we used Pennsylvania FIA plots remeasured during 2007–2011 (n = 1,186). For each plot, the minimum vegetation condition score from the 5 years previous to an FIA remeasurement was extracted from the smoothed vegetation condition score rasters (i.e., for an FIA plot measured in 2007, the minimum vegetation condition score was determined based on assessment results from 2002–2006). We used this minimum condition score over the 5-year period prior to remeasurement as an indicator of the severity of peak defoliation, and we also computed the number of years where condition scores fell below a given threshold, i.e., -1.0 or -2.0, as a basic indicator of the frequency/persistence of vegetation condition changes.

We estimated plot-level mortality, growth, growth/volume ratio, and mortality/volume ratio for oak species in plots in the oak-hickory forest type group. We fit general linear models (GLMs) with oak mortality and oak growth as the dependent variables and HCM metrics as independent variables with the models weighted by live oak volume. Both mortality and growth models trended in the expected directions, with mortality increasing for more severe and more frequent disturbances while growth exhibits a decreasing trend (fig. 9.3). Although slope terms were found to be significant for all models (p <0.01), the relationships with HCM-generated vegetation condition scores were quite weak, with R^2 values around 0.01. When relating growth and mortality with frequency of disturbance, i.e., the number of years with scores below -1.0 versus below -2.0, the slopes tended to be greater for the "number of -2 years" metric (fig. 9.4). However, it is important to note that the sample size for plots that intersected pixels with strong decreases in HCM scores was too small to be able to robustly test for differences in mortality and growth across the range of HCM vegetation condition scores, i.e., only 7 plots had 2 or more years <-2 HCM in the 5-year window and 43 plots had 1 year <-2 HCM score.

Although we designed the spatial and temporal scope of this exploratory analysis to match that of Morin and Liebhold (2016), the results suggest a much weaker relationship between defoliation and mortality. This difference is likely due to differences between the aerial sketch-map

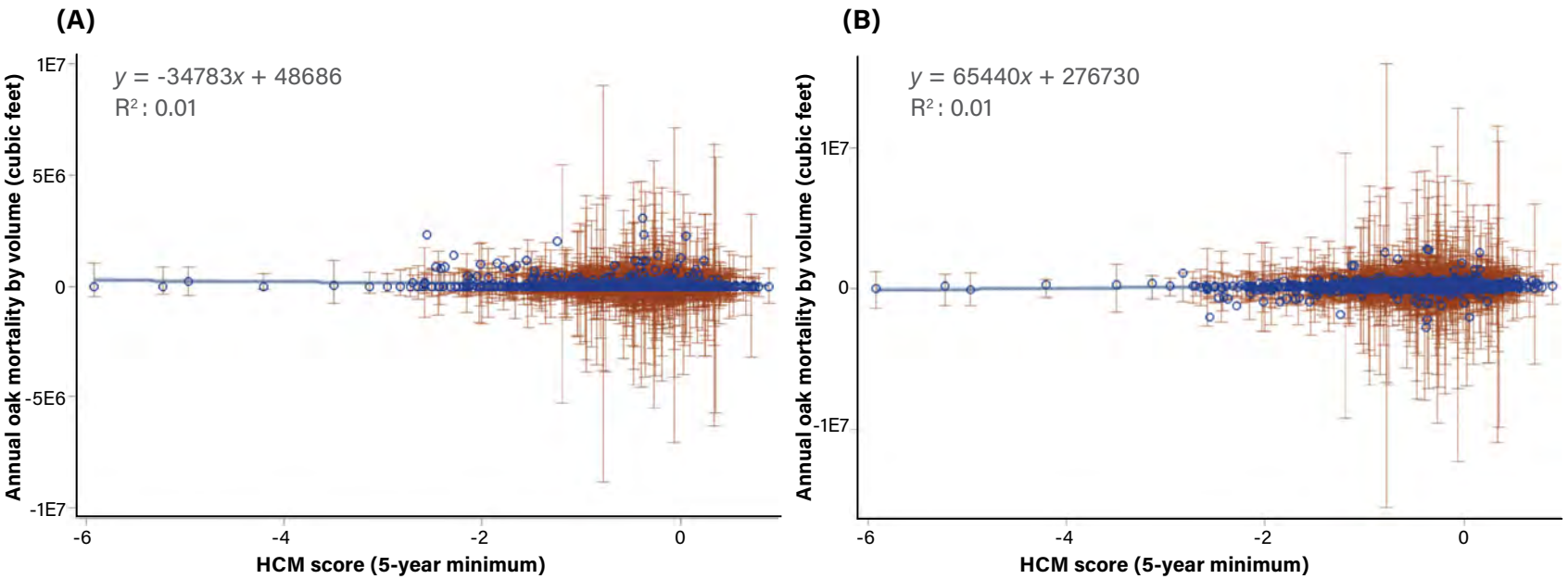

Figure 9.3—(A) Oak mortality and (B) growth by volume as a function of 5-year minimum harmonic condition monitoring (HCM) scores with error bars corresponding to 95-percent prediction limits (weighted). The model suggests mortality is higher and growth is lower for plots with more negative minimum condition scores during the 5-year remeasurement period. Both the slope and intercept terms are significant at $p < 0.01$*; however, the correlations are very weak.*

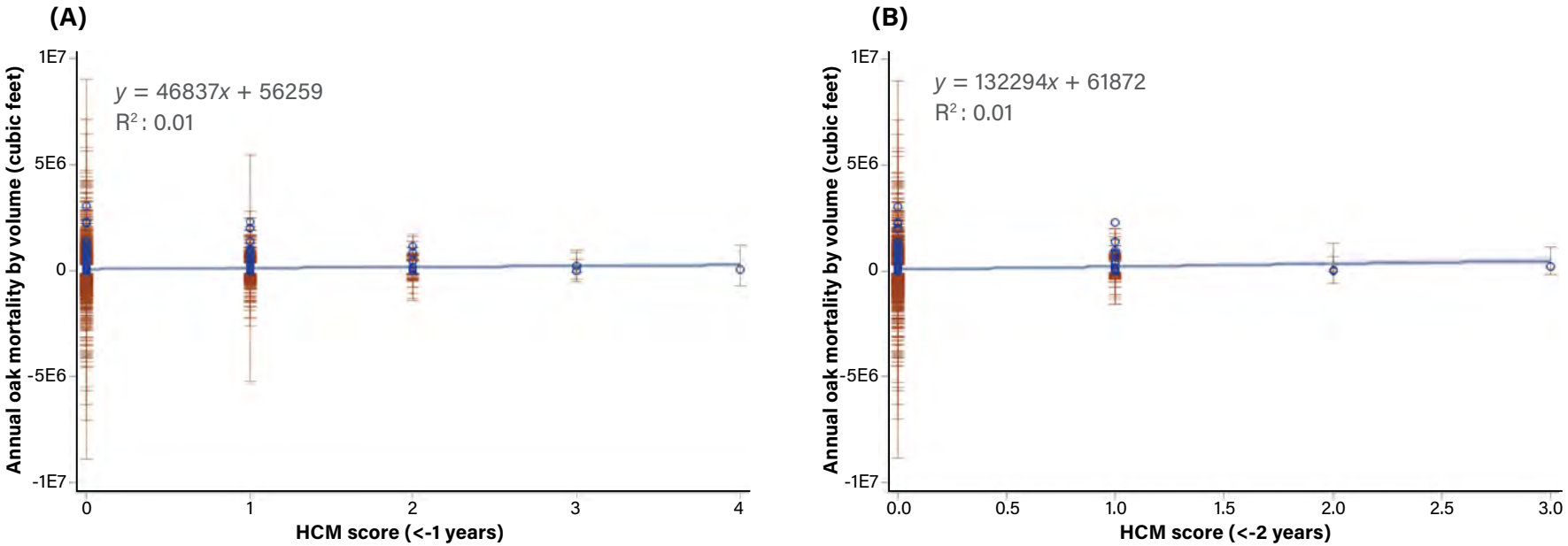

Figure 9.4—Oak mortality by volume as a function of the number of years the 5-year minimum harmonic condition monitoring (HCM) scores fell below -1.0, i.e., showed a Tasseled Cap Greenness (TCG) anomaly two or more times the estimated root mean square error of the (A) baseline models and (B) -2. Error bars correspond to 95-percent prediction limits (weighted). The model suggests increased mortality with increased frequency of anomalously negative HCM scores, and both the slope and intercept terms are significant at p *<0.01; however, the correlations are very weak, and there are relatively few sampled plots that show repeated, high-magnitude changes in TCG.*

polygons used for the original analysis and the HCM-based vegetation condition score rasters used here, which have a finer resolution and increased precision, and are more directly tied to objective measures of change in vegetation greenness. It is also possible that moving-window baselines produce more conservative assessments when multiyear decreases in canopy greenness are included in baseline modeling. Thus, differences observed in this preliminary reanalysis warrant further consideration.

SUMMARY AND CONCLUSIONS

In this project, we introduced an HCM approach that identifies anomalous canopy conditions by fitting a series of harmonic regression models to 5-year moving windows of remotely sensed observations from the Landsat series of satellites rather than relying on a single baseline model derived from a fixed set of years. We share our HCM code as well as an interactive tool for exploring results over a large multistate area (Pasquarella 2021). Our workflow and tool are expected to be a valuable resource for both historic and near-real-time assessments of changes in vegetation condition. Key findings:

- An ensemble of 5-year harmonic baseline models fit using a moving-window approach allows us to characterize the magnitude of spectral change as well as uncertainty in predictions given multiple predictions and dates of observation, and this improved characterization of uncertainty is one of the primary benefits of this approach. This HCM approach is also more flexible than previous fixed-baseline approaches because the baseline period adapts dynamically rather than being specified *a priori*.
- Our comparisons suggest that vegetation condition scores estimated with a moving-window HCM approach are consistent with previous fixed-baseline assessments given the same baseline and monitoring years, though they may diverge more given a greater difference between baseline and monitoring periods. We recommend the moving-window approach for general monitoring over large spatial extents where it would be difficult to prescribe an ideal baseline, although there may be cases where fixing the baseline period to a specific reference period may be preferable, particularly at more localized scales.
- The relationship between vegetation condition scores and mortality of oak in oak/hickory FIA plots in Pennsylvania was difficult to assess based on low numbers of samples that fell into "high disturbance" areas. However, the inconsistency between these results and previous investigations using aerial survey data warrants further consideration, and a larger sample size of impacted plots would be particularly helpful.

It is important to note that the current version of the HCM workflow characterizes spectral anomalies without specific attribution beyond the direction of the change (i.e., an observed area appears more or less green relative to prior years). Future work focusing on combining vegetation condition scores with other spectral inputs and ancillary datasets to differentiate among

different types of disturbance, i.e., defoliation, harvest, urban development, is important to consider. There are also opportunities to increase monitoring frequency by extending the Landsat-based approach presented here to other remote sensing instruments and datasets. For example, the Landsat 8 and Sentinel-2 sensors have complementary spectral and spatial resolutions and the combined constellation can provide at least 3- to 4-day revisit time (Li and Roy 2017), and the increased spatial resolution of Sentinel-2 (10- and 20-m bands) could improve detection of finer scale patterns of defoliation and mortality. Differences in estimates of defoliation location, magnitude, and frequency between aerial surveys and Landsat-based estimates are important to be considered for further investigation in terms of both timing and extent of detections.

For more information:
Valerie Pasquarella
vpasquarella@fas.harvard.edu

ACKNOWLEDGMENTS

We thank Audrey Barker Plotkin and Richard MacLean for providing the Quabbin Reservoir Watershed dataset used in this analysis. We also thank Christopher Brown for assistance implementing the moving-window approach for harmonic condition monitoring in Google Earth Engine. Funding for this project was provided by a grant (18-CA-11420004-293) from the USDA Forest Service, Forest Health Protection, Evaluation Monitoring Program. We would like to acknowledge additional support for this work from the Harvard Forest Long Term Ecological Research (LTER) program (NSF DEB #1832210).

LITERATURE CITED

Barker Plotkin, A.; Blumstein, M.; Laflower, D. [and others]. 2021. Defoliated trees die below a critical threshold of stored carbon. Functional Ecology. 35(10): 2156–2167. https://doi.org/10.1111/1365-2435.13891.

Chastain, R.A.; Fisk, H.; Ellenwood, J.R. [and others]. 2015. Near-real time delivery of MODIS-based information on forest disturbances. In: Lippitt, C.D.; Stow, D.A.; Coulter, L.L., eds. Time-sensitive remote sensing. New York: Springer: 147–164. https://doi.org/10.1007/978-1-4939-2602-2_10.

Cohen, W.B.; Healey, S.P.; Yang, Z. [and others]. 2017. How similar are forest disturbance maps derived from different Landsat time series algorithms? Forests. 8(4): 98. https://doi.org/10.3390/f8040098.

Cohen, W.B.; Yang, Z.; Stehman, S.V. [and others]. 2016. Forest disturbance across the conterminous United States from 1985–2012: the emerging dominance of forest decline. Forest Ecology and Management. 360: 242–252. https://doi.org/10.1016/j.foreco.2015.10.042.

Coleman, T.W.; Graves, A.D.; Heath, Z. [and others]. 2018. Accuracy of aerial detection surveys for mapping insect and disease disturbances in the United States. Forest Ecology and Management. 430: 321–336. https://doi.org/10.1016/j.foreco.2018.08.020.

Conrad-Rooney, E.; Barker Plotkin, A.; Pasquarella, V.J. [and others]. 2020. Defoliation severity is positively related to soil solution nitrogen availability and negatively related to soil nitrogen concentrations following a multi-year invasive insect irruption. AoB Plants. 12(6): laa059. https://doi.org/10.1093/aobpla/plaa059.

Crist, E.P. 1985. A TM tasseled cap equivalent transformation for reflectance factor data. Remote Sensing of Environment. 17(3): 301–306. https://doi.org/10.1016/0034-4257(85)90102-6.

Crist, E.R.; Kauth, R.J. 1986. The tasseled cap de-mystified. Photogrammetric Engineering and Remote Sensing. 52: 81–86.

Elkinton, J.S.; Bittner, T.D.; Pasquarella, V.J. [and others]. 2019. Relating aerial deposition of *Entomophaga maimaiga* conidia (Zoopagomycota: Entomophthorales) to mortality of gypsy moth (Lepidoptera: Erebidae) larvae and nearby defoliation. Environmental Entomology. 48(5): 1214–1222. https://doi.org/10.1093/ee/nvz091.

Hall, R.J.; Skakun, R.S.; Arsenault, E.J. 2007. Remotely sensed data in the mapping of insect defoliation. In: Wulder, M.A.; Franklin, S.E., eds. Understanding forest disturbance and spatial pattern; remote sensing and GIS approaches. Boca Raton, FL: CRC Taylor & Francis: 85–111. https://doi.org/10.1201/9781420005189.ch4.

Koltunov, A.; Ramirez, C.M.; Ustin, S.L. [and others]. 2020. eDaRT: the ecosystem Disturbance and Recovery Tracker system for monitoring landscape disturbances and their cumulative effects. Remote Sensing of Environment. 238: 111482. https://doi.org/10.1016/j.rse.2019.111482.

Li, J.; Roy, D.P. 2017. A global analysis of Sentinel-2A, Sentinel-2B and Landsat-8 data revisit intervals and implications for terrestrial monitoring. Remote Sensing. 9(9): 902. https://doi.org/10.3390/rs9090902.

Lister, A.J.; Andersen, H.; Frescino, T. [and others]. 2020. Use of remote sensing data to improve the efficiency of national forest inventories: a case study from the United States national forest inventory. Forests. 11(12): 1364. https://doi.org/10.3390/f11121364.

Lovett, G.M.; Canham, C.D.; Arthur, M.A. [and others]. 2006. Forest ecosystem responses to exotic pests and pathogens in eastern North America. BioScience. 56(5): 395–405. https://doi.org/10.1641/0006-3568(2006)056[0395:FERTEP]2.0.CO;2.

MacLean, R.; Pasquarella, V.; Barker Plotkin, A. 2021. Gypsy moth defoliation survey at the Quabbin Watershed in central Massachusetts 2017. Harvard Forest Data Archive: HF352 (v.3). Environmental Data Initiative. https://doi.org/10.6073/pasta/db7489f4d0e8b00b7c9066aaab554982.

Morin, R.S.; Liebhold, A.M. 2016. Invasive forest defoliator contributes to the impending downward trend of oak dominance in eastern North America. Forestry. 89(3): 284–289. https://doi.org/10.1093/forestry/cpv053.

Norman, S.P.; Christie, W.M. 2020. Satellite-based evidence of forest stress and decline across the conterminous United States for 2016, 2017, and 2018. In: Potter, K.M.; Conkling, B.L., eds. Forest Health Monitoring: national status, trends, and analysis 2019. Gen. Tech. Rep. SRS-250. Asheville, NC: U.S. Department of Agriculture, Forest Service, Southern Research Station: 151–166.

Norman, S.P.; Hargrove, W.W.; Spruce, J.P. [and others]. 2013. Highlights of satellite-based forest change recognition and tracking using the ForWarn system. Gen. Tech. Rep. SRS-180. Asheville, NC: U.S. Department of Agriculture, Forest Service, Southern Research Station. 30 p. https://doi.org/10.2737/SRS-GTR-180.

Pasquarella, V. 2021. Valpasq/condition_monitoring: v0.2-alpha (v0.2-alpha). Zenodo. https://doi.org/10.5281/zenodo.4565535.

Pasquarella, V.J.; Bradley, B.A.; Woodcock, C.E. 2017. Near-real-time monitoring of insect defoliation using Landsat time series. Forests. 8(8): 275. https://doi.org/10.3390/f8080275.

Pasquarella, V.J.; Elkinton, J.S.; Bradley, B.A. 2018. Extensive gypsy moth defoliation in southern New England characterized using Landsat satellite observations. Biological Invasions. 20(11): 3047–3053. https://doi.org/10.1007/s10530-018-1778-0.

Pasquarella, V.J.; Holden, C.E.; Kaufman, L.; Woodcock, C.E. 2016. From imagery to ecology: leveraging time series of all available Landsat observations to map and monitor ecosystem state and dynamics. Remote Sensing in Ecology and Conservation. 2(3): 152–170. https://doi.org/10.1002/rse2.24.

Pasquarella, V.J.; Mickley, J.G.; Barker Plotkin, A. [and others]. 2021. Predicting defoliator abundance and defoliation measurements using Landsat-based condition scores. Remote Sensing in Ecology and Conservation. 7(4): 592–609. https://doi.org/10.1002/rse2.211.

Rullan-Silva, C.D.; Olthoff, A.E.; de la Mata, J.A.D.; Pajares-Alonso, J.A. 2013. Remote monitoring of forest insect defoliation. A review. Forest Systems. 22(3): 377–391. https://doi.org/10.5424/fs/2013223-04417.

Schroeder, T.A.; Healey, S.P.; Moisen, G.G. [and others]. 2014. Improving estimates of forest disturbance by combining observations from Landsat time series with U.S. Forest Service Forest Inventory and Analysis data. Remote Sensing of Environment. 154: 61–73. https://doi.org/10.1016/j.rse.2014.08.005.

Sellers, P.J.; Tucker, C.J.; James Collatz, G. [and others]. 1996. A revised land surface parameterization (SiB2) for atmospheric GCMS. Part II: the generation of global fields of terrestrial biophysical parameters from satellite data. Journal of Climate. 9(4): 706–737. https://doi.org/10.1175/1520-0442(1996)009<0706:ARLSPF>2.0.CO;2.

Senf, C.; Seidel, R.; Hostert, P. 2017. Remote sensing of forest insect disturbances: current state and future directions. International Journal of Applied Earth Observation and Geoinformation. 60: 49–60. https://doi.org/10.1016/j.jag.2017.04.004.

Smith-Tripp, S.; Griffith, A.; Pasquarella, V.J.; Matthes, J.H. 2021. Impacts of a regional multiyear insect defoliation event on growing-season runoff ratios and instantaneous streamflow characteristics. Ecohydrology. 14(7): e2332. https://doi.org/10.1002/eco.2332.

Vogt, J.T.; Koch, F.H. 2016. The evolving role of Forest Inventory and Analysis data in invasive insect research. American Entomologist. 62(1): 46–58. https://doi.org/10.1093/ae/tmv072.

Wilson, B.T. 2015. Harmonic analysis of dense time series of Landsat imagery for modeling change in forest conditions. In: Stanton, S.M.; Christensen, G.A., comps. Pushing boundaries: new directions in inventory techniques and applications: Forest Inventory and Analysis (FIA) symposium 2015. 2015 December 8–10, Portland, OR. Gen. Tech. Rep. PNW-931. Portland, OR: U.S. Department of Agriculture, Forest Service, Pacific Northwest Research Station: 200–205.

Wilson, B.T.; Knight, J.F.; McRoberts, R.E. 2018. Harmonic regression of Landsat time series for modeling attributes from national forest inventory data. ISPRS Journal of Photogrammetry and Remote Sensing. 137: 29–46. https://doi.org/10.1016/j.isprsjprs.2018.01.006.

Wilson, B.T.; Lister, A.J.; Riemann, R.I. 2012. A nearest-neighbor imputation approach to mapping tree species over large areas using forest inventory plots and moderate resolution raster data. Forest Ecology and Management. 271: 182–198. https://doi.org/10.1016/j.foreco.2012.02.002.

Zhu, Z.; Woodcock, C.E.; Olofsson, P. 2012. Continuous monitoring of forest disturbance using all available Landsat imagery. Remote Sensing of Environment. 122: 75–91. https://doi.org/10.1016/j.rse.2011.10.030.

CHAPTER 10

Laurel Wilt Spread, Vector Flight Behavior, and Impacts in Sassafras Beyond the Gulf-Atlantic Coastal Plain

Albert E. Mayfield III,
Rabiu O. Olatinwo,
Jaesoon Hwang,
Bryan T. Mudder,
Alexandra Blevins, and
Stephen W. Fraedrich

How to cite this chapter:

Mayfield, Albert E. III; Olatinwo, Rabiu O.; Hwang, Jaesoon; Mudder, Bryan T.; Blevins, Alexandra; Fraedrich, Stephen W. 2023. Laurel wilt spread, vector flight behavior, and impacts in sassafras beyond the Gulf-Atlantic Coastal Plain. In: Potter, Kevin M.; Conkling, Barbara L., eds. Forest Health Monitoring: national status, trends, and analysis 2022. Gen. Tech. Rep. SRS-273. Asheville, NC: U.S. Department of Agriculture, Forest Service, Southern Research Station: 163–169. https://doi.org/10.2737/SRS-GTR-273-Chap10.

INTRODUCTION

Laurel wilt is a destructive vascular disease of woody plants in the family Lauraceae. The cause of laurel wilt, the fungus *Harringtonia lauricola*, is an ambrosial symbiont of the redbay ambrosia beetle (RAB) (*Xyleborus glabratus*) (de Beer and others 2022, Fraedrich and others 2008). The beetle and the pathogen are native to Asia (Hughes and others 2017, Wuest and others 2017) and were introduced to North America prior to 2002 when RAB was first detected in Georgia (Rabaglia and others 2006). Healthy plants become diseased when RAB bores into host stems and inoculates the xylem with *H. lauricola*. Laurel wilt has killed hundreds of millions of redbay (*Persea borbonia*) and swamp bay (*P. palustris*) and represents a serious threat to the plant family Lauraceae in North America and other parts of the world (Hughes and others 2017, Olatinwo and others 2021).

Sassafras (*Sassafras albidum*) is the most widely distributed member of the Lauraceae in the United States (Griggs 1990) and is susceptible to laurel wilt (Cameron and others 2008, Fraedrich and others 2008). It is intolerant of shade and commonly colonizes old fields, fencerows, burned areas, and other disturbed sites. Stems commonly occur in clusters due to vegetative reproduction via root sprouts (Griggs 1990). Like other members of the Lauraceae, sassafras is rich in essential oils and has numerous medicinal, culinary, cultural, and wildlife uses (Dills 1970, Immel 2016).

In 2018, the known distribution of laurel wilt remained primarily within the Gulf-Atlantic Coastal Plain. It was uncertain how quickly and with what impact laurel wilt would spread into the Piedmont and Mountains of the Eastern United States using sassafras as a host. To examine the spread and impact of laurel wilt in sassafras, we initiated an Evaluation Monitoring project in 2018 to establish sentinel sassafras plots, both within and ahead of the known laurel wilt distribution (Mayfield and others 2022). A comprehensive report on this project has been published previously (Mayfield and others 2022); the present document presents a shorter summary of the methods, results, and implications.

METHODS

Site Selection

We selected monitoring sites containing live sassafras trees ≥5 cm diameter at breast height (d.b.h.) in three regions of the Southeastern United States: (1) Gulf-Atlantic Coastal Plain, (2) Piedmont (including adjacent Sandhills), and (3) Central and Eastern Mountains (including the Southern Appalachian Mountains, Cumberland Plateau, and Highland Rim/Central Basin) (fig. 10.1). In the Coastal Plain, we targeted sites that were not known to be affected by laurel wilt (or only very recently affected), whereas in the Piedmont and Mountain regions, we targeted sites near RAB risk of entry points (mills, campgrounds, RV parks, etc.). We monitored a total of 46 sites, although not every site was monitored in every year due to personnel changes, COVID 19-related travel restrictions, or stand elimination.

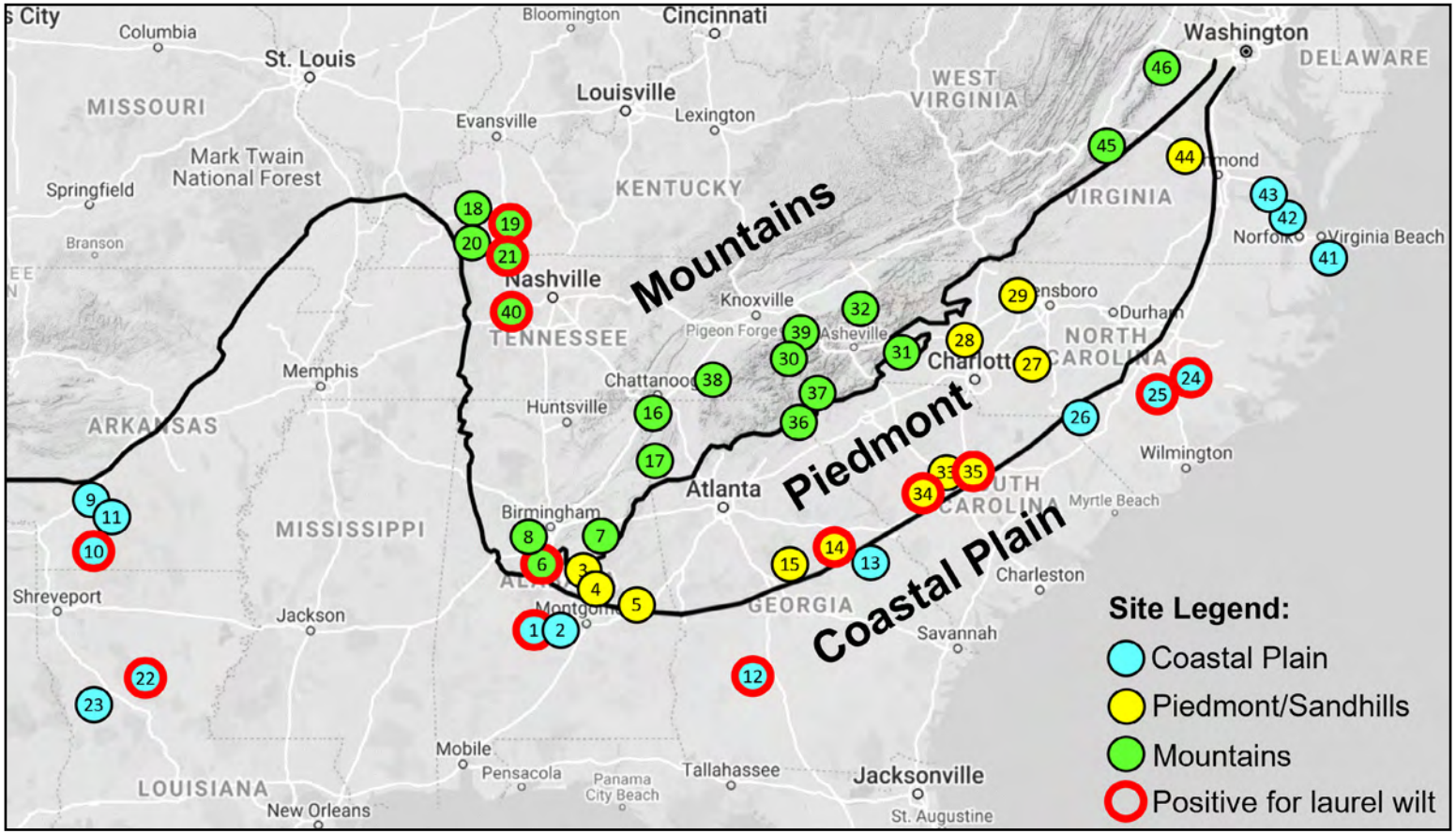

Figure 10.1—Locations of 46 laurel wilt monitoring plots with sassafras in the Southeastern United States, color coded by physiographic region. Red outline indicates laurel wilt pathogen detection in 2018–2020. (Map data © 2022 Google, INEGI [from Mayfield and others 2022])

Vegetation Monitoring and Laurel Wilt Assessment

We tagged a target of 20 live sassafras trees ≥5 cm d.b.h. per site (average n = 19, range 6–32) for annual monitoring of crown health and survival during the leaf-on season. We determined sassafras crown health by visually estimating the percentages of the entire tree crown represented by healthy, wilted/discolored, and missing foliage. Trees with no healthy foliage were considered dead. We sampled xylem from suspected diseased trees with a chisel, and then bagged and shipped the samples overnight to a U.S. Department of Agriculture, Forest Service, Southern Research Station plant pathology lab in Athens, GA, or Pineville, LA, for confirmation of *H. lauricola* (Dreaden and others 2014, Fraedrich and others 2008, Harrington and others 2008).

Redbay Ambrosia Beetle Monitoring

We monitored RAB flight activity at a subset of sites with suspected laurel wilt activity or that were of particular interest. At each trapping site, we baited two traps with a 50-percent α-copaene lure (product #3302, Synergy Semiochemical Corp., Burnaby, BC, Canada). One trap in each pair was a black 8-unit Lindgren funnel trap and the other was a black triple-vane multipanel trap (products #4072 and #4057, respectively, Synergy Semiochemical Corp.). Traps were deployed and checked biweekly for a total of 8 weeks between early June and October. We conducted trapping for an extended duration (3 to 24 months, depending on site) at select sites in each region where laurel wilt was suspected or confirmed.

Data Analysis

We used analysis of variance to evaluate all factorial combinations of Region, Pathogen, and Year as fixed effects and Site(Region*Pathogen) as a random effect, on percentage of sassafras mortality (square-root transformed). We evaluated the effect of trap type (funnel versus panel) on mean RAB per week using a Wilcoxon signed-rank test and by limiting the dataset to the "site x date" combinations on which at least one RAB was collected in a trap. We analyzed RAB flight activity graphically over time, and identified and counted all species of ambrosia beetles at two sites in Kentucky. See Mayfield and others (2022) for full methods and analysis.

RESULTS

Vegetation Monitoring and Laurel Wilt Assessment

Laurel wilt was detected at 28 percent of the monitoring sites during the 3-year project period (2018–2020), including six sites in the Coastal Plain, three in the Piedmont, and four in the Mountains (fig. 10.1). Four of these detections were previously unreported county records for laurel wilt (Chilton County, AL; Bibb County, AL; Columbia County, AR; Worth County, GA), generating new range information for the national Laurel Wilt Distribution Map (https://www.fs.usda.gov/Internet/FSE_DOCUMENTS/fseprd669956.pdf). In 2018, mean percentage of mortality of tagged sassafras trees at all disease-free sites did not differ significantly from the mean mortality at sites where laurel wilt would ultimately become detected between 2018 and 2020 (fig. 10.2). In

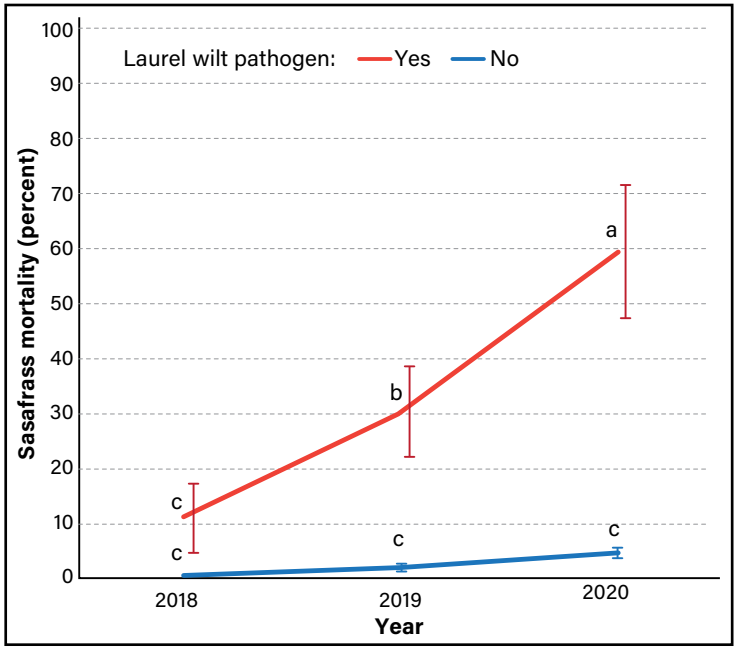

Figure 10.2—Mean percentage of mortality of tagged sassafras monitoring trees from 2018 through 2020 at sites where the laurel wilt pathogen was confirmed versus sites where it was not detected. Vertical bars denote standard error of the mean. Means labeled with the same letter are not significantly different (α = 0.05). (From Mayfield and others 2022)

2019 and 2020, however, mean sassafras mortality at diseased sites increased to 30 percent and 60 percent, respectively, whereas mortality in disease-free stands remained below 5 percent (fig. 10.2). Elevated sassafras mortality in diseased stands was evident in all diameter classes monitored. Sassafras mortality was notably rapid in a number of stands, progressing to 100 percent within 3 years at four sites (Mayfield and others 2022).

Redbay Ambrosia Beetle Monitoring

Redbay ambrosia beetles were captured in traps at a total of 11 sites including 5 sites in the Coastal Plain, 2 in the Piedmont, and 4 in the Mountains. Detection of the laurel wilt pathogen through sampling of host material usually preceded RAB detection or occurred in the same year. There was no significant difference between the mean number of RABs per week captured in panel traps versus paired funnel traps in any year, although statistical significance was marginal in 2019 when slightly more RABs were captured in panel traps. In the Coastal Plain of Louisiana, RAB captures occurred throughout the calendar year (including January) with modest peaks in late August and early December. At two Piedmont/Sandhill sites in South Carolina, RAB flight began as early as February, with two periods of peak capture in April and August through November. A similar pattern occurred in the Mountain region of Alabama where captures began in February with peaks in April and late summer (Mayfield and others 2022).

In western Kentucky, RAB flight activity began in April, peaked in June (with a lesser peak in

August), and persisted at low levels until November. A nearly tenfold decrease in peak RAB captures corresponded with an elimination of fresh sassafras host material from one summer to the next. Trap captures of the two most abundant ambrosia beetle species, the granulate ambrosia beetle (*Xylosandrus crassiusculus*) and the fruit-tree pinhole borer (*Xyleborinus saxesenii*), exhibited strong peak captures in early April or May at much higher abundances than RAB. Redbay ambrosia beetles were present in <9 percent of all the ambrosia beetle specimens captured, and >98 percent of all ambrosia beetle specimens comprised eight species, all of which were nonnative to North America (Mayfield and others 2022).

DISCUSSION

This project demonstrated the movement of laurel wilt beyond the Coastal Plain and into portions of the Piedmont/Sandhills and Mountain regions in Alabama, Georgia, South Carolina, Tennessee, and Kentucky. Four previously unreported county-level infestations were added to the national Laurel Wilt Distribution Map, demonstrating that supplemental Evaluation Monitoring projects can enhance State forestry agencies' baseline laurel wilt monitoring efforts. The impact of laurel wilt in sassafras in Piedmont and Mountain sites was substantial and rapid, with mortality progressions similar to those observed in redbay and sassafras in the Coastal Plain (Cameron and others 2015, Fraedrich and others 2008). Although we did not target sassafras stems <5 cm d.b.h. for monitoring, we documented mortality of stems of this size when they were occasionally tagged or observed informally. The likelihood of attack by RAB increases with stem diameter due to more apparent visual cues (Mayfield and Brownie 2013), which may allow small-diameter stems to escape inoculation by the insect. The clonal growth habit of sassafras, however, provides opportunity for even small sprouts to become infected with laurel wilt via root transmission, leading to the potential for accelerated sassafras mortality even when RAB populations are low.

Our results strongly suggest that deploying α-copaene-baited flight traps in the vicinity of sassafras trees, while useful for monitoring known RAB populations, may not substantially improve early-detection efforts for laurel wilt (compared to visually monitoring for symptoms). Detection and confirmation of the pathogen from symptomatic host material either preceded or coincided with the first trap catch of RAB at 92 percent of our laurel wilt-positive sites. Still, placing α-copaene-baited traps in stands with sassafras could help State surveyors evaluate the potential presence of RAB in certain situations, particularly if laurel wilt has been present and undetected for several years.

Similar to data from Florida reported by Brar and others (2012), we observed two peaks of RAB flight activity in this study in the Piedmont/Sandhills of South Carolina and the southern limit of the Mountain region in Alabama, suggesting two RAB generations annually, which peak in early spring, and then late summer/fall, respectively. However, farther north in Kentucky, RAB captures peaked slightly later (June), seasonal RAB flight activity was only weakly bimodal, and no flight activity was observed from December through March. These differences in RAB flight seasonality may be due to the

colder climate of interior Kentucky compared to warmer sites in the Piedmont and Coastal Plain. Furthermore, the notable reduction in beetle abundance in traps between 2020 and 2021 in Kentucky was likely due to the elimination of fresh sassafras host material for brood production.

Although traps in this study were baited with a primary host volatile attractant of the RAB (α-copaene) and thus were intended to mimic lauraceous trees, <9 percent of the all the ambrosia beetle specimens captured in Kentucky comprised RAB. This suggests that numerous other generalist ambrosia beetle species, many of which are nonnative to North America, may be attracted to α-copaene or are at least passively captured in traps deployed in diseased sassafras stands. Thus, the degree to which other ambrosia beetle species compete with the RAB for potential host material, or have a role as potential vectors, is worthy of additional investigation.

CONCLUSIONS

Laurel wilt has spread from the Coastal Plain of the Southeastern United States into the Piedmont and Mountain regions using sassafras as a primary host. Impact to sassafras populations is substantial and rapid, with the disease killing up to 100 percent of the sassafras stems ≥5 cm d.b.h. and the pathogen spreading via root transmission. There was no substantial difference in RAB trapping efficacy between the 8-unit Lindgren funnel trap and the triple-vane multipanel trap. Trapping with α-copaene lures in stands with sassafras was useful for monitoring known RAB populations but did not enhance early detection of latent laurel wilt infections. Seasonal flight activity of the RAB was bimodal in stands with sassafras in the Piedmont, with peak captures in April and a secondary peak between August and November. In western Kentucky, RAB flight was not observed from December through March, peaked in June, and declined markedly as fresh sassafras host material was eliminated from the stand. The georeferenced network of sassafras plots established during this project provides baseline data for future monitoring efforts and could be revisited in the future for possible evidence of trees that display resistance to, or tolerance of, laurel wilt.

For more information:
Albert E. Mayfield III
albert.e.mayfield@usda.gov

LITERATURE CITED

Brar, G.S.; Capinera, J.L.; McLean, S. [and others]. 2012. Effect of trap size, trap height and age of lure on sampling *Xyleborus glabratus* (Coleoptera: Curculionidae: Scolytinae), and its flight periodicity and seasonality. Florida Entomologist. 95: 1003–1011. https://doi.org/10.1653/024.095.0428.

Cameron, R.S.; Bates, C.; Johnson, J. 2008. Distribution and spread of laurel wilt disease in Georgia: 2006–08 survey and field observations. Georgia Forestry Commission Report. 28 p.

Cameron, R.S.; Hanula, J.; Fraedrich, S.; Bates, C. 2015. Progression and impact of laurel wilt disease within redbay and sassafras populations in southeast Georgia. Southeastern Naturalist. 14: 650–674. https://doi.org/10.1656/058.014.0408.

de Beer, Z.W.; Procter, M.; Wingfield, M.J. [and others]. 2022. Generic boundaries in the Ophiostomatales reconsidered and revised. Studies in Mycology. 101: 57–120. https://doi.org/10.3114/sim.2022.101.02.

Dills, G.G. 1970. Effects of prescribed burning on deer browse. Journal of Wildlife Management. 34: 540–545. https://doi.org/10.2307/3798860.

Dreaden, T.J.; Davis, J.M.; Harmon, C.L. [and others]. 2014. Development of multilocus PCR assays for *Raffaelea lauricola*, causal agent of laurel wilt disease. Plant Disease. 98: 379–383. https://doi.org/10.1094/PDIS-07-13-0772-RE.

Fraedrich S.W.; Harrington, T.C.; Rabaglia, R.J. [and others]. 2008. A fungal symbiont of the redbay ambrosia beetle causes a lethal wilt in redbay and other Lauraceae in the Southeastern United States. Plant Disease. 92: 215–224. https://doi.org/10.1094/PDIS-92-2-0215.

Griggs, M.M. 1990. *Sassafras albidum* (Nutt.) Nees. Sassafras. In: Burns, R.M.; Honkala, B.H., eds. Silvics of North America. Agric. Handb. 654. Washington, DC: U.S. Department of Agriculture: 773–777.

Harrington, T.C.; Fraedrich, S.W.; Aghayeva. D.N. 2008. *Raffaelea lauricola*, a new ambrosia beetle symbiont and pathogen on the Lauraceae. Mycotaxon. 104: 399–404.

Hughes, M.A.; Riggins, J.J.; Koch, F.H. [and others]. 2017. No rest for the laurels: symbiotic invaders cause unprecedented damage to Southern USA forests. Biological Invasions. 19: 2143–2157. https://doi.org/10.1007/s10530-017-1427-z.

Immel, D.L. 2016. Sassafras, *Sassafras albidum* (Nutt.) Nees. Plant guide. [Place of publication unknown]: U.S. Department of Agriculture, Natural Resources Conservation Service. https://plants.usda.gov/DocumentLibrary/plantguide/pdf/cs_saal5.pdf. [Date accessed: June 5, 2022].

Mayfield, A.E., III; Brownie, C. 2013. The redbay ambrosia beetle (Coleoptera: Curculionidae: Scolytinae) uses stem silhouette diameter as a visual host-finding cue. Environmental Entomology. 42: 743–750. https://doi.org/10.1603/EN12341.

Mayfield, A.E., III; Olatinwo, R.O.; Hwang, J. [and others]. 2022. Spread, vector flight behavior, and impact of laurel wilt in sassafras beyond the Gulf-Atlantic Coastal Plain. Journal of Forestry. 120(6): 633–645. https://doi.org/10.1093/jofore/fvac014.

Olatinwo, R.O.; Fraedrich, S.W.; Mayfield, A.E., III. 2021. Laurel wilt: current and potential impacts and possibilities for prevention and management. Forests. 12: 181. https://doi.org/10.3390/f12020181.

Rabaglia, R.J.; Dole, S.A.; Cognato, A.I. 2006. Review of American Xyleborina (Coleoptera: Curculionidae: Scolytinae) occurring north of Mexico, with an illustrated key. Annals of the Entomological Society of America. 99: 1034–1056. https://doi.org/10.1603/0013-8746(2006)99[1034:ROAXCC]2.0.CO;2.

Wuest, C.E.; Harrington, T.C.; Fraedrich, S.W. [and others]. 2017. Genetic variation in native populations of the laurel wilt pathogen, *Raffaelea lauricola*, in Taiwan and Japan and the introduced population in the United States. Plant Disease. 101: 619–628. https://doi.org/10.1094/PDIS-10-16-1517-RE.

CHAPTER 11

Effects of Spruce Beetle (*Dendroctonus rufipennis*) Outbreaks on Rocky Mountain Spruce-Fir Stand Characteristics

Camille Stevens-Rumann,
Donna Shorrock,
Chad Hoffman,
Zoe Schapira, and
Amy Chambers

How to cite this chapter:

Stevens-Rumann, Camille; Shorrock, Donna; Hoffman, Chad; Schapira, Zoe; Chambers, Amy. 2023. Effects of spruce beetle (*Dendroctonus rufipennis*) outbreaks on Rocky Mountain spruce-fir stand characteristics. In: Potter, Kevin M.; Conkling, Barbara L., eds. Forest Health Monitoring: national status, trends, and analysis 2022. Gen. Tech. Rep. SRS-273. Asheville, NC: U.S. Department of Agriculture, Forest Service, Southern Research Station: 171–176. https://doi.org/10.2737/SRS-GTR-273-Chap11.

INTRODUCTION

The recent impacts of climate change have threatened the health and functioning of forested ecosystems on a global scale. Due to the shifting global climate, the frequency and severity of disturbances are increasing, inevitably causing an increase in disturbances overlapping in time and space (Abatzoglou and Williams 2016, Hart and others 2014, Schoennagel and others 2017). Widespread tree mortality from altered disturbance regimes creates significant uncertainty about stand dynamics and recovery in many systems. Bark beetle epidemics and wildfires have historically shaped the disturbance regimes of western North American forests. The interactive effects of multiple disturbances are often inadequately studied, especially in high-elevation, often difficult to access forests, such as those dominated by Engelmann spruce (*Picea engelmannii*) and subalpine fir (*Abies lasiocarpa*); understanding these interactions is imperative to the management and health of forested ecosystems. This study focuses on the effects of epidemic spruce beetle (*Dendroctonus rufipennis*) outbreaks, high-severity fires, and the subsequent species and structural diversity of subalpine forest regeneration and structure in northern Colorado and southern Wyoming.

This project collected data across 80 sites (fig. 11.1) to address three main objectives: (1) quantify fuels structure and regeneration across a chronosequence of spruce beetle outbreaks in addition to areas impacted by outbreaks and wildfires, (2) age seedlings to understand tree regeneration and recruitment in relation to the disturbances and long-term climate, and (3) quantify fuels after spruce beetle disturbance for better assessment of fuel complexity in the event of wildfires.

METHODS AND RESULTS

To address objective 1, we collected fuels, stand structure, and tree regeneration data and modeled our plot design after Ott and others (2018), establishing 0.08-ha circular fixed area plots. Full methods can be found in Schapira and others (2021a). Analyses indicated a significant increase in fuel loading over time since outbreak, as aerial fuels were transferred to the forest floor following high tree mortality (fig. 11.2A). Tree seedling densities among outbreak and control sites differed significantly from burned areas, indicating that wildfires overrode the effects of spruce beetle disturbances on regeneration (fig. 11.2B). There was consistent Engelmann spruce seedling survival following beetle outbreaks, providing evidence for stable forest recovery following a single disturbance. We did not observe any life cycle changes in beetle phenology though we focused primarily on forest structural characteristics. However, fire was a dominant force in determining post-disturbance species composition, indicating continued prevalence of high-severity fire may prove detrimental for the persistence of spruce-fir species, while promoting shifts toward more drought- and fire-tolerant tree species (e.g., lodgepole pine [*Pinus contorta*]).

To address objective 2, we destructively sampled and aged 229 Engelmann spruce and subalpine fir seedlings on 30 of these original 80 sites. Here, we aged seedlings to understand age structure of understory trees within spruce beetle- and

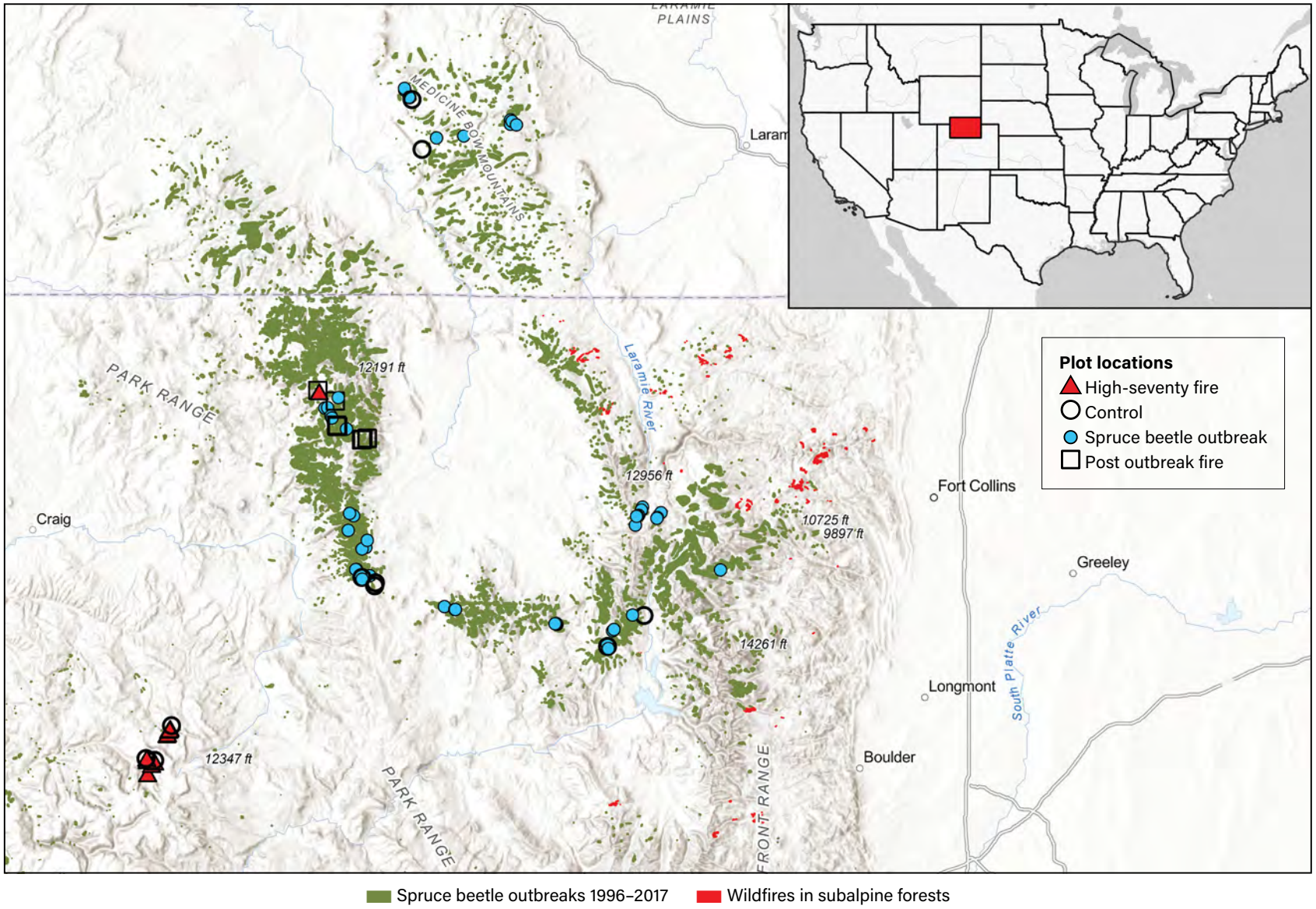

Figure 11.1—Study sites located in southern Wyoming and northern Colorado, across a chronosequence of spruce beetle outbreaks and area impacted by spruce beetle outbreaks and wildfires.

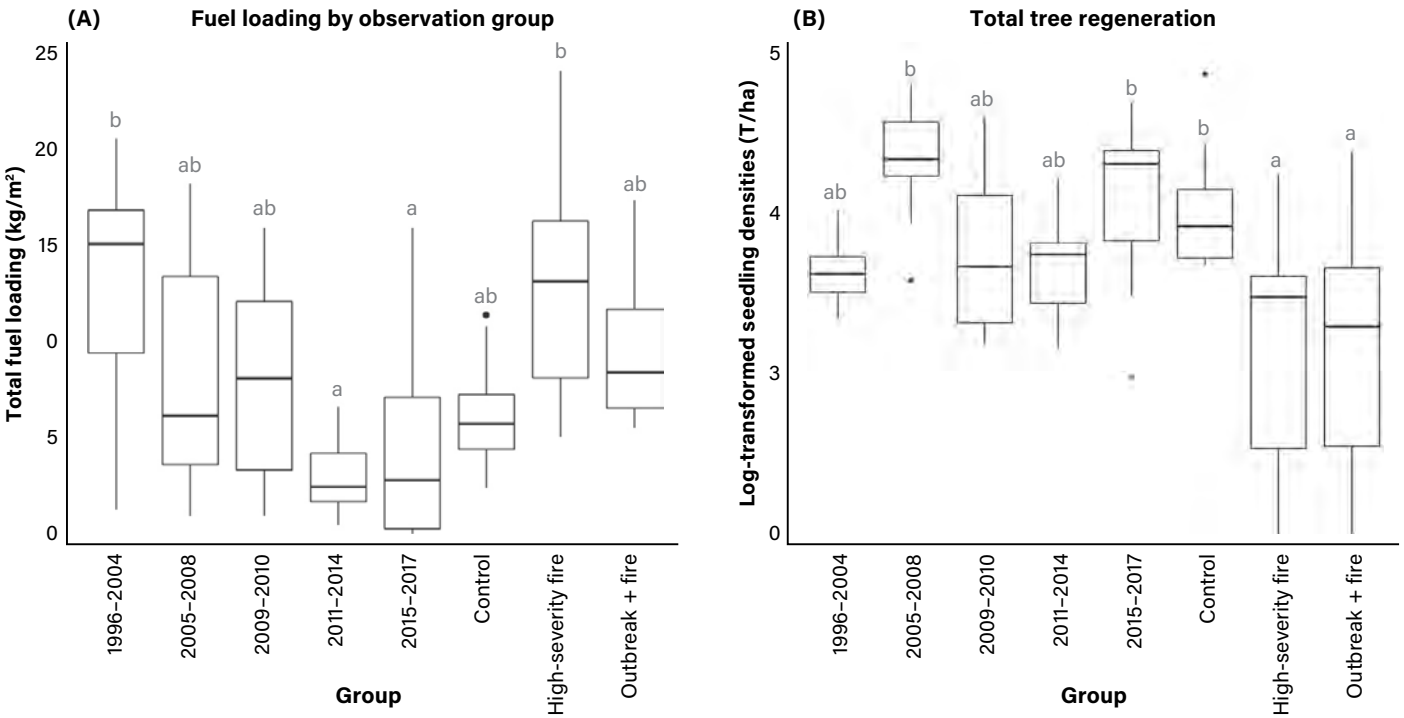

Figure 11.2—(A) Boxplots of total fuel loading by group; (B) boxplots of total tree seedling densities (all species) in each disturbance group. Bark beetle disturbances were pinned by year since outbreak, control sites were those with endemic levels of bark beetle activity and wildfire sites burned in 2002 and 2005, and "outbreak and fire" sites experienced a bark beetle outbreak prior to wildfires of these same years. Horizontal bars represent mean fuel loading of each disturbance group; height of boxes represents spread of 75 percent of data. Different letters indicate statistically significant differences between groups from a Tukey's honestly statistical difference (HSD) analysis. As shown on (B), analyses were conducted on log-transformed seedling densities; raw densities are graphically displayed. Units are in log transformed trees per hectare.

wildfire-affected stands. Full methods can be found in Schapira and others (2021b). We compared climatic conditions between years with high tree seedling establishment and nonestablishment years to ascertain regional drivers of tree seedling recruitment in subalpine forest. Both height and terminal bud scar counts were significant predictors of seedling age, although correlations were weaker in older seedlings that exhibited suppressed growth (tables 11.1 and 11.2). Growing season precipitation had a significant positive relationship with spruce-fir establishment, while minimum temperatures, annual vapor pressure, and climatic water deficits had significant negative correlations with subalpine tree establishment. Height and terminal bud scar counts did not accurately predict precise ages of subalpine tree establishment from beetle-affected stands but provided more accuracy in post-fire tree establishment. Average climate conditions compared to long-term climate may provide suitable conditions for low levels of tree establishment in spruce-fir stands. However, large spruce-fir establishment pulses occurred in cooler and wetter growing years compared to the long-term average.

To address objective 3, we created a post-outbreak fuels photo series and modeled it after the natural fuels photo series, which includes six volumes that represent different forest types across the United States (Ottmar and others 2000). This post-outbreak fuels photo series represents spruce-fir forests in different stages of spruce beetle outbreak recovery and spruce-fir stands unaffected by spruce beetles for comparison. This project was published through the Southern Rockies Fire Science Network (Schapira and others 2021c).

Table 11.1—Generalized linear models for predicting Engelmann spruce seedlings (R^2 = 0.8158)

Engelmann spruce	Estimate	Standard error	*t*-value	*p*-value[a]
(intercept)	-6.62	2.36	-2.81	*0.006*
Height (cm)	0.19	0.05	3.96	*0.0001*
Bud scar count	1.42	0.13	11.00	*<0.0001*
Disturbance type: burn[b]	-6.24	2.70	-2.31	*0.023*

[a] Significance indicated in italics, and *p*-values indicate significance of predictor variables on Engelmann spruce age.

[b] Outbreak sites are the baseline category for "disturbance type."

Table 11.2—Generalized linear models for predicting subalpine fir seedlings (R^2 = 0.7992)

Subalpine fir	Estimate	Standard error	*t*-value	*p*-value[a]
(intercept)	-4.69	2.34	-2.00	*0.048*
Height (cm)	0.095	0.04	2.41	*0.018*
Bud scar count	1.45	0.12	12.49	*<0.0001*
Disturbance type: burn[b]	-7.49	2.94	-2.55	*0.012*

[a] Significance indicated in italics, and *p*-values indicate significance of predictor variables on subalpine fir age.

[b] Outbreak sites are the baseline category for "disturbance type."

DISCUSSION AND CONCLUSIONS

This study demonstrates that subalpine forests are impacted differently by different disturbances. Tree regeneration was abundant following spruce beetle outbreak, but post-fire seedlings were less common and were predominantly lodgepole pine and aspen (*Populus* spp.), rather than Engelmann spruce and subalpine fir that previously dominated these landscapes. However, unlike concerns at lower elevation forests (Chambers and others 2016), all plots had tree seedlings. Climate change will likely continue to play a role in tree establishment in both burned and bark beetle-affected stands, and this pattern is likely more pronounced in burned sites due to the lack of canopy cover and favorable microsite conditions. Tree regeneration and forest recovery in these long-lived systems may take many decades or even centuries to recover to a similar species dominance, and these processes may be driven by current and future climate. In spruce beetle outbreak sites, tree regeneration was abundant and high fuels loads were common, especially at longer times since outbreak. Small trees do not necessarily equate to young trees, especially in these dense forests that are dominated by shade-tolerant species (Hankin and others 2018, Veblen 1986). We found tree seedlings on all 80 study sites; however, spruce beetle outbreak sites had a larger proportion of subalpine fir and, in some cases, thousand seedlings per hectare, and we may see a change in dominance as others have hypothesized and observed (DeRose and Long 2010, Schmid and Frye 1977). Burned sites had tree regeneration dominated by lodgepole pine and aspen, indicating at least short-term conversions in forest dominance, as others have found in fire-affected stands (Harvey and others 2014), but this may create conditions conducive in the years to come for Engelmann spruce and subalpine fir regeneration as they are more shade tolerant. Given the projections for both more wildfires and hotter and drier climatic conditions (Higuera and others 2021), the future of these forests is uncertain and continued monitoring of these complex forests at the top of the world is important to consider.

For more information:
Camille Stevens-Rumann
c.stevens-rumann@colostate.edu

LITERATURE CITED

Abatzoglou, J.T.; Williams, A.P. 2016. Impact of anthropogenic climate change on wildfire across Western US forests. Proceedings of the National Academy of Sciences. 113 (42): 11770–11775. https://doi.org/10.1073/pnas.1607171113.

Chambers, M.E.; Fornwalt, P.J.; Malone, S.L.; Battaglia, M.A. 2016. Patterns of conifer regeneration following high severity wildfire in ponderosa pine-dominated forests of the Colorado Front Range. Forest Ecology and Management. 378: 57–67. https://doi.org/10.1016/j.foreco.2016.07.001.

DeRose, R.J.; Long, J.N. 2010. Regeneration response and seedling bank dynamics on a *Dendroctonus rufipennis*-killed *Picea engelmannii* landscape. Journal of Vegetation Science. 21: 377–387. https://doi.org/10.1111/j.1654-1103.2009.01150.x.

Hankin, L.E.; Higuera, P.E.; Davis, K.T.; Dobrowski, S.Z. 2018. Accuracy of node and bud-scar counts for aging two dominant conifers in western North America. Forest Ecology and Management. 427: 365–371. https://doi.org/10.1016/j.foreco.2018.06.001.

Hart, S.J.; Veblen, T.T.; Eisenhart, K.S. [and others]. 2014. Drought induces spruce beetle (*Dendroctonus rufipennis*) outbreaks across northwestern Colorado. Ecology. 95(4): 930–939. https://doi.org/10.1890/13-0230.1.

Harvey, B.J.; Donato, D.C.; Turner, M.G. 2014. Recent mountain pine beetle outbreaks, wildfire severity, and postfire tree regeneration in the US Northern Rockies. Proceedings of the National Academy of Sciences. 111(42): 15120–15125. https://doi.org/10.1073/pnas.1411346111.

Higuera, P.E.; Shuman, B.N.; Wolf, K.D. 2021. Rocky Mountain subalpine forests now burning more than any time in recent millennia. Proceedings of the National Academy of Sciences. 118(25): e2103135118. https://doi.org/10.1073/pnas.2103135118.

Ott, D.S.; Fettig, C.J.; Ross, D.W.; Munson, A.S. 2018. Effects of spruce beetle (*Dendroctonus rufipennis*) outbreaks on fuels, carbon, and stand structure and composition in Utah and western Wyoming (Project INT-EM-F-13-02). In: Potter, K.M., Conkling, B.L., eds. Forest Health Monitoring: national status, trends, and analysis 2017. Gen. Tech. Rep. SRS-233. Asheville, NC: U.S. Department of Agriculture, Forest Service, Southern Research Station: 177–182.

Ottmar, R.D.; Vihnanek, R.E.; Wright, C.S. 2000. Stereo photo series for quantifying natural fuels. Volume III: lodgepole pine, quaking aspen, and gambel oak types in the Rocky Mountains. PMS 832. Boise, ID: National Wildfire Coordinating Group, National Fire Center. 85 p.

Schapira, Z.H.; Stevens-Rumann, C.S.; Shorrock, D. [and others]. 2021a. Beetlemania: is the bark worse than the bite? The ecological effects of bark beetle and wildfires in Rocky Mountain subalpine forests. Forest Ecology and Management. 482: 118879. https://doi.org/10.1016/j.foreco.2020.118879.

Schapira, Z.H.; Stevens-Rumann, C.S.; Shorrock, D. 2021b. Subalpine tree seedlings: assessing aging methodology and drivers of establishment. Forest Ecology and Management. 497(42): 119516. https://doi.org/10.1016/j.foreco.2021.119516.

Schapira, Z.H.; Stevens-Rumann, C.; Shorrock, D. [and others]. 2021c. Photo series for quantifying post-disturbance fuels. Spruce beetle-affected subalpine forest type in the Rocky Mountains. SRFSN Publication 2021-1. Fort Collins, CO: Southern Rockies Fire Science Network. 25 p.

Schmid, J.M.; Frye, R.H. 1977. Spruce beetle in the Rockies. Gen. Tech. Rep. RM-49. Fort Collins, CO: U.S. Department of Agriculture, Forest Service, Rocky Mountain Forest and Range Experiment Station. 38 p.

Schoennagel, T.; Balch, J.K.; Brenkert-Smith, H. [and others]. 2017. Adapt to more wildfire in western North American forests as climate changes. Proceedings of the National Academy of Sciences. 114 (18): 4582–4590. https://doi.org/10.1073/pnas.1617464114.

Veblen, T.T. 1986. Age and size structure of subalpine forests in the Colorado Front Range. Bulletin of the Torrey Botanical Club. 113(3): 225–240. https://doi.org/10.2307/2996361.

ACKNOWLEDGMENTS

This research presented in this report was supported in part through the project "Forest Health Monitoring and Assessment" of Cost Share Agreement (July 19, 2021 through January 15, 2023) and the project "Forest Health Monitoring, Analysis, and Assessment" (August 25, 2022 through September 30, 2023) between North Carolina State University (this institution is an equal opportunity provider) and the U.S. Department of Agriculture, Forest Service, Southern Research Station, Asheville, NC. This research was supported by funds provided by the U.S. Department of Agriculture, Forest Service, Southern Research Station, Asheville, NC.

The editors and authors of this report thank the following for their reviews and constructive comments: Thomas Albright, Chris Asaro, Stephen Burr, Robert Cain, Jennifer Costanza, Susan Crocker, Robert Haack, Ryan Hanavan, Robert Jetton, Phillip Marshall, Bruce McCune, Toby Petrice, Andrea Pipp, Roger Rosentreter, Robert Smith, Tom Smith, Eric Sprague, and Barry Ty Wilson.

AUTHOR INFORMATION

Sections 1 and 2, Forest Health Monitoring Research

Mark J. Ambrose, Research Assistant, North Carolina State University, Department of Forestry and Environmental Resources, Raleigh, NC 27695.

William M. Christie, Geospatial Analyst, U.S. Department of Agriculture, Forest Service, Southern Research Station, Eastern Forest Environmental Threat Assessment Center, Asheville, NC 28804.

Sarah Jovan, Research Ecologist, U.S. Department of Agriculture, Forest Service, Pacific Northwest Research Station, Portland, OR 97214.

Steven P. Norman, Research Ecologist, U.S. Department of Agriculture, Forest Service, Southern Research Station, Eastern Forest Environmental Threat Assessment Center, Asheville, NC 28804.

Jeanine L. Paschke, Geographic Information Systems Analyst, RedCastle Resources, Inc., Fort Collins, CO 80526.

Kevin M. Potter, Research Professor, North Carolina State University, Department of Forestry and Environmental Resources, Raleigh, NC 27695 (now Research Ecologist, U.S. Department of Agriculture, Forest Service, Eastern Forest Environmental Threat Assessment Center, Research Triangle Park, NC 27709).

KaDonna C. Randolph, Research Mathematical Statistician, U.S. Department of Agriculture, Forest Service, Southern Research Station, Knoxville, TN 37919.

Susan Will-Wolf, Senior Scientist II emerita, University of Wisconsin-Madison, Department of Botany, Madison, WI 53706.

AUTHOR INFORMATION

Section 3, Evaluation Monitoring Project Summaries

Jordan D. Bernard, Student, Washington & Jefferson College, Environmental Studies Program, Washington, PA 15301.

Alexandra Blevins, Forest Health Specialist, Kentucky Energy and Environment Cabinet, Division of Forestry, Frankfort, KY 40601.

Amy Chambers, Biological Technician, U.S. Department of Agriculture, Forest Service, Rocky Mountain Regional Office, Lakewood, CO 80401.

Charles E. Flower, Research Ecologist, U.S. Department of Agriculture, Forest Service, Northern Research Station, Delaware, OH 43085.

Timothy D. Fox, Ecologist, U.S. Department of Agriculture, Forest Service, Northern Research Station, Delaware, OH 43085.

Stephen W. Fraedrich, Research Plant Pathologist (retired), U.S. Department of Agriculture, Forest Service, Southern Research Station, Athens, GA 30602.

Kyle J. Haynes, Research Professor, University of Virginia, Blandy Experimental Farm, Boyce, VA 22620.

Chad Hoffman, Associate Professor, Colorado State University, Department of Forest and Rangeland Stewardship, Fort Collins, CO 80523.

Brian M. Hoven, Visiting Assistant Professor, Centre College, Department of Biology, Danville, KY 40422.

Jaesoon Hwang, Plant Pathologist, U.S. Department of Agriculture, Forest Service, State and Private Forestry, Forest Health Protection, Southern Region, Pineville, LA 71360.

Rachel H. Kappler, Great Lakes Basin Forest Health Collaborative Coordinator, Holden Forests & Gardens, Kirtland, OH 44094.

Jason S. Kilgore, Professor of Biology, Washington & Jefferson College, Department of Biology, Washington, PA 15301.

Kathleen S. Knight, Research Ecologist, U.S. Department of Agriculture, Forest Service, Northern Research Station, Delaware, OH 43085.

Andrew M. Liebhold, Research Entomologist, U.S. Department of Agriculture, Forest Service, Northern Research Station, Morgantown, WV 26505.

AUTHOR INFORMATION

Robert P. Long, Research Plant Pathologist, U.S. Department of Agriculture, Forest Service, Northern Research Station, Irvine, PA 16329.

Albert E. Mayfield III, Research Entomologist, U.S. Department of Agriculture, Forest Service, Southern Research Station, Asheville, NC 28804.

Randall S. Morin, Research Forester, U.S. Department of Agriculture, Forest Service, Northern Research Station, Forest Inventory and Analysis, York, PA 17402.

Bryan T. Mudder, Forestry Research Technician, U.S. Department of Agriculture, Forest Service, Southern Research Station, Asheville, NC 28804.

Rabiu O. Olatinwo, Research Plant Pathologist, U.S. Department of Agriculture, Forest Service, Southern Research Station, Pineville, LA 71360.

Valerie J. Pasquarella, Research Assistant Professor, Boston University, Department of Earth & Environment, Boston, MA 02215.

Clare A. Rodenberg, Graduate Student, University of Virginia, Department of Environmental Sciences, Charlottesville, VA 22903.

Alejandro A. Royo, Research Ecologist, U.S. Department of Agriculture, Forest Service, Northern Research Station, Irvine, PA 16329.

Zoe Schapira, Graduate Student, Colorado State University, Department of Forest and Rangeland Stewardship, Fort Collins, CO 80523.

Donna Shorrock, Ecologist, U.S. Department of Agriculture, Forest Service, Rocky Mountain Regional Office, Lakewood, CO 80401.

Nathan W. Siegert, Forest Entomologist, U.S. Department of Agriculture, Forest Service, State and Private Forestry, Forest Health Protection, Eastern Region, Durham, NH 03824.

Camille Stevens-Rumann, Associate Professor, Colorado State University, Department of Forest and Rangeland Stewardship, Fort Collins, CO 80523.

Joshua S. Wigal, Biological Science Technician, U.S. Department of Agriculture, Forest Service, Northern Research Station, Delaware, OH 43085.

Potter, Kevin M.; Conkling, Barbara L., eds. 2023. Forest health monitoring: national status, trends, and analysis 2022. Gen. Tech. Rep. SRS-273. Asheville, NC: U.S. Department of Agriculture Forest Service, Southern Research Station. 180 p. https://doi.org/10.2737/SRS-GTR-273.

The annual national report of the Forest Health Monitoring (FHM) program of the U.S. Department of Agriculture, Forest Service, presents forest health status and trends from a national or multistate regional perspective using a variety of sources, introduces new techniques for analyzing forest health data, and summarizes results of recently completed Evaluation Monitoring projects funded through the FHM national program. In this 22nd edition in a series of annual reports, national survey data are used to identify recent geographic patterns of insect and disease activity. Satellite data are employed to detect geographic patterns of forest fire occurrence. Fine-scale changes in Normalized Difference Vegetation Index (NDVI) are used to detect broad patterns of forest disturbance across the conterminous United States. Data collected by the Forest Inventory and Analysis (FIA) program are employed to detect regional differences in tree mortality. Twenty years of crown dieback trends are presented for the most common tree species and genera in the Eastern United States. The new National FIA Lichen Database and the National Lichen Atlas are described to illustrate the breadth of 23 years of lichen indictor data. Four recently completed Evaluation Monitoring projects are summarized, addressing forest heath concerns at smaller scales.

Keywords—Change detection, disturbance, fire, forest health, forest insects and disease, lichens, tree canopy, tree crown dieback, tree mortality.

Download a copy
www.srs.fs.usda.gov/pubs/

Southern Research Station
200 W.T. Weaver Blvd.
Asheville, NC 28804
www.srs.fs.usda.gov